AN ABSTRACT OF THE DISSERTATION OF

Sofyan Kurnianto for the degree of Doctor of Philosophy in Fisheries Science presented on August 14, 2017.

Title: The Eco-hydrology of Tropical Peatlands Associated with Land Cover Changes.

Abstract approved:

_____

James T. Peterson

Tropical peatlands play an important role in global climate system by storing an immense of carbon that had been accumulated over thousands of years. Peatlands provide another important ecosystem service by regulating the hydrology. It is believed that peatlands act like a giant sponge by absorbing substantial amounts of water in wet season and gradually releasing the water in the following dry season. Nonetheless, there is a lack of information about the hydrological processes that occur in tropical peatlands, especially the effects of land cover change on peat and peat hydraulic properties. In this study, I conducted field surveys to evaluate two main peat hydraulic properties: saturated hydraulic conductivity (K_s) and moisture retention characteristics at different land cover types in tropical peatlands of West Kalimantan, Indonesia. I also explored the potential of ground penetrating radar (GPR) to determine peat properties in tropical peatlands.

Across all sites, K_s varied over four orders of magnitude with depth (ca 0.001 – 13.9 m d^{-1}). The saturated hydraulic conductivity in forested sites at the depth of 50-100 cm (1.08 ± 0.39 m day^{-1}) was significantly higher than K_s at deeper layers. In addition, K_s at the upper layer of forested sites was significantly higher than K_s at the same depth in other land cover types, i.e., recently burned forests, seral community, and oil palm plantation. The best-approximating hierarchical model for estimating K_s included depth, forest cover, a depth and forest cover interaction, and the von Post degree of decomposition. There was no evidence that K_s was related to other peat physical and chemical properties.

The peat moisture retention characteristics presented in the van Genuchten (VG) model indicated that bulk density was strongly and negatively related to the α parameter and there was no evidence that peat properties were strongly related to the m shape parameter of VG model. The proportion of macro-porosity in the drained sites with the distance < 50 m from canal was less than those the drained-seral sites > 50 m from canal and forested sites. Peat pore distribution (i.e., the proportion of macro-, meso- and micro-porosity) also was strongly related to bulk density.

The GPR results indicated that dielectric varied from 5.8 to 84.9 across all sites and were significantly lower at the 50-100 cm depth than those measured at 300-400 cm and 500-600 cm. Parameter estimates from hierarchical models indicated that ash content and carbon concentration were strongly positively related to dielectric and the relationship varied among sites.

My results suggest that tropical peatlands provide essential environmental services by storing huge amounts of water. We estimated that the potential amount of water that can be stored by undrained peat swamp forests in Borneo, Sumatra, and Peninsular Malaysia was about 51.1 – 52.5 km^3 of freshwater. However, the tropical peatlands release water relatively easily when the water table is lowered since it is mostly composed by macro-porosity. Therefore, maintaining the water table close to the peat surface is crucial to prevent water loss from peat. My results also suggest that GPR can be useful for mapping peatland distribution, providing estimates of peat depth and insights into its properties. However, the manual coring is still needed to improve the accuracy and quality of peat property measurement data.

The Eco-hydrology of Tropical Peatlands Associated with Land Cover Changes

by
Sofyan Kurnianto

A DISSERTATION

submitted to

Oregon State University

in partial fulfillment of
the requirements for the
degree of

Doctor of Philosophy

Presented August 14, 2017
Commencement June 2018

Doctor of Philosophy dissertation of Sofyan Kurnianto presented on August 14, 2017

APPROVED:

Major Professor, representing Fisheries Science

Head of the Department of Fisheries and Wildlife

Dean of the Graduate School

I understand that my dissertation will become part of the permanent collection of Oregon State University libraries. My signature below authorizes release of my dissertation to any reader upon request.

Sofyan Kurnianto, Author

ACKNOWLEDGEMENTS

Alhamdulillahirabbil'alamin. All praises belongs to Allah, Lord of all the worlds.

I would like to express the deepest gratitude to my major supervisor, James Peterson, for his guidance, motivation, and knowledge sharing. His insightful comments in the writing process helps a lot to improve this dissertation and my writing skills. I would like to thank Boone Kauffman for the opportunity gave to me to pursue PhD degree at Oregon State University. My gratitude also was delivered to my other committee members: John Selker and Daniel Murdiyarso for providing me great suggestions to establish my PhD research. I would like to thank my graduate representative council, Yvette Spitz for her support and time.

My sincere thanks go to my parents, wife, and big family who always give me their supports, prays and motivations to reach my dream in getting higher education.

My gratitude thanks goes to Ibu Asih in soil biotechnology laboratory, Bogor Agricultural University, Mas Jati and Pak Arif from the soil physic laboratory, soil research center, Bogor for helping me in the soil analysis. This research could not be successful without any helps from them.

My sincere thanks goes to the villagers from Desa Sungai Pelang, Kecamatan Matan Hilir Selatan, Kabupaten Ketapang especially to Bapak Samsudin for his assistance while I was having the field surveys and coordinating the local worker. My thanks go to Robi, Mas Daryono, Pak Dikin, Kang Warga, Harun for helping me getting dirty in the field.

My thanks also go to my Peterson's lab colleague: Adam, Steve, Ty, and Miguel for the brainstorming, giving important ideas, teaching me the statistical analysis for this study and all of the joyful. To my Indonesian graduate friends, thanks for all support. To my brothers in "Hemarnos Bersaudara", VTCOMM, BVC, BMAC, keep the brotherhoods forever.

My study and research was funded by USAID through Kalimantan Wetlands and Climate Studies Project (KWACS). Part of this study was also funded by Sustainable Wetlands Adaptation and Mitigation Program (SWAMP), a joint program between the Center for International Forestry Research (CIFOR) and the US Forest Service joint program. My deepest thanks goes to USAID, USAID-Indonesia, IIE, IIEF and to all officers (Ibu Raya Soendjoto, Pak Hanif Saleh, Pak Donald Tambunan, Debby Gultom, Marcela Zeballos, Christiana Ebiasah) for all the administrative works and making sure my study went well at OSU.

CONTRIBUTION OF AUTHORS

Dr. James T. Peterson was involved in determining the study design, data analysis and writing of this dissertation. Dr. John Selker was involved in selecting the field survey and laboratory methods used in this study as well as reviewed the dissertation. Dr. Boone Kauffman and Dr. Daniel Murdiyarso were involved in designing the study and reviewing the dissertation.

TABLE OF CONTENTS

Page

TABLE OF CONTENTS (Continued)

Page

TABLE OF CONTENTS (Continued)

Page

TABLE OF CONTENTS (Continued)

Page

LIST OF FIGURES

LIST OF FIGURES (Continued)

Figure Page

LIST OF FIGURES (Continued)

Figure Page

LIST OF FIGURES (Continued)

Figure Page

LIST OF TABLES (Continued)

LIST OF TABLES (Continued)

Table Page

I would like to dedicate my dissertation

to my beloved Almarhum Bapak, Ibu-ibu, Istri dan Anak-anakku

CHAPTER 1. INTRODUCTION

Peat is made up by the partially undecomposed plants and mosses that is maintained in wet condition (Andriesse 1988). Globally, peatlands cover an area of approximately 4 million km^2 (~3% of global land area) but play an important role in global carbon cycles. The development of most of these peatlands began in the early Holocene about 11 – 9,000 year before present (BP) and accumulated at rates of 19, 13, and 22 g C m^{-2} y^{-1} for northern, tropical, and southern Patagonia peatlands, respectively (Yu et al., 2010). The total carbon stored in peatlands is estimated to be 600 Gt C, approximately 90% of which occurs in the northern peatlands. Tropical peatlands is defined as the all organic soil that is located between latitude 35° N and 35° S including high altitude peatlands (Andriesse 1988; Wust et. al. 2003).. It covers approximately 440,000 km^2 and contain about 90 Gt C, 80% of which is located in South East Asia (Page et al., 2010). The tropical peatland long-term mean carbon accumulation rate during the Holocene is estimated to be as high as 90 g C m^2 y^{-1} (Page et al. 2004; Yu et al. 2010). These high rates of organic matter accumulation have been attributed high productivity and litter production of tropical forest ecosystems and low decomposition rates due to soil saturation, leading to organic matter accumulation as peat (Chimner and Ewel 2004). The flat topography and high rainfall of tropical areas combined to create the soil saturation necessary for peat development (Page et al. 2010).

Most research conducted in the tropical peatlands focused on biogeochemical studies, such as the carbon dynamics in peatlands since the Holocene (Page et al.

2004; Yu et al. 2010; Dommain et al. 2011) and estimating total carbon stocks (Jaenicke et al. 2008; Murdiyarso et al. 2009). Some research efforts also were focused on carbon flux measured in both pristine peat swamp forests (Jauhiainen et al. 2005), and other land cover types overlain peatlands (Melling et al. 2005b; Jauhiainen et al. 2012). In addition to CO_2 emissions, other greenhouse gas emissions have been measured in tropical peatlands, such as methane and nitrous oxide (Inubushi et al. 2003; Hadi et al. 2005; Melling et al. 2005a; Novita 2016.)

It had been reported that hydrology affects the biogeochemical processes responsible for peat development by controlling the gaseous diffusion within the peat column (i.e., donor and electron acceptor in redox reaction) vegetation structure, composition, and diversity (Holden et al. 2005). The water table influences the decomposition processes of organic matter and, in turn, probably influences the greenhouse gas emissions in peatlands (Couwenberg et al. 2009; Undari et al. 2012). In addition to its influence on peat biogeochemical processes, there also is a link between peat hydraulic properties and the forest structure and composition. Trees with buttress roots that commonly exist in tropical peatlands reduce the surface water flow and, hence, will maintain the peat in a saturated condition (Dommain et al. 2010). This hydraulic condition, then, probably influences the nutrient status in the forest and eventually influences the forest composition (Page et al. 1999; Gunawan et al. 2012)

Some studies on the tropical eco-hydrolgy had been initiated, especially the relationship between peat properties and the water table. Wösten *et al.*, (2006) modeled the dynamics of the peat water table and its implication on the frequency

of peat fires. However, there is a general lack of knowledge related to peat hydrology especially the linkage between land cover changes, peat properties and peat hydraulic characteristic for describing the eco-hydrology in the tropical peatlands especially at the landscape level. Therefore, further research is needed to understand and predict the effects of peat disturbances on tropical peatland eco-hydrology.

To describe the peatland eco-hydrology, two main peat hydraulic properties were estimated, i.e., saturated hydraulic conductivity and peat moisture retention characteristics. The hydraulic properties were determined at different land cover types including undrained and drained sites to evaluate the impact of land cover changes on the peat eco-hydrology. This study was conducted to address following questions:

- What is the effect of land cover change and drainage canal development on peat saturated hydraulic conductivity and how do the peat properties affect saturated hydraulic conductivity?
- How would peat properties be used to quantify the influence of tropical peatlands in regulating water given the range of disturbance regimes?
- How useful are non-destructive geophysical methods as an alternative to conventional methods used to estimate the peat properties?

Based on these scientific questions, my dissertation is organized and presented as the following chapter sections:

Chapter 2. The effect of land cover change on the peat saturated hydraulic conductivity and the influence of peat properties. My hypothesis is that hydraulic conductivity in pristine forest is greater than non-forested areas.

Chapter 3. The peat pore distribution (i.e., macro-, meso, and micro-porosity) at two contrasting land cover types: undrained peat swamp forests and drained seral community. The water retention curve for those sites also were developed to understand the peat moisture dynamics within the range of water table fluctuation. This chapter evaluates the relationship between peat properties, pore distribution, and moisture retention characteristics.

Chapter 4. The peat properties presented in Chapter 2 and Chapter 3 were estimated by conventional methods of collecting peat samples from the field and analyzing them in the laboratory. In chapter 4, I explore an alternative, less-labor intensive method - ground penetrating radar survey, to estimate the peat properties.

Chapter 5. General conclusions and synthesis of information in the previous 3 chapters. I also identify knowledge gaps and provide suggestions for future research to fill those gaps.

CHAPTER 2. THE INFLUENCE OF LAND COVER CHANGES ON THE VARIABILITY OF SATURATED HYDRAULIC CONDUCTIVITY IN TROPICAL PEATLANDS

Abstract

Understanding the movement of water through tropical peat landscapes is essential for developing effective conservation and management strategies for these systems that contain considerable labile carbon. Saturated hydraulic conductivity, K_s is one of the most important parameters that is used to describe water movement through soil profiles, but there is little understanding of the spatial variability of K_s in tropical peatlands and the effects of land conversion on peat characteristics. To describe the vertical distribution of saturated hydraulic conductivity within the peat profile, we utilized the slug test method in tropical peatlands of West Kalimantan, Indonesia at three depths (0.5-1, 3-4, and 5-6 m) on undrained forests, recently burned forests, early seral communities, and oil palm plantations. We found strong spatial autocorrelation among measurements collected at our 19 study sites and evaluated the relationship between hydraulic conductivity and land cover types, peat properties, and depth of measurement with a hierarchical linear model. Hydraulic conductivity varied over four orders of magnitude (ca 0.001 – 13.9 m d^{-1}). The best-approximating hierarchical model for estimating K_s had dependencies on depth, forest cover, a depth and forest cover interaction, and the von Post degree of decomposition. Parameter estimates indicated that K_s in forested communities at the 50 -100 cm depth was two- orders of magnitude greater than non-forested sites and decreased with increasing depth and decomposition stage. This suggested that the peat swamp forest conversion likely reduced the ability of peat to transfer

water. Our results suggest that K_s should be measured directly in tropical peatlands rather than estimated as a function of peat properties. Additionally, the strong spatial dependence observed in our study suggests that similar research designs should examine the sample data for spatial dependence and if necessary incorporate hierarchical models to incorporate the spatial variation of K_s that could not be captured by using ordinary linear regression.

Keywords: hydroecology, permeability, forests conversion, land cover change, eco-hydrology, peat properties

2.1. Introduction

Tropical peatlands are estimated to store 90 Gt of carbon, which is 15 – 19% of the carbon stored in peatlands globally (Page et al. 2011) and represents thousands of years of accumulation. Undisturbed peat forests are a carbon sink that have been sequestering carbon from the atmosphere at millennial time-scales (Yu et al. 2010). Approximately 60% of tropical peatlands are located in Southeast Asia (SEA), which currently store ca. 69 GtC of belowground carbon. Additionally, tropical peatlands also provide a wide range of ecosystem services, such as habitat for endangered species, biodiversity-rich ecosystems, and regulating hydrology and flood prevention (Evers et al. 2016).

Saturated hydraulic conductivity (K_s) is an important property that describes the ability of water to flow through the peat profile (Rycroft et al. 1975). In the application of peat hydrology in tropics, information on K_s is required to estimate the amount of water needed to maintain saturated conditions in the peat dome (Dommain et al. 2010), identify fire prone areas (Wösten et al. 2006a), and design drainage canals for better water management (Ritzema et al. 1998).

In recent decades, land use/cover changes have greatly altered tropical peatlands, with forest conversion to other land cover types such as industrial plantations of oil palm, wood, and other agricultural activities (Koh et al. 2011; Miettinen et al. 2012b, a; Gaveau et al. 2016). Tropical peat swamp deforestation for plantation development usually includes construction of drainage canals to facilitate rapid runoff and dropping the water table. This practice has several effects on the physical and chemical properties of peat, increasing bulk density, ash content, base

cation concentration (Kool et al. 2006; Anshari et al. 2010); and decreasing nitrogen concentration (Könönen et al. 2015). Previous studies conducted in northern boreal peatlands demonstrated that K_s varies with vegetation type, structure, and composition (Whittington et al. 2007; Crockett et al. 2015).

Estimates of the vertical variability of K_s within the peat profile is needed for a greater understanding of the hydrological processes within these soil types such as simulating the groundwater flow (Jiang et al. 2009). To simulate the spatial distribution of a water table using a groundwater model, Wösten et al. (2006b) divided the peat column into two layers: upper layer (<100 cm) had greater conductivity than the deeper layer. Studies conducted in boreal peatlands reported that K_s was inversely related to depth in the upper profile (depth < 100 cm), with conductivity decreasing several orders of magnitude with increased depth from the peat surface (Clymo 2004; Whittington et al. 2007; Quinton et al. 2008; Moore et al. 2015). The hydraulic conductivity measured in the permanently saturated zone (i.e., generally > 100 cm) varied much less with depth (Chason and Siegel 1986). In the Peruvian tropical peatlands, Kelly et al. (2014) reported that hydraulic conductivity at 50 cm in depth was greater than at 90 cm. However, estimates of K_s at deeper layers in the peat profile and the effects of peat properties and land cover on Ks in tropical peatlands remain poorly understood.

The relationship between K_s and other physical and chemical peat properties can be used to estimate conductivity and serve as the proxies of degree of peat decomposition. Previous research in northern peatlands indicated that conductivity was negatively correlated to bulk density (Boelter 1969; Grover and Baldock 2013;

Mustamo et al. 2016) and the degree of decomposition in von Post scale (Rycroft et al. 1975; Mustamo et al. 2016) and positively correlated to fiber content (Boelter 1969) and the proportion of macro-porosity (Rizzuti et al. 2004). In addition, carbon to nitrogen ratios (C/N) are inversely related with degree of humification (Kuhry and Vitt 1996) and can be used to estimate the mass remaining after to the decomposition process that are related to K_s (Morris et al. 2015). Furthermore, the statistical relationships between K_s and peat properties have been used to model the carbon accumulation over millennia in northern boreal and tropical peatlands (Frolking et al. 2010; Kurnianto et al. 2014).

There have been few published hydraulic conductivity studies conducted in tropical peatlands, and most of the available hydraulic conductivity information is published in grey literature, especially from South East Asia (see Dommain *et al.*, 2010). In South East Asia (SEA) peatlands, the relationship between K_s and depth for the whole peat profile (i.e., the surface to mineral layer) remains unclear. In addition, the influence of land cover change on K_s in this region is unknown but is needed to estimate the amount of groundwater draining from the peat dome. To fill these gaps, we evaluated the relationships between K_s and peat properties across different land cover types (*i.e.* forests, burned forests, early seral, and oil palm plantation) in tropical peatlands of West Kalimantan to address the following research objectives:

- Quantify differences of K_s within the peat column and within and across four different land cover types.

- Evaluate the statistical relationship between physical and chemical peat properties and K_s and estimate how these relationships vary with land cover change. We hypothesize that K_s is higher in forested sites than other types and affected by the degree of decomposition.

2.2. Methods

2.2.1. Study Area

The field study was conducted in Ketapang, West Kalimantan, Indonesia, which is a coastal peatland because its edge is located less than 20 km from the sea (Karimata Strait). This region was selected because it contained multiple land cover types in close proximity on peat soils hat represented the trajectory of typical land cover changes occurring in Indonesian peatlands. The study site was characterized by a peat dome with the peat depth up to 11 m. The peat dome is located between two rivers: the Pawan River in the northern part and the Kepuluk River in the southern part (Figure 2.1). The gradient in this region is very low with the elevation ranging from 5 to 50 m a.s.l. (meter above mean sea level) across the peat dome.

The study area is characterized as wet-tropics with a mean annual rainfall of 3,200 mm based on measurements from 1980 to 2014 (http://dataonline.bmkg.go.id). There were no distinct differences between wet and dry seasons that might be affected by the southward and northward shifting of the inter-tropical convergence zone (ITCZ) (Aldrian and Dwi Susanto 2003). Additionally, the rainfall in this region has two peaks of rainfall that typically occurred in March to May and October to December (Figure 2.2). Contrary to

rainfall, the average monthly temperature in this region was very stable ranging only from 23.1 to 24.3 ^{o}C. Over the diurnal cycle, the mean maximum daily temperature ranged from 30.4 to 32.0^{o}C, and the minimum daily temperature from 26.7 to 27.6 ^{o}C (Figure 2.2).

2.2.2. Study design

To assess the effect of land cover type on saturated hydraulic conductivity (hereafter, K_s), measurements were performed at 19 sites across four different land cover types. These included forests (n=7), recently burned forests (n=3), early seral (n=5), and oil palm plantations (n=4) (Table 2.1). The trees density in the forested sites were up to 1,906 ± 185 trees ha^{-1} with the tree basal area up to 33.1 ± 2.6 (Basuki 2017). The distance of the canal to the forested sites were longer than 500 m. Other land cover types were categorized as drained peatlands since they were close to the drainage canals. The burned sites were burned in a wildfire from August to October 2014. Vegetative cover of the early seral sites were primarily ferns and herbaceous woody plant community (hereafter, seral). The oil palm plantation sites were established in five-year old plantations that at establishment were drained to lower the water table and planted by the smallholder local villagers with minimum soil tillage or fertilization.

At each site, a 150 m transect was established with six 2-m in diameter circular plots on 30 m intervals (Figure 2.3). Piezometer wells were established within each plot with screening spanning three depths (hereafter identified by the mid-point): 50–100 cm (75 cm mid-point), 300–400 cm (350 cm mid-point) and 500 – 600 cm

(550 cm mid-point). If the peat depth in a plot was < 600 cm, the deepest measurement was taken above the mineral layer and if the peat depth was less than 500 cm, we did not collect the third measurement. For seral and oil palm plantation sites, transects were established perpendicular to drainage canals with the first plot located 20 m away from a canal.

In addition to the three piezometer wells, we also collected peat samples at each plot and depth where the K_s was measured using a peat auger (Eijkelkamp, Giesbeek, Netherland) with a core diameter of 5.6 cm. At each plot depth (i.e., 75 cm, 350 cm and 550 cm), 10 cm long peat subsamples were extracted, wrapped in aluminum foil, and placed in sealed whirl packs (Nasco whirl-pak®). These subsamples then were transferred to the soil laboratory of Bogor Agricultural University for peat analysis that included carbon (*C*), nitrogen concentration (*N*), bulk density (*BD*), and ash content. The degree of decomposition was determined in the field qualitatively using the von Post (*VP*) scale, H1 – H10, following the method of Verry *et al.* (2011).

The peat subsamples were oven dried at 70 ^{o}C for 48 hours or until weight reached a constant value, indicating that all the lightly-held peat moisture had evaporated. This was performed by weighing the samples after dried for 48 hours, put them back in oven for the next 24 hours and, then, reweigh the sub samples. The dry weights of sub-samples were considered constant when consecutive measurements, rounded to the nearest tenth, were equal. The dry bulk density was determined as the ratio between the peat dry weight and fresh subsample volume. After the dry weights were recorded, the dry subsamples were placed in a muffle

furnace at 550 ^{o}C for approximately 2 hr. The ash content was determined as the ratio between the weight after ashing at 550 ^{o}C and dry weight. A portion of the dry weight subsamples were ground, homogenized and analyzed for carbon and nitrogen concentration using a LECO TruSpec elemental CN analyzer (LECO Corp, St. Joseph, Michigan, USA). This method had previously been applied to quantify the peat carbon stocks at various sites of Indonesian peatlands (Warren et al. 2012).

2.2.3. Slug test procedures

Field measurements to determine K_s were performed using a slug test, an easy, practical, and relatively inexpensive method that requires a piezometer well (Bouwer and Rice 1976). We made a piezometer using polyvinyl chloride (PVC) pipes with an inner and outer diameter of 55.5 and 59.9 mm, respectively. The lower 30 cm of the pipe was perforated by drilling holes in the pipe and cutting slots that would allow the free flow of water into and out of the piezometer (Figure 2.4). The perforated area was made by cutting twelve rectangular holes with the dimension of 1.5 cm x 13 cm and equivalent to ca. 41% of the surface area that was available for the water to pass. The perforated section of the pipe was covered by stainless steel screen to prevent peat material from entering the piezometer and was sealed at the base with a wooden cone. The well installations were established August to October, 2014.

The piezometers were inserted into the peat after a hole was created with a Russian peat auger with the diameter of about 5.6 cm. After creating the hole, the piezometer was inserted by hand to prevent damage to the piezometer. Prior to

conducting hydraulic conductivity measurements, we performed piezometer 'development' to ensure that the stainless steel piezometer screens were not clogged by material that could affect the measurements. Piezometer development was conducted using a wooden piston-like tool equipped with a one-way valve that served as the surge block with a diameter that fit snugly inside the well. The piston was moved up and down within the well to force water into and out of the tube through stainless steel screen covering the perforated area. This process loosened the peat immediately outside the screening, and removed materials that might have clogged the screen.

After piezometer development, we waited a minimum of 24 hours before conducting the slug test. The slug test method is generally performed by rapidly lowering the water level in a well by removing water or by increasing the water-level by submerging an object in a well (Bouwer and Rice 1976). In this study, we removed water with each well with a hand-made bailer that removed approximately 840 cm^3 water from the 350 and 550-cm and 340 cm^3 for the 75-cm wells.
The depth of the water within the well before and after bailing was recorded using HOBO® pressure transducer water level data logger (part number: U20-001-01). The time resolution for the logger was set to 10 s. We placed the data logger at least 150 cm below the water table at the 350- and 550-cm wells and at the bottom of the 75-cm wells. We then inserted the bailer into the wells to displace water, waited several minutes after the water level reached equilibrium condition (i.e., the initial water depth), and removed the bailer quickly from a well to initiate the test. The amount of time that the depth of water within the well took to reach equilibrium

condition after the bailer was removed was recorded and used in the K_s calculation. The slug test measurements were conducted from 27 November to 16 December 2014.

2.2.4. Data analysis

The logged water pressure data in the slug test procedure was transferred to a computer directly in the field by using HOBO® waterproof shuttle (part number: U-DTW-1). The water pressure data was converted to water table depth using HOBOware® Pro with the barometric compensation assistant extension that requires absolute air pressure and manual water level measurements to calibrate the absolute water pressure recorded by the logger. We used the same HOBO® data logger to record air pressure as the study site is characterized by relatively flat topography.

2.2.4.1. K_s calculation

The saturated hydraulic conductivity, K_s was analyzed using the Bouwer & Rice (1976) method using the following equation

$$K_s = \frac{{r_c}^2 \ln\left({R_e}/{r_w}\right)}{2(L-d)} \frac{1}{t} ln \frac{H_0}{H_w}$$

where H_o is the initial head change (m) and H_w is the head change over time (m), r_c is effective radius of the well casing in which the water lever change is occurred (m), r_w is effective radius of the well (m), L is the vertical distance of the static water table to the bottom of well screen (Figure 2.4). Since K_s, r_c, R_e, r_w, and L are constant,

the value of $\frac{1}{t} ln \frac{H_0}{H_w}$ should be constant and can be estimated by fitting a straight line in a H_w/H_0 – *time* semi logarithmic plot. The term ln $\left({R_e}/{r_w}\right)$ was calculated as:

$$ln\left({R_e}/{r_w}\right) = \left(\frac{1.1}{ln\left({L}/{r_w}\right)} + \frac{A + B.ln\left({(m-L)}/{r_w}\right)}{{(L-d)}/{r_w}}\right)^{-1}$$

where *m* is the aquifer saturated thickness, *A, B,* and *C* are dimensionless and their values were determined using the polynomial equations developed by Yang & Yeh (2004):

$$A(x) = 1.353 + 2.157x - 4.027x^2 + 2.777x^3 - 0.460x^4$$

$$B(x) = -0.401 + 2.619x - 3.267x^2 + 1.548x^3 - 0.210x^4$$

$$C(x) = -1.605 + 9.496x - 12.317x^2 + 6.528x^3 - 0.986x^4$$

where x is $\log\left(\frac{L-d}{r_w}\right)$.

2.2.4.2. Statistical modeling

We evaluated the influence of the land cover, depth of measurement and their interaction on the peat properties (e.g. bulk density, carbon content) using a nested analysis of variance (ANOVA) with plots nested within sites. Bulk density, carbon content, ash content, carbon to nitrogen ratio and von Post degree of decomposition were treated as the dependent variable and the depth of measurement and land cover as independent variables. The ANOVA test was performed using the *lmerTest* package implemented in R statistical software with the *p-value* and the degrees of freedom calculated using Satterthwate's approximation (Kuznetsova et. al. 2016).

We initially evaluated the relationship between quantified peat properties, (i.e., carbon, carbon to nitrogen ratio, ash content, bulk density, and von Post degree of decomposition) and land cover types of tropical peatland K_s using linear regression models. However, the K_s measurements were taken in 19 sites in which six plots were nested within each site and three K_s measurements were made at different depths within each plot. This research design suggests that there was the possibility of the spatial autocorrelation among plots nested within sites that would preclude the use of ordinary linear regression. To evaluate whether spatial dependency of the K_s existed, we fitted a global model containing all predictor variables using linear regression and plotted the residuals ordered by site. The plots indicated that there was spatial dependency among plots nested within sites at different land cover types.

To account for the spatial dependence among plots within sites, we used hierarchical linear models to evaluate the factors related to K_s. One of the benefits of utilizing hierarchical models compared to ordinary linear regression is that dependence among K_s measurements performed at a site, defined as lower-level units (plots) within upper-level units (sites), is accounted for by including random effect for the lower-level intercept and slopes (Raudenbush and Bryk 2002). Here, the lower-level model treated the intercept (β_0) and the effect of peat characteristics (β_1) as varying among sites (j):

$$Y_{ij} = \beta_{0j} + \beta_{1j}X_{1ij} + \ldots \beta_{Pj}X_{Pij} + r_{ij},$$

where Y_{ij} is the dependent variable (e.g., K_s) and X_P is the plot-level explanatory variables (e.g., bulk density) measured in plot *i* at site *j*, and *r* are the residuals that are assumed normally distributed with a mean of zero. The upper level models modeled the intercept, β_{0j} and slope β_{1j} as functions of site-specific characteristics (e.g., land cover types) using the following:

$$\beta_{0j} = \gamma_{00} + \gamma_{01}W_{1j} + \ldots + \gamma_{0s}W_{sj} + u_{0j},$$

$$\beta_{1j} = \gamma_{10} + \gamma_{11}W_{1j} + \ldots + \gamma_{1s}W_{sj} + u_{1j},$$

where W_s is a site specific (upper level) characteristic (Table 2.1); γ_{00} and γ_{10} are the mean intercept and mean effect (slope) of the plot-level characteristics on the response, respectively; γ_{0s} is the mean effect of the site-specific characteristic on the intercept; γ_{1s} is the average effect of the plot-level attributes at the site level; and u_{0j} and u_{1j} are the random effects that that were assumed to be normally distributed with mean of zero and random effect-specific variance (Raudenbush and Bryk 2002).

Prior to hierarchical model fitting, we coded the land cover types using a binary indicator variable. Forest was coded as 1 when the land cover of sites was forests and 0 otherwise, oil palm plantation was coded as1 if the land cover was oil palm and 0 otherwise. Similar binary coding was used for seral land cover and burnt forest was the baseline land cover category. The depths of the measurement were standardized to a mean of zero and standard deviation of one to facilitate model fitting (later called *depth*).

We utilized an information-theoretic approach (Burnham and Anderson 2002) to assess the relationship between K_s, peat properties and land cover types. Firstly,

we developed a global model that contained all of the variables potentially related to K_s including: carbon, bulk density, ash content, C/N, and depth, and land cover types and used it to determine the random effects that best accounted for the spatial dependence. There were several potential sources of statistical dependence. Therefore, we evaluated the relative fit of alternative variance structures for all possible combinations of random effects for the intercept and plot-level explanatory variables. The best approximating variance structure was selected as the model with the smallest Akaike's Information Criteria (*AIC*; Akaike 1973) with the small-sample bias adjustment (AIC_c; Hurvich and Tsai 1989). The variance structure with the smallest AIC_c was considered the best and was to evaluate of the fit of the candidate models, discussed below. The goodness-of-fit (GOF) of the best approximating global model variance structure was assessed by examining the relationship between the residual and fitted values of the global model, quantile plots of the residuals, and plots of residuals ordered by site. All models were fit using the *lmer* function in the R package *lme4* (Bates et al. 2015a).

Using best approximating random effects structure, we fit 50 alternative candidate models comprising different combinations of explanatory variables. The candidate models represented hypothesis of the relationship between peat properties, land cover, depth, and interaction among those variables with the K_s (Table 2.2). The relative support for these alternative models were evaluated by calculating AIC_c. The model with the smallest AIC_c was considered the best approximating model. To facilitate interpretation, we calculated ΔAIC_c for each

candidate model (*i*) and Akaike weight following Burnham and Anderson (2002) that range from 0 to 1 with the best fitting model having the greatest weight.

We created a confidence set of models by selecting the candidate models with the Akaike weights within 10% of the highest Akaike weights, which is similar to the minimum cut-point (i.e. 1/8) as a rule of thumb for evaluating the strength of evidence, as suggested by Royall (1997). All of our interpretations were made using the confidence set of models. We also calculated 90% confidence intervals for fixed effect parameters in the confidence model set. All model selection was performed by using R software with the MuMIn package (Bartoń 2016).

We employed a random effects analysis of variance (ANOVA) with plots nested within sites to partition variation in K_s within and among sites. To evaluate the explanatory power of the best approximating K_s model, we also estimated the amount of variation explained by the model using the methods described in Nakagawa and Schielzeth (2013).

2.3. Results

2.3.1. Peat properties

Across all land cover types, carbon concentration at the 50-100 cm depth was significantly higher than the 300-400 cm depth (DF = 39; p-value=0.0091) and 500-600 cm depth (DF = 19.7; p-value = 0.0001). Carbon concentration at the depth of 50 - 100 cm was similar among land cover types and varied from 52.3 ± 0.39% (mean ± standard error) in forests to 53.4 ± 0.80% in burned forests (Figure 2.5). At the deeper layer (500–600 cm), carbon concentration for forests, seral, and oil palm

was lower than shallower depths and averaged 42.5 ± 1.8% (p-value = 0.0038), 40.2 ± 2.4% (p-value = 0.0048), and 35.0 ± 2.3 (p-value = 0.0032), respectively.

Ash content had a different vertical pattern (Figure 2.5). Ash content increased toward to the deeper layer for all land cover types except burnt forest in which ash content at 50–100 cm was greater than at 300–400 cm (Figure 2.5). At the depth of 50-100 cm and 300-400 cm regardless the land cover types, the average of ash content was significantly lower than 500-600 m strata (DF 1.9; p-value = 0.0000). Within the same layer depth, there was no significant difference of ash content at the 50-100 cm depth among different land cover types. At the depth of 300-400 cm, ash content in oil palm was significantly greater than the forested (DF = 42.6; p-values =0.0335) and burned forest sites (DF = 46.8; p-values = 0.0233). At the deepest layer, 500 – 600 cm, ash content of oil palm was significantly greater than ash measured in burned forest sites (DF = 52.0; p-value = 0.0197).

Similar with the ash content, the average of bulk density across land cover types at the deepest layer was significantly higher than upper (DF = 19.6; p-value = 0.0005) and middle layer (DF = 85.5; p-value = 0.0000). At the 50–100 cm depth, bulk density was similar among land cover types ranging from 0.102 ± 0.007 g cm^{-3} in burnt forest to 0.112 ± 0.005 in oil palm sites. However, bulk densities at the 300–400 cm depth differed significantly among land cover types with bulk density in oil palm in average of 0.148 ± 0.007 g cm^{-3} was significantly higher than forests (DF = 42.6; p-value = 0.0335).

The degree of decomposition for most of the sites in this study varied from medium to highly decomposed peat with the von Post scale ranging from H5 to H8

(Figure 2.5). There were some sites that still had lightly decomposition status of H4 scale. The peat at the layer closer to the surface (50–100 cm) was more significantly decomposed than the deeper layer (DF = 20.9; p-value = 0.0001).

The Carbon to nitrogen ratio (C/N) at the 50 – 100 cm depth were significantly lower than 300-400 cm depth (DF = 53.4; p-value = 0.0000) and 500-600 cm (DF = 19.3; p-value = 0.0000). When comparing C/N ratio among land cover types, C/N in forested sites was significantly lower than oil palm (DF = 17.1; p-value = 0.0047) and early seral communities (DF = 17.7; p-value = 0.0091). At 50–100 cm, burnt forest had the lowest C/N with 41.8 ± 2.1, followed by forest, shrub, and oil palm with the value of 49.8 ± 2.3, 62.0 ± 3.7 and 63.5 ± 1.1, respectively (Figure 2.5).

2.3.2. Hydraulic conductivity

Hydrologic conductivity varied greatly both within and among sites, ranging from ca. 0.001 to 13.9 m day^{-1} (Figure 2.6). High variability of K_s was observed at all sites. Estimated variance components from random effect ANOVA indicated that the hydraulic conductivity varied 19% among sites, 1% among plots within sites, and 80% within plots. The outliers, points located outside of the boxplots tails, were also occurred consistently at all study sites. The skewness of K_s, however, was slightly different among land cover types in which forests tend to have right skewness, while K_s in oil palm plantations and seral skewed to left.

Across different land cover types, K_s at the depth at 50-100 cm was significantly greater than 300-400 cm (DF = 37.4; p-value = 0.0234) and 500-600 cm (DF = 20; p-value = 0.0424). The hydraulic conductivity in forested sites at the depth of 50-100

cm (1.08 ± 0.39 m day^{-1}) was significantly higher than K_s at deeper layers, i.e., 300-400 cm (DF = 35.9; p-value = 0.0001) and 400-500 cm (DF=18.7; p-value = 0.0067. In addition, K_s at the upper layer of forested sites was significantly higher than K_s at the same depth in seral sites (DF = 37.5; p-value = 0.0162), at 300-400 cm in burnt forests (DF=55.1; p-value = 0.0021), at 400 – 500 cm in burnt forests (DF = 50.2; p-value = 0.0475). Hydraulic conductivity in oil palm, burnt forest, and seral did not vary substantially with depth (Figure 2.6).

2.3.3. Factors related to hydraulic conductivity

The best-approximating hierarchical model for determining K_s contained depth, forest land cover, the interaction between depth and forest land cover and the von Post degree of decomposition (Table 2.3). The second best approximating model was only slightly less supported than the best based on Akaike weights. It contained von Post and depth and their interaction. The third best approximating model that was also similar to the best model but contained the interaction between forested land cover and ash content. These models were more than 20 times more likely explanations for the variation in K_s within and among sites compared to the global model containing all variables. There also was no evidence that the relationship between K_s and peat properties varied with land cover as indicated by the Akaike weights near to zero for models containing peat properties by land cover interactions (Table 2.3). The confidence model set included 18 models with weights within 10% of the best model in which all of them contained depth and von Post variables.

The best approximating models indicated that hydraulic conductivity was negatively related to depth and von Post score (Table 2.4). The model accounted for 47% of the variation in hydraulic conductivity within and among sites. The interaction between forest and depth indicated that the decrease in hydraulic conductivity with depth was greater in forested land cover compared to other land types and K_s was reduced in the upper peat layer due to the forest conversion (Figure 2.7). However, at the deeper layer, the K_s was constantly low and was not related to either land cover types or von Post scale (Figure 2.7). The von Post parameter estimates in the best approximating model were relatively precise as shown by their 90% confidence interval that did not span zero (Table 2.4). The depth random effect from the best approximating model indicated that the relationship between log transformed hydraulic conductivity and depth varied about 210% $\left(\frac{\sqrt{0.308}}{|-0.263|}\right)$ among sites. The remaining models in the confidence set suggested that ash content, C/N, and bulk density were negatively related to hydraulic conductivity (Table 2.4, Figure 2.7). However those estimates were imprecise as indicated by 90% confidence intervals that were relatively wide and spanned zero.

2.4. Discussion

Hydraulic conductivity is a very important property needed to evaluate the dynamics of groundwater in tropical peatland ecosystems (Wösten et al. 2006b; Dommain et al. 2010). However, information about the factors affecting hydraulic conductivity in tropical peatlands, particularly those located in South East Asia,

remain scarce. This is likely due to the complexity associated with measuring saturated hydraulic conductivity in-situ. To our knowledge, our study was the first comprehensive study on hydraulic conductivity and related properties in tropical peatlands across different land cover types and its relationship with physical and chemical peat properties within a peat profile.

2.4.1. The influence of peat properties on K_s

Developing statistical or mathematical relationships between hydraulic conductivity, K_s and other peat physical properties that can be measured with relative ease (e.g., bulk density and degree of decomposition) has been the subject of study for several decades (Boelter 1969; Rycroft et al. 1975; Chason and Siegel 1986; Grover and Baldock 2013). We found that the most plausible model for estimating K_s contained von Post degree of decomposition classes. The parameter estimate indicated a strong negative relationship between K_s and von Post, especially for the forested sites at the depth of 75 cm, which is similar with the studies reviewed by Rycroft *et al.*, (1975). They reported that K_s abruptly decreased with increasing von Post scale from H1 to H3 then stabilized when the degree of decomposition greater than H5. Our study results were also consistent with those reported for Finnish peatlands, K_s declining with an increase of degree of decomposition and the slopes of decrease were dependent on the vegetation type overlying the peat (Päivänen 1973). This suggests that the ability of peat to transmit water can be estimated by determining the degree of decomposition using the von Post scale, which is easily and practical tested in the field.

The total porosity of peat comprises two main parts: macro-porosity in which the most of the water transmission occurs, and the closed, dead-end, micro-porosity where water movement has been previously found to be negligible (Rezanezhad et al. 2016). Quinton et al. (2008) reported that the decrease in K_s within a peat profile was related to the reduction of the macro-porosity proportion and was likely related with the state of peat decomposition. As peat decomposes, microbial activities digest the organic material and reduce the portion of the macro-porosity of peat (Rizzuti et al. 2004). Therefore, we hypothesize that our observed negative relationship between peat decomposition state and K_s is due, in part, to the loss of macro-porosity associated with peat decomposition.

Vegetation type is one of the main components in determining the peat properties since it develops from partly undecomposed overlying vegetation (Page et al. 1999). Therefore, vegetation cover types that influence peat substrate characteristics likely influence K_s. For instance, Crockett et al. (2015) measured K_s at shallow depths at several locations with different vegetative communities and concluded that it varied greatly among the vegetation types. This is further supported by the observations that K_s measured at a depth of 90 cm in Peruvian tropical peat swamp forest (Kelly et al. 2014) was similar to our forested field sites at 75 cm depth. However, K_s measured our forested sites was also similar to that measured in northern Minnesota; an area that was mostly covered by non-tree vegetation (Boelter 1969). The similarity in K_s values is probably due to the decomposition process that had occurred at our sites at 75 cm depth, so that the degree of decomposition in our forested sites was similar with Minnesota peat. This

suggests that the influence of vegetation type may be less important than peat substrate quality as measured by the decomposition state when estimating K_s (Preston et al. 2012).

Statistical models of the relationship between K_s and bulk density have proved useful for environmental models of peatland dynamics. For example, Frolking et al. (2010) developed long-term carbon accumulation models for northern boreal peatlands by coupling the carbon and hydrological models in which the hydraulic conductivity was estimated as a function of bulk density. A recent study in sub-alpine peatlands in Australia also reported a significant relationship between bulk density and hydraulic conductivity (Grover and Baldock 2013). Our study, however, differed from previously cited studies in that K_s was not related to bulk density as shown by small (close to zero) parameter estimates and wide confidence intervals that included zero. The weak relationship between bulk density and K_s observed in our study was likely due to the low variability in bulk density among sites. Bulk density measured at the 75 cm depth was similar among sites and ranged from 0.076 – 0.162 g cm^{-3} among samples. This is in contrast to studies that reported a strong statistical relationship between bulk density and K_s with much higher bulk density ranging from ca 0.3 – 0.9 g cm^{-3} (Grover and Baldock 2013). However, our results are similar to Chason and Siegel (1986), who reported low variability of bulk density among the samples that ranged from ca 0.07 – 0.1 g cm^{-3} sampled from Minnesota peatlands.

We evaluated the relationship between K_s and peat chemical properties because we expected that these characteristics were potential proxies of peat decaying

status. During the decomposition processes, the carbon rich organic material in peat is digested by the microbial community so that *N* content increases since it is retained in microbial biomass resulting lower C/N values for well decomposed peat located deep in the profile (Malmer and Holm 1984; Kuhry and Vitt 1996). Thus, we used the C/N to evaluate the hypotheses that K_s was influenced by peat chemical properties. However our result indicated that the relationship between K_s and C/N is imprecise. Anderson (2002) reveled that C/N determined from the peat samples from Scottish peatlands increased following the decomposition processes spanning from less to more decomposed peat. This positive relationship was also commonly found in the tropical peatlands (e.g. Lampela *et al.*, 2014; Könönen *et al.*, 2015). Therefore, we suggest that inconsistent relationship between C/N with the degree of decomposition was one of the factors that influenced the weak relationship between C/N and K_s.

2.4.2. The effect of land cover change on K_s

The peat swamp forest conversion to other land cover types that has been occurring for decades in South East Asia (Miettinen and Liew 2010; Miettinen et al. 2016) reportedly affects both physical and chemical peat properties (Anshari et al. 2010; Könönen et al. 2015). Land cover change in tropical peatland and associated drainage canal development generally results in peat subsidence, which is comprised three main processes: decomposition, compaction, and consolidation was generated by which also (Hooijer et al. 2012). The surface layers of peat are also

often lost due to the wildfire that occurs frequently in drained peatlands (Page et al. 2002; Heil et al. 2006). Therefore, the age of the peat at the surface is likely older than in the undrained forested sites (Dommain et al. 2014). Hydraulic conductivity measured in the shallow depths of our non-forested sites, which was likely measured from older peat than the undrained forested sites at the same depth, were lower than at our forested site, suggesting that the deforestation led to a decrease in K_s that occurred primarily in the upper portion of peat profile. This suggests that peat swamp conversion was not only altering the peat properties at the upper part of profile (Basuki 2017) but also changing the hydraulic properties considered in this study. The peat swamp forests conversion to other land cover types that is usually accompanied by drainage canal installation will likely result in greater groundwater discharge due to the higher saturated hydraulic conductivity at the forested sites. The greater decrease in K_s at the upper level profile from forest to non-forest sites is consistent with what would be expected to occur due to the alteration of peat properties following deforestation. Deforestation of tropical peatlands for plantation and agricultural activities requires the creation of a drainage canals to lower the water table to obtain soil moisture content and aeration suitable for plant growth (Carlson et al. 2015). Previous studies reported that uppermost layers of disturbed peatlands with drainage canal development have higher bulk densities than undrained peatlands (Kool et al. 2006; Couwenberg and Hooijer 2013), which was not found in our site at the 75 cm depth. The deeper water table due to the canal ditching also could increase the microbial activity in decomposing organic matter due to the expanding of aerated zone (Hooijer et al.

2010, 2012), potentially increasing the peat degree of decomposition, reducing the proportion of macro-porosity (Quinton et al. 2008) and, in turn, lowering K_s. Therefore, we hypothesize that the decrease of K_s due to the peat swamp forests conversion is primarily due to peat decomposition, which in turn generated the loss of macro-porosity.

We also found a strong negative relationship between K_s and depth only in forested sites, in which K_s at the shallowest depth was about two orders of magnitude greater than at deeper strata. This pattern was similar to, but of different magnitude, the measurements in Ellergower Moss bogs, Scotland (Clymo 2004) and Michigan peatlands, USA (Moore et al. 2015). However, in our study K_s was constantly low and less dependent depth for the non-forested types and depth, which is consistent with several other studies in northern peatlands (Holden & Burt, 2003a; Chason & Siegel, 1986). We hypothesize the lower K_s values in the disturbed non-forest sites, and the deeper layer of peat profile for all land covers, is in part due to gas accumulation as a byproduct of decomposition process in the saturated zone (Comas et al. 2014) which inhibit the water movement within the substrates (Reynolds et al. 1992; Fry et al. 1997a; Beckwith and Baird 2001). Unfortunately, there are no studies of the spatial and vertical distribution of gas accumulation in tropical peatlands and its influence on the conductivity to support this hypothesis. The very small K_s measured in the deeper layer is plausibly explained by compression due to the loss of buoyant support following drainage, decreasing macro-porosity. This potentially occurred in our sites since we occasionally encountered transition layers where mineral and peat material were well mixed,

shown by higher ash content in that layer, so that the peat depth was relatively difficult to distinguish. This implies that the K_s was not solely determined by single environmental factor such as peat physical, chemical properties, land cover or depth but was influenced by the interaction among different variables.

Two-layer peat profiles have been reported in northern temperate or boreal peatland ecosystems for decades, with the upper layers consisting of acrotelm, a more active layer with higher hydraulic conductivity and a catotelm layer in fully saturated zone with three order of magnitude difference of K_s compared to the uppermost layer (Clymo 1984). This two layer system had been used to describe and model biogeochemical processes and hydrological regime in northern peatlands (Holden and Burt 2003b). We found that the range of K_s in forested peatland between upper and the deeper layer, which were different by about two orders of magnitude, were consistent with the two-layer system. We did not measure K_s in the surface strata (< 50 cm) since the slug test measured K_s below the water table and water table in most of the sites in the drained peatland were below 50 cm at the time we conducted the slug test. We expect that K_s in the zone very close to surface is higher than our shallowest measurements since the peat porosity was likely dominated by macro-porosity. This suggests that the acrotelm-catotelm zonation is applicable to tropical peat swamp forests.

2.5. Conclusions

We undertook a comprehensive assessment of the effect of land cover types and peat properties on hydraulic conductivity in tropical peat under several

management practices. Despite high variability of hydraulic conductivity within and among sites, we found that it was strongly affected by the land cover types. In the upper layer of forested sites, hydraulic conductivity was much higher than non-forested sites regardless the measurement depth. We did not find evidence that peat properties, including bulk density, ash content, and carbon to nitrogen ratio, were primarily related to K_s. However, the degree of decomposition determined in the field using von Post scale had relationship with hydraulic conductivity and it was more pronounced in the upper layer of forested sites.

We measured K_s only once in the late November to early December 2014, which is the peak of the rainy season in this region. At this time, the peat water tables were close to surface so that we could measure K_s at the depth of 75 cm. The variability of K_s values through time and the influence of season weather patterns (i.e., dry or rainy season) are unknown. In the northern peatlands, the variability of dry-wet periods influence the peat hydraulic properties due to the peat shrinkage and swelling (Price and Schlotzhauer 1999). Additionally, intra-annual variability of K_s has been attributed to growing and non-growing seasonal vegetation dynamics that influenced the concentration of the gas bubbles in the peat saturated zone (Kettridge et al. 2013). However, the effect of dry and wet season on the peat properties still remain unclear in tropical peatlands and need further investigation to relate them with variation K_s.

This is, to our knowledge, the first study that assessed the effect of land cover conversion on tropical peats K_s and linked it to both peat physical and chemical properties within the peat profiles. However, the large variability of hydraulic

conductivity within and among sites and inconsistent relationships with peat properties suggests that K_s should be measured directly rather than estimated with peat properties. To evaluate these relationships, we recommend that future research with a sample designs similar to ours use hierarchical models to evaluate the statistical relationship between K_s and peat characteristics and land cover.

References:

Akaike H (1973) Information theory and an extension of the maximum like- lihood principle. In: Petrov B, Csaki F (eds) Second International Symposium on Information Theory. Akademiai Kiado, Budapest, Hungary, pp 267–281.

Anshari G, Kershaw AP, Van Der Kaars S, Jacobsen G (2004) Environmental change and peatland forest dynamics in the Lake Sentarum area, West Kalimantan, Indonesia. J Quat Sci 19:637–655. doi: 10.1002/jqs.879.

Anshari GZ, Afifudin M, Nuriman M, et al (2010) Drainage and land use impacts on changes in selected peat properties and peat degradation in West Kalimantan Province, Indonesia. Biogeosciences 7:3403–3419. doi: 10.5194/bg-7-3403-2010.

Basuki I (2017) Carbon dynamics in response to land cover change in tropical peatland, Kalimantan, Indonesia. PhD thesis. Oregon State University.

Boelter DH (1969) Physical Properties of Peats as Related to Degree of Decomposition. Soil Sci Soc Am Proc 33:606–609.

Burnham K, Anderson D (2002) Model Selection and Inference: An Information-theoretic Approach, 2nd edition. Springer-Verlag, New York.

Campos CA, Hernández ME, Moreno-Casasola P, et al (2011) Soil water retention and carbon pools in tropical forested wetlands and marshes of the Gulf of Mexico. Hydrol Sci J 56:1388–1406. doi: 10.1080/02626667.2011.629786.

Couwenberg J, Dommain R, Joosten H (2009) Greenhouse gas fluxes from tropical peatlands in south-east Asia. Glob Chang Biol 16:1715–1732. doi: 10.1111/j.1365-2486.2009.02016.x.

Dray S, Legendre P, Peres-Neto PR (2006) Spatial modelling: a comprehensive framework for principal coordinate analysis of neighbour matrices (PCNM). Ecol Modell 196:483–493. doi: 10.1016/j.ecolmodel.2006.02.015.

Frolking S, Talbot J, Jones MC, et al. (2011) Peatlands in the Earth's 21 st century climate system. Environ Rev 19:371–396.

Gandois L, Cobb AR, Hei IC, et al. (2013) Impact of deforestation on solid and dissolved organic matter characteristics of tropical peat forests: Implications for carbon release. Biogeochemistry 114:183–199. doi: 10.1007/s10533-012-9799-8.

Gnatowski T, Szatyłowicz J, Brandyk T, Kechavarzi C (2010) Hydraulic properties of fen peat soils in Poland. Geoderma 154:188–195. doi: 10.1016/j.geoderma.2009.02.021.

Grover SPP, Baldock JA (2013) The link between peat hydrology and decomposition: Beyond von Post. J Hydrol 479:130–138. doi: 10.1016/j.jhydrol.2012.11.049.

Hallema DW, Périard Y, Lafond J a., et al. (2015) Characterization of Water Retention Curves for a Series of Cultivated Histosols. Vadose Zo J 14:0. doi: 10.2136/vzj2014.10.0148.

Hardjamulia A, Suwignyo P (1987) The present status of the reservoir fisheries in Indonesia. In: Silva SS De (ed) Reservoir fishery management and development in Asia. International Development Research Centre, Kathmandu, Nepal, pp 23–28.

Hergoualc'h K, Verchot L V. (2011) Stocks and fluxes of carbon associated with land use change in Southeast Asian tropical peatlands: A review. Global Biogeochem Cycles 25:doi:10.1029/2009GB003718. doi: 10.1029/2009GB003718.

Hooijer A, Page S, Jauhiainen J, et al. (2012) Subsidence and carbon loss in drained tropical peatlands. Biogeosciences 9:1053–1071. doi: 10.5194/bg-9-1053-2012.

Huijnen V, Wooster MJ, Kaiser JW, et al. (2016) Fire carbon emissions over maritime southeast Asia in 2015 largest since 1997. Sci Rep 6:26886. doi: 10.1038/srep26886.

Hurvich CM, Tsai C-L (1989) Regression and time series model selection in small samples. Biometrika 76:297–307. doi: 10.1093/biomet/76.2.297.

Jaenicke J, Wösten H, Budiman A, Siegert F (2010) Planning hydrological restoration of peatlands in Indonesia to mitigate carbon dioxide emissions. Mitig Adapt Strateg Glob Chang 15:223–239. doi: 10.1007/s11027-010-9214-5.

Jauhiainen J, Hooijer A, Page SE (2012) Carbon dioxide emissions from an Acacia plantation on peatland in Sumatra, Indonesia. Biogeosciences 9:617–630. doi:

10.5194/bg-9-617-2012.

Kellner K (2016) jagsUI: A Wrapper Around “rjags” to Streamline “JAGS” Analyses.

Kettridge N, Tilak AS, Devito KJ, et al. (2016) Moss and peat hydraulic properties are optimized to maximize peatland water use efficiency. Ecohydrology 9:1039–1051. doi: 10.1002/eco.1708.

Kool DM, Buurman P, Hoekman DH (2006) Oxidation and compaction of a collapsed peat dome in Central Kalimantan. Geoderma 137:217–225. doi: 10.1016/j.geoderma.2006.08.021.

Kuo L, Mallick B (1998) Variable Selection for Regression Models. Sankhyā Indian J Stat Ser B 60:65–81. doi: 10.2307/25053023.

Kurnianto S, Warren M, Talbot J, et al. (2014) Carbon accumulation of tropical peatlands over millennia: A modeling approach. Glob Chang Biol 1–14. doi: 10.1111/gcb.12672.

Lal R (2004) Soil Carbon Sequestration Impacts on Global Climate Change and Food Security. Science (80) 304:1623–1627. doi: 10.1126/science.1097396.

Legendre P, Borcard D, Blanchet FG, Dray S (2013) PCNM: MEM spatial eigenfunction and principal coordinate analyses.

Limpens J, Berendse F, Blodau C, et al. (2008) Peatlands and the carbon cycle: from local processes to global implications - a synthesis. Biogeosciences 5:1475–1491. doi: 10.5194/bgd-5-1379-2008.

Mccarter CPR, Price JS (2014) Ecohydrology of Sphagnum moss hummocks : mechanisms of capitula water supply and simulated effects of evaporation. 44:33–44. doi: 10.1002/eco.1313.

Miettinen J, Shi C, Liew SC (2012) Two decades of destruction in Southeast Asia’s peat swamp forests. Front Ecol Environ 10:124–128. doi: 10.1890/100236.

Miettinen J, Shi C, Liew SC (2016) Land cover distribution in the peatlands of Peninsular Malaysia, Sumatra and Borneo in 2015 with changes since 1990. Glob Ecol Conserv 6:67–78. doi: 10.1016/j.gecco.2016.02.004.

Moore PA, Morris PJ, Waddington JM (2015) Multi-decadal water table manipulation alters peatland hydraulic structure and moisture retention. Hydrol Process 29:2970–2982. doi: 10.1002/hyp.10416.

Moore S, Evans CD, Page SE, et al. (2013) Deep instability of deforested tropical peatlands revealed by fluvial organic carbon fluxes. Nature 493:660–3. doi:

10.1038/nature11818.

Murdiyarso D, Donato D, Kauffman JB, et al. (2009) Carbon storage in mangrove and peatland ecosystems: A preliminary account from plots in Indonesia. Bogor, Indonesia.

Murdiyarso D, Hergoualc'h K, Verchot L V (2010) Opportunities for reducing greenhouse gas emissions in tropical peatlands. Proc Natl Acad Sci U S A 107:19655–19660. doi: 10.1073/pnas.0911966107.

Nemati MR, Caron J, Banton O, Tardif P (2000) Determining Air Entry Value in Peat Substrates. Soil Sci Soc Am J 367–373.

Oksanen J, Blanchet FG, Friendly M, et al. (2017) vegan: Community Ecology Package. R package version 2.4-3. https://CRAN.R-project.org/package=vegan

Page SE, Rieley JO, Banks CJ (2011) Global and regional importance of the tropical peatland carbon pool. Glob Chang Biol 17:798–818. doi: 10.1111/j.1365-2486.2010.02279.x.

Page SE, Siegert F, Rieley JO, et al. (2002) The amount of carbon released from peat and forest fires in Indonesia during 1997. Nature 1999:61–65. doi: 10.1038/nature01141.1.

Page SE, Wűst R a. J, Weiss D, et al. (2004) A record of Late Pleistocene and Holocene carbon accumulation and climate change from an equatorial peat bog(Kalimantan, Indonesia): implications for past, present and future carbon dynamics. J Quat Sci 19:625–635. doi: 10.1002/jqs.884.

Peres-Neto PR, Legendre P, Dray S, Borcard D (2006) Variation Partitioning of Species Data Matrices : Estimation and Comparison of Fractions. Ecology 87:2614–2625.

Phillips VD (1998) Peatswamp ecology and sustainable development in Borneo. Biodivers Conserv 7:651–671.

Plummer M (2003) JAGS: A program for analysis of Bayesian graphical models using Gibbs sampling. In: Proceedings of the 3rd International Workshop on Distributed Statistical Computing (DSC 2003). pp 20–22.

Quinton WL, Elliot T, Price JS, et al. (2009) Measuring physical and hydraulic properties of peat from X-ray tomography. Geoderma 153:269–277. doi: 10.1016/j.geoderma.2009.08.010.

Raudenbush SW, Bryk AS (2002) Hierarchical linear models: Applications and data analysis methods, 2nd editio. Sage Publications, Thousand Oaks, CA, USA.

Rezanezhad F, Quinton WL, Price JS, et al. (2010) Influence of pore size and geometry on peat unsaturated hydraulic conductivity computed from 3D computed tomography image analysis. Hydrol Process 24:2983–2994. doi: 10.1002/hyp.7709.

Ritzema HP, Hassan AM., Moens R. (1998) A new approach to water management of tropical peatlands: a case study from Malaysia. Irrig Drain Syst 12:123–139. doi: 10.1023/A:1005976928479

Rocha Campos JR Da, Silva AC, Fernandes JSC, et al. (2011) Water retention in a peatland with organic matter in different decomposition stages. Rev Bras Ciência do Solo 35:1217–1227. doi: 10.1590/S0100-06832011000400015.

Saharjo BH, Munoz CP (2005) Controlled burning in peat lands owned by small farmers: a case study in land preparation. Wetl Ecol Manag 13:105–110. doi: 10.1007/s11273-003-5110-z.

Schwärzel K, Šimůnek J, van Genuchten MT, Wessolek G (2006) Measurement modeling of soil-water dynamics evapotranspiration of drained peatland soils. J Plant Nutr Soil Sci 169:762–774. doi: 10.1002/jpln.200621992.

Sherwood JH, Kettridge N, Thompson DK, et al. (2013) Effect of drainage and wildfire on peat hydrophysical properties. Hydrol Process 27:1866–1874. doi: 10.1002/hyp.9820.

Taufik M, Torfs PJJF, Uijlenhoet R, et al. (2017) Amplification of wildfire area burnt by hydrological drought in the humid tropics. Nat Clim Chang. doi: 10.1038/nclimate3280..

R Core Team (2017). R: A language and environment for statistical computing. R Foundation for Statistical Computing, Vienna, Austria. URL https://www.R-project.org/.

Walczak R, Rovdan E, Witkowska-Walczak B (2002) Water retention characteristics of peat and sand mixtures. Int Agrophysics 16:161–165.

Warren MW, Kauffman JB, Murdiyarso D, et al. (2012) A cost-efficient method to assess carbon stocks in tropical peat soil. Biogeosciences 9:4477–4485. doi: 10.5194/bg-9-4477-2012.

Watanabe S (2010) Asymptotic Equivalence of Bayes Cross Validation and Widely Applicable Information Criterion in Singular Learning Theory. J Mach Learn Res 11:3571–3594.

Weiss R, Alm J, Laiho R, Laine J (1998) Modeling moisture retention in peat soils. Soil Sci Soc Am J 62:305–313. doi: 10.2136/sssaj1998.03615995006200020002x

Yu Z, Loisel J, Brosseau DPDP, et al. (2010) Global peatland dynamics since the Last Glacial Maximum. Geophys Res Lett 37:L13402. doi: 10.1029/2010GL043584.

Figures

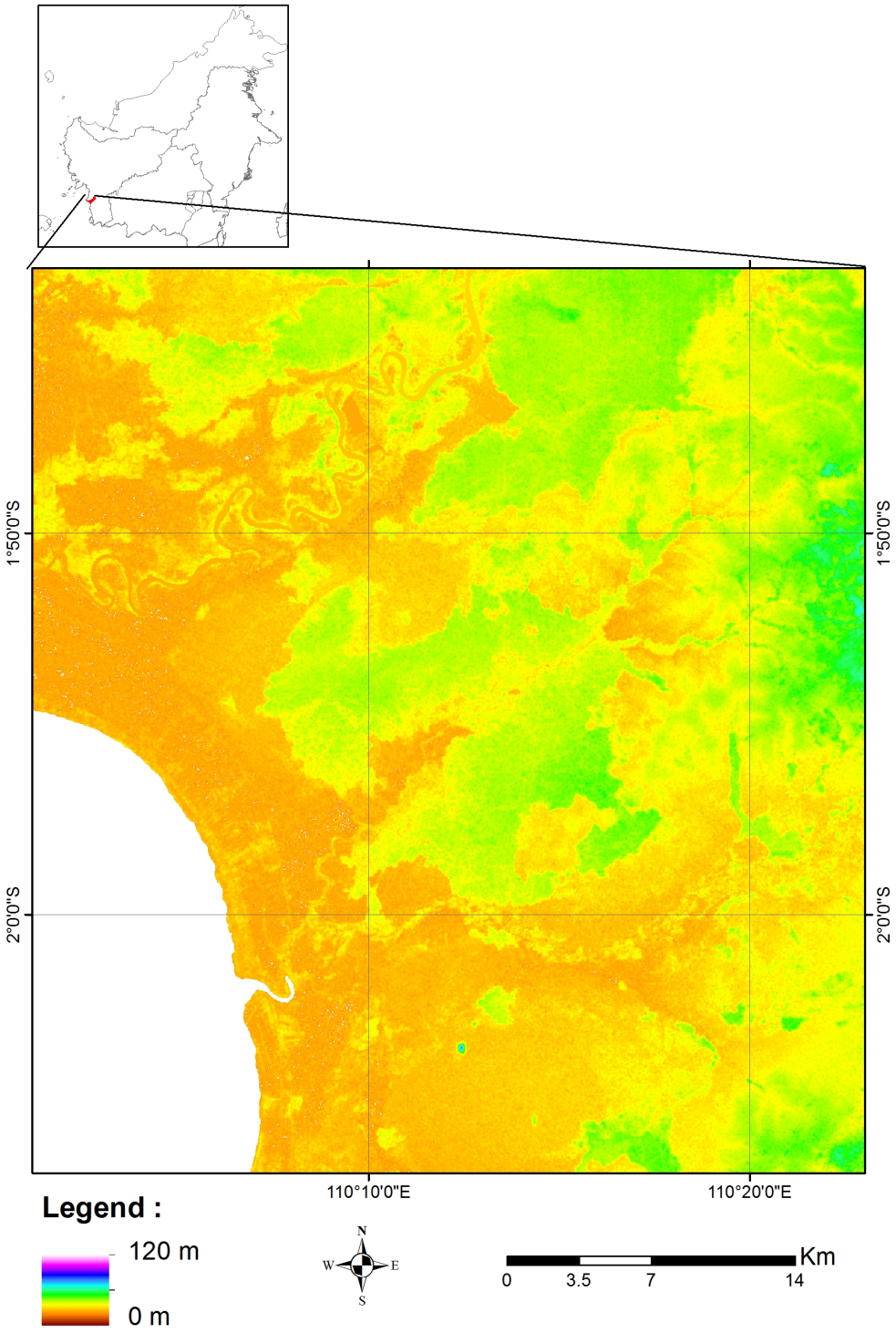

Figure 2.1. The 30-m SRTM digital elevation model of our study sites.

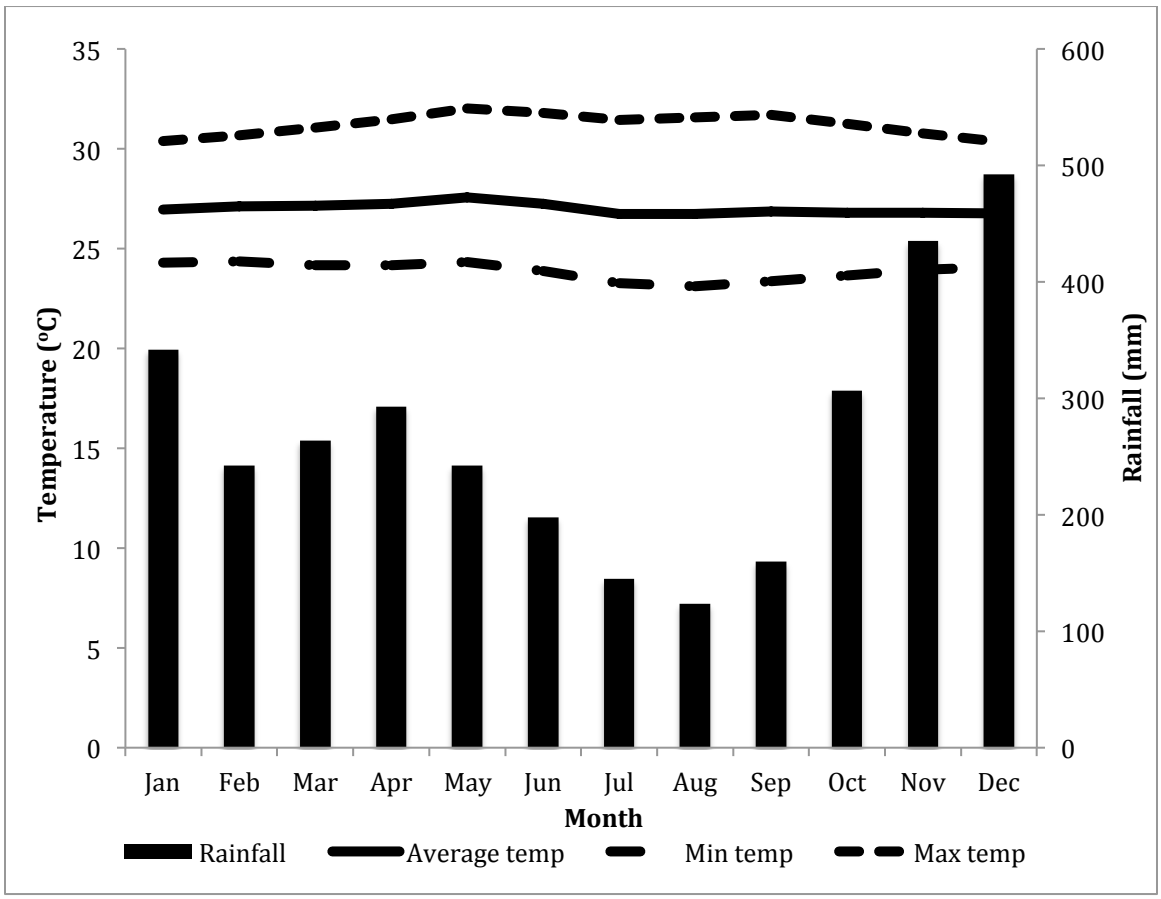

Figure 2.2. Mean monthly rainfall, minimum, maximum, and mean temperature measured at the Rahadi Oesman meteorological station, Ketapang, West Kalimantan. Recorded from 1980 to 2014.

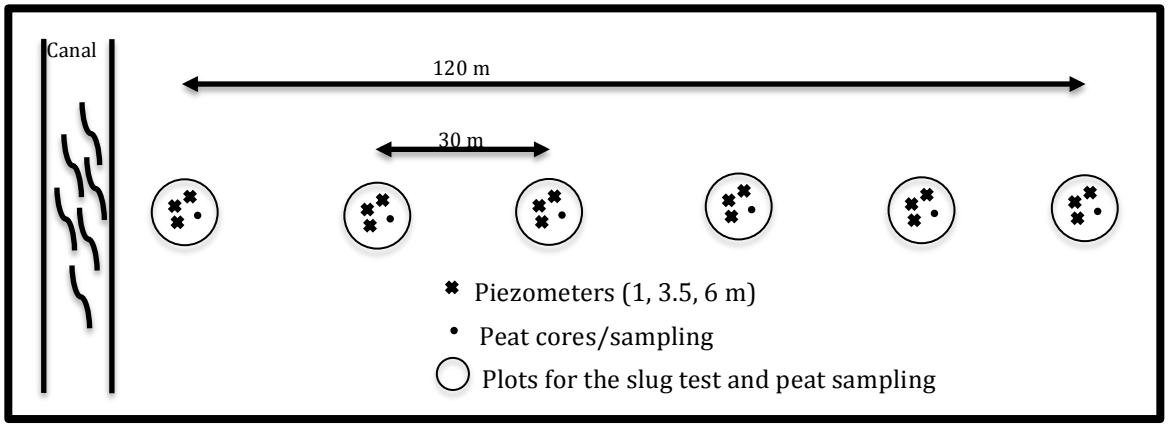

Figure 2.3. The experimental design using a transect line method implemented for each site. For oil palm plantation and seral communities, the transect line is perpendicular to canal. For undrained forests and recently burned forests, the direction of transect is random.

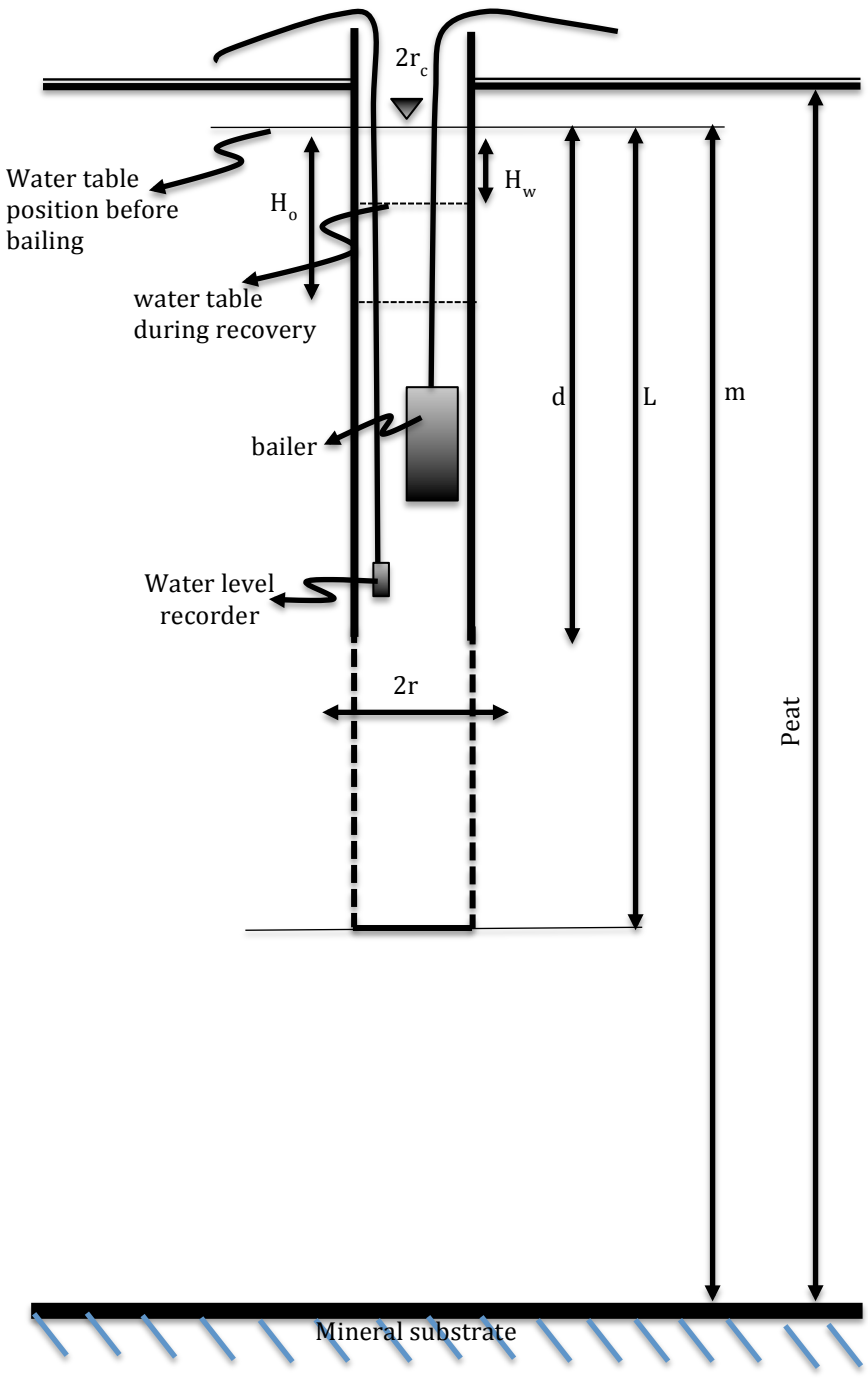

Figure 2.4. The piezometer well schematic used in the slug-test based on the Bouwer and Rice (1976) method.

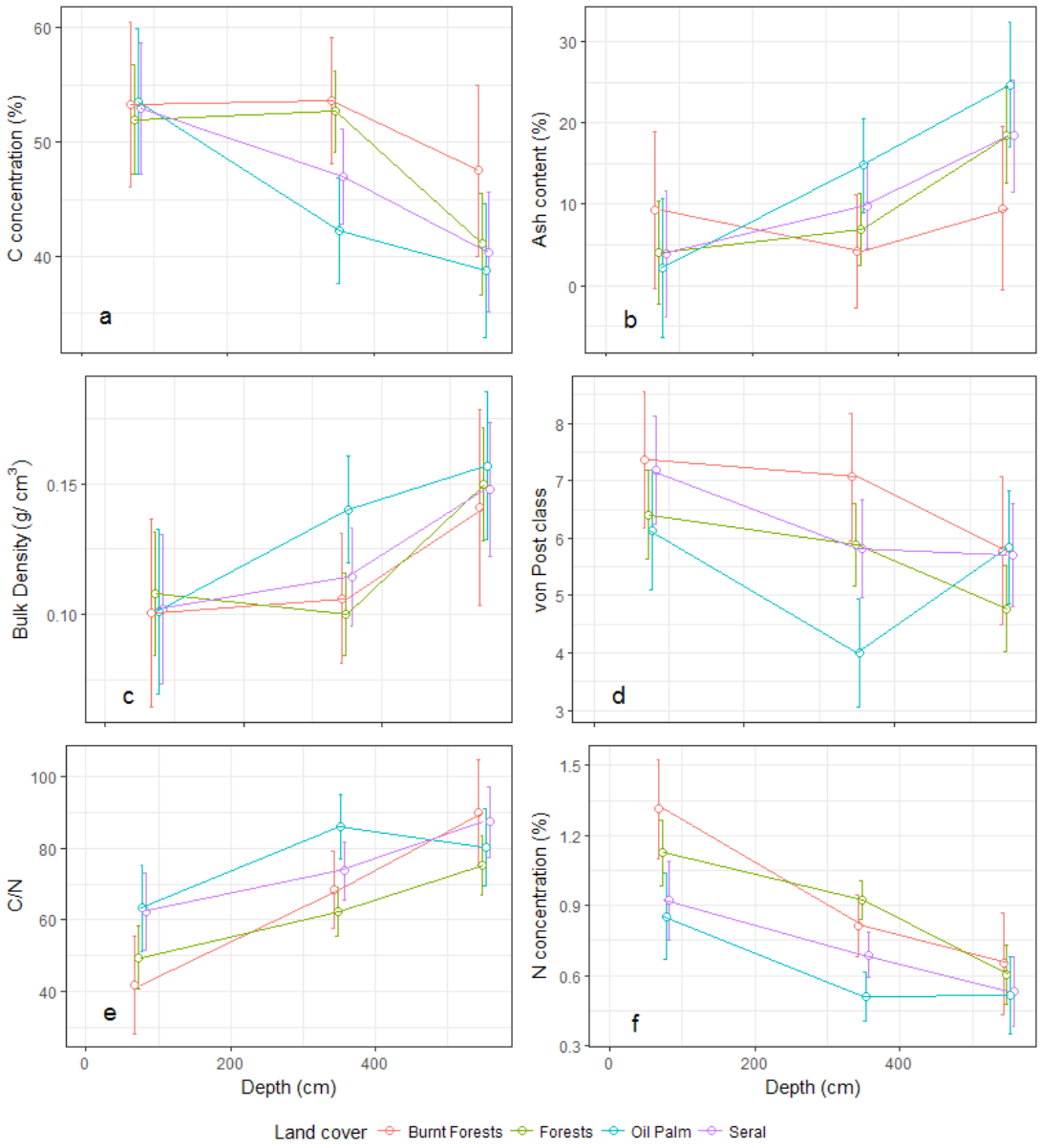

Figure 2. 5. **a**. The mean carbon (C) concentration, **b**. ash content, **c.** bulk density, **d**. degree of humification in von Post scale, **e.** carbon to nitrogen ratio, C/N, and **f**. nitrogen (N) concentration within the peat column at three different depth. Error bars represent 95% confidence intervals.

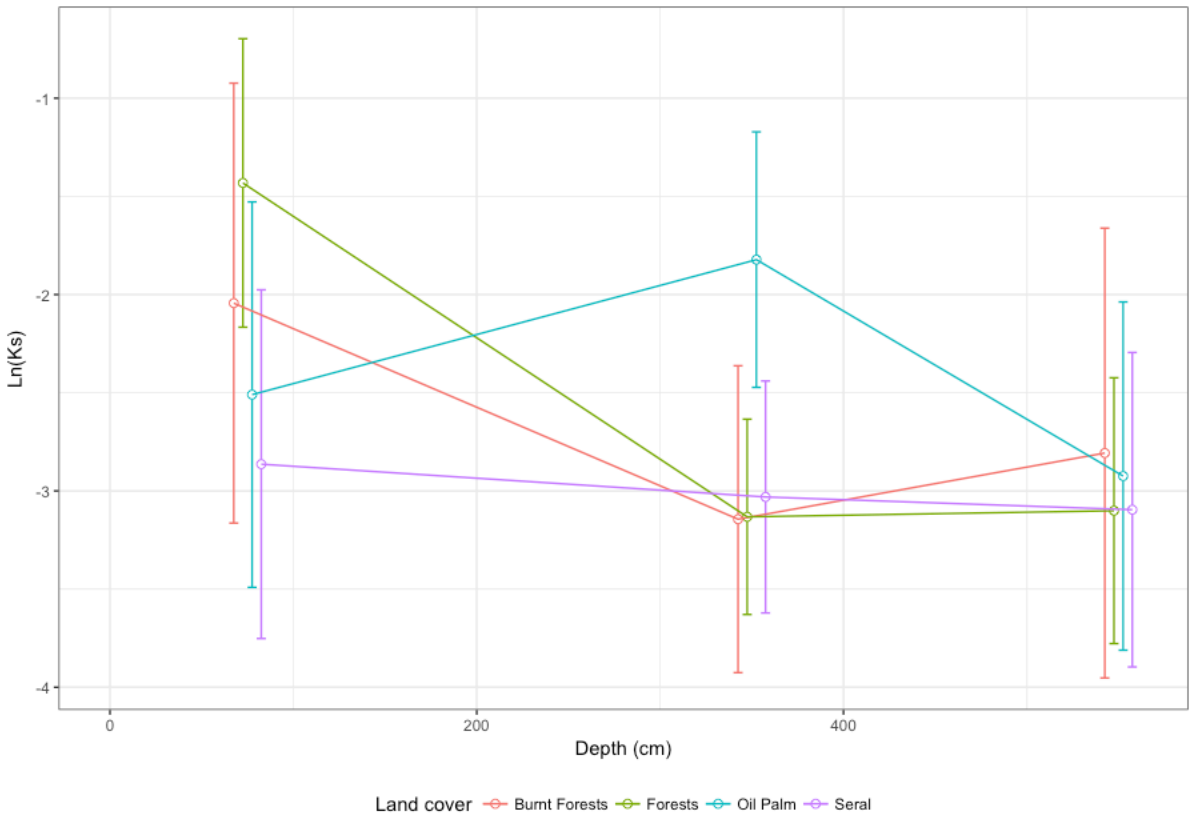

Figure 2.6. The natural log transformed of saturated hydraulic conductivity within the peat profile in four different land cover types. Error bars represent 95% confidence intervals.

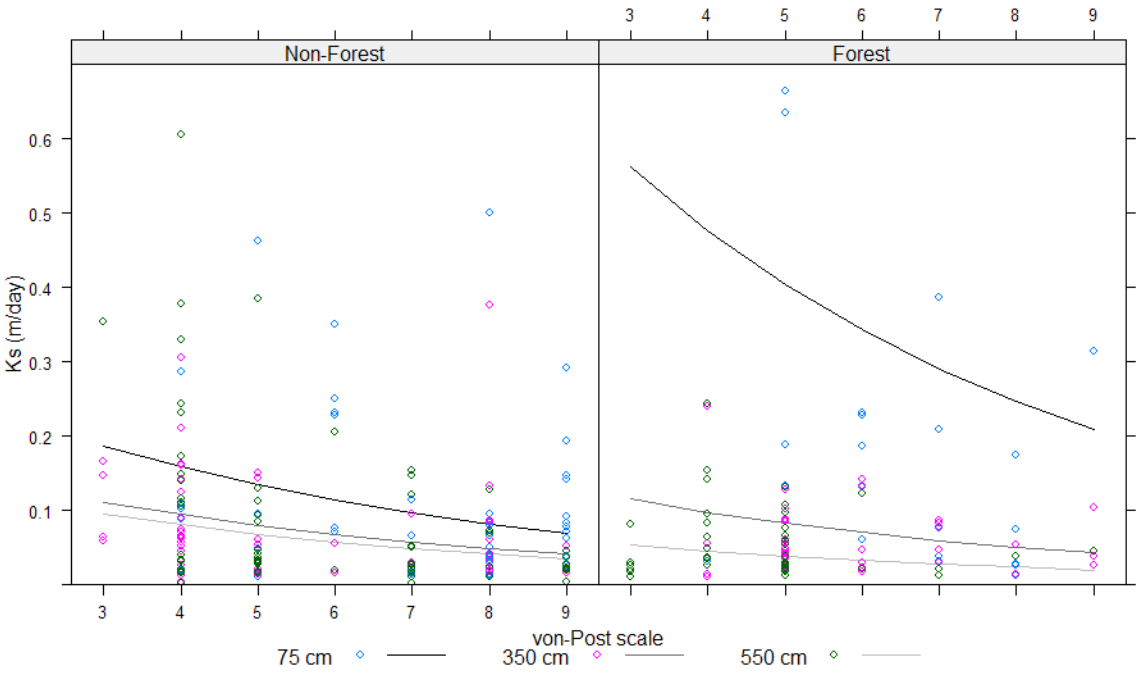

Figure 2.7. Predicted hydraulic conductivity (K_s) from 19 sites grouped by land cover types (non-forests and forests) and depths (75, 350 and 550 cm) showing the relationship between K_s and von Post degree of decomposition generated by the best approximating model.

Tables

Table 2.1. Mean (standard error in parenthesis) of carbon (*C*), bulk density (*BD*), ash content, carbon to nitrogen ratio (*C/N*), and von-Post of degree of decomposition (VP) for each site at the recently burnt forest (*BF*), undrained logged over forests (*F*), oil palm plantation (*OP*), and seral land cover (*S*) with the number of sample, *n*

	Sites	Depth	n	C(%)	BD (g cm^{-3})	Ash (%)	C/N	VP
1	BF1	75	5	57.60(0.61)	0.07(0.01)	19.22(5.43)	46.74(4.69)	8(0.58)
2	BF1	350	5	55.18(2.22)	0.09(0.01)	1.84(0.26)	78.46(10.2)	7(0.63)
3	BF1	550	4	39.65(10.56)	0.17(0.05)	15.84(6.01)	118.9(30.63)	5(0.95)
4	BF2	75	6	51.82(0.55)	0.1(0)	2.6(0.37)	39.78(1.9)	6(0.68)
5	BF2	350	5	52.10(1.91)	0.12(0.01)	7.09(2.19)	60.72(0.85)	7(0.68)
6	BF2	550	1	51.70(NA)	0.11(NA)	4.03(NA)	73.9(NA)	5(NA)
7	BF3	75	5	50.36(0.4)	0.13(0.01)	6.65(2.55)	39.24(4.33)	8(0.4)
8	BF3	350	5	53.62(0.63)	0.11(0.01)	3.69(1.78)	65.92(5.91)	8(0.51)
9	BF3	550	5	53.50(0.17)	0.12(0)	3.71(1.43)	71.14(3.59)	7(1.02)
10	F1	75	4	54.70(0.93)	0.1(0.01)	4.05(2.2)	36.83(2.49)	8(0.29)
11	F1	350	4	58.48(0.42)	0.06(0)	28.07(15.09)	71.3(8.24)	6(0.75)
12	F1	550	4	40.92(6.66)	0.13(0.02)	3.83(2.5)	79.65(7.2)	6(0.65)
13	F2	75	5	50.28(0.43)	0.1(0.01)	2.08(0.33)	38.44(2.02)	6(0.55)
14	F2	350	6	53.48(0.57)	0.1(0.01)	2.47(0.64)	60.88(2.02)	7(0.75)
15	F2	550	6	27.03(4.73)	0.24(0.03)	41.4(7.82)	78.2(5.59)	5(0.76)
16	F3	75	6	52.05(0.35)	0.1(0.01)	3.8(1.52)	45.07(2.17)	7(0.87)
17	F3	350	6	53.07(0.30)	0.09(0)	2.27(0.28)	57.25(2.25)	5(0.48)
18	F3	550	6	33.12(1.32)	0.15(0.02)	24.93(5.06)	84.48(10.88)	3(0.33)
19	F4	75	5	52.12(2.02)	0.12(0.01)	1.94(0.43)	67.96(4.7)	7(0.55)
20	F4	350	6	53.1(1.35)	0.12(0.01)	6.3(5.04)	54.65(7.11)	5(0.48)
21	F4	550	5	54.02(0.3)	0.12(0.01)	6.36(3.45)	69.96(3.56)	5(0.93)
22	F5	75	6	54.22(0.23)	0.14(0.01)	5.17(3.31)	64.75(5.09)	6(0.58)
23	F5	350	6	54.42(0.28)	0.11(0)	2.25(0.25)	71.28(2.17)	5(0.17)
24	F5	550	6	54.07(0.14)	0.12(0)	2.82(0.51)	64.73(5.92)	5(0.26)
25	F6	75	5	48.76(1.12)	0.11(0)	6.02(2.56)	42.74(5.51)	6(0.24)
26	F6	350	6	54.31(1.07)	0.11(0.01)	4.22(1.27)	60.52(6.22)	6(0.31)
27	F6	550	6	43.75(3.8)	0.15(0.03)	17.42(6.56)	65.9(6.89)	5(0.4)
28	F7	75	6	51.3(0.79)	0.09(0)	3.8(0.46)	48.37(3.96)	6(0.42)
29	F7	350	6	43.3(4.22)	0.11(0.01)	9.1(4.95)	63.33(12.42)	6(0.67)
30	F7	550	6	34.95(3.63)	0.15(0.01)	27.97(5.5)	82.75(8.34)	4(0.17)
31	OP1	75	6	54.37(1.69)	0.11(0)	2.17(1)	66.77(1.74)	8(0.56)

32	OP1	350	6	48.58(2.84)	0.12(0.01)	8.47(3.28)	82.47(6.01)	4(0.31)
33	OP1	550	6	48.98(3.9)	0.09(0.01)	8.9(4.29)	76.05(2.8)	7(0.42)
34	OP2	75	6	52.58(0.43)	0.1(0)	3.8(0.2)	60.88(1.73)	6(0.89)
35	OP2	350	6	34.95(1.75)	0.14(0.01)	27.2(2.97)	93.05(5.91)	4(0)
36	OP2	550	6	43.52(2.54)	0.14(0.01)	15.07(3.97)	67.43(3.05)	5(0.6)
37	OP3	75	3	52.27(0.98)	0.12(0.01)	3.07(0.52)	60.47(2.26)	5(0.33)
38	OP3	350	6	40.22(2.39)	0.17(0.02)	13.87(3.12)	90.4(5)	4(0.17)
39	OP3	550	6	28.73(4.6)	0.24(0.04)	39.37(7.88)	88.48(13.63)	7(0.76)
40	OP4	75	5	53.94(0.65)	0.09(0.01)	2.06(0.25)	64.42(2)	5(0.58)
41	OP4	350	6	45.13(1.13)	0.14(0.01)	9.52(1.74)	78.27(4.05)	4(0)
42	OP4	550	6	33.77(1.49)	0.16(0)	35.58(3.69)	89.08(5.86)	5(0.48)
43	S1	75	6	54(2.02)	0.09(0.01)	3.32(1.77)	65.45(3.9)	6(0.85)
44	S1	350	6	46.51(3.43)	0.15(0.01)	10.13(3.94)	90.2(5.79)	4(0.17)
45	S1	550	6	51.19(2.8)	0.14(0.04)	6(1.4)	73.37(1.8)	6(0.67)
46	S2	75	5	52.9(0.21)	0.1(0.01)	3.73(1.41)	39.8(1.98)	8(0.58)
47	S2	350	6	46.86(2.83)	0.14(0.01)	11.86(3.17)	62.15(3.97)	7(0.92)
48	S2	550	6	33.26(5)	0.2(0.03)	33.73(7.98)	77.57(9.64)	7(0.83)
49	S3	75	3	53.7(0.43)	0.13(0.01)	5.14(3.52)	75.23(7.64)	7(0.33)
50	S3	350	5	53.93(0.08)	0.1(0)	1.55(0.27)	59.4(2.74)	8(0.2)
51	S3	550	6	54.47(0.17)	0.1(0.01)	1.65(0.12)	65.62(2.15)	8(0.65)
52	S4	75	3	55.21(0.28)	0.14(0.01)	3.25(0.55)	72.77(9.27)	5(0.33)
53	S4	350	5	40.23(3.85)	0.09(0.01)	17.84(4.52)	77.78(5.04)	4(0.2)
54	S4	550	4	31.12(0.78)	0.15(0.01)	33.54(2.83)	122.22(9.03)	4(0.25)
55	S5	75	6	49.71(4.63)	0.07(0)	4.32(0.97)	64.93(8.51)	8(0)
56	S5	350	6	47.05(3.91)	0.1(0.02)	7.63(2.25)	76.63(9.75)	6(0.8)
57	S5	550	6	31.17(5.02)	0.16(0.04)	18.82(7.49)	104.28(14.63)	4(0.34)

Table 2. 2. Interpretation of predictor variables contained in the candidate models in predicting hydraulic conductivity.

Predictor variables	Hypothesis
Land cover types	Different land cover types influence conductivity
Peat properties	Physical and/or chemical peat properties such as C, C/N, ash content, and degree of decomposition influence conductivity.
Depth	The vertical position within the peat column influence the conductivity.
Peat properties × depth	The influence of the peat properties on conductivity varies within the peat column.
Land cover × depth	The influence of the vertical position within the peat column on conductivity varies among different land cover types.
Peat properties × land cover	The influence of the peat properties in determining conductivity varies with land cover types.

Table 2.3. Twenty-five model candidates with the number of parameter (*K*), log of likelihood (*logL*), Akaike information criteria with the small sample adjustment (AIC_c) and Akaike weights (w_i) for explaining the hydraulic conductivity.

Model	*K*	*logL*	*AICc*	ΔAIC_c	w_i
*Depth*Forest+VP*	8	-488.13	992.75	0.000	0.123
*Depth*VP*	7	-489.34	993.05	0.305	0.106
*Depth*Forest+VP+Ash*Forest*	10	-486.20	993.15	0.399	0.101
Forest+VP+Depth	7	-489.69	993.75	1.000	0.075
*Depth*Forest+Depth*VP*	9	-487.58	993.77	1.021	0.074
*Depth*Forest+CNratio+VP*	9	-487.61	993.84	1.091	0.071
*Depth*Forest+VP+Ash*	9	-487.98	994.58	1.828	0.049
*Depth*Forest+VP+BD*	9	-488.11	994.83	2.077	0.044
*Depth*VP+Ash*	8	-489.21	994.90	2.153	0.042
*Depth*VP+Ash*	8	-489.21	994.90	2.153	0.042
*Depth*Forest+VP+BD*Forest*	10	-487.09	994.93	2.178	0.041
*C*Forest+BD*Forest+Ash*Forest+VP*Forest+Depth*Forest*	15	-481.81	995.29	2.542	0.035
C+BD+Ash+VP+Depth	9	-488.4	995.41	2.665	0.032
*Depth*Forest+CNratio+Ash+VP*	10	-487.58	995.92	3.166	0.025
*Depth*Forest+CNratio+BD+VP*	10	-487.61	995.97	3.218	0.025
*Depth*BD+Depth*VP*	9	-488.69	996.00	3.249	0.024
*Depth*Forest+VP+BD*Forest+Ash*	11	-486.87	996.64	3.892	0.018
*Depth*Forest+VP+BD+Ash*	10	-487.98	996.72	3.967	0.017
*Depth*Ash+Depth*VP*	9	-489.17	996.94	4.194	0.015#
*C*Seral+BD*Seral+Ash*Seral+VP*Seral+Depth*Seral*	15	-482.87	997.4	4.650	0.012#
*C*OP+BD*OP+Ash*OP+VP*OP+Depth*OP*	15	-483.58	998.83	6.083	0.006#
C+BD+Ash+VP+Forest+OP+Seral+Depth	12	-486.91	998.89	6.143	0.006#
Forest+VP	6	-493.33	998.94	6.192	0.006#
*Forest*VP*	7	-493.17	1000.72	7.974	0.002#
*Forest*VP*	7	-493.17	1000.72	7.974	0.002#

Note: the notation of *A*B means A + B + A×B; *VP* is von Post degree of decomposition, *BD* is dry bulk density, *C* is carbon concentration, *C/N* is carbon to nitrogen ratio, *Ash* is ash content. *Forest* is binary indicator variables indicated by 1 for forested site and 0 otherwise. *Seral* and *OP* are also binary indicator variables for seral land cover and oil palm plantation respectively. # indicates that those models were excluded from the confidence set of models.

Table 2.4. The parameter estimates with standard error in parenthesis of the fixed effect and random effect parameters of the three best-approximating models in predicting hydraulic conductivity. Random effects are variance estimates.

Parameter estimates	estimate	90% confidence interval	
		Lower	Upper
Depth + Forest + VPt + Depth x Forest			
Fixed effect			
Intercept	-1.734(0.300)	-2.239	-1.239
Depth	-0.263(0.182)	-0.573	0.046
Forest	0.090(0.241)	-0.321	0.500
VP	-0.165(0.043)	-0.237	-0.092
Depth x Forest	-0.545(0.296)	-1.048	-0.039
Random effect			
Intercept	0.180		
Depth	0.310		
Residual	1.220		
Depth + VP + Depth x VP			
Fixed effect			
Intercept	-1.733(0.282)	-2.209	-1.265
Depth	-0.215(0.314)	-0.734	0.308
VP	-0.163(0.043)	-0.236	-0.091
Depth x VP	-0.041(0.044)	-0.114	0.032
Random effect			
Intercept	0.179		
Depth	0.390		
Residual	1.214		
Depth + Forest + VP + ash + Depth x Forest + Forest x Ash			
Fixed effect			
Intercept	-1.589(0.316)	-2.117	-1.068
Depth	-0.184(0.189)	-0.506	0.136
Forest	-0.154(0.273)	-0.616	0.306
VP	-0.163(0.043)	-0.235	-0.090
ash	-0.014(0.008)	-0.028	0.000
Depth x Forest	-0.671(0.306)	-1.192	-0.152
Forest x ash	0.023(0.012)	0.003	0.043
Random effect			
Intercept	0.184		
Depth	0.317		
Residual	1.200		

Note: *Forest* is the binary variable (*i.e.* 1 is for forested and 0 otherwise), *VP* is von Post degree of decomposition, *ash* is the ash content.

CHAPTER 3. THE IMPORTANCE OF TROPICAL PEAT SWAMP FOREST IN REGULATING WATER RELATED TO LAND COVER CHANGES: BEYOND CARBON STOCKS AND EMISSIONS

Abstract

Information on peat moisture characteristics are essential for evaluating the role of tropical peatlands in water regulation and determining the efficacy of peatland management, conservation, and restoration actions. Nonetheless, there is a lack of information about the moisture characteristics of tropical peatlands. In this study, we conducted field surveys to collect peat samples from two contrasting land covers types in West Kalimantan peatlands, Indonesia: undrained-forests and drained degraded/deforested community sites. We proposed a new integrated method to simultaneously parameterize the van Genuchten (VG) model and evaluate the relationship between the VG model parameters and peat characteristics using Markov Chain Monte Carlo (MCMC). The results indicated that bulk density strongly (negatively) related to α, however without evidence of a relationship with m shape parameter of VG model. Since to α is most closely associated with the mean grain size, this would appear to indicate a fining of the pore structure (loss of macroporosity). The proportion of macro-porosity in the drained sites with the distance < 50 m from a drainage canal was less than those the drained-seral sites > 50 m from canal and forested sites. Peat pore distribution (i.e. the proportion of macro-, meso- and micro-porosity) also was strongly related to bulk density. We estimated that the potential amount of water that can be stored by undrained peat

swamp forests was 9.5 x 10^6 L ha^{-1} m^{-1} and about 51.1 – 52.5 km^3 of freshwater stored in undrained peat swamp forests in Borneo, Sumatra, and Peninsular Malaysia. Our results suggest tropical peatland provide crucial environmental services by storing considerable water for use by tropical plants and biota and for anthropogenic uses. However, this ecosystem also prone to loss water due to the lowering water table since it mostly composed by macro-porosity.

Keywords: integrated hierarchical model, Bayesian statistic, eco-hydrology, drainage canals, water retention curve, peatlands restoration

3.1. Introduction

Peatlands play an important role in the global carbon balance by storing an estimated 400 – 600 Gt of carbon (Yu et al. 2010; Page et al. 2011) or about one-third of the global soil organic carbon (Lal 2004). Tropical peatlands cover approximately 440,000 km^2, about 10% of the global peatland area. In terms of carbon sequestration, they accumulate about 90 Gt C, of which 80% is in South East Asia (SEA; Page *et al.*, 2011). The role of tropical peatlands as a carbon sink, sequestering carbon from atmosphere, began in the Late Pleistocene, around 20,000 years ago (Anshari et al. 2004; Page et al. 2004; Kurnianto et al. 2014) with the carbon accumulation rate of 8 g C m^{-2} y^{-1} (Yu et al. 2010).

In addition to its importance in the global carbon cycle, peatlands provide another ecosystem service by moderating hydrologic extremes, such as preventing floods and drought in settlements and agriculture areas close to peatlands (Phillips 1998). Peatlands, composed of partly undecomposed organic matter likely act as giant "sponges" as the organic-rich materials absorb and store considerable water during the wet season and steadily release the water during the dry season (Campos et al. 2011). However, the amount of water that could potentially absorb and release by peatlands especially those are located tropical regions are uncertain due to the lack information of peat hydrological properties.

Despite its function in carbon cycles as well as providing many others ecological services, tropical peatlands are currently facing existential challenges, one which is

land cover change. Tropical peatlands in South East Asia are generally covered by lowland forests in their natural condition (Murdiyarso et al. 2009), but are being converted to other land cover types (i.e., industrial plantations, smallholder plantations agriculture, and settlement). Within an 8 year period (from 2007-2015), the annual peatland deforestation rate in peninsular Malaysia, Sumatra – Indonesia, and Borneo was 4.1% y^{-1} (Miettinen et al. 2016), which is slightly higher than rates between 2000 – 2010 of 3.7% y^{-1} (Miettinen et al. 2012b), indicating well over half of the peatlands were deforested since 2000 alone, with the pace accelerating. The forest conversion to oil palm plantations, industrial plantations or agricultural activities are commonly followed by development of drainage canals for lowering the water table (Ritzema et al. 1998).

Drainage canal installation as part of the peat swamp forest conversion causes significant changes to peat properties. The decreasing water table associated with canal development accelerates peat subsidence, which is the result of three main processes: oxidation, peat compaction, and consolidation leading the increase of peat bulk density (Kool et al. 2006; Hooijer et al. 2012). Drainage development also affects the biogeochemical processes in tropical peat resulting in changes to peat chemical properties such as increasing the peat pH, total nitrogen concentration, and decreasing the carbon to nitrogen ratio (Anshari et al. 2010). The amount of water retained by peat is strongly affected by peat physical properties, such as bulk density and fiber content (Boelter 1969), as well as peat chemical properties (Grover and Baldock 2013). However, the peat physical and chemical properties changes that result from peat swamp forest conversion and drainage development

and their effects on the peat hydrological characteristics, especially at landscape scales remains unclear.

The lower water table that results from drainage canal development increases the susceptibility of peat to wildfire (Saharjo and Munoz 2005). Tropical peat fires emit a large amount of carbon to the atmosphere within a range of 100 to 300 Mg C ha^{-1} for each peat fire event and depending on the burn depth (Page et al. 2002; Kurnianto et al. 2014). The most recent large scale peat burning occurred during the 2015 El-Nino year in Borneo and caused haze trans-boundary over areas in SEA countries was estimated emitting CO_2 to atmosphere in amount of 11.3 Tg CO_2 per day within the period of September to October 2015 (Huijnen et al. 2016). Taufik *et al.* (2017) reported that groundwater recharge that influences peat moisture condition is one of the important factors in determining the burnt area extent in Borneo. However, the information about the peat moisture characteristics that could be used to estimate moisture content is still scarce.

Many biogeochemical processes that occur in peatlands are also affected by the hydrological changes that result from peat forests land conversion and drainage ditching. Furukawa et al. (2005) reported that CO_2 emission from tropical peatland increased following a decrease in the water table and, conversely, CH_4 emission decrease due to shallower water table. Furthermore, the tropical peatland carbon cycle was also affected by the water table dynamic indicated by the closely relationship between water table with respiration, photosynthesis, and net ecosystem CO_2 exchange (NEE) (Hirano et al. 2012). The effect of tropical peat swamp forest conversion, drainage canal development, and fires on the GHG

emission is well studied (Murdiyarso et al. 2010; Hergoualc'h and Verchot 2011; Jauhiainen et al. 2012, Novita 2016, Basuki 2017). However to our knowledge, no studies have been conducted to evaluate the effect of land cover change on the hydraulic properties of tropical peatlands, especially the water retention characteristics of unsaturated zone; the zone in the peat profile that is highly affected by the human intervention.

Assessments of the effects of peat swamp forest conversion and drainage ditching in the tropical peatlands, particularly on moisture characteristics, remain scarce. Thus, the aims of our study were to: (1) determine the peat pore distribution and develop a peat water retention model for the undrained forested and drained-seral plant community sites in tropical peat lands; and (2) evaluate the influence of peat properties and land cover on peat moisture characteristics. We hypothesized that peat forest conversion followed by the canal development alters the peat pore distribution and the shape of the retention curve due to the changes of the peat properties.

3.2. Methods

3.2.1. Study sites

The study was conducted in tropical peatlands of Ketapang, West Kalimantan, Indonesia that can be classified as the coastal peatlands. The peat dome is situated between two main rivers: the Pawan River in the northern part and the Kepuluk River in the southern part (Figure 2.1) and has a maximum peat depth of up to 11 m.

Part of these peat swamp forests have been converted to other land cover types such, oil palm plantation, abandoned lands, and settlement areas. Drainage ditches have been installed as part of the development of plantation and agricultural land to lower the water table.

3.2.2. Field sampling

We collected peat samples from two different land cover types with contrasting hydrology: undrained forested and drained seral community sites. The seral sites was the abandoned-degraded lands that were mostly covered by ferns, shrubs, and non-woody vegetation. We randomly selected three sites in the peat swamp forests and established a 150 m long transect at each site. Within each transect, sample plots were placed at 30 m intervals for a total of six plots per transect.

A different sampling design was implemented in the drained seral community to evaluate the effect of drainage canals on the moisture characteristics. Five sampling sites were placed perpendicularly to a drainage canal that was, on average, 8-m wide and 1-m deep. There was no documentation of the purpose of the canal or the date of installation. However, based on the interview with a local villager, the canal was installed in 2008 by the public works agency of Ketapang Regency. To evaluate the effects of the canal on peat soil moisture characteristics, each sampling site was placed systematically at distances of 1, 10, 50, 100, and 200 m perpendicular from the canal. For each sampling site, three sampling plots were set up parallel to the canal with the interval of 200 m (Figure 3.1). At the time when sampling was

conducted, the canal was a single primary canal and there was no lateral canals connected to it.

At all sampling sites, we collected peat samples with two different collection methods: 1) using ring samplers for determining retention characteristics, ash, carbon, and nitrogen content, and 2) using a peat corer for estimating peat bulk density and fiber content.

The peat samples were collected at each plot using ring samplers with the dimension of 5 cm diameter and 5 cm length at the depth of 50 cm below the peat surface. This depth of measurement was chosen since it could be classified as the unsaturated zone of peat profile in which most of the peat-water exchange occurred in that layer. At each plot, we created a 40 cm deep pit and a ring sampler was then carefully pushed from the surface of pit to a depth of 10 cm to avoid sample disturbance. The ring sampler containing the peat sample was then dug out from the pit, any peat attached below the ring sampler was removed using serrated knife, and the ring sampler was sealed at the both sided using lids. For each plot, additional 142.9 cm^3 peat samples also were collected with peat corer (Eijkelkamp, Giesbeek, Netherland) located adjacent to the pit.

3.2.3. Laboratory analysis

The peat from the ring samplers were removed using the wooden cylinder with the diameter slightly smaller than the ring's diameter. Each sample was cut into five sub-samples with the thickness of about 1.5 cm for determining the gravimetric

water content at six different pressure heads: 10, 31.6, 100, 316.2, and 1,000 cm H_2O (-0.98, -3.10, -9.81, -31.0, and -98.1 kPa respectively). We placed the sub-samples on 1-bar air entry pressure plate which had been saturated for 24 hours, and then put those inside the pressure chamber extractor (Soil Moisture Equipment Corps., Santa Barbara, CA, USA) and maintained pressure for 24 hours or until water ceased coming out of pressure chamber, which meant that equilibrium moisture content at the pressure head had been achieved. The remaining samples from each ring were air-dried and sieved using 2 mm mesh to determine the water content at pressure of 1,554.2 kPa (Rocha Campos et al. 2011). After water extraction for each pressure head, we weighed and then dried the sub-samples at 70 ^{o}C for approximately 24 hours or until the dry weight of those sub-samples were constant and the gravimetric water content was calculated using the weight measured before and after drying.

The dried remaining samples from the soil moisture analysis were used to determine ash content, carbon and nitrogen concentration. Ash content of each sample was estimated using a 1 g sub-sample and burning them in a muffle furnace at 550 ^{o}C for approximately 2 h. The ash content was determined as the ratio between the weight after ashing at 550 ^{o}C and dry weight at 70 ^{o}C. The remaining portion of each sample was then ground, homogenized and analyzed to determine the carbon and nitrogen concentration using a LECO TruSpec induction furnace C analyzer.

Because it was difficult to obtain bulk density and fiber content using the same samples used to determine the moisture characteristic, we analyzed both bulk

density and fiber content using different samples that were collected by using the Russian peat auger from the same depth and close to the pit soil where the ring core samples were collected. We weighed the 10 cm length of samples prior to conducting fiber content and bulk density determination. A 25 cm^3 subsample was extracted from the sample with a graduated syringe and used to estimate fiber content. The subsample was transferred to a 100-mesh sieve and washed using tap water. The samples on the mesh were rubbed using the thumb and first finger with the flowing tap water until the color of water was clear. The samples were transferred back to a graduated syringe to determine the volume of the remaining samples. The fiber content was determined as the ratio of sample volume measured after and before rubbing (Rocha Campos et al. 2011). To estimate bulk density, the peat samples were dried in the oven at 105 ^oC for minimum 24 h or until the weight reached the constant value and it was determined as the ratio between the peat dry weight and fresh sample volume (Chambers et al. 2011). The bulk density for each sample was then used to transform the gravimetric to volumetric water content for each pressure step.

The peat pore distribution (i.e., the percentage proportion of macro-, meso-, and micro- porosity) was determined using the measured volumetric content. The pore size larger than 30 μm was classified as the macro-porosity and calculated as the difference of the total porosity and water content at the suction of 9.81 kPa (100 cm H_2O). The meso-porosity was classified with the pores between 0.2 – 30 μm and calculated as the difference of water content at 9.81 kPa and 1,554 kPa suction. The

remaining pores were classified as the micro-porosity with the dimension less than 0.2 μm (Walczak et al. 2002).

3.2.4. Statistical analysis

3.2.4.1. Hierarchical model to estimate pore distribution

Because our sampling design included sites and plots within sites, we used the hierarchical linear model to incorporate the spatial dependence for predicting the proportion of macro-, meso-, and micro-porosity using the peat physical and chemical properties. Using this method, the intercept and the coefficient of peat properties were modeled as randomly varying among sites:

$$Y_{ij} = \beta_{0j} + \beta_{1j}X_{1ij} + \ldots \beta_{Pj}X_{Pij} + r_{ij},$$

where Y_{ij} is the macro-, meso-, and micro-porosity measured in site plot *i* and site *j,* and *r* are residuals that were assumed normally distributed with mean of zero. β_{0j} and β_{1j} are the site-specific upper level (sites) intercept and slope, respectively that can be modeled as functions of site-specific characteristics:

$$\beta_{0j} = \gamma_{00} + \gamma_{01}W_{1j} + \ldots + \gamma_{0s}W_{sj} + u_{0j},$$

$$\beta_{1j} = \gamma_{10} + \gamma_{11}W_{1j} + \ldots + \gamma_{1s}W_{sj} + u_{1j},$$

where W_s is a site specific (upper level) characteristic; γ_{00} and γ_{10} are the mean intercept and mean effect (slope) of the plot-level characteristics on the response (e.g., macro-porosity), respectively; γ_{0s} is the mean effect of the site-specific characteristic on the intercept; γ_{1s} is the average effect of the plot-level attributes at the site level; and u_{0j} and u_{1j} are the random effects that that were assumed to be normally distributed with mean of zero and random effect-specific variance

(Raudenbush and Bryk 2002). Goodness-of-fit was assessed for all candidate models by examining plots of lower level residuals, normal probability plots, and plots of upper level residuals (Raudenbush and Bryk 2002).

We used the information-theoretic approach (Burnham and Anderson 2002) to evaluate the relationship of the peat pore distribution with peat properties. We initially developed a global model that contained all of the predictors variables that were pairwise uncorrelated ($r^2 < |0.49|$) and corresponded to hypothesis about the influence of the peat physical and chemical properties on the pore distribution. Prior to model selection, we determined the best variance structure (i.e., the random effects) since there were several potential sources of statistical dependence by combining random effect for the intercept and plot level explanatory variables, i.e. peat properties. We selected the best approximating variance structure with the lowest Akaike's Information Criteria (*AIC*; Akaike, 1973) with the small-sample bias adjustment (AIC_c; Hurvich & Tsai, 1989), which included both fixed and random effect. Random effects associated to water retention curve were estimates of the predictable variability of the effect of a predictor (e.g., bulk density, ash content) among sites and site random effect represented predictable variation among sites that were not accounted for by the site predictors. The best approximating variance structure was used for all candidate models during model selection procedure, described below.

Prior to model selection, we fit a random effects ANOVA to partition variation in macro-, meso- and micro-porosity within and among sites. We then fit candidate models that contained the combinations of explanatory variables to predict pore

distribution (i.e. the proportion of micro-, meso- and macro-porosity) and evaluated the relative support for each using AIC_c. The candidate model with the smallest AIC_c was considered the best approximating model to explain peat pore distribution. Then, we also calculated ΔAIC_c for each candidate model (i) and Akaike weight following Burnham and Anderson (2002) ranging from 0 to 1 with the best fitting model having the greatest weight.

3.2.4.2. Water retention model

We used the van Genuchten (1980) model to evaluate the relationship between the pressure head and water contents as:

$$\theta(h)_{ij} = \theta_{rij} + \frac{(\theta_{sij} - \theta_{rij})}{\left(1 + \left(\alpha_{ij} h_{ij}\right)^{n_{ij}}\right)^{m_{ij}}}$$

where h is pressure head (cm), θ_r is the residual water content ($cm^3\ cm^{-3}$), θ_s is the saturated water content ($cm^3\ cm^{-3}$), and α (cm^{-1}), n, and m (dimensionless) is the estimated parameters for each plot i and site j. The saturated water content θ_s was estimated using the particle density (PD) and bulk density (BD) for each plot and site as:

$$\theta_{sij} = 1 - \frac{BD_{ij}}{PD_{ij}},$$

with particle density was estimated as:

$$PD_{ij} = \frac{1 + F_{ij}}{F_{ij}/_{1.55} + 1/_{2.65}},$$

where F is the ratio between organic content and ash content and assuming that particle density of organic and mineral matter were 1.55 and 2.65 g cm^{-3},

respectively. The values of parameters α and m are restricted to a range of zero to one (van Genuchten, 1980) and n was calculated from m as:

$$n_{ij} = \frac{1}{1-m_{ij}},$$

where it is evident from construction that $n > 1$.

Previous studies of peat water retention properties estimated the van Genuchten parameters using optimization algorithms such as conjugate gradient, Nelder and Mead Simplex algorithm, and simulated annealing (Hallema et al. 2015). The calibrated van Genuchten parameters were then used to evaluate their relationship with peat properties using linear regression (Weiss et al. 1998). Here, we proposed a new integrated method to simultaneously parameterize the van Genuchten model and evaluate the relationship between the model parameters and peat characteristics using Markov Chain Monte Carlo (MCMC) method implemented with JAGS software v.4.2.0 (Plummer 2003) and R statistical software (R Core Team, 2016) with package *jagsUI* (Kellner 2016). With this method, the parameterization of van Genuchten model utilized all of the observed water content values for all plots and pressure head steps (i.e., 33 plots x 6 pressure head steps for 198 total) and allowed us to estimate the variability among plots and evaluate the relations with peat properties. We assumed that the residual variation between observed and modeled water content θ was normally distributed with a mean of zero and standard deviation that was equivalent to the standard error of a linear regression. Each candidate model was fit using three independent chains consisting of 100,000 iterations, 50,000 adaptation iterations, and diffuse priors. The model convergence

was determined with two approaches: visual inspection of trace plots of the parameters and by calculating the Brooks and Gelman diagnostic statistic ($\hat{R}$) for all parameters. Convergence was assumed when trace plots indicated good mixing and $\hat{R}$ values were all less than 1.03 (Kuo and Mallick 1998).

To evaluate the relationship between peat properties and water retention curve, we modeled both α and m as logit linear functions of the measured peat properties, such as bulk density, ash content, fiber content, carbon, nitrogen, and carbon to nitrogen ratio (C/N), using hierarchical linear models:

$$Logit\ (Y_{ij}) = \beta_{0j} + \beta_1 X_{1ij} + \beta_2 X_{2ij} + \ldots\ldots \beta_p X_{pij} + r_{ij}$$

where Y is α and m shape parameters, $X_1, X_2 \ldots X_p$ is the plot level explanatory variables (e.g., bulk density, ash content) measured in plot i and site j and, b_{0j} is an intercept that varies normally among plots with mean of zero and variance. Several candidate models were developed to explain the variation in α and m among sites using various combinations of the peat properties (Table 3.1). Previous studies assumed that θ_r was equal to zero (Sherwood et al. 2013). Here, we assumed θ_r was constant at a site, but varied among sites assuming a logit-normal distribution. That is, we used the above hierarchical linear but only included a randomly varying intercept, b_{0j}.

Prior to model fitting, we calculated the Pearson correlation coefficient among the potential predictor variables and excluded the pair of high correlated predictor variables ($r^2 > 0.55$). We also created the binary indicator variables (i.e., 0 and 1) where drained shrubs sites were coded as 1 and undrained forested sites were 0.

We implemented an information theoretic approach (Burnham and Anderson 2002) to evaluate the plausibility of each candidate model that related peat physical and chemical properties with the water retention curve parameters. To determine the fit of each candidate model, we calculated Watanabe-Akaike Information Criterion (Watanabe 2010). The best approximating model for estimating water retention curve was the model with the lowest *WAIC* is considered the best plausible model. We also calculated the *WAIC* weight for each model to ease the interpretation of the relative support for these model candidates. The weights ranged from 0 to 1 with the best-fitted model was having the highest weight (Burnham and Anderson 2002).

3.2.4.3. Multivariate analysis

To assess the effect of spatial component of variation of the moisture characteristics and pore distribution, we used the principal coordinates of neighbor matrices to quantifying the spatial pattern (PCNM; Borcard & Legendre, 2002). PCNM is a distance-based eigenvector analysis that estimates linearly independent spatial variables at multiple scales ranging from broad to finer scales. Eigenvectors with high absolute value of eigenvalues represent high spatial auto-correlation (Dray et al. 2006). We used the coordinate of each plot that had been already converted to Universal Transverse Mercator (UTM) zone 49 S as the spatial data input. We only selected the positive auto-correlation shown by positive Morran's *I* values higher than expected Morran's value (Borcard et al. 2011). The PCNM analysis was conducted by using PCNM package run in R statistical software (Legendre et al. 2013), which calculates Morran's *I* value automatically.

We performed the variation portioning based on redundancy analysis to determine the amount of variation of the van Genuchten parameters representing the moisture characteristic and the proportion of pore distribution that could be explained exclusively by peat properties, land cover, and spatial components (Borcard et al. 1992; Peres-Neto et al. 2006). We used the adjusted R^2 to evaluate the amount of variation of response variables that could be explained since the unadjusted R^2 values are biased (Peres-Neto et al. 2006). To implement variation portioning, we used the function *varpart* in *vegan* package in the R statistical software (Oksanen et al. 2017).

To simultaneously evaluate the relationships between peat moisture characteristic (*i.e. m, n,* α*,* θ_s*,* θ_r, macro-, meso-, and micro-porosity) with the other peat properties (i.e., bulk density, particle density, fiber content, carbon, nitrogen, and carbon to nitrogen ratio) and display them visually, we used the partial redundancy analysis (pRDA) by excluding the spatial autocorrelation components (i.e. PCNM eigenvectors). Redundancy analysis is an ordination technique that extracts the main pattern of variation among objects (e.g., peat moisture characteristic) and among attributes (e.g., peat properties). The relationships among objects and among attributes are displayed in two-dimensional planes with a point for each object and attribute, respectively (Borcard et al. 1992). Peat moisture metrics with similar characteristics are located closer together in the object two-dimensional plane, while the attributes responsible for relationships among the objects are located in a similar position. Prior doing the redundancy analysis, we standardized each of the environment variable to a mean zero and standard

deviation of one due to the different scale among those variables. pRDA was performed by using R statistical software with the installed *vegan* package (Oksanen et al. 2017).

3.3. Results

3.3.1. Pore distribution

The moisture retention analysis indicated that a majority of the peat pores were occupied by the macro- and meso-porosity. In forested sites, the proportion of macro-porosity was 45±3%, greater than those of meso-porosity (37±8%) and micro-porosity (12±2%; Table 3.1).The proportion of macro-porosity in the drained sites < 50 m away from canal was less than those the drained-seral sites > 50 m from canal and forested sites. A random effects ANOVA indicated that variability of macro-, meso- and micro-porosity at 50 cm depth was greater within sites than among sites with within- site variation estimated to be 18.6%, 17.1%, and 4.1% among sites, respectively.

Using the global model for predicting the macro-porosity, all of the uncorrelated variables were included as covariates, we found that the variance structure of the best approximating global model contained the ash coefficient that varied among sites and the model intercept was constant for all sites. Based on the selected variance structure, we found that the best approximating model for predicting the proportion of macro-porosity contained bulk density and ash content without interaction between both variables (Table 3.2). The Akaike importance weight (w_i) indicates that this model was about 3 times more likely than the second best

approximating model in which these models contained bulk density and ash content as well as the interaction of both covariates. The best approximating model can explain the proportion of macro-porosity variability of about 62% by fixed effect only (bulk density and ash content) and 77% by both fixed and random effect indicating that hierarchical model can explain more the variability of macro-porosity than ordinary linear model.

Parameter estimates for the top-two best approximating models shows that the proportion of macro-porosity was negatively related with bulk density (Table 3.3). The model coefficient also indicates that the relationship was strong and precise as depicted by confidence intervals that did not include zero. The estimated macro-porosity proportion decreased with an increase of bulk density and lower macro-porosity was estimated for the drained-seral sites compare to forested sites (Figure 3.2). The ash content was a parameter included in the best approximating model. However, the relationship between the proportions of macro-porosity and ash content was weak and imprecise shown by small coefficient and confidence interval spanned zero. The ash random effect from the best approximating model to predict the proportion of macro-porosity indicated that the relationship between proportion of macro-porosity and ash content varied about 126% (0.044/0.034) among sites.

Similar to macro-porosity model, the variance structure for predicting meso-porosity proportion indicated that ash coefficient varied among sites with the model intercept set to constant. The model selection indicates that a model contained bulk density and ash content was considered as the best approximating model for

predicting meso-porosity proportion (Table 3.2). This model was about three times more likely than the second best approximating model that contained bulk density, ash content, and their interaction. The variability of meso-porosity proportion that could be explained by the best approximating model was about 75% by both fixed and random effects. The Akaike weights indicated only two candidate models comprised in the confidence model set.

The confidence model set depicted that meso-porosity proportion was positively related to bulk density but its effect size was weaker than macro-porosity (Table 3.3). The estimates of bulk density coefficient indicated that the relationship between bulk density and meso-porosity proportion was relatively precise as shown by confidence interval that did not contain zero. In the seral sites within 50 m from the ditch, the estimated meso-porosity proportion was greater than those in the forested sites for similar values of bulk density (Figure 3.2). For example, a bulk density between 0.08 to 0.09 g cm^{-3}, the meso-porosity proportion in forested site was 40-50% and in drained site < 50 m from canal was about 50 – 60%. In addition, the meso-porosity proportion in the seral sites > 50 m from the canal was similar to the forested site assuming similar values for bulk density. The best approximating model indicated that ash content was negatively related with meso-porosity proportion. However, the effect of ash content was very small and imprecise shown by confidence interval that spanned zero and greatly varied among sites.

The best approximating random effects structure for predicting micro-porosity proportion included a bulk density coefficient that varied among sites and the model intercept was constant. The best approximating model contained not only bulk

density, similar to macro-, meso-porosity model, but also included carbon to nitrogen ratio and their interaction (Table 3.1). This model was similar to the next best approximating model containing the same covariates but without interaction. The fixed and random component of the best approximating model explained approximately 61% of the variability of micro-porosity proportion.

Micro-porosity was positively related with the bulk density. The confidence interval of bulk density coefficient also was relatively precise and the confidence limit did not include zero (Table 3.2). However, the relationship between micro-porosity proportion and carbon to nitrogen ratio was small and imprecise as indicated by the confidence interval that spanned zero. The relationship between micro-porosity proportion and bulk density was similar among sites as indicated by small the random effect estimate for bulk density (the standard deviation of bulk density coefficient was close to zero).

3.3.2. Peat moisture model

The best approximating model from 14 candidate models to estimate peat water content from varying pressure head using the van Genuchten model indicated that the α shape parameter was related to peat bulk density and the m shape parameter was a function of ash content (Table 3.3). This model was slightly more supported, based on WAIC, than the second-best approximating model in which only α was related to peat properties, *i.e.* bulk density and m only varied among plots. Furthermore, the best approximating model was also about 37 times more likely to

be the best model of peat water content than a model containing α and m shape parameter that varied among plots but were not related to any peat properties.

Based on the best approximating model, the mean α across all sites was 0.366 cm^{-1} (95% confidence interval CI: 0.24 – 0.548 cm^{-1}). On average, α shape parameter varied 9.5% among plots (0.82/8.659; Table 3.4). The bulk density was negatively related to α and the estimate was precise as depicted by 95% confidence interval did not include zero. After accounting for the effects of bulk density, forested sites generally had greater shape parameter α than those in the drained-seral sites within 10 m distance from the canal (Figure 3.3). The best approximating model also indicated that m increased with ash content (Figure 3.4). However, the estimates were imprecise with wide 95% confidence interval and spanned zero. The overall mean of shape parameter m also varied of 4% among plots.

3.3.3. Peat properties, land cover and spatial effects

The variation portioning indicated that the combination of peat properties, land cover, spatial components explained about 83% variability of the multiple response variables (i.e., macro,-meso, and micro-porosity proportion, n, m, α, θ_r, θ_s). By excluding the land cover and spatial components, the peat properties explained about 57.5% of the moisture characteristic and pore distribution variability. Only 3.7% of the variability could be explained by land cover types exclusively (Figure 3.5).

After partialing out the spatial component of variation, the first axis of redundancy analysis (*RDA1*) explained the most variation of the peat moisture

characteristic, i.e. 98.2% and it was highly related with the shape parameter α, macro-and meso-porosity (Figure 3.6). Only 1.6% of the moisture characteristic variability that could be explained by the second axis of redundancy analysis (RDA2). Other moisture characteristic such as m, n, θ_r, θ_s, and micro-porosity had weak relationship with both *RDA1* and *RDA2*. The biplot indicates that bulk density was negatively related with macro-porosity and α and were positively related with meso-porosity (Figure 3.6). Sites situated less than 50 m from the ditch were mostly positioned in the left space of the RDA1 meaning that those sites had greater meso-porosity, lower α and macro-porosity due to the higher bulk density (Figure 3.6).

Based on the position of each site over the two-dimensional RDA space, we placed our sites into three groups: close (1 and 10 m perpendicular to ditch), far (50, 100, and 200 m perpendicular to ditch), and undrained forested sites (Figure 3.7). The grouping indicated that the saturated water content in the sites close to canal was 0.93 ± 0.004 cm^3 cm^{-3} and significantly lower than sites far from canal (DF = 33; p-value = 0.0404) and undrained forested sites (DF = 33; p-value = 0.0092). Similarly, α shape parameter in the sites close to canal was significantly lower than the sites far from canal (DF = 33; p-value = 0.008) and forested sites (DF = 33; p-value = 0.001).

For these groupings, we also calculated the mean values of the van Genuchten parameters using group predictor variables and used those values to calculate the estimated water content (Figure 3.8). Plots of predicted water retention for each group indicated that the peat from sites close to the ditch retained more water than those sites far from the canal and forested land cover and under the same pressure

head (Figure 3.8). For the pressure head under 100 cm, the decreasing of the retained moisture with an increase of pressure head in sites close to the ditch was lower than those from forested sites.

3.4. Discussion

3.4.1. The effect of forest conversion on saturated water content

Saturated water content is one of the most important hydrologic characteristics since it represents the maximum of total water that can be stored by peatlands. Saturated water content estimates in our study were relatively similar to those estimated from the temperate boreal peatlands (e.g. Boelter, 1969; Gnatowski *et al.*, 2010; Grover & Baldock, 2013; Moore *et al.*, 2015). Very high saturated water content in our sites was likely due to the very high organic content as depicted by high carbon concentration, low ash content and bulk density of the peat samples. If we assume that whole pores of the peat from forested sites can be occupied by water, the potential total volume of water per unit volume of the peat was about 0.95 m^3 m^{-3} or equivalent to 9.5 x 10^6 L ha^{-1} m^{-1}. Page *et al.*, (2011) reported that the best estimate of the average peat depth in Indonesia, Malaysia and Brunei is 5.5 m, although we found up to 12 m peat depth in our study sites, which was similar with the deepest peat measured by Warren *et al.*, (2012) and Basuki (2017). Using this (5.5 m) mean peat depth and the area of pristine peat swamp forests in 2015 (Miettinen et al. 2016), we estimated that the peat swamp forests in Sumatera,

Borneo, and Peninsular Malaysia stored about 51.1 – 52.5 km^3 of freshwater. To put this value into perspective, the volume of Jatiluhur, one of major reservoirs in Indonesia is about 83 km^2 in surface area with a volume of 2.97 km^3 (Hardjamulia and Suwignyo 1987). This suggests that peat swamp forests provide a crucial environmental service through storing water equivalent to about 17 times of water stored in Jatiluhur reservoir.

The amount of the water storage capacity loss caused by the peat swamp forest conversion due to the increasing of bulk density are not well quantified. Our results suggest that the reduction of macro-porosity due to increased bulk density likely results in substantial water loss from the peat swamp forests. We quantified the approximate water loss due to the conversion of forest to industrial plantation using our estimates and assuming the mean peat depth of Indonesian, Malaysia, and Brunei (Page et al. 2011), the area of pristine peat swamp forests in 1990 (Miettinen et al. 2012b), and the area of industrial (i.e. oil palm and pulp) plantation in 2015 (Miettinen et al. 2016). Using this approach, the estimates of the water loss due to the peat swamp forest conversion to drained peatlands, i.e. oil palm and pulp plantation was approximately 257.9 to 265 km^3 of water (Table 3.5). This is similar with the water loss rate of 10.3 – 10.6 $km^3\,y^{-1}$ due to 25 years of deforestation (1990 – 2015). In other words, the amount of water exported from the basin annually due to the peat swamp forests conversion was about three times of water stored in Jatiluhur reservoir. This suggests that pristine peat swamp forest could also deliver another ecosystem services by storing water and preventing floods.

Part of this fluvial carbon storage is likely lost due to the conversion of the peat swamp forests to industrial plantations. Again, using estimates of the water loss rate and the DOC concentration from pore water, the exported DOC in Sumatera, Borneo and Peninsular Malaysia associated with the forest conversion is about 0.74 to 0.82 Tg y^{-1}, which is smaller than the estimated total DOC and POC increase by 2.1 Tg y^{-1} reported by Moore *et al.* (2013). This suggests that the peat forest store substantial amounts of carbon in the fluvial form and potentially release it not only to atmosphere as greenhouse gas emission, but also as fluvial organic matter due to the peat forests conversion.

3.4.2. The effect of land cover change on moisture characteristic

Land cover change in tropical peatland, especially the conversion of peat swamp forest to other land cover types such as oil palm and other industrial plantation, has been occurring for decades in South East Asia (Miettinen and Liew 2010; Miettinen et al. 2016). The peat swamp forest conversion, which is usually accompanied by drainage canal development, causes peat subsidence and reportedly affect both physical and chemical peat properties (Anshari et al. 2010; Könönen et al. 2015). One of component of peat subsidence is decomposition (Hooijer et al. 2012) in which the organic matter digested by microbial activities in the large organic fragments and converts them to smaller particles and, thus, reduces the proportion of large pores relative to smaller ones (Quinton et al. 2009; Rezanezhad et al. 2010). We found that the macro-porosity proportion in the drained peatlands with < 50 m from canal was 21% and lower than those from undrained forested peatlands.

Conversely, the meso-and micro-porosity in the drained peatlands were greater than those from undrained peatlands. This suggested that the increasing bulk density in the drained peatlands was related to the changes in the peat pore distribution, i.e., decreasing macro-porosity and transformed to meso- and micro-porosity. However, our results indicated that peatland areas most affected by drainage development were located within only 50 m from canal as shown by the profound differences in moisture characteristics of these sites relative to undrained peat swamp forests. This was likely due to the fact that our study sites were covered by shrubs and herbaceous plants with no intense soil tillage and the presence of only a single primary canal. That is, there were no secondary and tertiary canals when we were conducting the field sampling. During the conversion of peat swamp forests to industrial plantations, massive drainage canal networks consisting of primary, secondary and tertiary canals are developed with a spacing between the tertiary canal are less than 500 m (e.g. Jaenicke *et al.*, 2010). Thus, industrial plantations developed in peatlands likely have a moisture characteristic similar to our highly-affected canal sites.

The pressure head threshold in which the water began to drain is graphically located at the inflection point of the water retention curve (Nemati et al. 2000). It was quantified by α shape parameter and was closely related with peat properties. In our study sites, α shape parameters varied between 0.014 to 0.914 cm^{-1}, which is greater than those measured from the fen peat in Poland that ranged from 0.004 – 0.166 cm^{-1} (Gnatowski et al. 2010) but fell within the range of estimated α from Michigan, USA peatlands (Moore et al. 2015). In addition, the best approximating

model for predicting water content as a function of pressure head indicated that α shape parameter was strongly and negatively related to bulk density. This result was similar to that reported for peat samples from the Finnish peatlands (Weiss et al. 1998). The upper layer peat (~50 cm below the surface) of the forested peatlands in our study sites also tended to have lower bulk density (0.085 ± 0.003 g cm^{-1}) than the drained seral community at the same layer. This relationship was also reported by a variety of studies from different locations in tropical peatlands (e.g. Kool *et al.*, 2006; Anshari *et al.*, 2010; Hooijer *et al.*, 2012). These observations suggest that maintaining the high water table in the peatlands is very crucial for avoiding the loss of water content from peat. When pristine peatlands are converted to other land cover types followed by drainage canal development, the water table drops and increases the pressure head (more negative pressure) at the peat surface. Water in peat from undrained-forested sites was more readily released from the peat matrix compared to drained areas. Therefore, the large amount of water is likely to be drained from the peat and the fluvial carbon exported from the system.

3.5. Conclusions

To our knowledge, this is the first study that assessed the importance of peat swamp forest in regulating water by determining the peat moisture characteristics. We found that intact peat swamp forest provide a valuable ecological service by storing substantial amounts of water and releasing it slowly when the water table drops. By converting the undrained peatlands to drained peatlands, the amount of water are likely to be lost from that ecosystem. We estimated that the potential

amount of water that can be stored by undrained peat swamp forests in Borneo, Sumatra, and Peninsular Malaysia was about 51.1 – 52.5 km^3 of freshwater stored and the water loss rate of 10.3 – 10.6 $km^3 y^{-1}$ due to 25 years of deforestation (1990 – 2015).

The modeled water retention curve indicated that about 20% of the water drains from undrained forest when the water table drops from surface level to 10 cm below the surface, but only 5% of water drains from the highly-affected-canal sites. This suggests that the undrained peat swamp forests release water relatively easily when the water table drops since it is mostly composed of macro-pores. Therefore, the conservation efforts should be considered to maintain the high water table to keep the peat wet and thus reduce the CO_2 emission and wildfire vulnerability.

Our estimates of moisture retention characteristics can be used as input to hydrological models to obtain more detailed understanding on how land cover change affects the hydrologic dynamics of peatlands. For example, HYDRUS numerical modeling has been applied to study the eco-hydrological function of peatlands in temperate-boreal peatlands (Schwärzel et al. 2006; Mccarter and Price 2014; Kettridge et al. 2016). By simulating the water moisture dynamics in tropical peatlands, some importance insights can be determined. These insights include: (1) more accurate estimates of peatland area prone to fire since the peat subsurface hydrological condition is closely related with peatlands drought condition (Taufik et al. 2017a); (2) the ability to identify and prioritize disturbed peatlands for restoration and the kinds of restoration actions that may be more effective; and (3) the evaluation of alternative designs for channel networks that minimizing the

negative impact of the plantations (e.g. fire risks, greenhouse gas emission), while maintaining or maximizing the harvest productivity.

Peat physical properties had an important role in determining the pore-peat water exchange. The statistical models relating peat characteristics to the van Genuchten model parameters and hierarchical modeling for predicting the peat pores distribution indicated that bulk density has several roles in determining: (1) the maximum water that can be hold by peat, (2) the threshold pressure head at which the peat matrices release water due to the lowering water table from the saturated condition; and (3) the pore distribution size (i.e., macro-, meso, and micro-porosity). Utilizing multivariate analysis, bulk density also explained approximately 60% the variability in peat water characteristics after excluding the effect of spatial and land cover variability. This was much greater than that amount of variability that could be explained by land cover only and spatial variability only. This suggests that the quick and low-cost preliminary appraisal to determine the peat-water exchange under the different land cover types in tropical peatlands can be implemented by determining the peat bulk density.

References:

Akaike H (1973) Information theory and an extension of the maximum like- lihood principle. In: Petrov B, Csaki F (eds) Second International Symposium on Information Theory. Akademiai Kiado, Budapest, Hungary, pp 267–281.

Anshari G, Kershaw AP, Van Der Kaars S, Jacobsen G (2004) Environmental change and peatland forest dynamics in the Lake Sentarum area, West Kalimantan, Indonesia. J Quat Sci 19:637–655. doi: 10.1002/jqs.879.

Anshari GZ, Afifudin M, Nuriman M, et al (2010) Drainage and land use impacts on changes in selected peat properties and peat degradation in West Kalimantan Province, Indonesia. Biogeosciences 7:3403–3419. doi: 10.5194/bg-7-3403-2010.

Basuki I (2017) Carbon dynamics in response to land cover change in tropical peatland, Kalimantan, Indonesia. Oregon State University

Boelter DH (1969) Physical Properties of Peats as Related to Degree of Decomposition. Soil Sci Soc Am Proc 33:606–609.

Borcard D, Gillet F, Legendre P (2011) Numerical Ecology with R. Springer.

Borcard D, Legendre P (2002) All-scale spatial analysis of ecological data by means of principal coordinates of neighbour matrices. Ecol Modell 153:51–68. doi: 10.1016/S0304-3800(01)00501-4.

Borcard D, Legendre P, Drapeau P (1992) Partialling out the spatial component of ecological variation. Ecology 73:1045–1055.

Burnham K, Anderson D (2002) Model Selection and Inference: An Information-theoretic Approach, 2nd edition. Springer-Verlag, New York.

Campos CA, Hernández ME, Moreno-Casasola P, et al (2011) Soil water retention and carbon pools in tropical forested wetlands and marshes of the Gulf of Mexico. Hydrol Sci J 56:1388–1406. doi: 10.1080/02626667.2011.629786.

Chambers FM, Beilman DW, Yu Z (2011) Methods for determining peat humification and for quantifying peat bulk density , organic matter and carbon content for palaeostudies of climate and peatland carbon dynamics. Mires Peat 7:1–10.

Dray S, Legendre P, Peres-Neto PR (2006) Spatial modelling: a comprehensive framework for principal coordinate analysis of neighbour matrices (PCNM). Ecol Modell 196:483–493. doi: 10.1016/j.ecolmodel.2006.02.015.

Furukawa Y, Inubushi K, Ali M, et al (2005) Effect of changing groundwater levels caused by land-use changes on greenhouse gas fluxes from tropical peat lands. Nutr Cycl Agroecosystems 71:81–91. doi: 10.1007/s10705-004-5286-5.

Gandois L, Cobb AR, Hei IC, et al (2013) Impact of deforestation on solid and dissolved organic matter characteristics of tropical peat forests: Implications for carbon release. Biogeochemistry 114:183–199. doi: 10.1007/s10533-012-9799-8.

Gnatowski T, Szatyłowicz J, Brandyk T, Kechavarzi C (2010) Hydraulic properties of fen peat soils in Poland. Geoderma 154:188–195. doi: 10.1016/j.geoderma.2009.02.021.

Grover SPP, Baldock JA (2013) The link between peat hydrology and decomposition: Beyond von Post. J Hydrol 479:130–138. doi: 10.1016/j.jhydrol.2012.11.049.

Hallema DW, Périard Y, Lafond J a., et al (2015) Characterization of Water Retention Curves for a Series of Cultivated Histosols. Vadose Zo J 14:0. doi: 10.2136/vzj2014.10.0148.

Hardjamulia A, Suwignyo P (1987) The present status of the reservoir fisheries in Indonesia. In: Silva SS De (ed) Reservoir fishery management and development in Asia. International Development Research Centre, Kathmandu, Nepal, pp 23–28.

Hergoualc'h K, Verchot L V. (2011) Stocks and fluxes of carbon associated with land use change in Southeast Asian tropical peatlands: A review. Global Biogeochem Cycles 25:doi:10.1029/2009GB003718. doi: 10.1029/2009GB003718.

Hirano T, Segah H, Kusin K, et al (2012) Effects of disturbances on the carbon balance of tropical peat swamp forests. Glob Chang Biol 18:3410–3422. doi: 10.1111/j.1365-2486.2012.02793.x.

Hooijer A, Page S, Jauhiainen J, et al (2012) Subsidence and carbon loss in drained tropical peatlands. Biogeosciences 9:1053–1071. doi: 10.5194/bg-9-1053-2012.

Huijnen V, Wooster MJ, Kaiser JW, et al (2016) Fire carbon emissions over maritime southeast Asia in 2015 largest since 1997. Sci Rep 6:26886. doi: 10.1038/srep26886.

Hurvich CM, Tsai C-L (1989) Regression and time series model selection in small samples. Biometrika 76:297–307. doi: 10.1093/biomet/76.2.297.

Jaenicke J, Wösten H, Budiman A, Siegert F (2010) Planning hydrological restoration of peatlands in Indonesia to mitigate carbon dioxide emissions. Mitig Adapt Strateg Glob Chang 15:223–239. doi: 10.1007/s11027-010-9214-5.

Jauhiainen J, Hooijer A, Page SE (2012) Carbon dioxide emissions from an Acacia plantation on peatland in Sumatra, Indonesia. Biogeosciences 9:617–630. doi: 10.5194/bg-9-617-2012.

Kellner K (2016) jagsUI: A Wrapper Around "rjags" to Streamline "JAGS" Analyses.

Kettridge N, Tilak AS, Devito KJ, et al (2016) Moss and peat hydraulic properties are optimized to maximize peatland water use efficiency. Ecohydrology 9:1039–1051. doi: 10.1002/eco.1708.

Könönen M, Jauhiainen J, Laiho R, et al (2015) Physical and chemical properties of tropical peat under stabilised land uses. Mires Peat 16:1–13.

Kool DM, Buurman P, Hoekman DH (2006) Oxidation and compaction of a collapsed peat dome in Central Kalimantan. Geoderma 137:217–225. doi: 10.1016/j.geoderma.2006.08.021.

Kuo L, Mallick B (1998) Variable Selection for Regression Models. Sankhyā Indian J Stat Ser B 60:65–81. doi: 10.2307/25053023.

Kurnianto S, Warren M, Talbot J, et al (2014) Carbon accumulation of tropical peatlands over millennia: A modeling approach. Glob Chang Biol 1–14. doi: 10.1111/gcb.12672.

Lal R (2004) Soil Carbon Sequestration Impacts on Global Climate Change and Food Security. Science (80-) 304:1623–1627. doi: 10.1126/science.1097396.

Legendre P, Borcard D, Blanchet FG, Dray S (2013) PCNM: MEM spatial eigenfunction and principal coordinate analyses.

Mccarter CPR, Price JS (2014) Ecohydrology of Sphagnum moss hummocks :

mechanisms of capitula water supply and simulated effects of evaporation. 44:33–44. doi: 10.1002/eco.1313.

Miettinen J, Liew SC (2010) Status of Peatland Degradation and Development in Sumatra and Kalimantan. Ambio 39:394–401. doi: 10.1007/s13280-010-0051-2.

Miettinen J, Shi C, Liew SC (2012) Two decades of destruction in Southeast Asia's peat swamp forests. Front Ecol Environ 10:124–128. doi: 10.1890/100236.

Miettinen J, Shi C, Liew SC (2016) Land cover distribution in the peatlands of Peninsular Malaysia, Sumatra and Borneo in 2015 with changes since 1990. Glob Ecol Conserv 6:67–78. doi: 10.1016/j.gecco.2016.02.004.

Moore PA, Morris PJ, Waddington JM (2015) Multi-decadal water table manipulation alters peatland hydraulic structure and moisture retention. Hydrol Process 29:2970–2982. doi: 10.1002/hyp.10416.

Moore S, Evans CD, Page SE, et al (2013) Deep instability of deforested tropical peatlands revealed by fluvial organic carbon fluxes. Nature 493:660–3. doi: 10.1038/nature11818.

Murdiyarso D, Donato D, Kauffman JB, et al (2009) Carbon storage in mangrove and peatland ecosystems: A preliminary account from plots in Indonesia. Bogor, Indonesia.

Murdiyarso D, Hergoualc'h K, Verchot L V (2010) Opportunities for reducing greenhouse gas emissions in tropical peatlands. Proc Natl Acad Sci U S A 107:19655–19660. doi: 10.1073/pnas.0911966107.

Nemati MR, Caron J, Banton O, Tardif P (2000) Determining Air Entry Value in Peat Substrates. Soil Sci Soc Am J 367–373.

Novita N.(2016) Carbon Stocks and Soil Greenhouse Gas Emissions Associated with Forest Conversion to Oil Palm Plantations in Tanjung Puting Tropical Peatlands, Indonesia. Oregon State University.

Oksanen J, Blanchet FG, Friendly M, et al (2017) vegan: Community Ecology Package. R package version 2.4-3. https://CRAN.R-project.org/package=vegan

Page SE, Rieley JO, Banks CJ (2011) Global and regional importance of the tropical peatland carbon pool. Glob Chang Biol 17:798–818. doi: 10.1111/j.1365-2486.2010.02279.x.

Page SE, Siegert F, Rieley JO, et al (2002) The amount of carbon released from peat and forest fires in Indonesia during 1997. Nature 1999:61–65. doi: 10.1038/nature01141.1.

Page SE, Wűst R a. J, Weiss D, et al (2004) A record of Late Pleistocene and Holocene carbon accumulation and climate change from an equatorial peat bog(Kalimantan, Indonesia): implications for past, present and future carbon dynamics. J Quat Sci 19:625–635. doi: 10.1002/jqs.884.

Peres-Neto PR, Legendre P, Dray S, Borcard D (2006) Variation Partitioning of Species Data Matrices : Estimation and Comparison of Fractions. Ecology 87:2614–2625.

Phillips VD (1998) Peatswamp ecology and sustainable development in Borneo. Biodivers Conserv 7:651–671.

Plummer M (2003) JAGS: A program for analysis of Bayesian graphical models using Gibbs sampling. In: Proceedings of the 3rd International Workshop on Distributed Statistical Computing (DSC 2003). pp 20–22.

Quinton WL, Elliot T, Price JS, et al (2009) Measuring physical and hydraulic properties of peat from X-ray tomography. Geoderma 153:269–277. doi: 10.1016/j.geoderma.2009.08.010.

Raudenbush SW, Bryk AS (2002) Hierarchical linear models: Applications and data analysis methods, 2nd editio. Sage Publications, Thousand Oaks.

Rezanezhad F, Quinton WL, Price JS, et al (2010) Influence of pore size and geometry on peat unsaturated hydraulic conductivity computed from 3D computed tomography image analysis. Hydrol Process 24:2983–2994. doi: 10.1002/hyp.7709.

Ritzema HP, Hassan AM., Moens R. (1998) A new approach to water management of tropical peatlands: a case study from Malaysia. Irrig Drain Syst 12:123–139. doi: 10.1023/A:1005976928479

Rocha Campos JR Da, Silva AC, Fernandes JSC, et al (2011) Water retention in a peatland with organic matter in different decomposition stages. Rev Bras Ciência do Solo 35:1217–1227. doi: 10.1590/S0100-06832011000400015.

Saharjo BH, Munoz CP (2005) Controlled burning in peat lands owned by small farmers: a case study in land preparation. Wetl Ecol Manag 13:105–110. doi: 10.1007/s11273-003-5110-z.

Schwärzel K, Šimůnek J, van Genuchten MT, Wessolek G (2006) Measurement modeling of soil-water dynamics evapotranspiration of drained peatland soils. J Plant Nutr Soil Sci 169:762–774. doi: 10.1002/jpln.200621992.

Sherwood JH, Kettridge N, Thompson DK, et al (2013) Effect of drainage and wildfire on peat hydrophysical properties. Hydrol Process 27:1866–1874. doi: 10.1002/hyp.9820.

Taufik M, Torfs PJJF, Uijlenhoet R, et al (2017) Amplification of wildfire area burnt by hydrological drought in the humid tropics. Nat Clim Chang. doi: 10.1038/nclimate3280.

Team R Core (2016) R: A Language and Environment for Statistical Computing. R Foundation for Statistical Computing, Vienna, Austria. URL https://www.R-project.org/.

van Genuchten MT (1980) A Closed-form Equation for Predicting the Hydraulic Conductivity of Unsaturated Soils. Soil Sci Soc Am J 44:892–898. doi:

10.2136/sssaj1980.03615995004400050002x.

Walczak R, Rovdan E, Witkowska-Walczak B (2002) Water retention characteristics of peat and sand mixtures. Int Agrophysics 16:161–165.

Warren MW, Kauffman JB, Murdiyarso D, et al (2012) A cost-efficient method to assess carbon stocks in tropical peat soil. Biogeosciences 9:4477–4485. doi: 10.5194/bg-9-4477-2012.

Watanabe S (2010) Asymptotic Equivalence of Bayes Cross Validation and Widely Applicable Information Criterion in Singular Learning Theory. J Mach Learn Res 11:3571–3594.

Weiss R, Alm J, Laiho R, Laine J (1998) Modeling moisture retention in peat soils. Soil Sci Soc Am J 62:305–313. doi: 10.2136/sssaj1998.03615995006200020002x.

Yu Z, Loisel J, Brosseau DPDP, et al (2010) Global peatland dynamics since the Last Glacial Maximum. Geophys Res Lett 37:L13402. doi: 10.1029/2010GL043584.

Figures

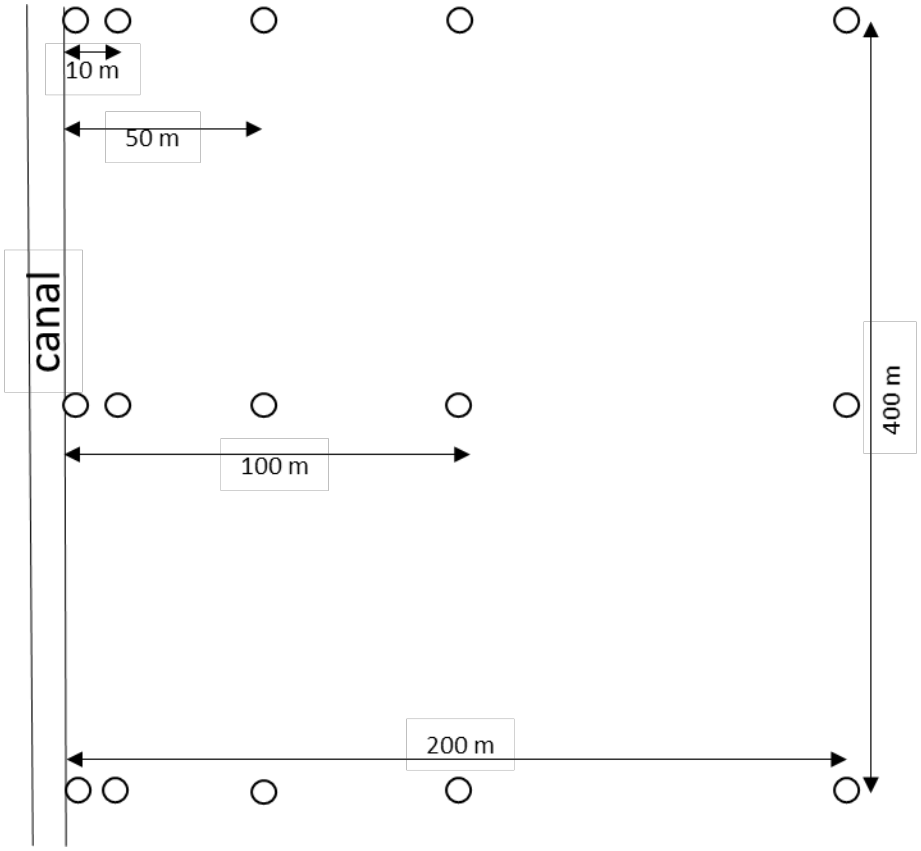

Figure 3.1. Experimental design used in drained seral community to take the peat samples for determining peat properties and moisture characteristics. Three transects were installed perpendicular to canal with the 200 m spacing between two adjacent transect. The first plot for each transect was 1 m away from drainage canal ditching.

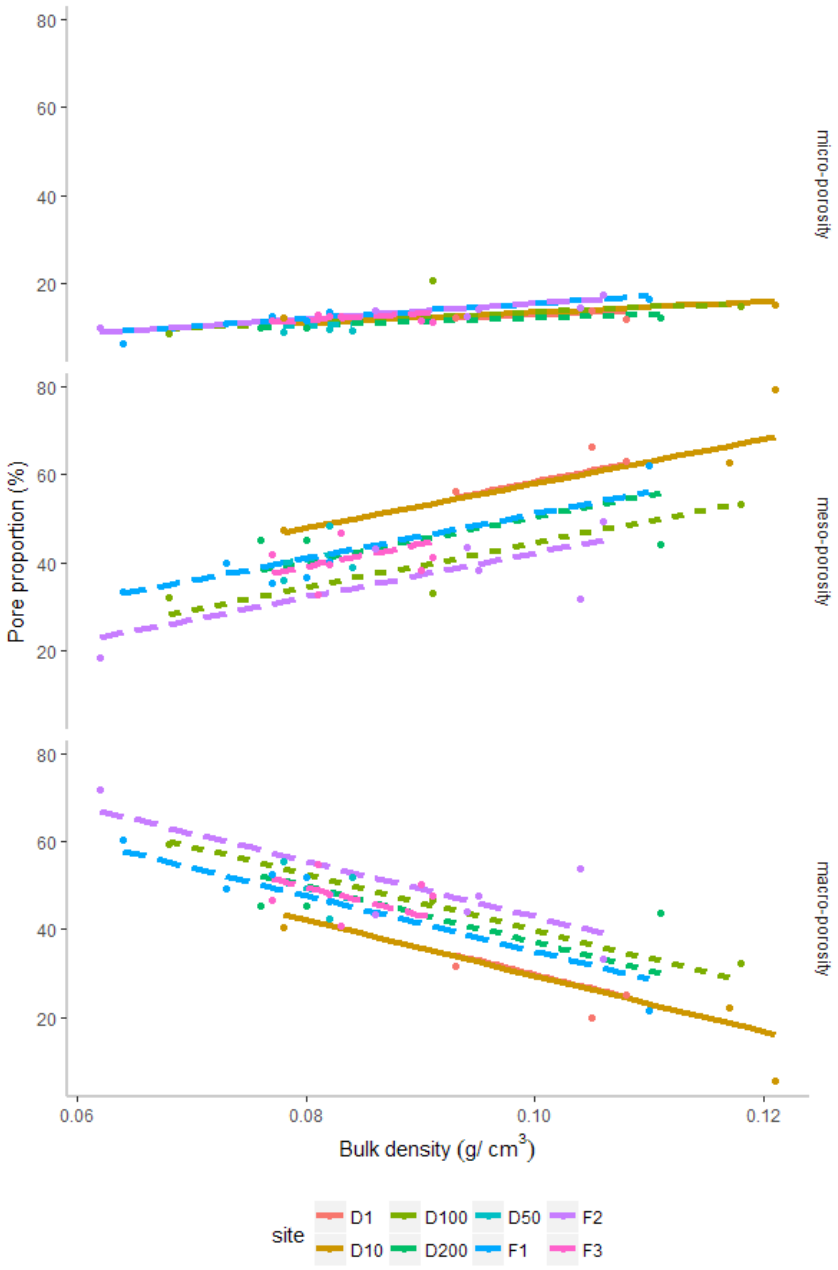

Figure 3.2. Estimated macro-, meso-, and micro-porosity proportion under varying bulk density for eight sites. The estimates were made by using the best approximating model to predict porosity proportion and study site characteristic. *D1, D10, D50, D100, D200* are drained seral communities sites with 1, 10, 50, 100, and 200 m perpendicular from the ditch, respectively. *F1, F2, F3* are the undrained forested sites.

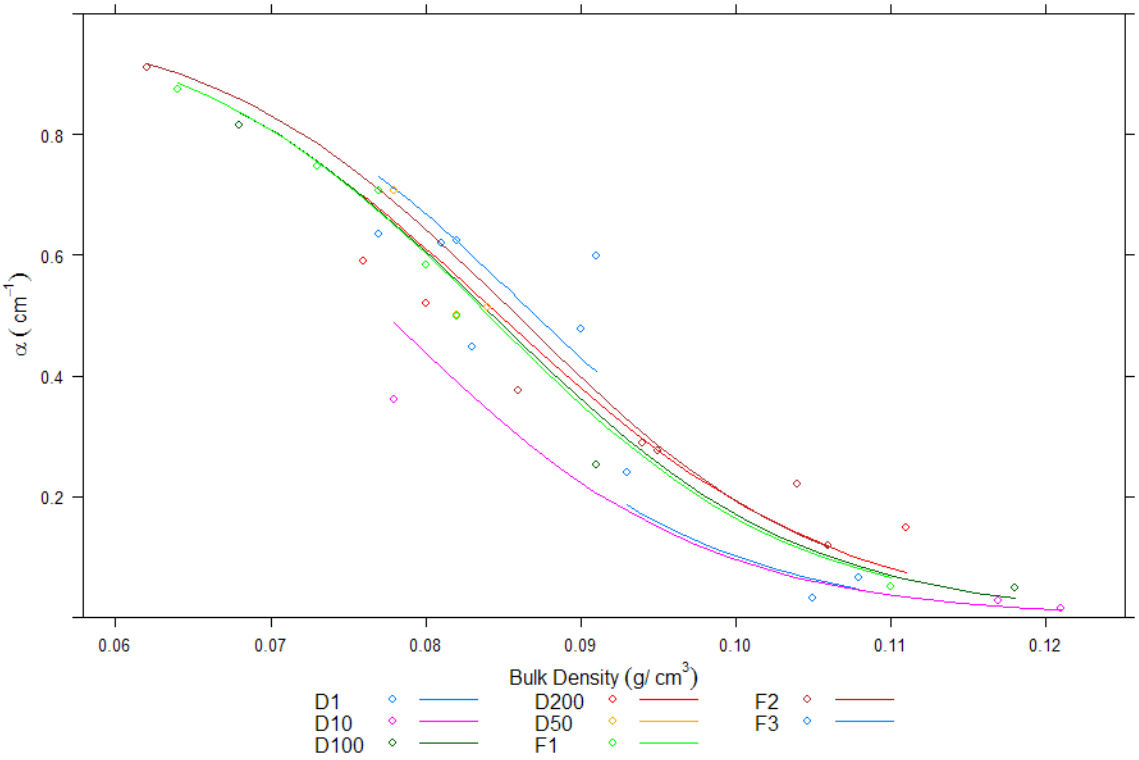

Figure 3.3. Estimated van Genuchten shape parameter α under varying bulk density for eight sites. The estimates were made by using the best approximating model to predict peat moisture content and study site characteristic. D1. D10, D50, D100, D200 are drained seral communities sites with 1, 10, 50, 100, and 200 m from the ditch, respectively. F1, F2, F3 are the undrained forested sites.

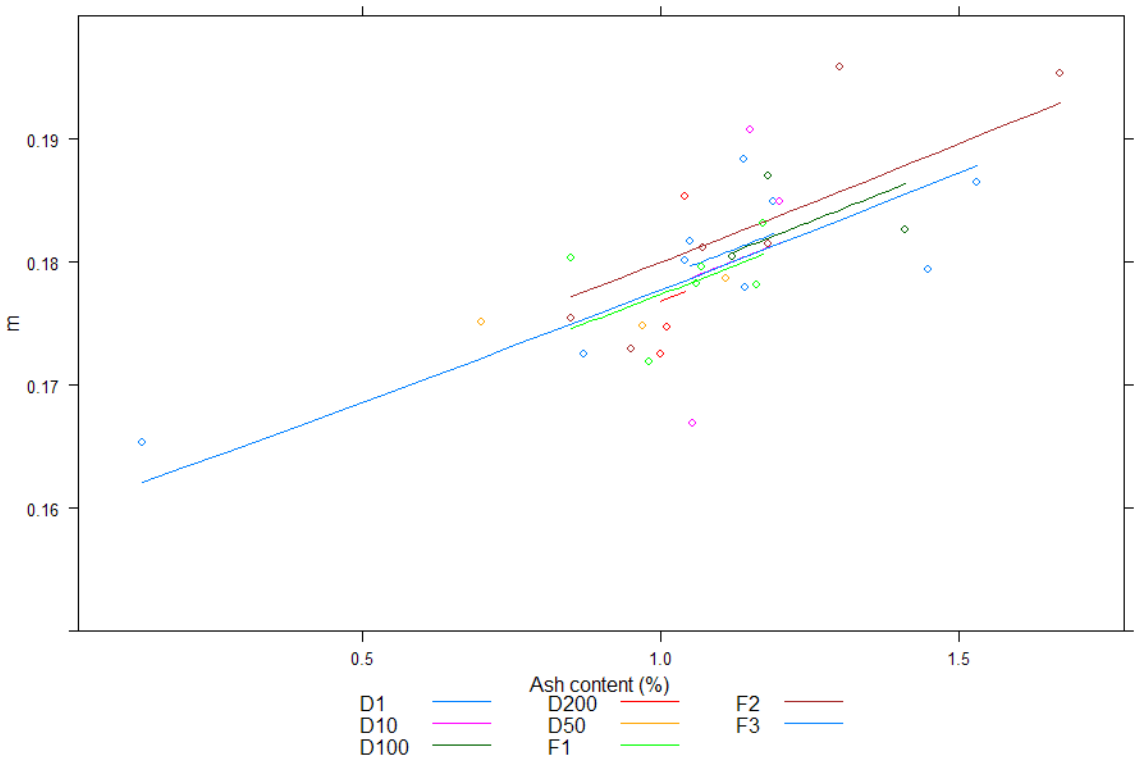

Figure 3.4. Estimated van Genuchten shape parameter *m* under varying ash content for eight sites. The estimates were made by using the best approximating model to predict peat moisture content and study site characteristic. D1. D10, D50, D100, D200 are drained seral communities sites with 1, 10, 50, 100, and 200 m from the ditch, respectively. F1, F2, F3 are the undrained forested sites.

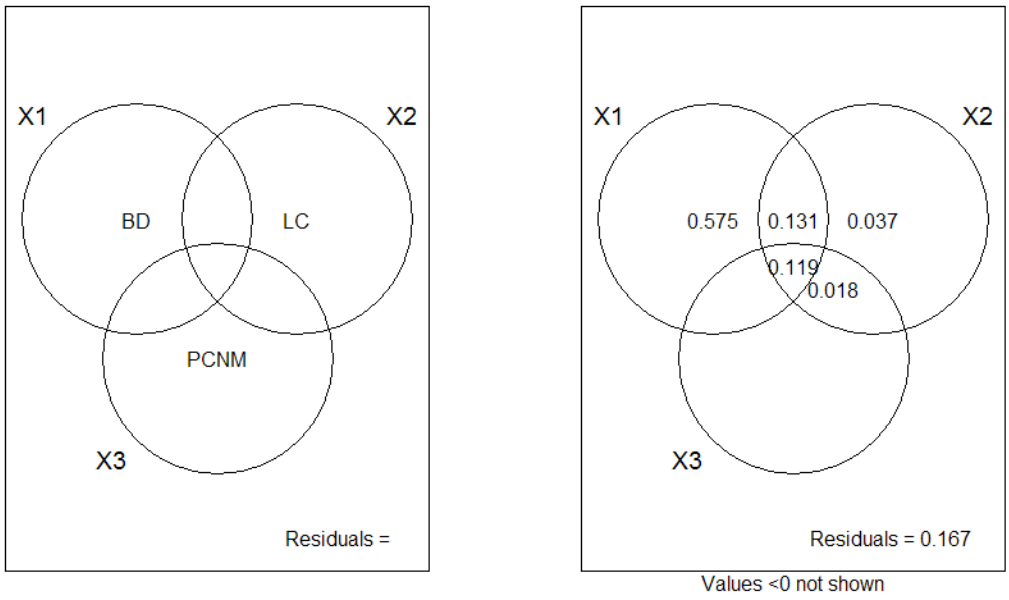

Figure 3.5. Partioning variation of peat moisture characteristics depicted by van Genuchten model parameters (n, m, α, θ_r, θ_s) and pore distribution, i.e. the proportion of macro-, meso-, and micro-porosity that can be explained by three main components: BD: bulk density, LC: land cover types (undrained forested sites and drained seral community that was classified into two groups, i.e. close from canal (< 50 m) and far from canal (>= 50 m), PCNM: the spatial auto-correlation that was calculated by using principal coordinates of neighbor matrices (PCNM). Left chart is the name of predictor variables components and right chart is the amount of respond variables variation.

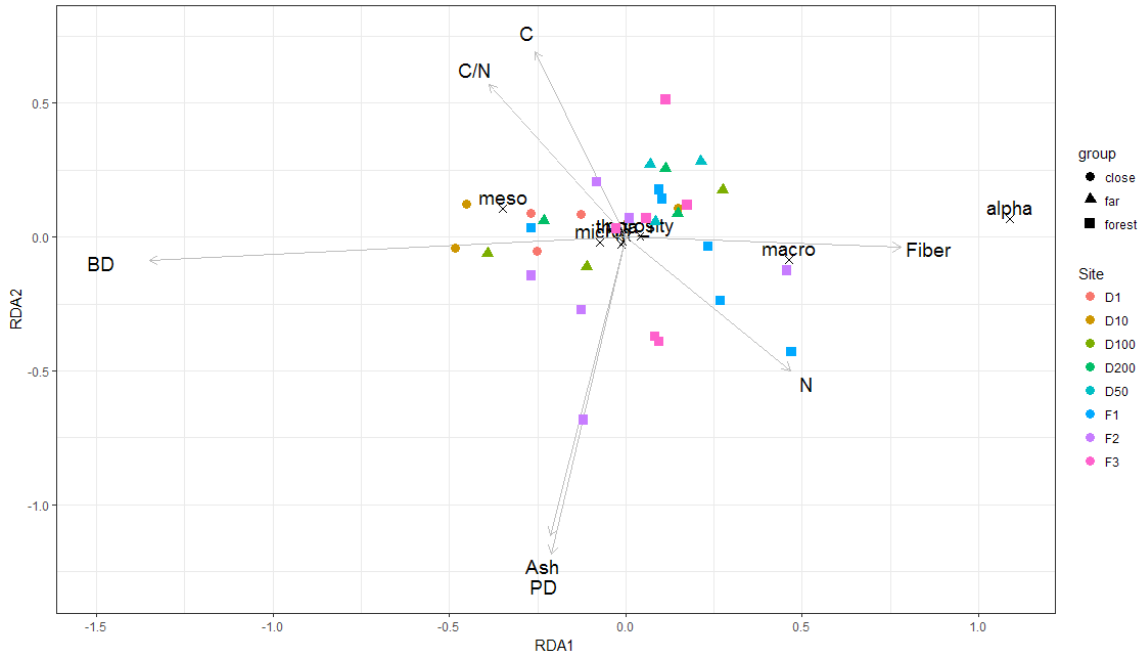

Figure 3.6. Redundancy analysis ordination of sites and peat moisture characteristic including van Genuchten model parameters (i.e. α, m, n, θ_s, θ_r) and pore distribution: macro-,meso-, and micro-porosity in two dimensional planes. RDA1 is the redundancy function for the first axis explaining about 80% variation of peat moisture characteristic. RDA2 is the second redundancy axis explaining only 1% of the peat moisture characteristic variability. The biplot shows the relationship between the peat physical (i.e. *Ash*: ash content, PD: particle density, *N*: nitrogen concentration, C: carbon concentration, C/N: carbon to nitrogen ratio, BD: bulk density) on each axis.

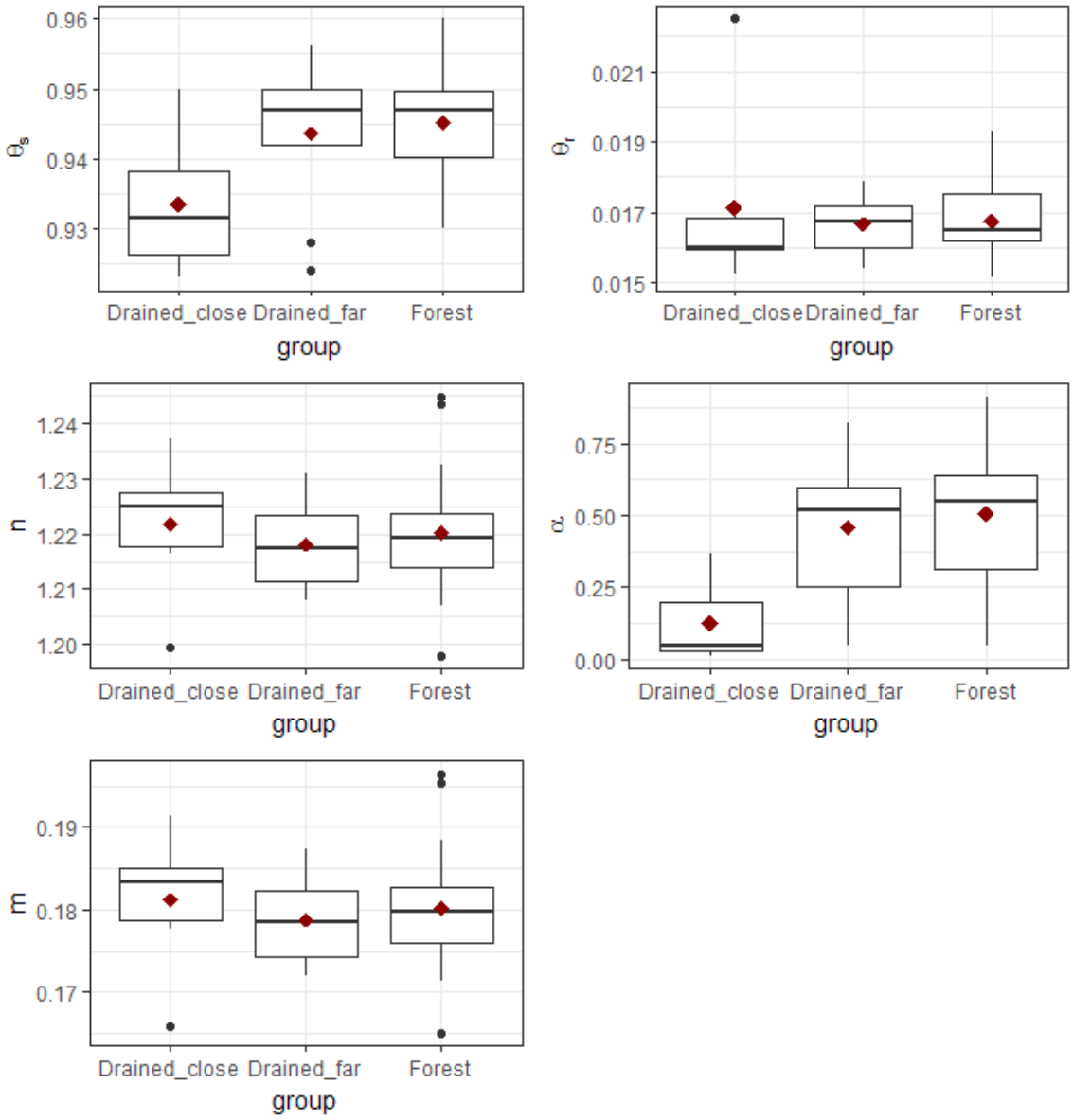

Figure 3.7. Boxplot of van Genuchten model parameter (shape parameter *α, m*, and *n*, saturated water content θ_s, and residual water content θ_r) for each group. Forest group consisted of all forested sites; drained close group included drained-seral community with the distance from the ditch is 1 and 10 m. Drained far group included 50, 100, and 200 m from the ditch. The boxes represent the interquartile range (25% - 75% percentile of data), the vertical lines in the boxes show the median values. The filled diamond shapes represent the mean values. Horizontal lines outside the boxes represent the maximum and minimum of data if there were no outliers. Outliers were calculated as 1.5 times of interquartile range and showed as black filled dots.

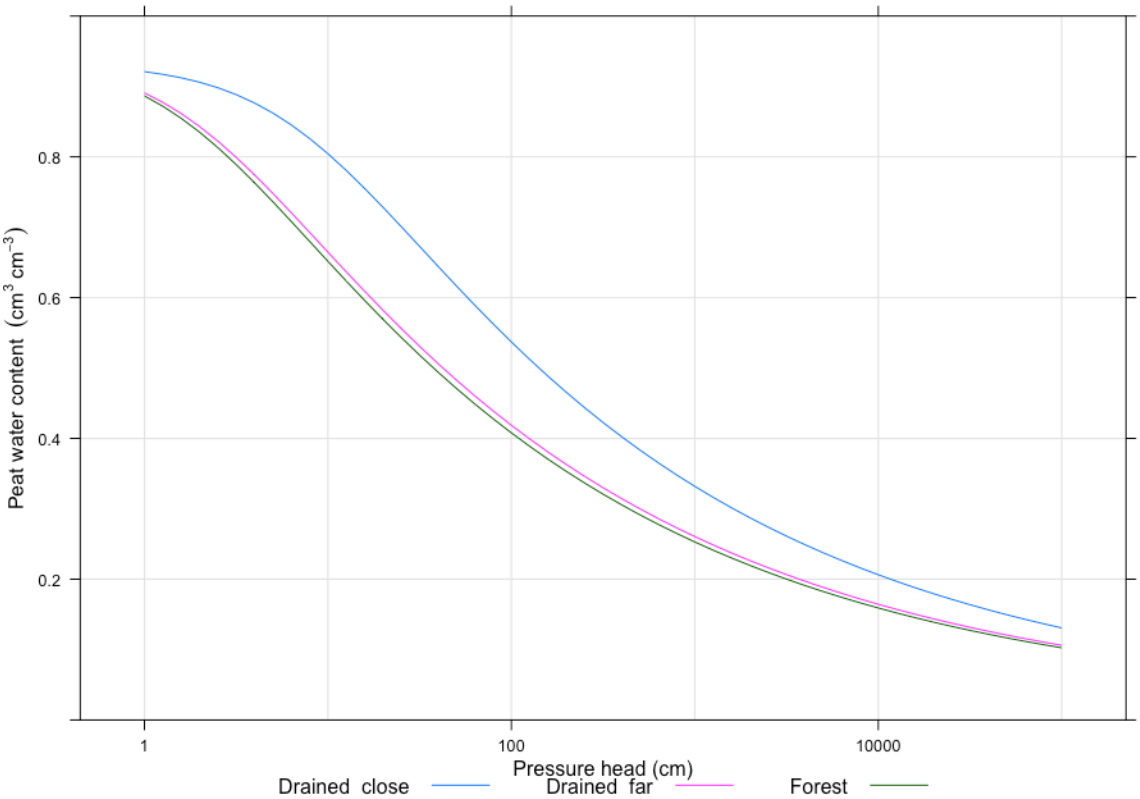

Figure 3. 8. Peat water retention moisture characteristic for three groups: undrained forested sites, drained sites close to canal (1 and 10 m from canal), and drained sites far from canal (50, 100, and 200 m from canal).

Tables

Table 3. 1. Mean and standard error (SE) of peat pore distribution in drained seral community and undrained forested sites.

Sites	Distance to canal (m)	N	Macro-porosity (%)		Meso-porosity (%)		Micro-porosity (%)	
			Mean	SE	Mean	SE	Mean	SE
Drained seral	1	3	24	3	58	3	12	1
	10	3	21	10	59	8	13	1
	50	3	47	4	39	4	9	0
	100	3	44	8	37	6	14	3
	200	3	42	1	42	1	10	1
Undrained forest		18	45	2	37	2	12	1

Table 3.2. Candidate models to predict peat macro-, meso-, and micro-porosity at the 50 cm depth with the number of parameter (*K*), log of likelihood (*logL*), Akaike information criteria with small sample adjustment (AIC_c), and Akaike weights (w_i).

Model	K	LogL	AIC_c	delta	w_i
Macro-porosity					
Bulk density+Ash content	5	42.89	-73.55	0	0.752
Bulk density *Ash content	6	43.28	-71.33	2.221	0.248
Ash content	4	22.88	-36.33	37.223	0
Ash content *Seral	6	25.45	-35.66	37.888	0
Ash content *carbon to nitrogen ratio	6	24.85	-34.46	39.083	0
Ash content + carbon to nitrogen ratio	5	23.3	-34.38	39.171	0
Meso-porosity					
Bulk density + Ash content	5	43.71	-75.19	0	0.728
Bulk density * Ash content	6	44.23	-73.22	1.97	0.272
Ash content	4	29.67	-49.9	25.287	0
Ash content + Seral	5	30.78	-49.33	25.86	0
Ash content + carbon to nitrogen ratio	5	30.2	-48.18	27.013	0
Ash content * Seral	6	31.51	-47.78	27.406	0
Micro-porosity					
Bulk density * carbon to nitrogen ratio	6	88.33	-161.44	0	0.481
Bulk density + carbon to nitrogen ratio	5	86.75	-161.27	0.165	0.443
Bulk density	4	83.02	-156.62	4.818	0.043
Bulk density *Seral	6	85.03	-154.83	6.604	0.018
Bulk density +Ash content	5	83.36	-154.5	6.935	0.015

Note *Seral* is a binary variables in which 1 for drained seral community and 0 for undrained forested peatlands**.** + is additive model. * represents the main effects and interaction between the covariates.

Table 3.3. Estimates of fixed and random effects, their standard error (S.E), 90% lower (LCL) and upper confidence interval (UCL) for the two best-approximating models in predicting macro-, meso-, and micro-porosity contained in the confidence model set. Random effects are standard deviation estimates.

	Estimate	S.E	Lower	Upper
	Macro-porosity (wi = 0.752)			
Fixed				
Intercept	0.928	0.072	0.805	1.054
Bulk density	-6.272	0.710	-7.562	-5.051
Ash content	0.034	0.044	-0.040	0.109
Random				
Ash content	0.041			
Residual	0.057			
	Macro-porosity (wi = 0.248)			
Fixed				
Intercept	1.304	0.427	0.587	2.042
Bulk density	-10.712	5.012	-19.411	-2.293
Ash content	-0.295	0.371	-0.929	0.328
Bulk density x Ash content	3.867	4.329	-3.404	11.297
Random effect				
Ash content	0.040			
Residual	0.056			
	Meso-porosity (wi = 0.782)			
Fixed				
Intercept	0.059	0.069	-0.060	0.174
Bulk density	4.492	0.674	3.346	5.695
Ash content	-0.032	0.043	-0.105	0.041
Random				
Ash	0.048			
Residual	0.053			
	Meso-porosity (wi = 0.272)			
Fixed				
Intercept	-0.345	0.399	-1.032	0.325
Bulk density	9.261	4.688	1.389	17.352
Ash content	0.322	0.347	-0.261	0.913
Bulk density x Ash content	-4.160	4.049	-11.089	2.643
Random effect				
Ash content	0.047			
Residual	0.052			
	Micro-porosity (wi = 0.481)			
Fixed				

(Intercept)	-0.090	0.079	-0.222	0.042
Bulk density	2.807	0.901	1.294	4.321
Carbon to nitrogen ratio (C/N)	0.002	0.002	-0.001	0.005
Bulk density x C/N	-0.036	0.020	-0.070	-0.003
Random				
BD	<0.001			
Residual	0.017			
	Micro-porosity (wi = 0.443)			
Fixed				
(Intercept)	0.049	0.020	0.016	0.083
Bulk density	1.200	0.203	0.860	1.541
C/N	-0.001	0.000	-0.001	0.000
Random				
Bulk density	<0.001			
Residual	0.017			

Notes: *Seral* is a binary variable with value 1 for drained seral community and 0 for undrained forested peatlands**.** + is additive model. * represents the main effects and interaction between the covariates.

Table 3.4. List of candidate models to predict peat water retention curve parameters based on van Genuchten model with the Watanabe-Akaike information criterion (*WAIC*), the difference of *WAIC* between the best approximating model and each model (*ΔWAIC*), and Akaike weight (w_i)

Model	WAIC	ΔWAIC	w_i
α ~ Bulk density; m ~ ash content	-414.56	0.00	0.37
α ~ Bulk density; m ~ constant	-414.35	0.21	0.33
α ~ Bulk density + fiber; m ~ ash content	-413.69	0.87	0.24
α ~ constant; m ~ ash content	-408.50	6.06	0.02
α ~ fiber; m ~ constant	-407.55	7.01	0.01
α ~ constant ; m ~ ash content	-407.06	7.50	0.01
α ~ constant; m ~ constant	-406.51	8.06	0.01
α ~ ash content; m ~ constant	-405.21	9.35	0.00
α ~ constant; m ~ Bulk density	-405.21	9.35	0.00
α ~ Carbon to nitrogen ratio; m ~ constant	-405.13	9.43	0.00
*α ~ constant; m ~ shrubs*distance*	-404.46	10.10	0.00
α ~ constant; m ~ fiber	-404.44	10.12	0.00
α ~ constant; m ~ Carbon to nitrogen ratio	-404.40	10.17	0.00
*α ~ seral*distance; m ~ constant*	-404.02	10.54	0.00

Notes: *m* and *α* are the van Genuchten model parameters. *Seral* is the binary variable in which 1 and 0 represent drained shrublands and undrained forested sites, respectively. *Constant* has no covariates (intercept only), + indicates models were additive and * indicates that there is an interaction among covariates.

Table 3.5. The van Genuchten model parameters estimated using an integrated hierarchical model and allowing parameters to vary among sites. Parameter estimates are the mean parameter values across plots, their standard deviation and 95% lower and upper confidence interval. The random effects are measures of their variability among plots expressed as a standard deviation.

	Mean	S.D	Lower	Upper
	α~ BD; m~ash; θ_r~constant			
Shape parameter, α				
Intercept	8.659	1.662	5.764	12.399
Bulk density	-103.128	16.049	-138.761	-74.299
Random effect	0.820	0.219	0.458	1.320
Residual water content, θ_r				
Intercept	−4.459	0.797	-6.227	-3.129
Random effect	0.565	0.461	0.021	1.701
Shape parameter, *m*				
Intercept	-1.656	0.123	-1.894	-1.405
Ash content	12.689	10.669	-8.774	33.804
Random effect	0.073	0.044	0.004	0.166
Residual error	0.075	0.004	0.067	0.084

Table 3.6. Predicted total water storage in undrained forested and drained industrial plantation peatlands in Sumatra, Borneo and Peninsular Malaysia.

	Minimum	Maximum
Saturated water content undrained peatlands (m^3 m^{-3})[a1]	0.932	0.959
Saturated water content in drained peat (m^3 m^{-3})[a2]	0.924	0.952
Best estimate of mean peat depth (m)[b]	5.5	
Pristine peat swamp forest area in 1990 (ha)[c]	10,227,400	
Pristine peat swamp forest area in 2015(ha)c	996,050	
Oil palm plantation area in 2015 (ha)[d1]	3,106,100	
Pulp plantation area in 2015 (ha)[d2]	1,131,150	
Total water stored in undrained; 1990 (km^3)[e1]	524.3	539.4
Total water stored in 2015 (km^3)[e2]	266.4	274.4
Water loss (km^3)[f]	257.9	265
Mean annual water loss rate (km^3/year)[g]	10.3	10.6
DOC in pristine peat swamp forest (mg l^{-1})[h]	60	64.4
DOC flux (Tg C yr^{-1})[i]	0.62	0.68

a. those values were calculated from this study; b. Page et al (2011); c. Miettinen et al. (2012b); d. Miettinen et al. (2016); e1 = a1 x b x c; e2 = a2 x b x (d1+d2); f = e1-e2; g = f/25; h. Gandois et al (2013); i = g x h

CHAPTER 4. CHARACTERIZING PEAT PROPERTIES USING THE GROUND PENETRATING RADAR (GPR) IN TROPICAL PEATLANDS.

Abstract

Currently, peat properties such as bulk density, ash content, carbon and nitrogen concentration are determined conventionally by collecting and analyzing peat samples from relatively few locations. Thus, most information is limited to small spatial scales (site level) with limited understanding of the magnitude or structure of heterogeneity. Ground penetrating radar (GPR) is non-invasive geophysical technique that records discontinuities in dielectric in the subsurface. It has been widely used to study northern boreal peatlands. In tropical peatlands, few studies have employed GPR and then primarily for determining peat depth. Here, we explore the potential of GPR to determine tropical peat properties, such as bulk density, ash, carbon content, and saturated hydraulic conductivity by evaluating the relationship between those properties with the relative dielectric permittivity produced by GPR. A common mid-point (CMP) GPR survey was conducted at two different land cover types: oil palm plantations and seral vegetative community sites in West Kalimantan, Indonesia to estimate the relative dielectric permittivity A hierarchical model was used to develop the relationship between relative dielectric permittivity and peat properties and incorporate spatial dependence. The results revealed that dielectric varied from 5.8 to 84.9 across all sites and were significantly lower at the 50-100 cm depth than those measured at 300-400 cm and 550 cm. Parameter estimates from the hierarchical models indicated that ash content and carbon concentration were strongly positively related to dielectric, with variation

among sites. In contrast, the relationship between dielectric and saturated hydraulic conductivity and bulk density were less precise shown by confidence interval of their coefficient included zero. Our results indicated that the ability of dielectric to estimate peat properties was good depicted by the root mean squared error (RMSE) calculated from the cross validation of those variables were within the range of measured peat properties variability. It suggests that GPR can be utilized to map the peatland distribution providing not only the peat depth but also its properties including ash content, carbon concentration, bulk density, and hydraulic conductivity. However, the conventional survey (e.g., sampling with a core) is still required to obtain more precise estimates and ensure data quality.

Keywords: geo-physical, land cover change, drained peatland, peat characteristics

4.1. Introduction

Tropical peatlands cover 440,000 km^2, about 10% of global peatland area and accumulate 90 Gt C of which 80% is located in South East Asia (SEA; Page *et al.*, 2011). More than 50% of tropical peatland area is believed to be located in Indonesia (Page et al. 2011). Tropical peatlands provide important ecosystem services, such as storing a huge amount of carbon (Murdiyarso et al. 2009; Warren et al. 2012; Basuki 2017) and water (Chapter 3). However, there are several challenges faced by tropical peatlands. These include the conversion of peat swamp forest to anthropogenic land uses (Miettinen et al. 2012b, 2016) and installation of drainage canals that lower the water table and potentially increase the susceptibility of peatlands to wildfire (Page et al. 2002; Taufik et al. 2017). The implementation of best peatland management practices requires information on peat depth and properties. In Indonesia, efforts are underway to develop peatland map that will provide information of peat depth (Wahyunto et al. 2003) but not peat properties. Currently, peat properties are determined with labor intensive methods that include collection of peat samples using a corer and transferring the samples to laboratory for analysis (Chapter 2; Chapter 3). These conventional methods, however, are limited to site-level measurements and require substantially more effort and resources if applied at the larger scales. Therefore, alternative cost-effective methods for characterizing peat properties for large-scale application should be explored.

Ground penetrating radar (GPR) is non-disturbing geophysical technique that records subsurface discontinuities in dielectric to depths <50 m. It involves

generating and receiving pulses of high-frequency of electromagnetic waves in the subsurface (Neal 2004). GPR has been widely used in peatland ecosystems, especially in boreal-temperate peatlands, to delineate the boundary between the peat and mineral layers (Gómez-Ortiz et al. 2010) and thus, it has been shown to be useful in determining peat depth (Plado et al. 2011; Parsekian et al. 2012b; Parry et al. 2014). As GPR continuously records peat depth, peat volume and stored carbon can be estimated with greater accurately than manual coring (Proulx-McInnis et al. 2013). GPR also has been successfully used to assess the hydrological conditions in peatlands, such as determining the water table position within the peat profile, peat water content (Parsekian et al. 2012a), the structure of pipe soil form in the peat profile, preferential flow, and macro-porosity for understanding sub-surface flow in peatland (Holden et al. 2013). In terms of evaluating the role of peatlands in regulating the greenhouse gas emission, GPR also could be used to estimate gas accumulation within the peat profile (Comas et al. 2005a, 2008, 2014; Parsekian et al. 2010).

Principally, the transmitter antenna of GPR unit sends high frequency electromagnetic pulses that penetrate the subsurface. Portions of the electromagnetic waves are reflected back to the surface and detected by the receiver antenna. The GPR unit records the two-way travel times of signal pulse from transmitter, sub-surface reflector, and receiver antenna that determines the wave velocity by the relative dielectric permittivity of the sub-surface material (Comas and Slater 2013). The relative dielectric permittivity is strongly related to the water content of the medium ranging from 1 for air and 81 for water (Neal 2004). The

relative dielectric permittivity likely varies within the peat profile since the characteristic of peat changes (e.g., ash content, bulk density,) due to the climate and other environmental variability (Page et al. 2004; Warren et al. 2012). The fraction of the electromagnetic which is reflected is determined by the difference in relative dielectric permittivity between adjacent materials. For example, peat with substantial organic material has a much greater total water content than clay material that will cause the relative dielectric permittivity to change abruptly at the peat-clay interchange layer and result in a strong reflectance signal arising from this boundary. Therefore, we hypothesize that GPR has the potential to estimate peat properties in tropical peatlands due to the variability of relative dielectric permittivity.

To our knowledge, there have been few studies that used GPR to evaluate the characteristics of tropical peatlands other than depth. For instance, Comas et al. (2015) reported the application of GPR in West Kalimantan peatlands, Indonesia and indicated that there was a good agreement between estimated peat depth using GPR and manual coring and, thus, suggested that it also can be utilized to estimate the peat depth and carbon stocks. However, information is currently lacking about whether GPR is useful for determining other peat properties, especially in the tropics. Here, we explore the potential use of GPR for estimating peat properties in the tropical peatlands with the following objectives: (1) measure dielectric permittivity with a GPR and peat properties with conventional methods in two land cover types; (2) evaluate the relationship between dielectric permittivity and peat properties. The results of this study could then potentially be used to develop a

peatland distribution map that is not only provides peat depth but also information on peat properties over large areas.

4.2. Methods

4.2.1. Study site

The study was conducted in a coastal-type tropical peatland in Ketapang regency, West Kalimantan, Indonesia. This peatland was considered to be a raised bog because the elevation of the central part of the peatland was higher than margin area (Figure 2.1). Based on previous studies (Chapter 2;), the peat properties between undrained forested sites and drained sites, i.e., oil palm plantation and seral community sites was similar (Figure 2.5). Therefore, we only conducted GPR surveys in drained peatlands that were dominated by two different land cover types: oil palm plantation and seral (non-forest) communities. Drainage ditch networks were developed at both sites at least 10 years prior to this study to lower the water table and presumably, facilitate agricultural activities. The oil palm plantations were owned and managed by a local villager with minimum soil tillage (no-use of heavy equipment). The seral community sites were abandoned drained peatlands that experienced repeated wildfires and were covered by shrubs and herbaceous vegetation at the time of the surveys.

4.2.2. Ground penetrating radar survey

The GPR survey was conducted using transect line method at the two different land cover types, i.e. three transect lines for each oil palm plantation and seral

community with six plots on 30 m intervals and set up perpendicular to the drainage canals. The locations of the transects and plots used in the GPR survey were the same as those used in the saturated hydraulic conductivity measurement presented in Chapter 2 of this dissertation.

We performed the GPR surveys using a MALÅ RAMAC system equipped with 100 MHz unshielded antennas (i.e., the transmitter and receiver antennas were separated). A common mid-point (CMP) GPR survey was used in this study to estimate the sub-surface electromagnetic wave velocity within a peat profile (one-dimension velocity profile) by changing the distance between transmitter and receiver antennas with the fixed midpoint between both antennas. In this study, the antennas moved sequentially from 0.1 to 7 m apart with the spacing of 0.1 m. For each transect, we conducted six CMP surveys with the interval between the midpoints of the CMP was 30 m. The transect layout was the same as in Chapter 2 of this dissertation (Figure 2.3).

The data collected during CMP surveys were recorded using a 700 ns time window for covering the signal reflection from the surface to the peat-mineral interface layer and 16 stacks or replicates that were used for each trace to improve the signal-to-noise ratio. Then, GPR data were post-processed using REFLEX-Win version 7.5.9 (Sandmeier 2015) that facilitated interpretation by increasing the signal-to-noise ratio. The following processing steps were performed to analyze the GPR data: (1) updating the start time in the file header data; (2) a “dewow” filter to reduce the low-frequency noise; (3) a manual gain to increase the visibility of the peat-mineral transitional zone; and (4) a band-pass filter to eliminate high and low

frequency of the reflectance. The semblance analysis provided in REFLEX-Win was utilized to estimate the 1-D velocity from CMP data. The electromagnetic wave velocity at a specific layer within a peat profile was determined by visually picking local maxima of semblance spectrum (Jacob and Urban 2016).

The electromagnetic wave velocities (v) estimated by using the CMP data, were used to estimate relative dielectric permittivity (ε_r) using the following equation (Neal 2004) as:

$$v = \frac{c_0}{\sqrt{\varepsilon_r \mu_r \frac{1+\sqrt{1+\left(\frac{\sigma}{\omega\varepsilon}\right)^2}}{2}}},$$

where c_o is the electromagnetic wave in the vacuum (3 x 10^8 m/s), μ_r is relative magnetic permeability, and $\left(\frac{\sigma}{\omega\varepsilon}\right)$ is a loss factor. Since peat material can be categorized as a low-loss medium in which conductivity of material, σ is much greater than displacement current ($\omega\varepsilon$) (Comas and Slater 2007), the electromagnetic wave velocity can be accurately calculated as:

$$v = \frac{c_0}{\sqrt{\varepsilon_r}},$$

where the parameters are defined above.

4.2.3. Peat properties

At each plot where the CMP surveys were conducted, we collected peat samples at three different depths: 50-100, 300-400 and 500-600 cm to represent the peat properties within the peat profile using an auger with a core diameter of 5.6 cm. The 10 cm length peat sub-samples were extracted from the auger, wrapped using

aluminum foil and placed in a sealed Nasco whirl-pak®. These subsamples were transferred to the soil laboratory of Bogor Agricultural University for peat analysis that included: carbon concentration (C), bulk density, and ash content. Bulk density was defined as the ratio of the dry weight, which was determined after oven drying at 70 ^{o}C for 48 hours or until weight reached a constant value and the volume of the fresh sub-samples. Ash content was determined as the ratio between the weights after ashing at 550 ^{o}C and dry weight at 70 ^{o}C. The dry weight subsamples then were ground, homogenized, and analyzed for carbon and nitrogen concentration using a LECO TruSpec elemental CN analyzer (LECO Corp, St. Joseph, Michigan, USA). We also measured the saturated hydraulic conductivity at the same depth as the collected peat samples using the piezometer slug-test. Since the slug-test method measures the hydraulic conductivity below the water table and it was very difficult to find the drained sites with the water table close to surface, we decided to take the measurement below 50 cm. The detailed method of the used well design, slug-test procedures, and the Bouwer-Rice method used to calculate saturated hydraulic conductivity are detailed in the Chapter 2 of this dissertation.

4.2.4. Statistical Analysis

We evaluated the influence of the land cover, depth of measurement and their interaction on the electromagnetic wave velocity using a nested analysis of variance (ANOVA) with plots nested within sites. Here, the electromagnetic wave velocity and relative dielectric permittivity was treated as the dependent variable and the depth and land cover as independent variables. The ANOVA test was performed using the

lmerTest package implemented in R statistical software with the *p-value* and the degrees of freedom calculated using Satterthwate's approximation (Kuznetsova et. al. 2016).

The peat measurements made in multiple plots nested within a site were likely statistically dependent, precluding the use of traditional linear regression methods to evaluate the relationship between peat properties and relative dielectric permittivity. To evaluate whether spatial dependency presence in the peat properties (e.g., bulk density), we fitted ordinary linear regression models with peat properties as response variable and relative dielectric permittivity as predictor and plotted the model residual ordered by site. The plots indicated site-level dependence. To incorporate the site-to-site dependence, the relationship between peat properties (i.e., bulk density, carbon concentration, ash content, and saturated hydraulic conductivity) and relative dielectric permittivity was evaluated using hierarchical linear models. The hierarchical model incorporates the dependence among the individual plot measurements made at a site, which are defined as plot measurements (lower-level) nested within a site (upper-level) using random effects for the lower intercept and slopes (Raudenbush and Bryk 2002). In this study, the lower-level model for predicting the peat properties (e.g., bulk density, carbon concentration) treated the intercept (β_0) and the effect of relative dielectric permittivity, depth, or land cover types (β_1) as potentially varying among sites (j):

$$Y_{ij} = \beta_{0j} + \beta_{Pj}X_{Pij} + r_{ij},$$

where Y_{ij} is the dependent variable (e.g., bulk density) and X_P is the plot-level explanatory variables (*i.e.*, relative dielectric permittivity) measured in plot *i* at site *j*, and *r* are the residuals that are assumed normally distributed with a mean of zero (Raudenbush and Bryk 2002).

We used the information-theoretic approach described by Burnham and Anderson (2002) to evaluate the relative plausibility of models relating the relative dielectric permittivity to bulk density, ash content, carbon, carbon to nitrogen ratio, and saturated hydraulic conductivity. For each response, we developed some candidate global models by incorporating relative dielectric permittivity as predictor variable to find the best variance structure (i.e. the random effect). The lowest Akaike's Information Criteria (*AIC*; Akaike, 1973) with the small-sample bias adjustment (AIC_c; Hurvich & Tsai, 1989), which included both fixed and random effect was considered as the best approximating variance structure. Random effects related to peat properties were estimates of the predictable variability of the effect of a predictor among sites. We then used the best approximating variance structure in all candidate models relating the relative dielectric permittivity to peat properties as describe below. Prior to model selection, we fit a random effects ANOVA to partition variation in peat properties within and among sites. All models were fit using the *lmer* function in the R package *lme4* (Bates et al. 2015b).

Goodness-of-fit of all hierarchical models was evaluated by examining the residuals. Data that indicated violations of homogeneity assumptions were natural log transformed to meet assumptions.

The predictive ability of the best approximating peat characteristic models were evaluated using leave-one-site-out cross-validation in which the data were portioned into two parts: training and testing data. The relative dielectric permittivity for each site was removed from the data set and used as the testing data. The remaining data was set up as the training data that was used to predict the peat properties (e.g. bulk density). The root mean squared error (RMSE) was used to evaluate the model validation and calculated as:

$$RMSE(Y) = \sqrt{\frac{\sum_{i=1}^{n} \hat{Y}_i - Y_i}{n}}$$

where $\hat{Y}_i$ is the predicted peat properties in plot *i,* Y_i is measured peat properties and *n* is the number of plots.

4.3. Results

4.3.1. Electromagnetic wave velocity and relative dielectric permittivity

Based on the semblance analysis from GPR data recorded on one specific plot, the electromagnetic wave velocity varied within the profile (Figure 4.1). Across all sites, the electromagnetic wave velocity ranged from 0.033 to 0.125 m ns^{-1}. At both land cover types, the 75 cm depth electromagnetic wave velocities were significantly greater than those measured at 350 cm (Figure 4.2; DF = 45.2; t-value = 4.93; p-value < 0.0001) and 550 cm (DF = 9.5; t-value = 5.31; p-value = 0.0004). In contrast, the electromagnetic wave velocity at the depth of 75 cm in oil palm plantation was 0.067 ± 0.004 (mean ± S.E) and was significantly lower than from identical depth at seral sites (DF = 53; t-value = 2.08; p-value = 0.042). However, at

the deeper depth of 350 and 550 cm the electromagnetic wave velocity in oil palm plantation was similar to seral community sites.

The relative dielectric permittivity across all sites varied between 5.8 to 84.9 and were significantly lower at the 75 cm depth than those measured at 350 cm (Figure 4.2; DF = 35.4; t-value = 3.56; p-value = 0.0011) and 550 cm (DF = 8.9; t-value = 4.48; p-value = 0.0016). The relative dielectric permittivity was not significantly different between the two land cover types with the average of 34.4 ± 2.3 and 33.7 ± 2.6 for oil palm plantation and seral community, respectively.

4.3.2. Relationship between peat properties and relative dielectric permittivity

The ash content was greatly varied across all sites ranging from 0.6 to 66%. At the upper layer, 50 – 100 cm, ash content was significantly lower than 300 – 400 cm (p-value = 0.056) and 500 – 600 cm (p-value = 0.0108). The random effects ANOVA indicated that ash content varied about 45% among sites. The best variance structure to predict natural log transformed ash content contained an intercept and relative dielectric permittivity parameters that varied among sites. The model indicated that relative dielectric permittivity was positively and strongly related to ash content (Figure 4.3) shown by the confidence interval of coefficient that did not include zero (Table 4.1). The relative dielectric permittivity model explained 20.8% of the variability in natural log transformed ash content. The relative dielectric permittivity random effect indicated that the relationship between relative dielectric permittivity and natural log transformed ash content varied by about 43%

(0.0087/0.0203) among sites (Table 4.1). In addition, the ability of this model to predict ash content was good depicted by the model RMSE of 1.24 (Table 4.2) that was about half of the average of observed natural log transformed ash content (2.14) and it was similar with the coefficient variability of log transformed ash content (57%).

Across all sites, the bulk density was varied between 0.047 to 0.335 g cm^{-3}. The bulk density at the 50-100 was significantly lower than those measured at 500 -600 cm (p-value = 0.0008). However, bulk density at 50-100 cm was not significantly different from 300 – 400 cm (p-value = 0.139). The random effects ANOVA indicated that the variability in bulk density within-site was much greater than among sites and constituted 85.6% of the variation. The random effect of the best approximating model contained intercept and relative dielectric permittivity coefficient that varied among sites. The hierarchical model parameters indicated that relative dielectric permittivity was positively related to bulk density. However, this relationship was weak and imprecise shown by the small coefficient with the confidence interval spanned zero (Table 4.1). In addition, the influence of relative dielectric permittivity varied site by site shown by the different model slope and intercept (Figure 4.4) in average of 87.7% among sites. The variability of bulk density that can be explained relative dielectric permittivity both fixed and random effect was 14.4%. The prediction error of this model with RMSE of 0.054 g cm^{-3} (Table 4.2) relative to the mean of measured bulk density of 0.128 g cm^{-3} which is similar with the bulk density variability of 41%. It indicates that this model was relatively good for predicting bulk density. Therefore, by using the GPR setting used in our study, i.e.

using 100 MHz unshielded antennas; the estimated bulk density using GPR falls within the range of the measured bulk density variability.

The carbon content across all sites was varied between 15 to 57%. The ANOVA indicated that the carbon content at the uppermost layer (50-100 cm) was significantly higher than those from 300 – 400 cm (p-value = 0.0091) and 500 – 600 cm (p-value = 0.0001). The random effect ANOVA showed that the variability of carbon concentration among sites was low and was estimated to constitute only 6% of the variation in carbon concentration. A model with varying intercept and relative dielectric permittivity parameters among sites was included as the best fitting variance structure of hierarchical model. The parameter estimates from the best approximating model indicated that carbon concentration was negatively relative dielectric permittivity (Figure 4.5). The effect of relative dielectric permittivity was precise shown by the confidence interval that did not include zero (Table 4.1). However, the influence of relative dielectric permittivity on carbon content varied considerably among sites as much as 65.5% (0.126/0.193). Both fixed and random effects of the model explained only 17.3% of the variability of carbon concentration. The prediction error of this model expressed by RMSE of 0.115 indicated that the ability of this model to predict carbon concentration was relatively better than other model predictions. It is depicted by the error of predicted carbon content was about 26% (0.115/0.436) of the observed carbon content which is about the same with the observed carbon content variability.

The random effects ANOVA indicated that the variability of saturated hydraulic conductivity among sites was low in amount of only 26.7% of variation in which

across all sites it varied between 0.001 to 4.3 m day^{-1}. The best variance structure to predict natural log transformed saturated hydraulic conductivity contained model intercept and relative dielectric permittivity that varied among sites. The model indicated that the influence of relative dielectric permittivity was, on average, weak and imprecise as shown by the small parameter estimate and 90% confidence interval that was wide and included zero (Table 4.1). The relationship between relative dielectric permittivity and natural log transformed saturated hydraulic conductivity also varied among sites as much as 128% with hydraulic conductivity in some sites decreased with increasing relative dielectric permittivity but for the remaining sites the relationship was positive (Figure 4.6). The prediction error of log transformed saturated hydraulic conductivity presented by RMSE was 1.3 which is about 46% of the mean observed saturated hydraulic conductivity and was lower than variability of log transformed saturated hydraulic conductivity (60%). It indicates that relative dielectric permittivity is a good predictor for estimating saturated hydraulic conductivity.

4.4. Discussion

The estimation of electromagnetic wave velocity is crucial since it is used to convert the two-way-travel-time recorded by GPR to depth information, which is required to locate the specific peat characteristic within the profile. This suggests that GPR is a useful tool for estimating the position of clay mineral layer, certain peat characteristics, and degree of decomposition at a 2-D space in peatlands (e.g. Plado et al. 2011; Parsekian et al. 2012b; Parry et al. 2014). There are few published

values of electromagnetic wave velocity in peatlands and fewer still for the relative dielectric permittivity in tropical peatlands. We found that in tropical peatlands, the wave velocity decreased as the depth increased with the average of 0.038 ± 0.002 m ns^{-1} or equivalent to a relative dielectric permittivity of 6 to 85. These estimates were similar with those estimated from the northern boreal peatlands (Parry et al. 2014). This suggests that peat properties in our site were likely similar to the northern boreal peatlands sites since the electromagnetic wave velocity and relative dielectric permittivity are primarily controlled by water content (Neal 2004).

We also estimated that the electromagnetic wave velocity in oil palm plantation and seral community sites at the upper layer (50-100 cm depth) were significantly greater than velocity estimated from the deeper layer (> 300 cm depth). This is likely due to the different peat water content of both land cover types within the peat profile. At the upper layer, the peat moisture content is likely lower than the deeper layer depending on the water table position. Since lower peat water content was associated with lower relative dielectric permittivity (Neal 2004; Kettridge et al. 2008; Parsekian et al. 2012a), the wave velocity is greater at that layer.

The tropical peatland development initiated over a thousands of years ago (Yu et al. 2010; Dommain et al. 2011, 2014) likely generated the varying peat characteristics within the profile (Shimada et al. 2001; Anshari et al. 2004; Page et al. 2004). The peat forest conversion followed by drainage canal ditching also likely altered both physical and chemical peat properties (Muniandy et al. 2009; Anshari et al. 2010; Könönen et al. 2015). Because peat properties varied across different land cover types and the peat profile, we expected that these properties would be

strongly related to relative dielectric permittivity. For example, the ash content and bulk density at deeper layers in the peat profile are likely greater than the upper layer due to the mixing that occurs between clay and organic matter in the deeper layer especially at the transition zone between peat and clay layer (e.g. Basuki 2017). Assuming peat is in a saturated condition, peat with lower ash content, which also has lower bulk density, tends to has higher water content and thus, has higher relative dielectric permittivity. However, our results indicated the relationship between relative dielectric permittivity and bulk density was positive, on average, but inconclusive as shown by confidence interval of bulk density coefficient spanned to zero. This is likely due to the low variability of bulk density measured in our sites at three depth interval that only varied about 14.4 %. In contrast, ash content was much more variable from site to site and its relationship with relative dielectric permittivity was much stronger and positive. Yet, relationship between relative dielectric permittivity and ash content varied among sites. This is likely due to the fact that peat with higher ash content tends to have a greater proportion of micro- and meso-porosity (Chapter 3) and thus, it has relatively lower water content (i.e., different dielectric permittivity). In addition, our results suggest that GPR also could be used to estimate carbon content suggested by the relatively low prediction error, RMSE relative to the variability of observed carbon content.

The relatively good ability of the GPR to estimate carbon content, bulk density, and ash content found in our study could enhance previous research in which GPR had been utilized to determine peat depth in tropical peatlands (Comas et al. 2015). This suggests that the GPR can be used as an alternative method to estimate the

carbon stored in peatlands by combining estimated bulk density, carbon content and peat depth. In addition, the ease at which GPR data are collect suggests that it can also be applied not only for the site-level measurements but also for larger scale measurements, e.g., for estimating the peat depth and peat volume for the whole dome continuously (Parry et al. 2014). Thus, GPR could add information related to peat properties in addition to existing peat depth information in the peatlands maps at regency, province or national scales in Indonesia (see Wahyunto et. al. 2003; Haryono et. al. 2011; Warren et. al. 2017). However, traditional surveys (e.g., sampling with a core) will also need to be implemented to incorporate the spatial variation and to calibrate the GPR to obtain more precise and better quality.

The gas content located in the saturated zone of the peat profile not only affects the greenhouse gas emission but also peat hydrological condition. A high gas content in the saturated zone of peat profiles could reduce the saturated hydraulic conductivity (Reynolds et al. 1992; Beckwith and Baird 2001). This also was observed in our study in which the hydraulic conductivity at the deeper layer was lower than conductivity measured in the upper layer of profile with the two order of magnitude difference, although the bulk density of those layers were similar. Using the estimated gas content along the peat profile based on the relative dielectric permittivity, the water content can also be calculated as the balance between porosity and gas content (Huisman et al. 2003). Our results indicated that in the saturated zone, the average peat water content was less than 80% (Figure 4.8) which is lower than the saturated water content estimated from the undrained forested sites (Chapter 3). This suggests that the peat water content in the saturated

zone is not only determined by the bulk density, which is frequently estimated as the same as total peat porosity, but also by the gas content. Therefore, gas content should also be taken into account when estimating water storage in the peat dome to provide a better understanding of this important ecological service.

4.5. Conclusions

This is the first study to explore the potential to estimate peat physical and chemical properties using a GPR, a noninvasive geophysical method in tropical peatlands. Our results indicated that the ability of relative dielectric permittivity to estimate ash content, carbon content, bulk density and saturated hydraulic conductivity was relatively good based on the cross-validation error estimates. It suggests that GPR method can be utilized to develop the map of peatland distribution in which it will not only provide the information of peat depth but also other peat properties such as carbon stock, the degree of decomposition, and the ability of water to transmit water. However, the relationship between relative dielectric permittivity and bulk density and saturated hydraulic conductivity was highly varied among sites. Together, these suggest that the application of GPR to estimate peat properties should be combined with conventional methods requiring peat coring to incorporate the spatial variability and calibrate the GPR measurements.

We also investigated the ability to estimate water content within the peat profile using the relative dielectric calculated from the GPR data. Our results indicated that gas accumulation occurred in the saturated zone of peat profile, which reduced the

water content in that zone. Future studies should evaluate the ability of the GPR to estimate gas content by collecting the gas samples and comparing known and GPR estimates. This will allow the composition of the gas trapped in the peat can (e.g. CH_4, CO_2) to be determined so that the important link between the low methane emission from the tropical peatlands (Jauhiainen and Takahashi 2005; Couwenberg et al. 2009) and the gas content in peat profile can be assessed. We also believe that it is important to conduct GPR surveys during multiple seasons (e.g., dry and rainy season) at the same site since it can be used to monitor the temporal variation of gas and water content in the peat profile. With this information, the connection between the water content dynamics and methane accumulation as well as the paths of its emission (ebullition, diffusion, and plants vascular) can be appraised.

References:

Akaike H (1973) Information theory and an extension of the maximum like- lihood principle. In: Petrov B, Csaki F (eds) Second International Symposium on Information Theory. Akademiai Kiado, Budapest, Hungary, pp 267–281.

Anshari G, Kershaw AP, Van Der Kaars S, Jacobsen G (2004) Environmental change and peatland forest dynamics in the Lake Sentarum area, West Kalimantan, Indonesia. J Quat Sci 19:637–655. doi: 10.1002/jqs.879.

Anshari GZ, Afifudin M, Nuriman M, et al (2010) Drainage and land use impacts on changes in selected peat properties and peat degradation in West Kalimantan Province, Indonesia. Biogeosciences 7:3403–3419. doi: 10.5194/bg-7-3403-2010.

Basuki I (2017) Carbon dynamics in response to land cover change in tropical peatland, Kalimantan, Indonesia. PhD thesis. Oregon State University.

Bates D, Mächler M, Bolker B, Walker S (2015) Fitting Linear Mixed-Effects Models Using **lme4**. J Stat Softw 67:1–48. doi: 10.18637/jss.v067.i01.

Beckwith CW, Baird AJ (2001) Effect of biogenic gas bubbles on water flow through poorly decomposed blanket peat. Water Resour Res 37:551–558.

Burnham K, Anderson D (2002) Model Selection and Inference: An Information-theoretic Approach, 2nd edition. Springer-Verlag, New York.

Comas X, Kettridge N, Binley A, et al (2014) The effect of peat structure on the spatial distribution of biogenic gases within bogs. Hydrol Process 28:5483–5494. doi: 10.1002/hyp.10056.

Comas X, Slater L (2007) Evolution of biogenic gases in peat blocks inferred from noninvasive dielectric permittivity measurements. Water Resour Res 43:1–10. doi: 10.1029/2006WR005562.

Comas X, Slater L, Reeve A (2005a) Spatial variability in biogenic gas accumulations in peat soils is revealed by ground penetrating radar (GPR). Geophys Res Lett 32:1–4. doi: 10.1029/2004GL022297.

Comas X, Slater L, Reeve A (2008) Seasonal geophysical monitoring of biogenic gases in a northern peatland: Implications for temporal and spatial variability in free phase gas production rates. J Geophys Res Biogeosciences 113:1–12. doi: 10.1029/2007JG000575.

Comas X, Slater L, Reeve A (2005b) Geophysical and hydrological evaluation of two bog complexes in a northern peatland: Implications for the distribution of biogenic gases at the basin scale. Global Biogeochem Cycles 19:1–10. doi: 10.1029/2005GB002582.

Comas X, Slater LD (2013) Noninvasive Field-Scale Characterization of Gaseous-Phase Methane Dynamics in Peatlands Using the Ground-Penetrating Radar Method. Carbon Cycl North Peatlands 159–171. doi: 10.1029/2008GM000810.

Comas X, Terry N, Slater L, et al (2015) Imaging tropical peatlands in Indonesia using ground penetrating radar (GPR) and electrical resistivity imaging (ERI): implications for carbon stock estimates and peat soil characterization. Biogeosciences Discuss 12:191–229. doi: 10.5194/bgd-12-191-2015.

Couwenberg J, Dommain R, Joosten H (2009) Greenhouse gas fluxes from tropical peatlands in south-east Asia. Glob Chang Biol 16:1715–1732. doi: 10.1111/j.1365-2486.2009.02016.x.

Dommain R, Couwenberg J, Glaser PH, et al (2014) Carbon storage and release in Indonesian peatlands since the last deglaciation. Quat Sci Rev 97:1–32. doi: 10.1016/j.quascirev.2014.05.002.

Dommain R, Couwenberg J, Joosten H (2011) Development and carbon sequestration of tropical peat domes in south-east Asia: links to post-glacial sea-level changes and Holocene climate variability. Quat Sci Rev 30:999–1010. doi: 10.1016/j.quascirev.2011.01.018.

Gómez-Ortiz D, Martín-Crespo T, Martín-Velázquez S, et al (2010) Application of ground penetrating radar (GPR) to delineate clay layers in wetlands. A case study in the Soto Grande and Soto Chico watercourses, Do??ana (SW Spain). J Appl Geophys 72:107–113. doi: 10.1016/j.jappgeo.2010.07.007.

Haryono, Sarwani M, Ritung S, et al. (2011) Peatland Map of Indonesia. Center for Research and Development of Agricultural Land Resources, Agricultural Research and Development Agency, Indonesia Ministry of Agriculture. Bogor, Indonesia.

Holden J, Smart RP, Chapman PJ, et al (2013) The Role of Natural Soil Pipes in Water and Carbon Transfer in and from Peatlands. Carbon Cycl North Peatlands 251–264. doi: 10.1029/2008GM000804.

Hooijer A, Page S, Jauhiainen J, et al (2012) Subsidence and carbon loss in drained tropical peatlands. Biogeosciences 9:1053–1071. doi: 10.5194/bg-9-1053-2012.

Huisman JA, Hubbard SS, Redman JD, Annan AP (2003) Measuring Soil Water Content with Ground Penetrating Radar: A Review. Vadose Zo J 2:476–491. doi: 10.2113/2.4.476.

Hurvich CM, Tsai C-L (1989) Regression and time series model selection in small samples. Biometrika 76:297–307. doi: 10.1093/biomet/76.2.297.

Jacob RW, Urban TM (2016) Ground-Penetrating Radar Velocity Determination and Precision Estimates Using Common-Midpoint (CMP) Collection with Hand-Picking, Semblance Analysis and Cross-Correlation Analysis: A Case Study and Tutorial for Archaeologists. Archaeometry 58:987–1002. doi: 10.1111/arcm.12214.

Jauhiainen J, Takahashi H (2005) Carbon fluxes from a tropical peat swamp forest floor. Glob Chang Biol 11:1788–1797. doi: 10.1111/j.1365-2486.2005.01031.x.

Kettridge N, Comas X, Baird A, et al (2008) Ecohydrologically important subsurface structures in peatlands revealed by ground-penetrating radar and complex conductivity surveys. J Geophys Res Biogeosciences 113:1–15. doi: 10.1029/2008JG000787.

Könönen M, Jauhiainen J, Laiho R, et al (2015) Physical and chemical properties of tropical peat under stabilised land uses. Mires Peat 16:1–13.

Kool DM, Buurman P, Hoekman DH (2006) Oxidation and compaction of a collapsed peat dome in Central Kalimantan. Geoderma 137:217–225. doi: 10.1016/j.geoderma.2006.08.021.

Kuznetsova A, Brockhoff PB, Christensen RHB (2016). lmerTest: Tests in Linear Mixed Effects Models. R package version 2.0-33. https://CRAN.R-project.org/package=lmerTest.

Melling L, Hatano R, Goh K (2005) Methane fluxes from three ecosystems in tropical peatland of Sarawak, Malaysia. Soil Biol Biochem 37:1445–1453. doi: 10.1016/j.soilbio.2005.01.001.

Miettinen J, Shi C, Liew SC (2012) Two decades of destruction in Southeast Asia's peat swamp forests. Front Ecol Environ 10:124–128. doi: 10.1890/100236.

Miettinen J, Shi C, Liew SC (2016) Land cover distribution in the peatlands of Peninsular Malaysia, Sumatra and Borneo in 2015 with changes since 1990. Glob Ecol Conserv 6:67–78. doi: 10.1016/j.gecco.2016.02.004.

Muniandy M, Ahmed OH, Majid NMA, Yusop MK (2009) Effects of Converting Secondary Forest to Oil Palm Plantation on Peat Soil Carbon and Nitrogen and other Soil Chemical Properties. Am J Environ Sci 5:406–412. doi: 10.3844/ajessp.2009.406.412.

Murdiyarso D, Donato D, Kauffman JB, et al (2009) Carbon storage in mangrove and peatland ecosystems: A preliminary account from plots in Indonesia. Bogor, Indonesia.

Neal A (2004) Ground-penetrating radar and its use in sedimentology: Principles, problems and progress. Earth-Science Rev 66:261–330. doi: 10.1016/j.earscirev.2004.01.004.

Page SE, Rieley JO, Banks CJ (2011) Global and regional importance of the tropical peatland carbon pool. Glob Chang Biol 17:798–818. doi: 10.1111/j.1365-2486.2010.02279.x.

Page SE, Siegert F, Rieley JO, et al (2002) The amount of carbon released from peat and forest fires in Indonesia during 1997. Nature 1999:61–65. doi: 10.1038/nature01141.1.

Page SE, Wűst R a. J, Weiss D, et al (2004) A record of Late Pleistocene and Holocene carbon accumulation and climate change from an equatorial peat bog(Kalimantan, Indonesia): implications for past, present and future carbon dynamics. J Quat Sci 19:625–635. doi: 10.1002/jqs.884.

Parry L, West L, Holden J, Chapman P (2014) Evaluating approaches for estimating peat depth. J Geophys Res Biogeosciences 119:567–576. doi: 10.1002/2013JG002411.Received.

Parsekian AD, Slater L, Comas X, Glaser PH (2010) Variations in free-phase gases in peat landforms determined by ground-penetrating radar. J Geophys Res Biogeosciences 115:1–13. doi: 10.1029/2009JG001086.

Parsekian AD, Slater L, Giménez D (2012a) Application of ground-penetrating radar

to measure near-saturation soil water content in peat soils. Water Resour Res 48:1–9. doi: 10.1029/2011WR011303.

Parsekian AD, Slater L, Ntarlagiannis D, et al (2012b) Uncertainty in Peat Volume and Soil Carbon Estimated Using Ground-Penetrating Radar and Probing. Soil Sci Soc Am J 76:1911. doi: 10.2136/sssaj2012.0040.

Plado J, Sibul I, Mustasaar M, Jõeleht a (2011) Ground-penetrating radar study of the Rahivere peat bog, eastern Estonia. Est J Earth Sci 60:31. doi: 10.3176/earth.2011.1.03.

Proulx-McInnis S, St-Hilaire A, Rousseau a. N, Jutras S (2013) A review of ground-penetrating radar studies related to peatland stratigraphy with a case study on the determination of peat thickness in a northern boreal fen in Quebec, Canada. Prog Phys Geogr 37:767–786. doi: 10.1177/0309133313501106.

Raudenbush SW, Bryk AS (2002) Hierarchical linear models: Applications and data analysis methods, 2nd editio. Sage Publications, Thousand Oaks.

Reynolds WD, Brown DA, Mathur SP, Overend RP (1992) Effect of in-situ gas accumulation on the hydraulic conductivity of peat. Soil Sci 135:397–408.

Shimada S, Takahashi H, Haraguchi A, Kaneko M (2001) The carbon content characteristics of tropical peats in Central Kalimantan, Indonesia: Estimating their spatial variability in density. Biogeochemistry 53:249–267.

Taufik M, Torfs PJJF, Uijlenhoet R., et al. (2017) Amplification of wildfire area burnt by hydrological drought in the humid tropics. Nat Clim Chang. doi: 10.1038/nclimate3280.

Wahyunto, Ritung S., Subagjo H. (2003) Maps of area of peatland distribution and carbon content in Sumatra, 1990–2002. Wetlands International-Indonesia Programme & Wildlife Habitat Canada (WHC), Bogor.

Warren MW, Kauffman JB, Murdiyarso D, et al (2012) A cost-efficient method to assess carbon stocks in tropical peat soil. Biogeosciences 9:4477–4485. doi: 10.5194/bg-9-4477-2012.

Yu Z, Loisel J, Brosseau DPDP, et al (2010) Global peatland dynamics since the Last Glacial Maximum. Geophys Res Lett 37:L13402. doi: 10.1029/2010GL043584.

Figures

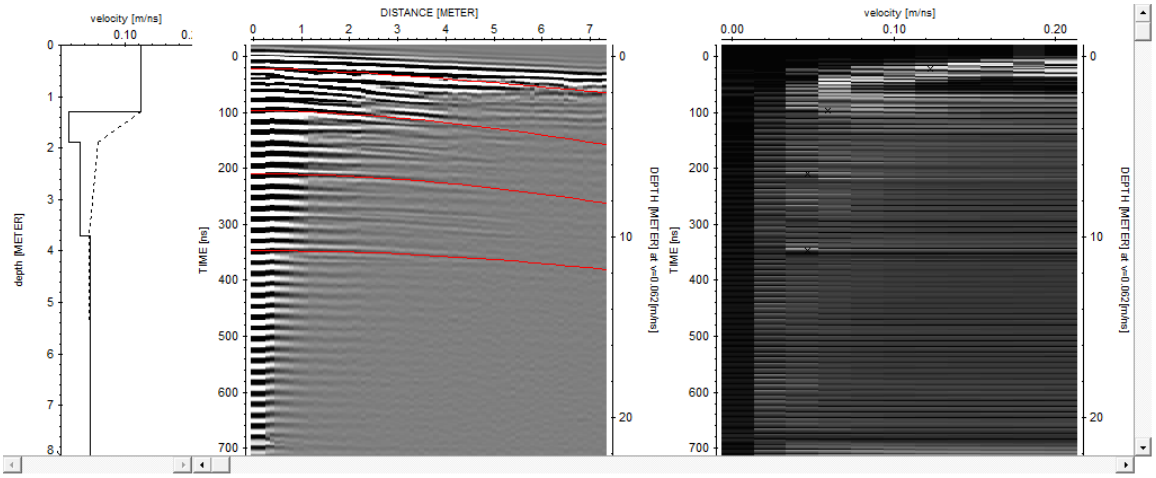

Figure 4.1. The calculated one-dimension electromagnetic wave velocity (left) based on the common midpoint ground penetrating radar survey using 100 MHz antennas (center) and semblance analysis (right). Dashed and solid lines represent root mean squared and interval velocity, respectively. The red line represents the hyperbolae reflection based on the manually picked local maxima semblance. Black and white spectrum in semblance analysis represent low and high semblance.

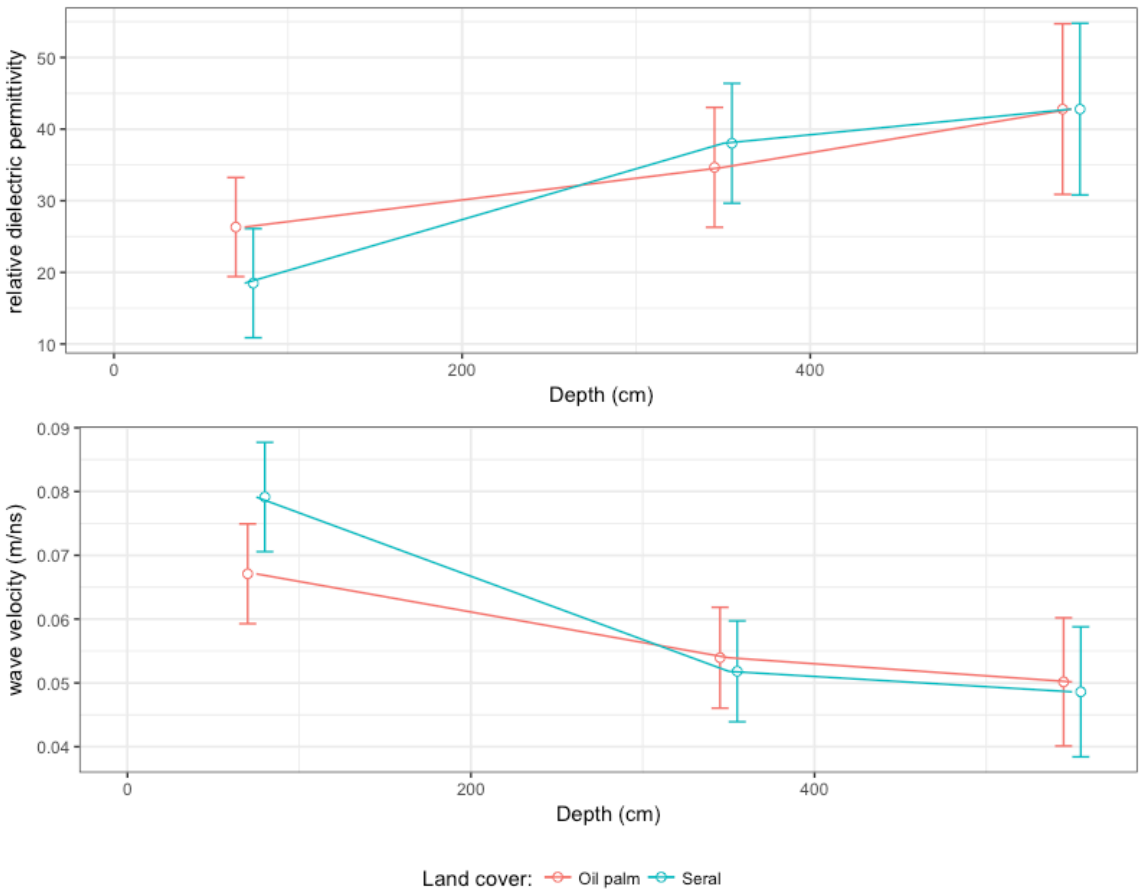

Figure 4.2. The mean relative dielectric permittivity (top) and electromagnetic wave velocity in oil palm plantation and seral community. Error bars represent the 90% confidence interval.

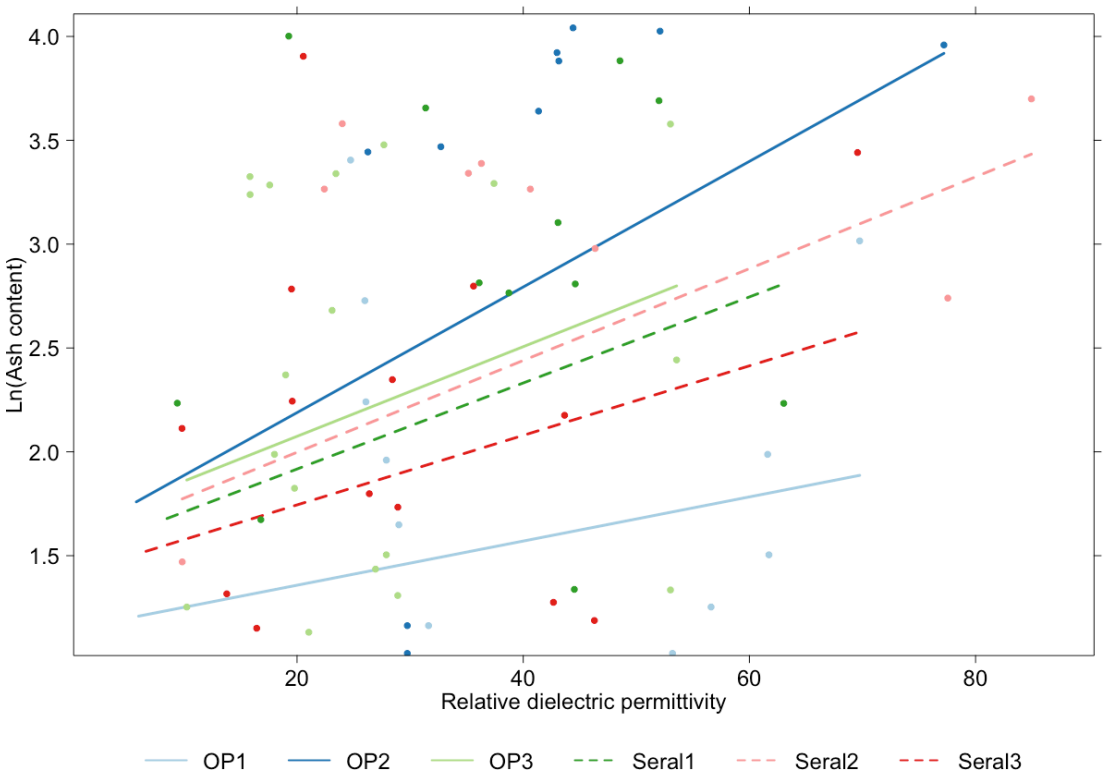

Figure 4.3. The estimated ash content under varying relative dielectric permittivity for six sites in oil palm plantation (OP) and seral community.

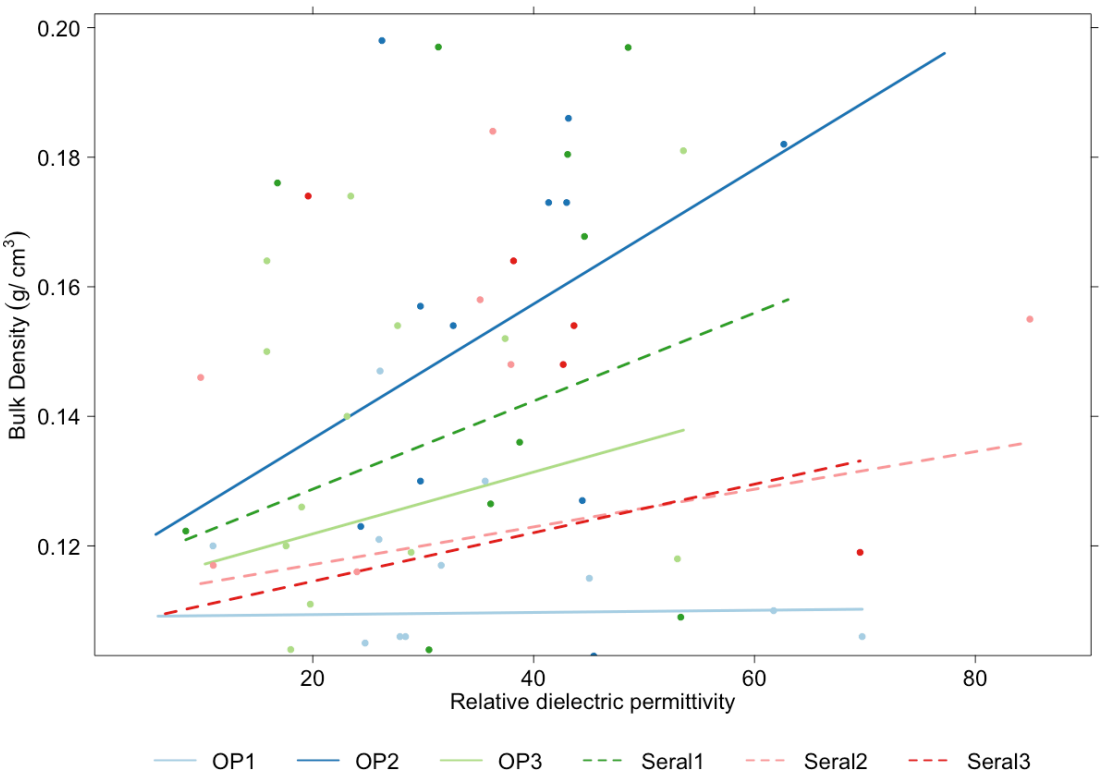

Figure 4.4. The estimated bulk density under varying relative dielectric permittivity for six sites in oil palm plantation (OP) and seral community

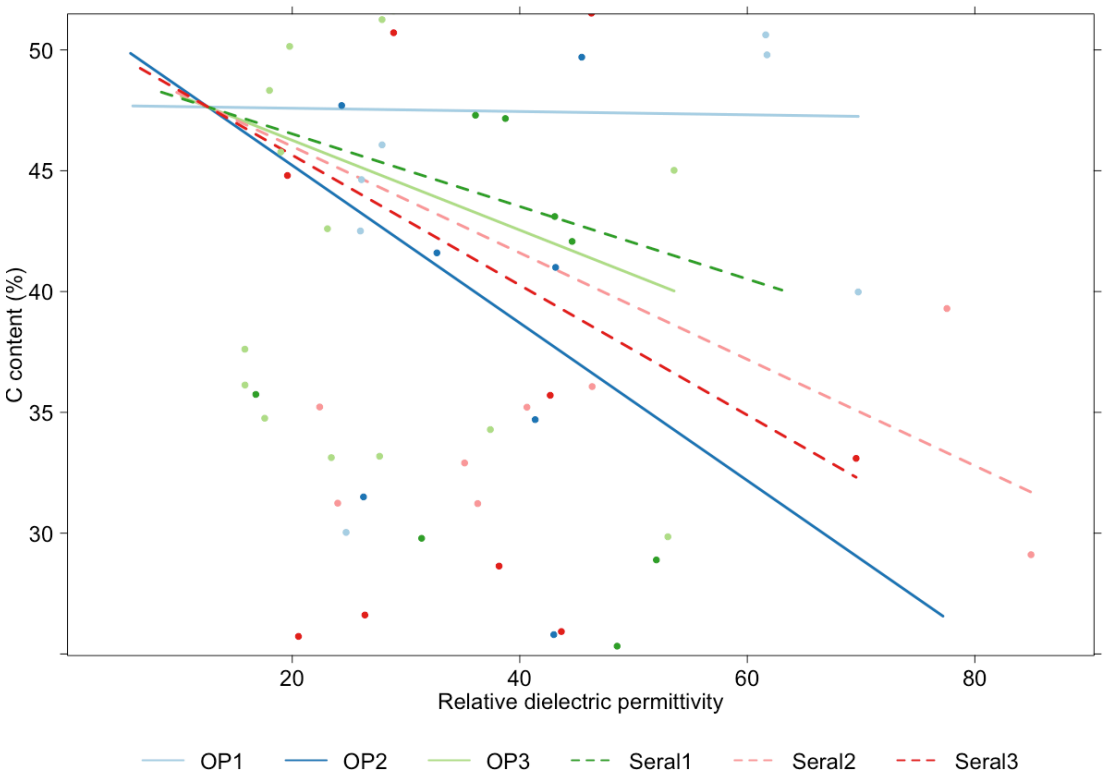

Figure 4.5. The estimated carbon concentration under varying relative dielectric permittivity for six sites in oil palm plantation (OP) and seral community.

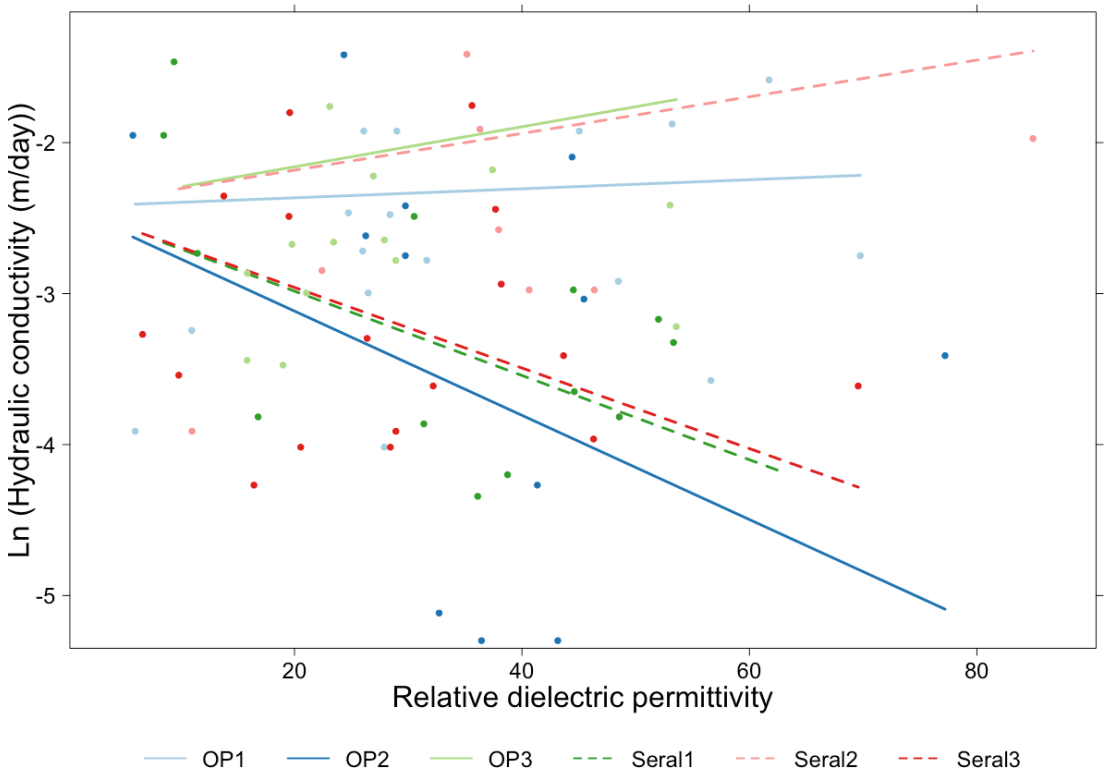

Figure 4.6. The estimated saturated hydraulic conductivity under varying relative dielectric permittivity for six sites in oil palm plantation (OP) and seral community.

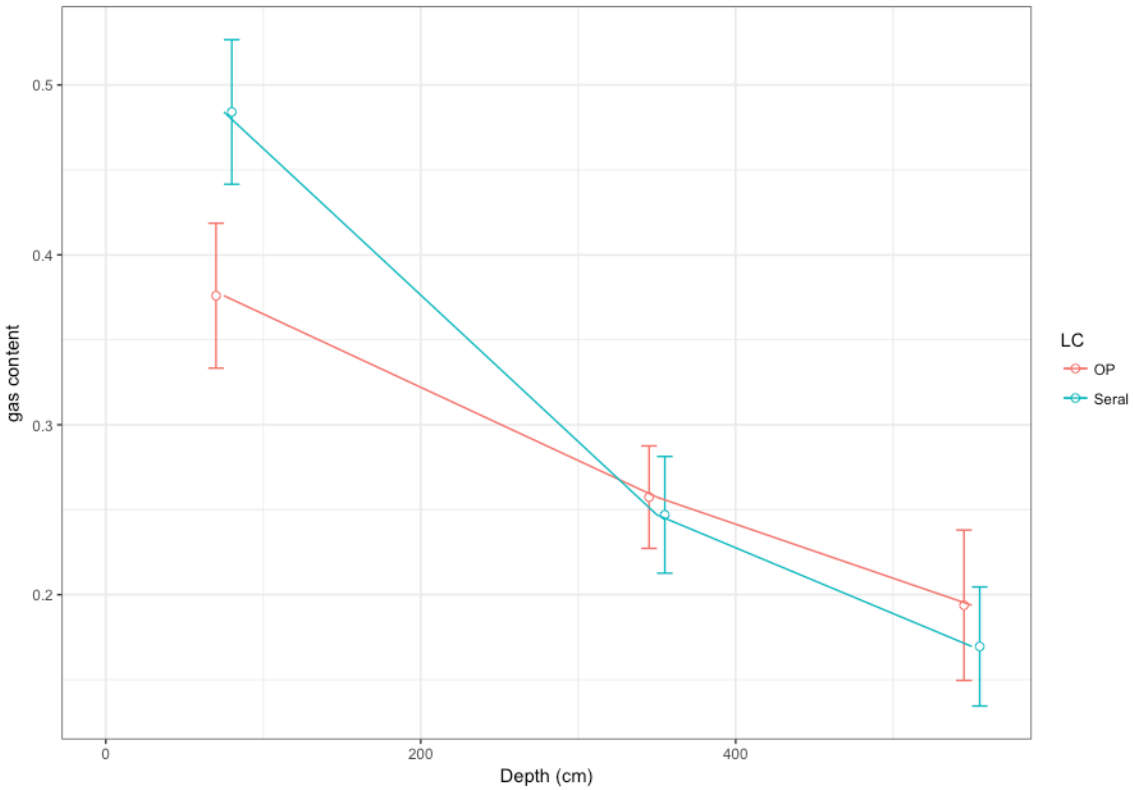

Figure 4.7. The estimated gas content using the complex refractive index model within the peat profile at three different depth in oil palm plantation (OP) and seral community sites. Error bars represent the standard error. CRIM was used by assuming the water and gas relative dielectric permittivity are 0 and 80, respectively.

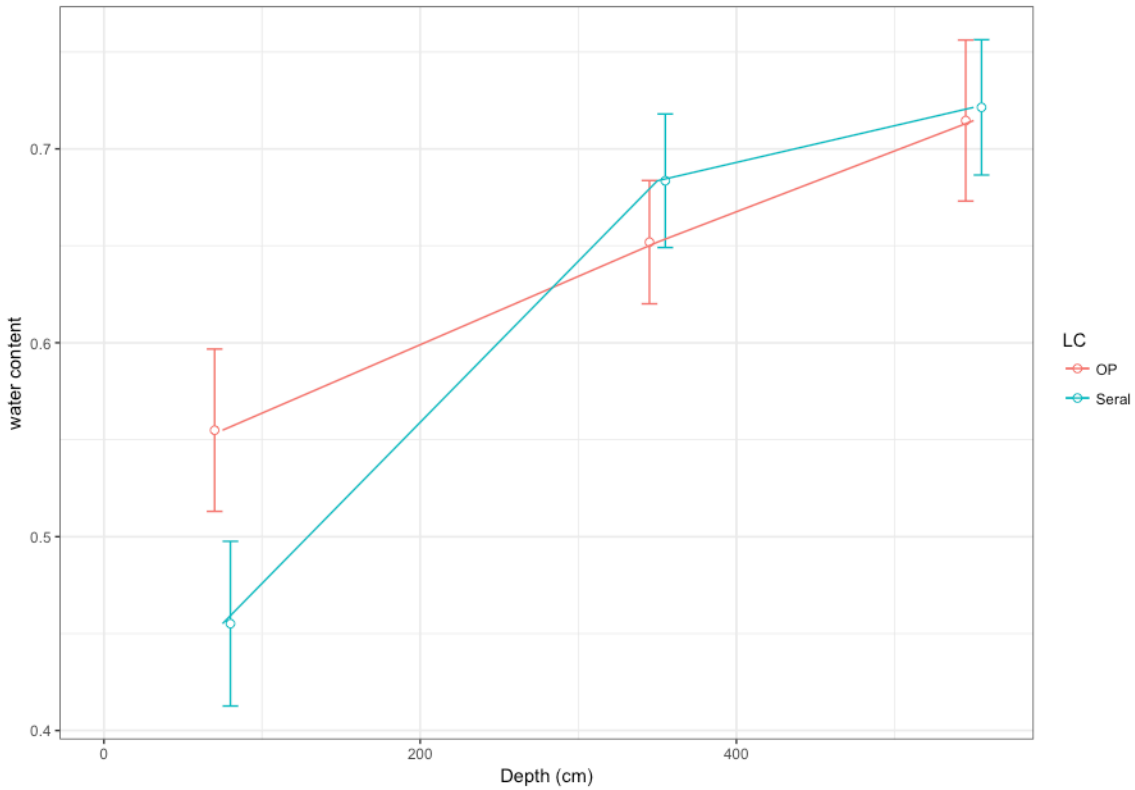

Figure 4.8. The estimated water content at three different depth in oil palm plantation (OP) and seral community sites. The water content is estimated as the difference between porosity and gas content. Error bars represent the standard error.

TABLES

Table 4.1. Estimates of fixed and random effects, their standard error (S.E), 90% lower (LCL) and upper confidence interval (UCL) for the best-approximating models in predicting ash content, bulk density, carbon content, and saturated hydraulic conductivity. Random effects are standard deviation estimates.

Parameter estimates			90% confidence interval	
	Estimate	S.E	LCL	UCL
		Ash content		
Fixed effect				
Intercept	1.473	0.274	0.997	1.954
Relative dielectric permittivity	0.020	0.007	0.007	0.033
Random effect				
Intercept	0.276			
Relative dielectric permittivity	0.009			
Residual	1.083			
		Bulk density		
Fixed effect				
Intercept	0.112	0.011	0.093	0.133
Relative dielectric permittivity	0.0005	0.0003	0.0001	0.001
Random effect				
Intercept	0.008			
Relative dielectric permittivity	<0.001			
Residual	0.048			
		Carbon concentration		
Fixed effect				
Intercept	50.068	2.467	45.867	54.282
Relative dielectric permittivity	-0.193	0.082	-0.341	-0.045
Random effect				
Intercept	1.594			
Relative dielectric permittivity	0.126			
Residual	10.417			
		Saturated hydraulic conductivity		
Fixed effect				
Intercept	-2.426	0.320	-2.959	-1.893
Relative dielectric permittivity	-0.010	0.012	-0.031	0.011
Random effect				
Intercept	<0.001			
Relative dielectric permittivity	0.022			
Residual	1.381			

Table 4.2. The amount of variability of each response variables that can be explained by fixed effect only (R^2_m) and both fixed and random effect (R^2_c) of relative dielectric permittivity and root mean squared error (RMSE) generated by cross-validation.

Model	R^2_m(%)	R^2_c(%)	RMSE
Ln(Ash) ~ permittivity	8.3	20.8	1.24
Bulk density ~ permittivity	2.6	14.4	0.05 g cm^{-3}
Carbon concentration ~ permittivity	8.5	17.3	11.55%
Ln(K_s) ~ permittivity	6.2	39.1	1.73

Note: Ln is natural logarithmic; *Ash* is ash content; permittivity is relative dielectric permittivity, and K_s is saturated hydraulic conductivity.

CHAPTER 5. GENERAL CONCLUSIONS

With respect to water movement through peat, peat total porosity can be classified into two components: macro-porosity where the most of the water transmission occurs and the closed, dead-end, micro-porosity where water movement has been previously found to be negligible (Rezanezhad et al. 2016). The results in chapter 2 indicated that hydraulic conductivity decreased with increasing the degree of decomposition. I also found that saturated hydraulic conductivity in the upper layer of undrained forested sites were greater than those measured in drained sites, such as recently burnt forest, oil palm plantation and seral community sites which suggests that the deforestation led to a decrease in saturated hydraulic conductivity that occurred primarily in the upper portion of peat profile. Therefore, when the undrained forested sites converted to other land cover types, followed by drainage canal development, the high discharge of groundwater will likely be produced due to the higher saturated hydraulic conductivity. I hypothesize that the observed negative relationship between peat decomposition state and saturated hydraulic conductivity is due, in part, to the loss of macro-porosity associated with peat decomposition since as peat decomposes, microbial activities digest the organic material and reduce the portion of the macro-porosity of peat (Rizzuti et al. 2004). This hypothesis is supported by the results of chapter 3 in which the proportion of macro-porosity, which was determined by the difference in total porosity and water content at the pressure head of 100 cm in drained-seral community, was smaller than those from undrained forested sites. In addition, macro-porosity was strongly

and positively related with bulk density, whereas bulk density was negatively related to fiber content (i.e., peat with low fiber content is classified as less decomposed).

In chapter 2, I also found a strong negative relationship between saturated hydraulic conductivity and depth, but only in forested sites, where I estimated two orders of magnitude difference in saturated hydraulic conductivity between upper and deeper layer. However, in drained-non forested sites, saturated hydraulic conductivity was constantly low and less dependent on depth, suggesting that the peat forest conversion only reduced the saturated hydraulic conductivity at the upper layer of peat profile. I hypothesized the lower saturated hydraulic conductivity in the disturbed non-forest sites, and the deeper layer of peat profile for all land cover types is, in part, due to gas accumulation as a byproduct of decomposition process in the saturated zone (Comas et al. 2014). The presence of gas in the saturated zone of peat profile probably inhibits water movement within the substrate (Reynolds et al. 1992; Fry et al. 1997b; Beckwith and Baird 2001). This hypothesis is supported by the estimated gas accumulation within the peat profile that was detected using common midpoint survey with a ground penetrating radar as reported in chapter 4. The results indicated that the biogenic gas was accumulated in the saturated zone of peat profile up to about 30%, which probably hindered water movement and, in turn, reduced the saturated hydraulic conductivity.

The two-layer peat profile system (i.e., acrotelm and catotelm) has been widely used to describe the biogeochemical and hydrological condition in northern

temperate or boreal peatland ecosystems. Acrotelm is located at the uppermost of peat profile with higher saturated hydraulic conductivity and the fluctuation of water table is mostly occurred in that zone. Meanwhile, the catotelm zone is fully saturated at most of the time (Holden 2005). I estimated about two orders of magnitude difference in the saturated hydraulic conductivity between upper and the deeper layer in forested peatland, which is consistent with the acrotelm-catotelm system applied in northern boreal peatlands. Although I did not measure saturated hydraulic conductivity in strata that was very close the peat surface (< 50 cm), I expect that saturated hydraulic conductivity in that zone is greater than our shallowest measurements since the peat porosity was likely dominated by macro-porosity. Conversely, the deeper zone is characterized by lower saturated hydraulic conductivity and greater portion of meso and micro-porosity. Therefore, the acrotelm-catotelm system could also applied in the tropical peatlands to obtain better understanding the eco-hydrology in that ecosystem.

The undrained peat swamp forest especially at the upper layer was primarily composed by less decomposed organic matter with greater saturated hydraulic conductivity (Chapter 2). It also was dominated by macro-porosity that easily released water when the water table decreased from the saturated condition, as depicted by higher α shape parameter of van Genuchten model (Chapter 3). For the application to peatland management practices, those results suggested that conserving peat swamp forest and maintaining high water table is essential for avoiding the loss of water content from peat. When undrained peatlands are converted to other land cover types and drained by canal development, the water

table drops and increases the pressure head (more negative pressure) at the peat surface. The greater α shape parameter suggests that water loss from the peat is likely initiated after only a few centimeters drop in the water table. Therefore, a substantial amount of water likely drains from the peat due to the higher saturated hydraulic conductivity. The accompanying drying out of the upper layers of the peat then accelerates the decomposition process increasing peat bulk density and reducing the water holding capacity of the peat. This loss also likely increased the amount of carbon that was exported from the system in the form of dissolve/particulate organic carbon.

In addition to its important role in regulating climate, peat swamp forests also provide another ecosystem services by storing substantial amounts of water with the potential total volume of water per unit volume of the peat of about 0.95 m^3 m^{-3} or equivalent to 9.5 x 10^6 L ha^{-1} m^{-1}. With the total area of undrained peat swamp forest in Borneo, Sumatra, and Peninsula Malaysia of 996,050 ha in 2015 (Miettinen et al. 2016), I estimated that peat swamp forests in Sumatra, Borneo, and Peninsular Malaysia stored about 51.1 – 52.5 km^3 km^3 of freshwater or about 17 times of water stored in Jatiluhur reservoir, one of main reservoir in Indonesia (Chapter 3). I also estimated that the water loss rate of 10.3 – 10.6 km^3 y^{-1} was yielded due to the peat swamp forest conversion to industrial plantation in Borneo, Sumatra, and Peninsular Malaysia within the period of 2010 – 2015. Based on the results of ground penetrating radar, the water content in the saturated zone of drained areas decreased due to the presence of the gas content in that zone (Chapter 4). Therefore, a correction factor should be developed to improve the estimate of water volume

stored in the peat dome to provide a better understanding of this important ecological service.

Based on the results of my study, I have identified future research priorities for filling important the gaps in our knowledge of peat dynamics and to allow a greater understanding of the role of peatlands in regulating water. I discuss these below.

- The study of peat properties in the tropics should be expanded to capture seasonal dynamics. I was unable to evaluate seasonal dynamics because I measured saturated hydraulic conductivity only once in the late November to early December 2014, which is the peak of the rainy season in this region. Thus, the variability of K_s values through time and the influence of seasonal patterns (i.e., dry or rainy season) remain unknown. In the northern peatlands, the variability of dry-wet season influences peat hydraulic properties due to the peat shrinkage and swelling (Price and Schlotzhauer 1999). Additionally, previous studies have attributed the intra-annual variability of K_s to growing and non-growing seasonal vegetation dynamics that influenced the concentration of the gas bubbles in the peat saturated zone (Kettridge et al. 2013). However, the effect of dry and wet season on the peat properties still remain unclear in tropical peatlands and need further investigation to relate them to variation K_s.
- The GPR study also should expanded to cover dry and rainy seasons to allow the evaluation of seasonal effects. Again, the GPR surveys conducted during my research were only performed once in November 2015, which was the El Nino

year. By doing the multiple surveys covering the different season, the temporal variation of gas and water content in the peat profile can be determined so that the relationship between hydrological condition and biogeochemical system can be evaluated spatially and temporally.

- Hydrologic models should be developed and used to estimate the hydrological dynamic in the peatlands and to provide insights into the best management strategies. Such models can be developed and calibrated using the measured peat hydraulic properties such as saturated hydraulic conductivity from Chapter 2 and moisture characteristic from Chapter 3, By simulating the water moisture dynamics in tropical peatlands, some importance insights can be determined. These insights include: (1) more accurate estimates of peatland area prone to fire; (2) the ability to identify and prioritize disturbed peatlands for restoration and the kinds of restoration actions that may be more effective; and (3) the evaluation of alternative designs for channel networks that minimizing the negative impact of the plantations (e.g. fire risks, greenhouse gas emission), while keep maximizing the harvest productivity.

Bibliography

Akaike H (1973) Information theory and an extension of the maximum like- lihood principle. In: Petrov B, Csaki F (eds) Second International Symposium on Information Theory. Akademiai Kiado, Budapest, Hungary, pp 267–281.

Aldrian E, Dwi Susanto R (2003) Identification of three dominant rainfall regions within Indonesia and their relationship to sea surface temperature. Int J Climatol 23:1435–1452. doi: 10.1002/joc.950.

Anderson DE (2002) Carbon accumulation and C / N ratios of peat bogs in North - West Scotland Carbon Accumulation and C / N Ratios of Peat Bogs in North-west Scotland. Scottish Geogr J 118:323–341.

Anshari G, Kershaw AP, Van Der Kaars S, Jacobsen G (2004) Environmental change and peatland forest dynamics in the Lake Sentarum area, West Kalimantan, Indonesia. J Quat Sci 19:637–655. doi: 10.1002/jqs.879.

Anshari GZ, Afifudin M, Nuriman M, et al (2010) Drainage and land use impacts on changes in selected peat properties and peat degradation in West Kalimantan Province, Indonesia. Biogeosciences 7:3403–3419. doi: 10.5194/bg-7-3403-2010.

Bartoń K (2016) MuMIn: Multi-Model Inference.

Basuki I (2017) Carbon dynamics in response to land cover change in tropical peatland, Kalimantan, Indonesia. Oregon State University.

Bates D, Mächler M, Bolker B, Walker S (2015a) Fitting Linear Mixed-Effects Models Using **lme4**. J Stat Softw 67:1–48. doi: 10.18637/jss.v067.i01.

Bates D, Mächler M, Bolker B, Walker S (2015b) Fitting Linear Mixed-Effects Models Using **lme4**. J Stat Softw 67:1–48. doi: 10.18637/jss.v067.i01.

Beckwith CW, Baird AJ (2001) Effect of biogenic gas bubbles on water flow through poorly decomposed blanket peat. Water Resour Res 37:551–558.

Boelter DH (1969) Physical Properties of Peats as Related to Degree of Decomposition. Soil Sci Soc Am Proc 33:606–609.

Borcard D, Gillet F, Legendre P (2011) Numerical Ecology with R. Springer.

Borcard D, Legendre P (2002) All-scale spatial analysis of ecological data by means of principal coordinates of neighbour matrices. Ecol Modell 153:51–68. doi: 10.1016/S0304-3800(01)00501-4.

Borcard D, Legendre P, Drapeau P (1992) Partialling out the spatial component of ecological variation. Ecology 73:1045–1055.

Bouwer H, Rice R (1976) A slug test for determining hydraulic conductivity of unconfined aquifers.pdf. Water Resour Res 12:423–428.

Burnham K, Anderson D (2002) Model Selection and Inference: An Information-theoretic Approach, 2nd edition. Springer-Verlag, New York.

Campos CA, Hernández ME, Moreno-Casasola P, et al (2011) Soil water retention and carbon pools in tropical forested wetlands and marshes of the Gulf of Mexico. Hydrol Sci J 56:1388–1406. doi: 10.1080/02626667.2011.629786.

Carlson KM, Goodman LK, May-Tobin CC (2015) Modeling relationships between water table depth and peat soil carbon loss in Southeast Asian plantations. Environ Res Lett 10:74006. doi: 10.1088/1748-9326/10/7/074006.

Chambers FM, Beilman DW, Yu Z (2011) Methods for determining peat humification and for quantifying peat bulk density , organic matter and carbon content for palaeostudies of climate and peatland carbon dynamics. Mires Peat 7:1–10.

Chason D., Siegel DI (1986) Hydraulic conductiviy and related physical properties of peat, Lost River peatland, Northern Minnesota. Soil Sci 142:91–99.

Chimner RA, Ewel KC (2004) Differences in carbon fluxes between forested and cultivated micronesian tropical peatlands. Wetl Ecol Manag 12:419–427. doi: 10.1007/s11273-004-0255-y.

Clymo RS (2004) Hydraulic conductivity of peat at Ellergower Moss, Scotland. Hydrol Process 18:261–274. doi: 10.1002/hyp.1374.

Clymo RS (1984) The Limits to Peat Bog Growth. Philos Trans R Soc B Biol Sci 303:605–654. doi: 10.1098/rstb.1984.0002.

Comas X, Kettridge N, Binley A, et al (2014) The effect of peat structure on the spatial distribution of biogenic gases within bogs. Hydrol Process 28:5483–5494. doi: 10.1002/hyp.10056.

Comas X, Slater L (2007) Evolution of biogenic gases in peat blocks inferred from noninvasive dielectric permittivity measurements. Water Resour Res 43:1–10. doi: 10.1029/2006WR005562.

Comas X, Slater L, Reeve A (2005a) Spatial variability in biogenic gas accumulations in peat soils is revealed by ground penetrating radar (GPR). Geophys Res Lett 32:1–4. doi: 10.1029/2004GL022297.

Comas X, Slater L, Reeve A (2008) Seasonal geophysical monitoring of biogenic gases in a northern peatland: Implications for temporal and spatial variability in free phase gas production rates. J Geophys Res Biogeosciences 113:1–12. doi: 10.1029/2007JG000575.

Comas X, Slater L, Reeve A (2005b) Geophysical and hydrological evaluation of two bog complexes in a northern peatland: Implications for the distribution of biogenic gases at the basin scale. Global Biogeochem Cycles 19:1–10. doi: 10.1029/2005GB002582.

Comas X, Slater LD (2013) Noninvasive Field-Scale Characterization of Gaseous-Phase Methane Dynamics in Peatlands Using the Ground-Penetrating Radar Method. Carbon Cycl North Peatlands 159–171. doi: 10.1029/2008GM000810.

Comas X, Terry N, Slater L, et al (2015) Imaging tropical peatlands in Indonesia using ground penetrating radar (GPR) and electrical resistivity imaging (ERI): implications for carbon stock estimates and peat soil characterization. Biogeosciences Discuss 12:191–229. doi: 10.5194/bgd-12-191-2015.

Couwenberg J, Dommain R, Joosten H (2009) Greenhouse gas fluxes from tropical peatlands in south-east Asia. Glob Chang Biol 16:1715–1732. doi: 10.1111/j.1365-2486.2009.02016.x.

Couwenberg J, Hooijer A (2013) Towards robust subsidence-based soil carbon emission factors for peat soils in south-east Asia , with special reference to oil palm plantations. Mires Peat 12:1–13.

Crockett AC, Ronayne MJ, Cooper DJ (2015) Relationships between vegetation type, peat hydraulic conductivity, and water table dynamics in mountain fens. Ecohydrology 1038:1028–1038. doi: 10.1002/eco.1706.

Dommain R, Couwenberg J, Glaser PH, et al (2014) Carbon storage and release in Indonesian peatlands since the last deglaciation. Quat Sci Rev 97:1–32. doi: 10.1016/j.quascirev.2014.05.002.

Dommain R, Couwenberg J, Joosten H (2010) Hydrological self-regulation of domed peatlands in south-east Asia and consequences for conservation and restoration. Mires Peat, Artic 6:1–17.

Dommain R, Couwenberg J, Joosten H (2011) Development and carbon sequestration of tropical peat domes in south-east Asia: links to post-glacial sea-level changes and Holocene climate variability. Quat Sci Rev 30:999–1010. doi: 10.1016/j.quascirev.2011.01.018.

Dray S, Legendre P, Peres-Neto PR (2006) Spatial modelling: a comprehensive framework for principal coordinate analysis of neighbour matrices (PCNM).

Ecol Modell 196:483–493. doi: 10.1016/j.ecolmodel.2006.02.015.

Evers S, Yule C, Padfield R, et al (2016) Keep Wetlands Wet: The Myth of Sustainable Development of Tropical Peatlands - Implications for Policies and Management. Glob Chang Biol 1–16. doi: 10.1111/gcb.13422.

Frolking S, Roulet NT, Tuittila E, et al (2010) A new model of Holocene peatland net primary production, decomposition, water balance, and peat accumulation. Earth Syst Dyn 1:1–21. doi: 10.5194/esd-1-1-2010.

Fry VA, Selker JS, Gorelick SM (1997a) Experimental investigations for trapping oxygen gas in saturated porous media for in situ bioremediation. Water Resour Res 33:2687–2696. doi: 10.1029/97WR02428.

Fry VA, Selker JS, Gorelick SM (1997b) Experimental investigations for trapping oxygen gas in saturated porous media for in situ bioremediation. Water Resour Res 33:2687–2696. doi: 10.1029/97WR02428.

Furukawa Y, Inubushi K, Ali M, et al (2005) Effect of changing groundwater levels caused by land-use changes on greenhouse gas fluxes from tropical peat lands. Nutr Cycl Agroecosystems 71:81–91. doi: 10.1007/s10705-004-5286-5.

Gandois L, Cobb AR, Hei IC, et al (2013) Impact of deforestation on solid and dissolved organic matter characteristics of tropical peat forests: Implications for carbon release. Biogeochemistry 114:183–199. doi: 10.1007/s10533-012-9799-8.

Gaveau DLA, Sheil D, Husnayaen, et al (2016) Rapid conversions and avoided deforestation: examining four decades of industrial plantation expansion in Borneo. Sci Rep 6:32017. doi: 10.1038/srep32017.

Gnatowski T, Szatyłowicz J, Brandyk T, Kechavarzi C (2010) Hydraulic properties of fen peat soils in Poland. Geoderma 154:188–195. doi: 10.1016/j.geoderma.2009.02.021.

Gómez-Ortiz D, Martín-Crespo T, Martín-Velázquez S, et al (2010) Application of ground penetrating radar (GPR) to delineate clay layers in wetlands. A case study in the Soto Grande and Soto Chico watercourses, Do??ana (SW Spain). J Appl Geophys 72:107–113. doi: 10.1016/j.jappgeo.2010.07.007.

Grover SPP, Baldock JA (2013) The link between peat hydrology and decomposition: Beyond von Post. J Hydrol 479:130–138. doi: 10.1016/j.jhydrol.2012.11.049

Gunawan H, Kobayashi S, Mizuno K (2012) Peat swamp forest types and their regeneration in Giam Siak Kecil-Bukit Batu Biosphere Reserve, Riau, East Sumatra, Indonesia. Mires Peat 10:1–17.

Hadi A, Inubushi K, Furukawa Y, et al (2005) Greenhouse gas emissions from tropical peatlands of Kalimantan,Indonesia. Nutr Cycl Agroecosystems 71:73–80. doi: 10.1007/s10705-004-0380-2.

Hallema DW, Périard Y, Lafond J a., et al (2015) Characterization of Water Retention Curves for a Series of Cultivated Histosols. Vadose Zo J 14:0. doi: 10.2136/vzj2014.10.0148.

Hardjamulia A, Suwignyo P (1987) The present status of the reservoir fisheries in Indonesia. In: Silva SS De (ed) Reservoir fishery management and development in Asia. International Development Research Centre, Kathmandu, Nepal, pp 23–28.

Heil A, Langmann B, Aldrian E (2006) Indonesian peat and vegetation fire emissions: Study on factors influencing large-scale smoke haze pollution using a regional atmospheric chemistry model. Mitig Adapt Strateg Glob Chang 12:113–133. doi: 10.1007/s11027-006-9045-6.

Hergoualc'h K, Verchot L V. (2011) Stocks and fluxes of carbon associated with land use change in Southeast Asian tropical peatlands: A review. Global Biogeochem Cycles 25:doi:10.1029/2009GB003718. doi: 10.1029/2009GB003718.

Hirano T, Segah H, Kusin K, et al (2012) Effects of disturbances on the carbon balance of tropical peat swamp forests. Glob Chang Biol 18:3410–3422. doi: 10.1111/j.1365-2486.2012.02793.x.

Holden J, Burt TP (2003a) Hydraulic conductivity in upland blanket peat: Measurement and variability. Hydrol Process 17:1227–1237. doi: 10.1002/hyp.1182.

Holden J, Burt TP (2003b) Hydrological studies on blanket peat: The significance of the acrotelm-catotelm model. J Ecol 91:86–102. doi: 10.1046/j.1365-2745.2003.00748.x.

Holden J, Smart RP, Chapman PJ, et al (2013) The Role of Natural Soil Pipes in Water and Carbon Transfer in and from Peatlands. Carbon Cycl North Peatlands 251–264. doi: 10.1029/2008GM000804.

Hooijer A, Page S, Canadell JG, et al (2010) Current and future CO2 emissions from drained peatlands in Southeast Asia. Biogeosciences 7:1505–1514. doi: 10.5194/bg-7-1505-2010.

Hooijer A, Page S, Jauhiainen J, et al (2012) Subsidence and carbon loss in drained tropical peatlands. Biogeosciences 9:1053–1071. doi: 10.5194/bg-9-1053-2012.

Huijnen V, Wooster MJ, Kaiser JW, et al (2016) Fire carbon emissions over maritime southeast Asia in 2015 largest since 1997. Sci Rep 6:26886. doi: 10.1038/srep26886.

Huisman JA, Hubbard SS, Redman JD, Annan AP (2003) Measuring Soil Water Content with Ground Penetrating Radar: A Review. Vadose Zo J 2:476–491. doi: 10.2113/2.4.476.

Hurvich CM, Tsai C-L (1989a) Regression and time series model selection in small samples. Biometrika 76:297–307. doi: 10.1093/biomet/76.2.297.

Hurvich CM, Tsai C-L (1989b) Regression and time series model selection in small samples. Biometrika 76:297–307. doi: 10.1093/biomet/76.2.297.

Inubushi K, Furukawa Y, Hadi a, et al (2003) Seasonal changes of CO(2), CH(4) and N(2)O fluxes in relation to land-use change in tropical peatlands located in coastal area of South Kalimantan. Chemosphere 52:603–8. doi: 10.1016/S0045-6535(03)00242-X.

Jacob RW, Urban TM (2016) Ground-Penetrating Radar Velocity Determination and Precision Estimates Using Common-Midpoint (CMP) Collection with Hand-Picking, Semblance Analysis and Cross-Correlation Analysis: A Case Study and Tutorial for Archaeologists. Archaeometry 58:987–1002. doi: 10.1111/arcm.12214.

Jaenicke J, Rieley J, Mott C, et al (2008) Determination of the amount of carbon stored in Indonesian peatlands. Geoderma 147:151–158. doi: 10.1016/j.geoderma.2008.08.008.

Jaenicke J, Wösten H, Budiman A, Siegert F (2010) Planning hydrological restoration of peatlands in Indonesia to mitigate carbon dioxide emissions. Mitig Adapt Strateg Glob Chang 15:223–239. doi: 10.1007/s11027-010-9214-5.

Jauhiainen J, Hooijer A, Page SE (2012) Carbon dioxide emissions from an Acacia plantation on peatland in Sumatra, Indonesia. Biogeosciences 9:617–630. doi: 10.5194/bg-9-617-2012.

Jauhiainen J, Takahashi H (2005) Carbon fluxes from a tropical peat swamp forest floor. Glob Chang Biol 11:1788–1797. doi: 10.1111/j.1365-2486.2005.01031.x.

Jauhiainen J, Takahashi H, Heikkinen JEP, et al (2005) Carbon fluxes from a tropical peat swamp forest floor. Glob Chang Biol 11:1788–1797. doi: 10.1111/j.1365-2486.2005.01031.x.

Jiang XW, Wan L, Wang XS, et al (2009) Effect of exponential decay in hydraulic conductivity with depth on regional groundwater flow. Geophys Res Lett 36:3–

6. doi: 10.1029/2009GL041251.

Kellner K (2016) jagsUI: A Wrapper Around “rjags” to Streamline “JAGS” Analyses.

Kelly TJ, Baird AJ, Roucoux KH, et al (2014) The high hydraulic conductivity of three wooded tropical peat swamps in northeast Peru: measurements and implications for hydrological function. Hydrol Process 28:3373–3387. doi: 10.1002/hyp.9884.

Kettridge N, Comas X, Baird A, et al (2008) Ecohydrologically important subsurface structures in peatlands revealed by ground-penetrating radar and complex conductivity surveys. J Geophys Res Biogeosciences 113:1–15. doi: 10.1029/2008JG000787.

Kettridge N, Kellner E, Price JS, Waddington JM (2013) Peat deformation and biogenic gas bubbles control seasonal variations in peat hydraulic conductivity. Hydrol Process 27:3208–3216. doi: 10.1002/hyp.9369.

Kettridge N, Tilak AS, Devito KJ, et al (2016) Moss and peat hydraulic properties are optimized to maximize peatland water use efficiency. Ecohydrology 9:1039–1051. doi: 10.1002/eco.1708.

Koh LP, Miettinen J, Liew SC, Ghazoul J (2011) Remotely sensed evidence of tropical peatland conversion to oil palm. Proc Natl Acad Sci U S A 108:5127–32. doi: 10.1073/pnas.1018776108.

Könönen M, Jauhiainen J, Laiho R, et al (2015) Physical and chemical properties of tropical peat under stabilised land uses. Mires Peat 16:1–13.

Kool DM, Buurman P, Hoekman DH (2006) Oxidation and compaction of a collapsed peat dome in Central Kalimantan. Geoderma 137:217–225. doi: 10.1016/j.geoderma.2006.08.021.

Kuhry P, Vitt DH (1996) Fossil carbon/nitrogen ratios as a measure of peat decomposition. Ecology 77:271–275.

Kuo L, Mallick B (1998) Variable Selection for Regression Models. Sankhyā Indian J Stat Ser B 60:65–81. doi: 10.2307/25053023.

Kurnianto S, Warren M, Talbot J, et al (2014) Carbon accumulation of tropical peatlands over millennia: A modeling approach. Glob Chang Biol 1–14. doi: 10.1111/gcb.12672.

Lal R (2004) Soil Carbon Sequestration Impacts on Global Climate Change and Food Security. Science (80-) 304:1623–1627. doi: 10.1126/science.1097396.

Lampela M, Jauhiainen J, Vasander H (2014) Surface peat structure and chemistry in a tropical peat swamp forest. Plant Soil 382:329–347. doi: 10.1007/s11104-014-2187-5.

Legendre P, Borcard D, Blanchet FG, Dray S (2013) PCNM: MEM spatial eigenfunction and principal coordinate analyses.

Malmer N, Holm E (1984) Variation in the C/N-quotient of peat in relation to decomposition rate and age determination with 210 Pb. Oikos 43:171–182.

Mccarter CPR, Price JS (2014) Ecohydrology of Sphagnum moss hummocks : mechanisms of capitula water supply and simulated effects of evaporation. 44:33–44. doi: 10.1002/eco.1313.

Melling L, Hatano R, Goh K (2005a) Methane fluxes from three ecosystems in tropical peatland of Sarawak, Malaysia. Soil Biol Biochem 37:1445–1453. doi: 10.1016/j.soilbio.2005.01.001.

Melling L, Hatano R, Goh KJ (2005b) Soil CO2 flux from three ecosystems in tropical peatland of Sarawak, Malaysia. Tellus B 57:1–11. doi: 10.1111/j.1600-0889.2005.00129.x.

Miettinen J, Hooijer A, Shi C, et al (2012a) Extent of industrial plantations on Southeast Asian peatlands in 2010 with analysis of historical expansion and future projections. GCB Bioenergy doi: 10.1111/j.1757-1707.2012.01172.x. doi: 10.1111/j.1757-1707.2012.01172.x.

Miettinen J, Liew SC (2010) Status of Peatland Degradation and Development in Sumatra and Kalimantan. Ambio 39:394–401. doi: 10.1007/s13280-010-0051-2.

Miettinen J, Shi C, Liew SC (2012b) Two decades of destruction in Southeast Asia's peat swamp forests. Front Ecol Environ 10:124–128. doi: 10.1890/100236.

Miettinen J, Shi C, Liew SC (2016) Land cover distribution in the peatlands of Peninsular Malaysia, Sumatra and Borneo in 2015 with changes since 1990. Glob Ecol Conserv 6:67–78. doi: 10.1016/j.gecco.2016.02.004.

Moore PA, Morris PJ, Waddington JM (2015) Multi-decadal water table manipulation alters peatland hydraulic structure and moisture retention. Hydrol Process 29:2970–2982. doi: 10.1002/hyp.10416.

Moore S, Evans CD, Page SE, et al (2013) Deep instability of deforested tropical peatlands revealed by fluvial organic carbon fluxes. Nature 493:660–3. doi: 10.1038/nature11818.

Morris PJ, Baird AJ, Belyea LR (2015) Bridging the gap between models and measurements of peat hydraulic conductivity. Water Resour Res 51:5353–5364. doi: 10.1002/2015WR017264.

Muniandy M, Ahmed OH, Majid NMA, Yusop MK (2009) Effects of Converting Secondary Forest to Oil Palm Plantation on Peat Soil Carbon and Nitrogen and other Soil Chemical Properties. Am J Environ Sci 5:406–412. doi: 10.3844/ajessp.2009.406.412.

Murdiyarso D, Donato D, Kauffman JB, et al (2009) Carbon storage in mangrove and peatland ecosystems: A preliminary account from plots in Indonesia. Bogor, Indonesia.

Murdiyarso D, Hergoualc'h K, Verchot L V (2010) Opportunities for reducing greenhouse gas emissions in tropical peatlands. Proc Natl Acad Sci U S A 107:19655–19660. doi: 10.1073/pnas.0911966107.

Mustamo P, Hyvärinen M, Ronkanen A-K, Kløve B (2016) Physical properties of peat soils under different land use options. Soil Use Manag 400–410. doi: 10.1111/sum.12272.

Nakagawa S, Schielzeth H (2013) A general and simple method for obtaining R2 from generalized linear mixed-effects models. Methods Ecol Evol 4:133–142. doi: 10.1111/j.2041-210x.2012.00261.x.

Neal A (2004) Ground-penetrating radar and its use in sedimentology: Principles, problems and progress. Earth-Science Rev 66:261–330. doi: 10.1016/j.earscirev.2004.01.004.

Nemati MR, Caron J, Banton O, Tardif P (2000) Determining Air Entry Value in Peat Substrates. Soil Sci Soc Am J 367–373.

Novita

N.(2016) Carbon Stocks and Soil Greenhouse Gas Emissions Associated with Forest Conversion to Oil Palm Plantations in Tanjung Puting Tropical Peatlands, Indonesia. Oregon State University.

Oksanen J, Blanchet FG, Friendly M, et al (2017a) vegan: Community Ecology Package.

Page S, Wüst R, Banks C (2010) Past and present carbon accumulation and loss in Southeast Asian peatlands. PAGES NEWS 18:25–27.

Page SE, Rieley JO, Banks CJ (2011) Global and regional importance of the tropical peatland carbon pool. Glob Chang Biol 17:798–818. doi: 10.1111/j.1365-

2486.2010.02279.x.

Page SE, Rieley JO, Shotyk W, Weiss D (1999) Interdependence of peat and vegetation in a tropical peat swamp forest. Philos Trans R Soc Lond B Biol Sci 354:1885–9187. doi: 10.1098/rstb.1999.0529.

Page SE, Siegert F, Rieley JO, et al (2002) The amount of carbon released from peat and forest fires in Indonesia during 1997. Nature 1999:61–65. doi: 10.1038/nature01141.1.

Page SE, Wűst R a. J, Weiss D, et al (2004) A record of Late Pleistocene and Holocene carbon accumulation and climate change from an equatorial peat bog(Kalimantan, Indonesia): implications for past, present and future carbon dynamics. J Quat Sci 19:625–635. doi: 10.1002/jqs.884.

Päivänen J (1973) Hydraulic conductivity and water retention in peat soils.

Parry L, West L, Holden J, Chapman P (2014) Evaluating approaches for estimating peat depth. J Geophys Res Biogeosciences 119:567–576. doi: 10.1002/2013JG002411.Received.

Parsekian AD, Slater L, Comas X, Glaser PH (2010) Variations in free-phase gases in peat landforms determined by ground-penetrating radar. J Geophys Res Biogeosciences 115:1–13. doi: 10.1029/2009JG001086.

Parsekian AD, Slater L, Giménez D (2012a) Application of ground-penetrating radar to measure near-saturation soil water content in peat soils. Water Resour Res 48:1–9. doi: 10.1029/2011WR011303.

Parsekian AD, Slater L, Ntarlagiannis D, et al (2012b) Uncertainty in Peat Volume and Soil Carbon Estimated Using Ground-Penetrating Radar and Probing. Soil Sci Soc Am J 76:1911. doi: 10.2136/sssaj2012.0040.

Peres-Neto PR, Legendre P, Dray S, Borcard D (2006) Variation Partitioning of Species Data Matrices : Estimation and Comparison of Fractions. Ecology 87:2614–2625.

Phillips VD (1998) Peatswamp ecology and sustainable development in Borneo. Biodivers Conserv 7:651–671.

Plado J, Sibul I, Mustasaar M, Jõeleht a (2011) Ground-penetrating radar study of the Rahivere peat bog, eastern Estonia. Est J Earth Sci 60:31. doi: 10.3176/earth.2011.1.03.

Plummer M (2003) JAGS: A program for analysis of Bayesian graphical models using Gibbs sampling. In: Proceedings of the 3rd International Workshop on

Distributed Statistical Computing (DSC 2003). pp 20–22.

Preston MD, Smemo KA, McLaughlin JW, Basiliko N (2012) Peatland microbial communities and decomposition processes in the James Bay Lowlands, Canada. Front Microbiol 3:1–15. doi: 10.3389/fmicb.2012.00070.

Price JS, Schlotzhauer SM (1999) Importance of shrinkage and compression in determining water storage changes in peat: The case of a mined peatland. Hydrol Process 13:2591–2601. doi: 10.1002/(SICI)1099-1085(199911)13:16<2591::AID-HYP933>3.0.CO;2-E.

Proulx-McInnis S, St-Hilaire A, Rousseau a. N, Jutras S (2013) A review of ground-penetrating radar studies related to peatland stratigraphy with a case study on the determination of peat thickness in a northern boreal fen in Quebec, Canada. Prog Phys Geogr 37:767–786. doi: 10.1177/0309133313501106.

Quinton WL, Elliot T, Price JS, et al (2009) Measuring physical and hydraulic properties of peat from X-ray tomography. Geoderma 153:269–277. doi: 10.1016/j.geoderma.2009.08.010.

Quinton WL, Hayashi M, Carey SK (2008) Peat hydraulic conductivity in cold regions and its relation to pore size and geometry. Hydrol Process 22:2829–2837. doi: 10.1002/hyp.

Raudenbush SW, Bryk AS (2002) Hierarchical linear models: Applications and data analysis methods, 2nd editio. Sage Publications, Thousand Oaks.

Reynolds WD, Brown DA, Mathur SP, Overend RP (1992) Effect of in-situ gas accumulation on the hydraulic conductivity of peat. Soil Sci 135:397–408.

Rezanezhad F, Price JS, Quinton WL, et al (2016) Structure of peat soils and implications for water storage, flow and solute transport: A review update for geochemists. Chem Geol 429:75–84. doi: 10.1016/j.chemgeo.2016.03.010.

Rezanezhad F, Quinton WL, Price JS, et al (2010) Influence of pore size and geometry on peat unsaturated hydraulic conductivity computed from 3D computed tomography image analysis. Hydrol Process 24:2983–2994. doi: 10.1002/hyp.7709.

Ritzema HP, Hassan AM., Moens R. (1998) A new approach to water management of tropical peatlands: a case study from Malaysia. Irrig Drain Syst 12:123–139. doi: 10.1023/A.

Rizzuti AM, Cohen AD, Stack EM (2004) Using hydraulic conductivity and micropetrography to assess water flow through peat-containing wetlands. Int J Coal Geol 60:1–16. doi: 10.1016/j.coal.2004.03.003.

Rocha Campos JR Da, Silva AC, Fernandes JSC, et al (2011) Water retention in a peatland with organic matter in different decomposition stages. Rev Bras Ciência do Solo 35:1217–1227. doi: 10.1590/S0100-06832011000400015

Rycroft DW, Williams DJA, Ingram HA. (1975) the transmisiion of water through peat.pdf. J Ecol 63:535–556.

Saharjo BH, Munoz CP (2005) Controlled burning in peat lands owned by small farmers: a case study in land preparation. Wetl Ecol Manag 13:105–110. doi: 10.1007/s11273-003-5110-z.

Schwärzel K, Šimůnek J, van Genuchten MT, Wessolek G (2006) Measurement modeling of soil-water dynamics evapotranspiration of drained peatland soils. J Plant Nutr Soil Sci 169:762–774. doi: 10.1002/jpln.200621992.

Sherwood JH, Kettridge N, Thompson DK, et al (2013) Effect of drainage and wildfire on peat hydrophysical properties. Hydrol Process 27:1866–1874. doi: 10.1002/hyp.9820.

Shimada S, Takahashi H, Haraguchi A, Kaneko M (2001) The carbon content characteristics of tropical peats in Central Kalimantan, Indonesia: Estimating their spatial variability in density. Biogeochemistry 53:249–267.

Taufik M, Torfs PJJF, Uijlenhoet R, et al (2017a) Amplification of wildfire area burnt by hydrological drought in the humid tropics. Nat Clim Chang. doi: 10.1038/nclimate3280.

Taufik M, Torfs PJJF, Uijlenhoet R, et al (2017b) Amplification of wildfire area burnt by hydrological drought in the humid tropics. Nat Clim Chang. doi: 10.1038/nclimate3280.

Team R Core (2016) R: A Language and Environment for Statistical Computing.

Undari SS, Irano TH, Amada HY, et al (2012) Effect of groundwater level on soil respiration in tropical peat swamp forests. 68:121–134.

van Genuchten MT (1980) A Closed-form Equation for Predicting the Hydraulic Conductivity of Unsaturated Soils. Soil Sci Soc Am J 44:892–898. doi: 10.2136/sssaj1980.03615995004400050002x.

Verry E, Boelter DH, Paivanen J, et al (2011) Physical properties of Organic Soils. In: Kolka RK, Sebestyen S, Verry E, Brooks K (eds) Peatland Biogeochemistry and Watershed Hydrology at the Marcell Experimental Forests. CRC Press, Boca Raton, FL, pp 135–176.

Walczak R, Rovdan E, Witkowska-Walczak B (2002) Water retention characteristics

of peat and sand mixtures. Int Agrophysics 16:161–165.

Warren MW, Kauffman JB, Murdiyarso D, et al (2012) A cost-efficient method to assess carbon stocks in tropical peat soil. Biogeosciences 9:4477–4485. doi: 10.5194/bg-9-4477-2012.

Watanabe S (2010) Asymptotic Equivalence of Bayes Cross Validation and Widely Applicable Information Criterion in Singular Learning Theory. J Mach Learn Res 11:3571–3594.

Weiss R, Alm J, Laiho R, Laine J (1998) Modeling moisture retention in peat soils. Soil Sci Soc Am J 62:305–313. doi: 10.2136/sssaj1998.03615995006200020002x.

Whittington PN, Strack M, van Haarlem R, et al (2007) The influence of peat volume change and vegetation on the hydrology of a kettle-hole wetland in Southern Ontario, Canada. Mires Peat 2:1–14.

Wösten H, Hooijer A, Siderius C, et al (2006a) Tropical Peatland water management modelling of the Air Hitam Laut catchment in Indonesia. Int J River Basin Manag 4:233–244.

Wösten JHM, Van Den Berg J, Van Eijk P, et al (2006b) Interrelationships between Hydrology and Ecology in Fire Degraded Tropical Peat Swamp Forests. Int J Water Resour Dev 22:157–174. doi: 10.1080/07900620500405973.

Yang S-Y, Yeh H-D (2004) A Simple Approach Using Bouwer and Rice's Method for Slug Test Data Analysis. Ground Water 42:781–784. doi: 10.1111/j.1745-6584.2004.tb02732.x.

Yu Z, Loisel J, Brosseau DPDP, et al (2010) Global peatland dynamics since the Last Glacial Maximum. Geophys Res Lett 37:L13402. doi: 10.1029/2010GL043584.

Appendices

Figure 1. The calculated one-dimension electromagnetic wave velocity (left) based on the common midpoint ground penetrating radar survey using 100 MHz antennas (center) and semblance analysis (right) for site oil palm plantation 1 and plot 2 (OP11). Dashed and solid lines represent root mean squared and interval velocity, respectively. The red line represents the hyperbolae reflection based on the manually picked local maxima semblance. Black and white spectrum in semblance analysis represent low and high semblance.

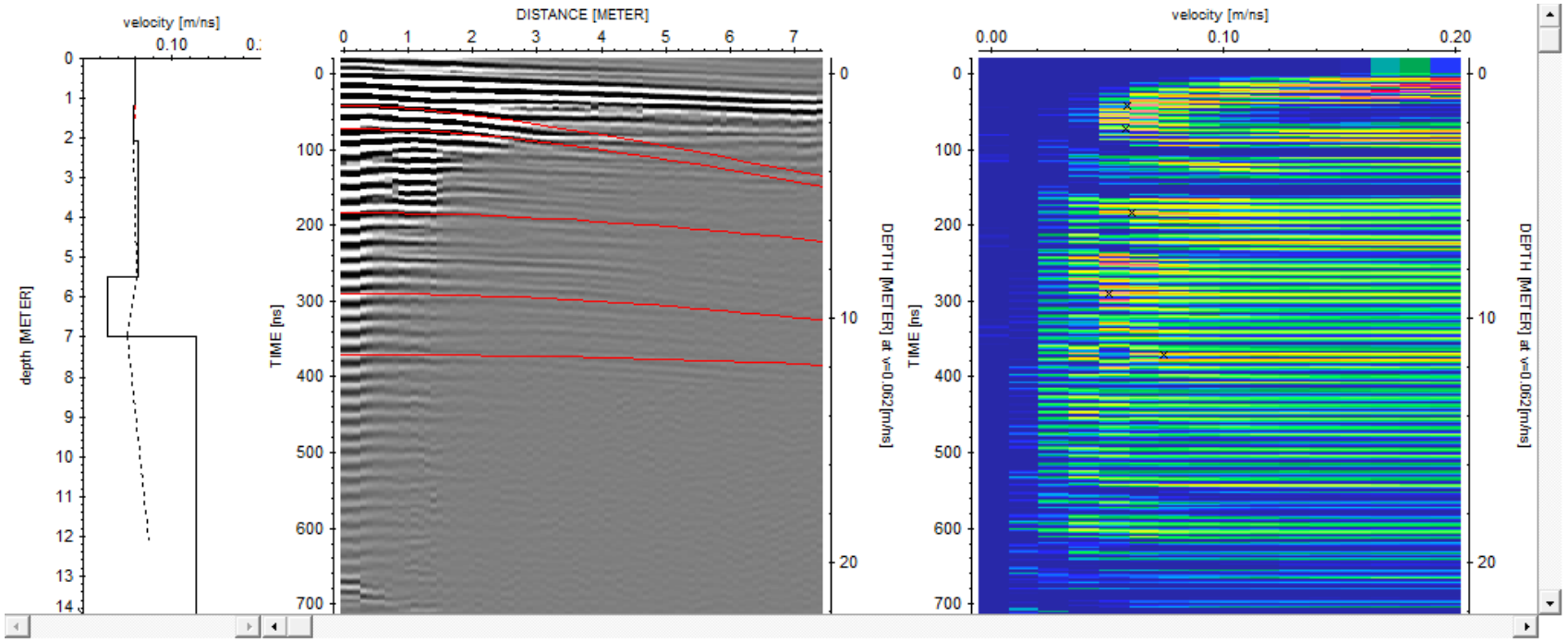

Figure 2. Same as Figure 1 but for oil plantation 1 plot 3.

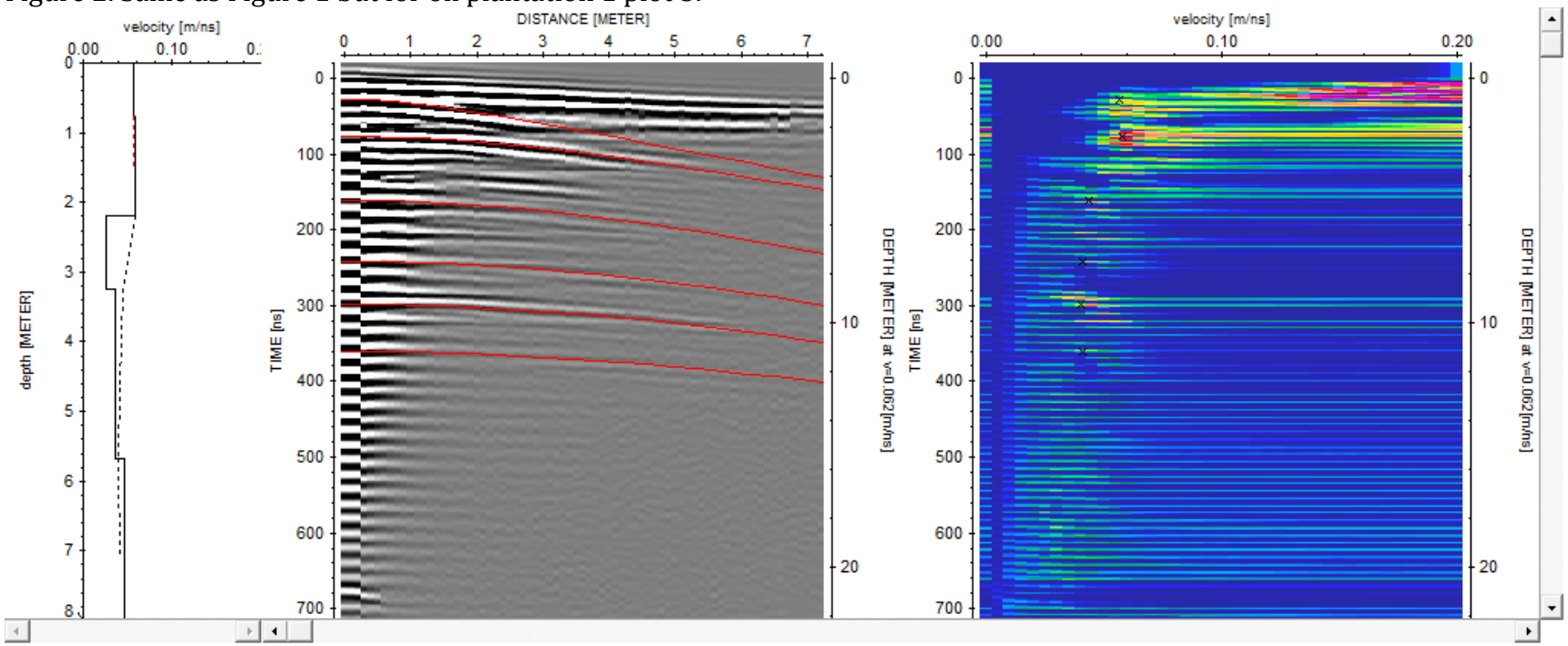

Figure 3. Same as Figure 1 but for oil plantation 1 plot 4.

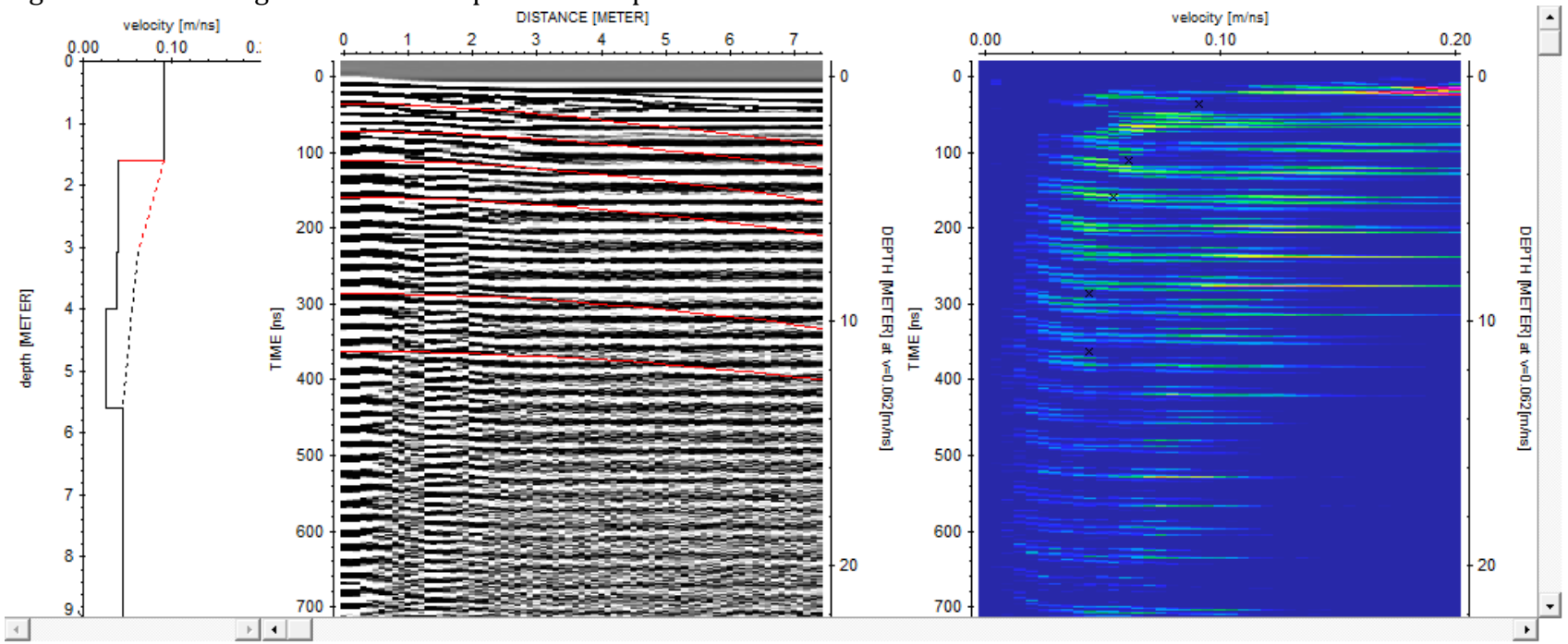

Figure 4. Same as Figure 1 but for oil plantation 1 plot 5

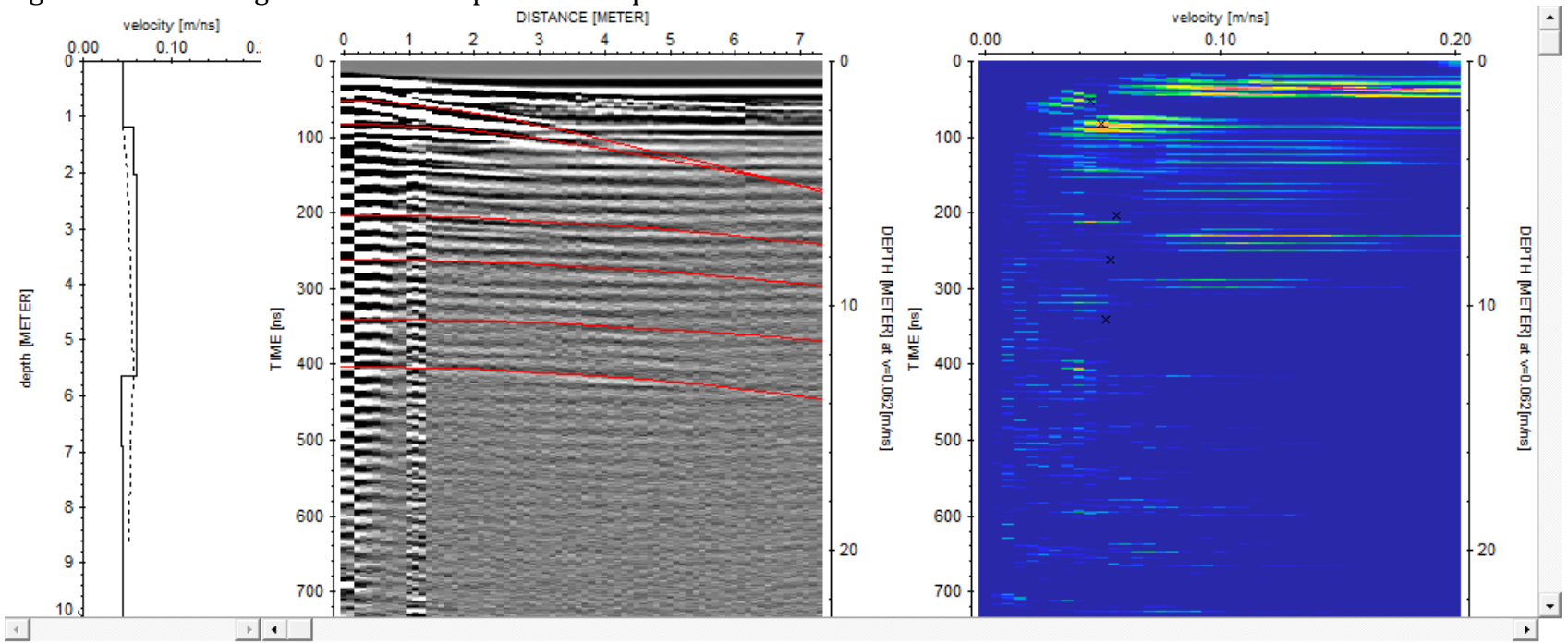

Figure 5. Same as Figure 1 but for oil plantation 1 plot 6

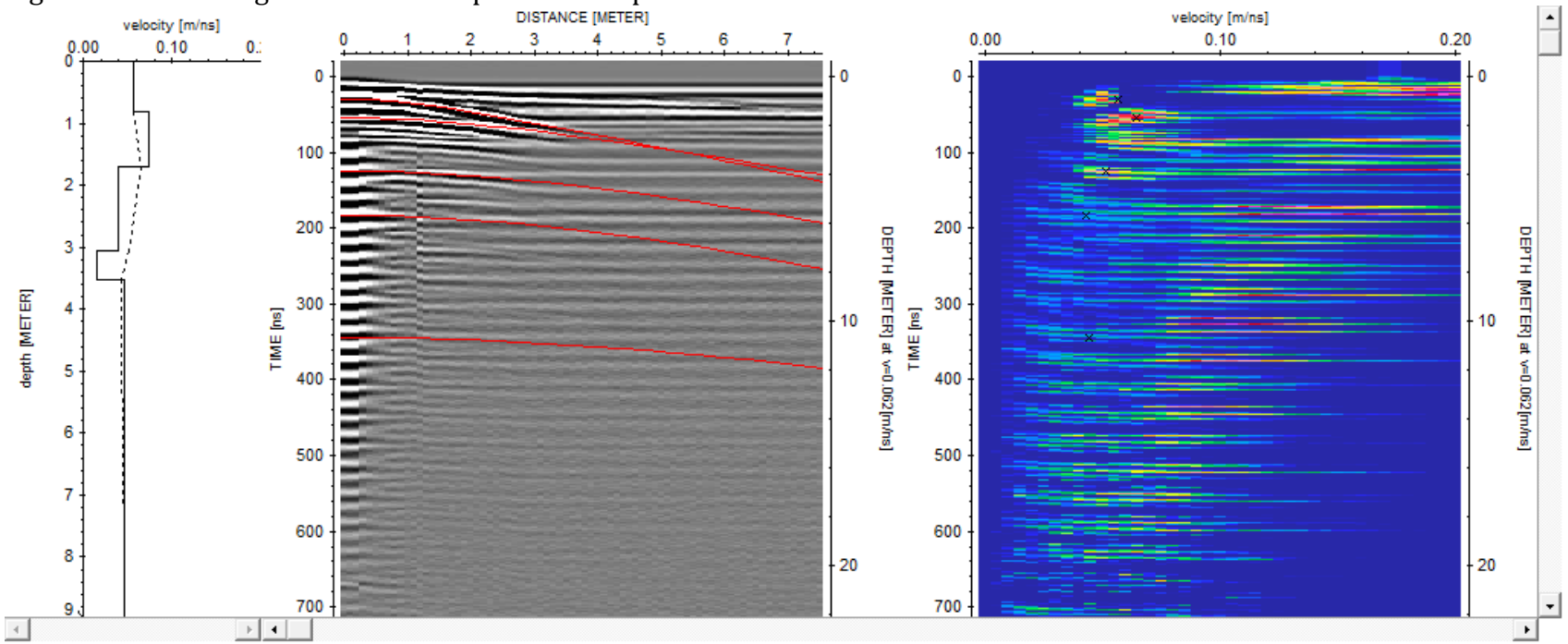

.

Figure 6. Same as Figure 1 but for oil plantation 2 plot 1.

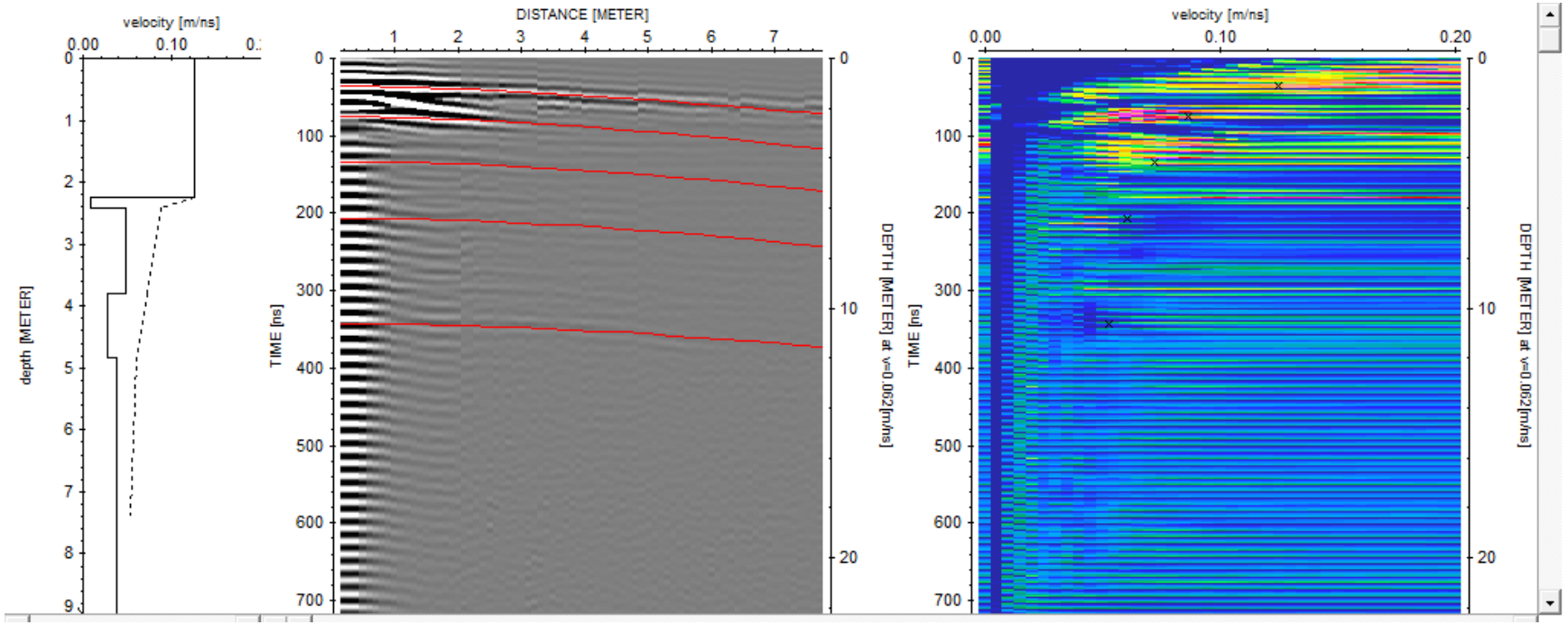

Figure 7. Same as Figure 1 but for oil plantation 2 plot 3

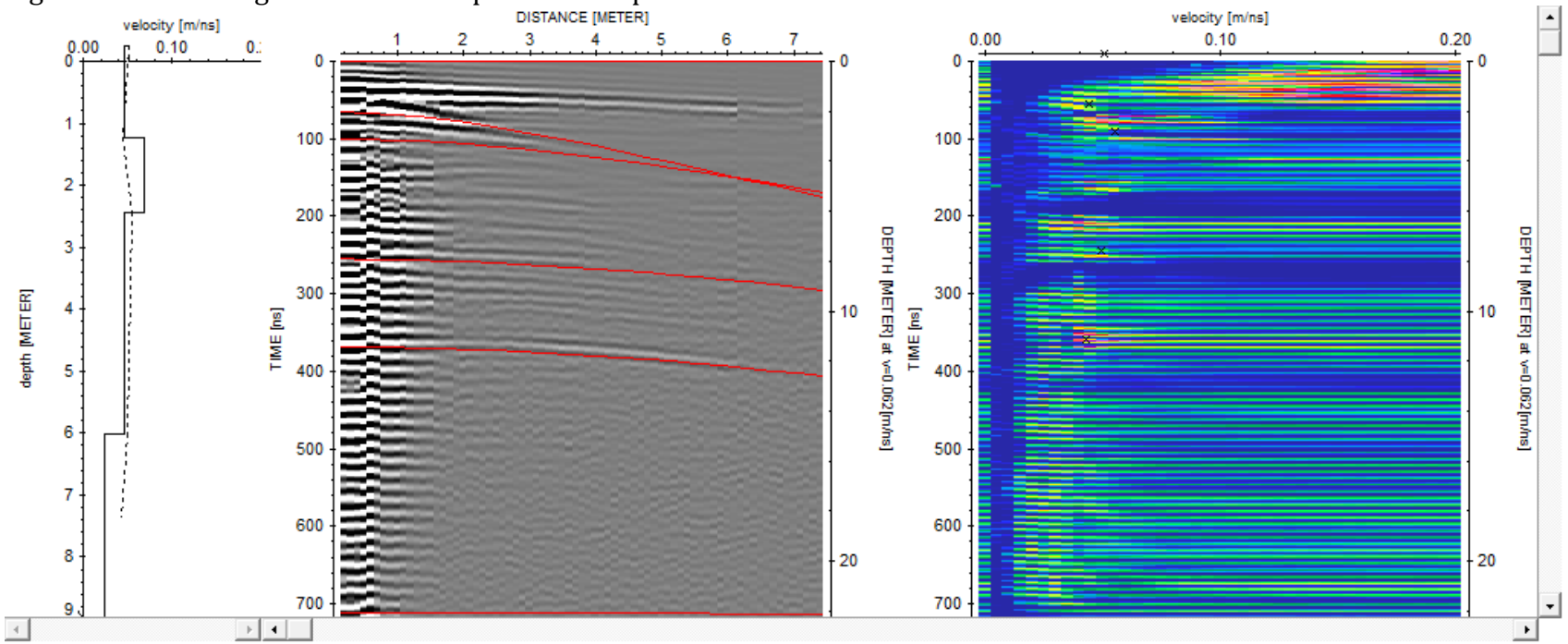

.

Figure 8. Same as Figure 1 but for oil plantation 2 plot 4.

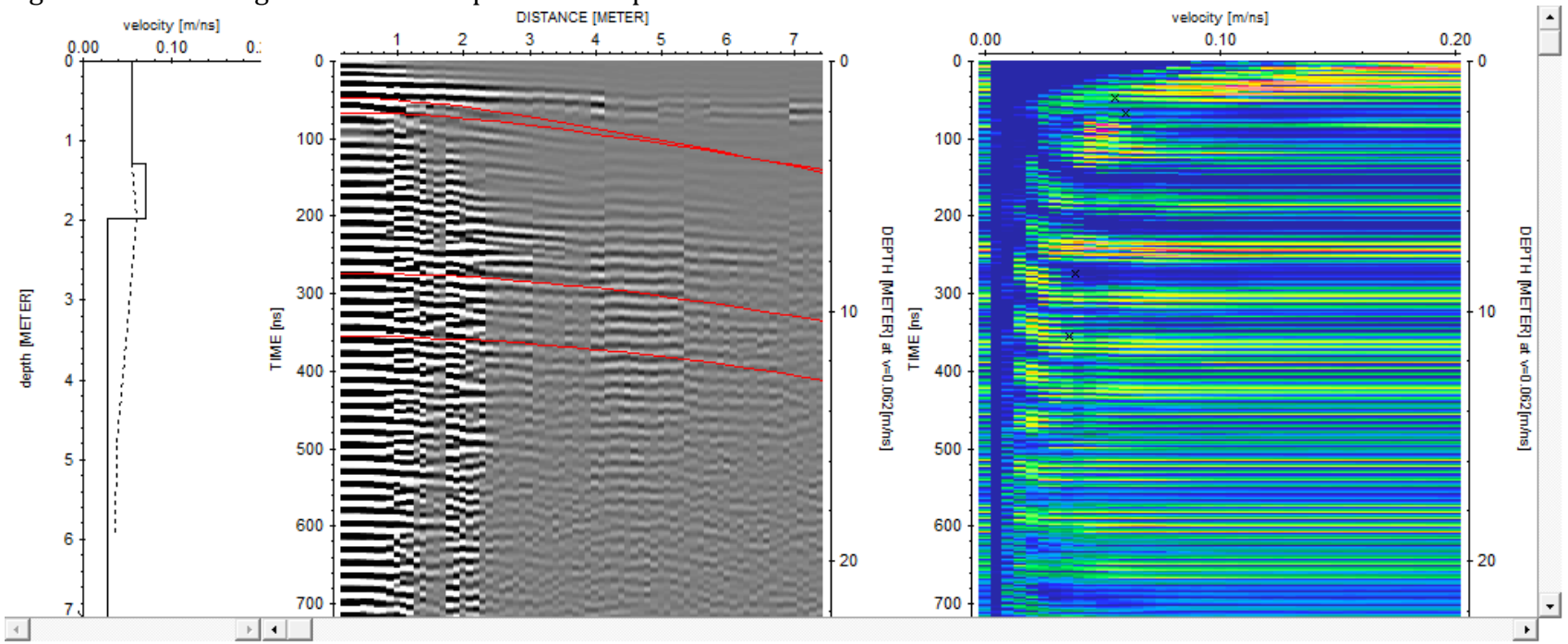

Figure 9. Same as Figure 1 but for oil plantation 2 plot 5.

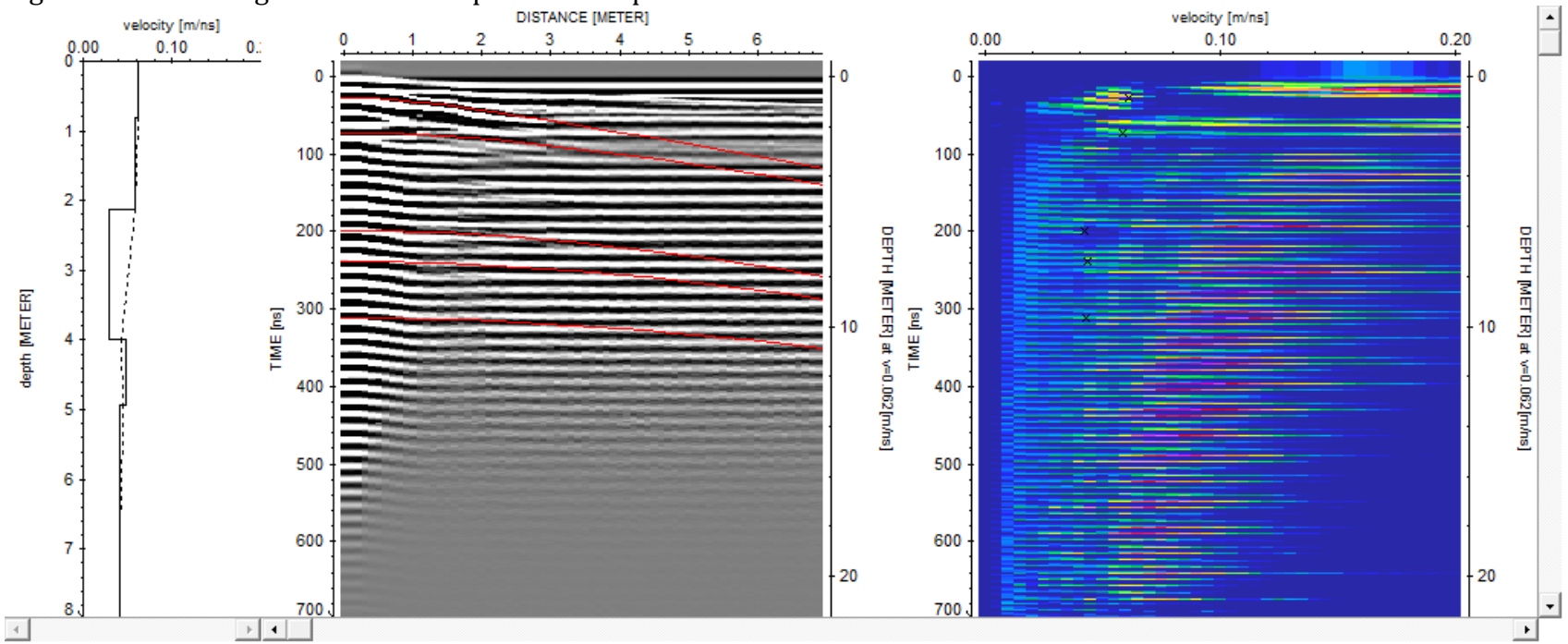

Figure 10. Same as Figure 1 but for oil plantation 2 plot 5.

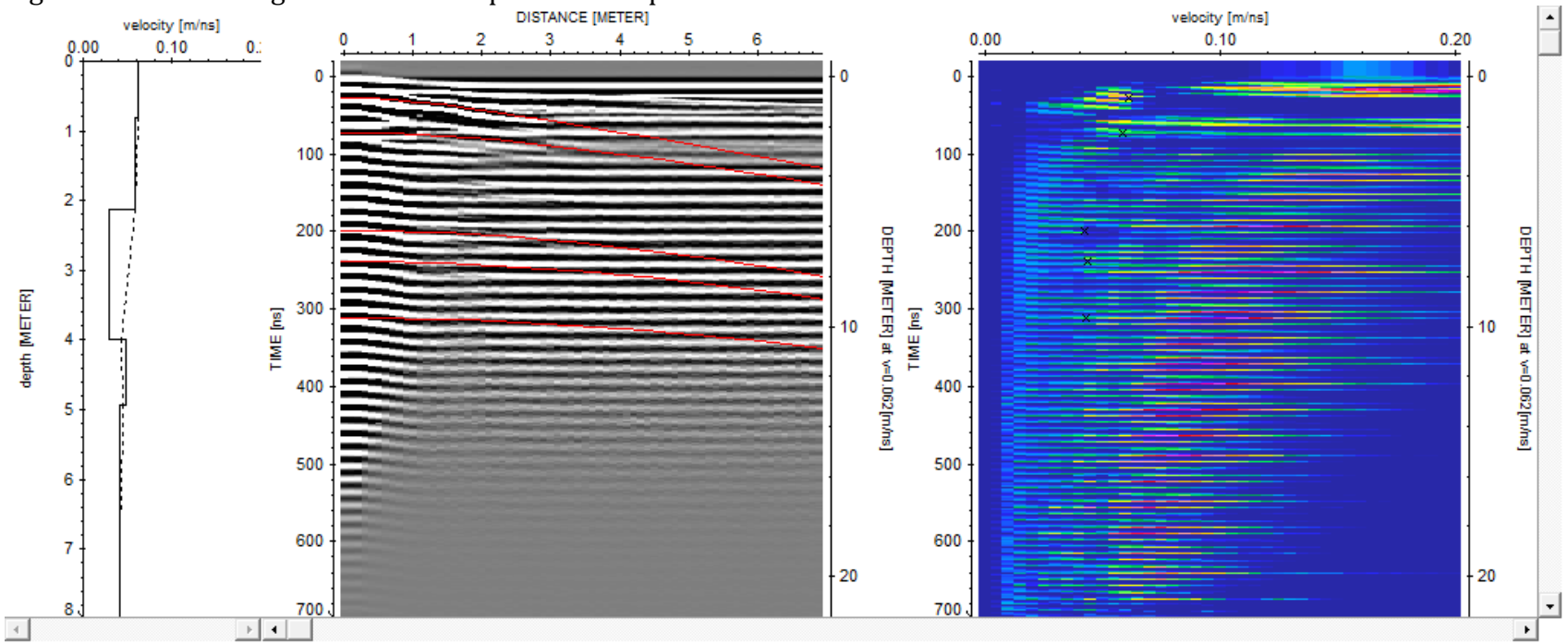

Figure 11. Same as Figure 1 but for oil plantation 2 plot 6.

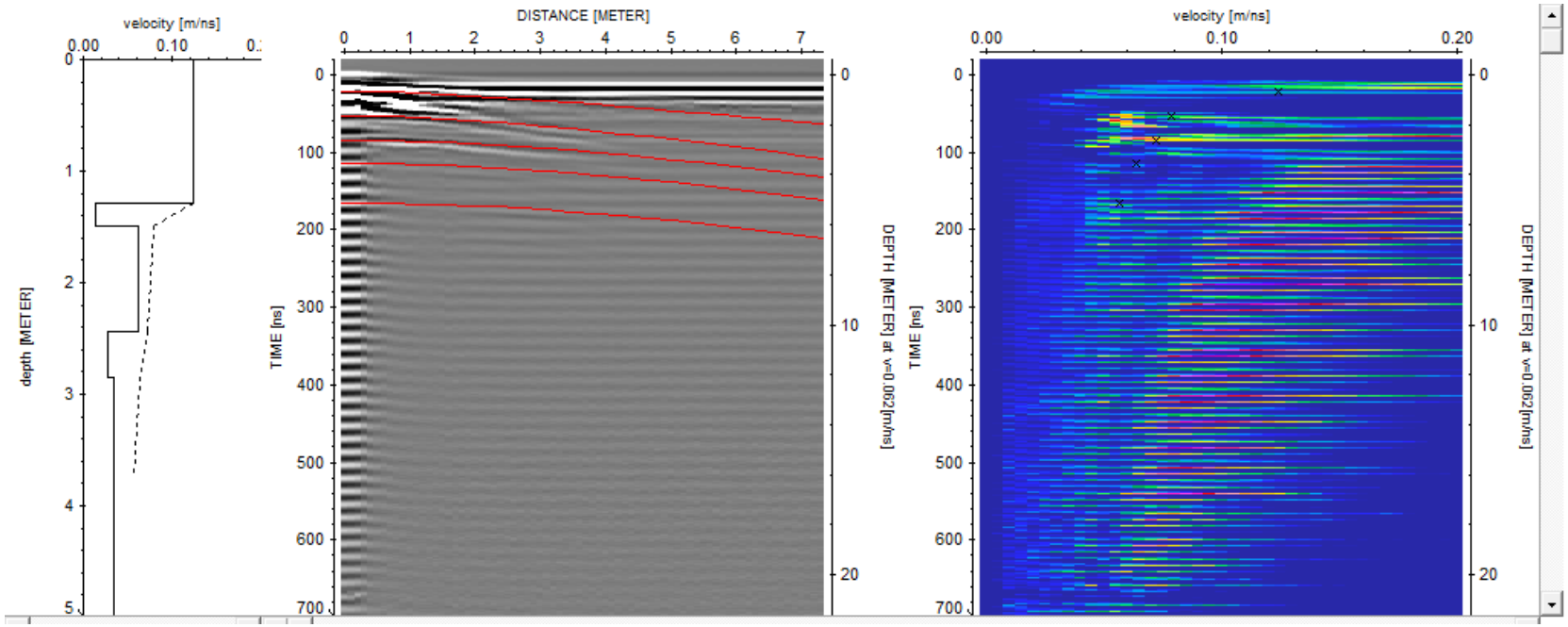

Figure 12. Same as Figure 1 but for oil plantation 3 plot 1.

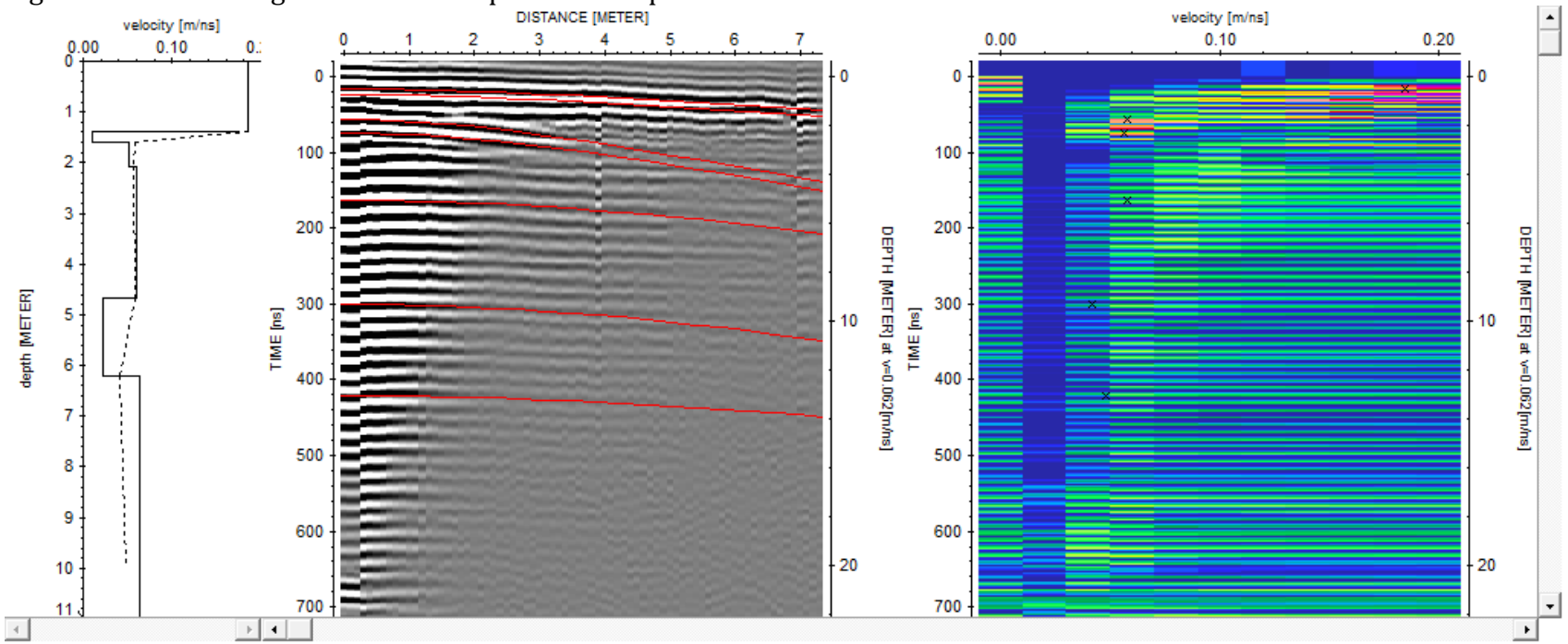

Figure 13. Same as Figure 1 but for oil plantation 3 plot 2.

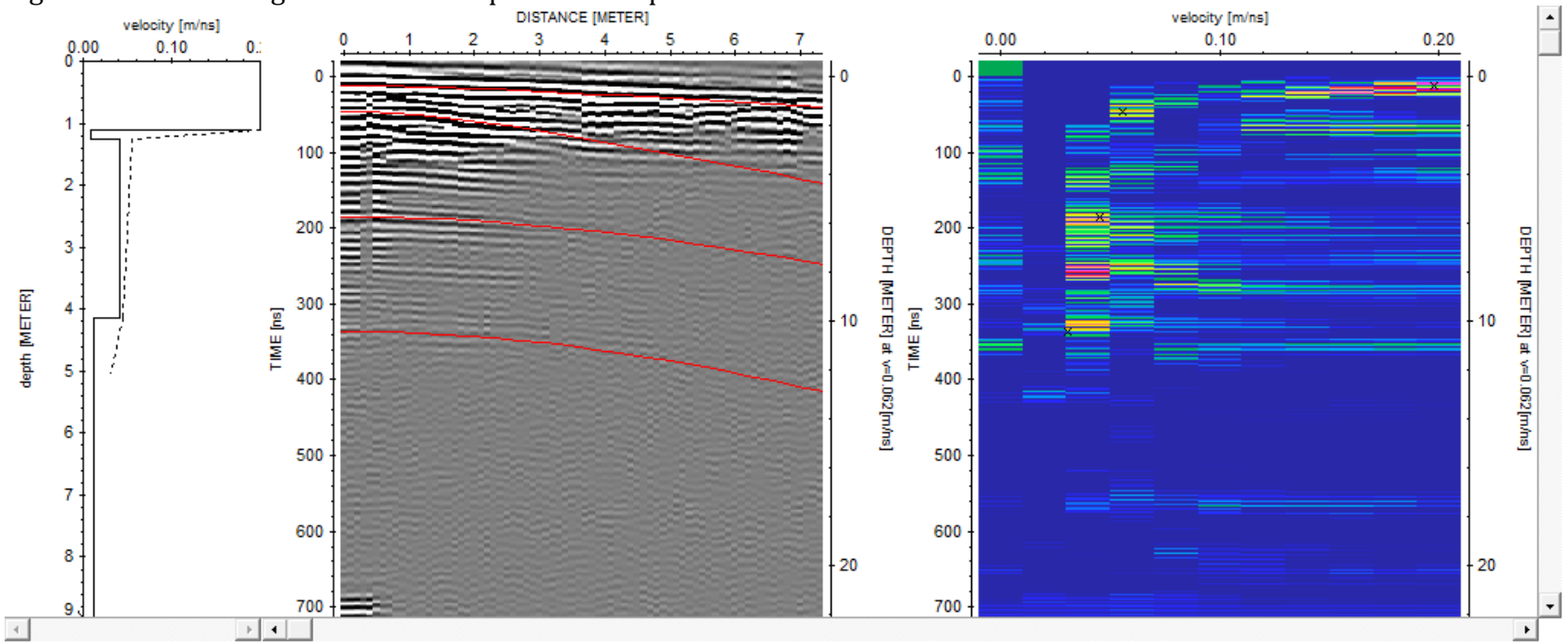

Figure 14. Same as Figure 1 but for oil plantation 3 plot 3.

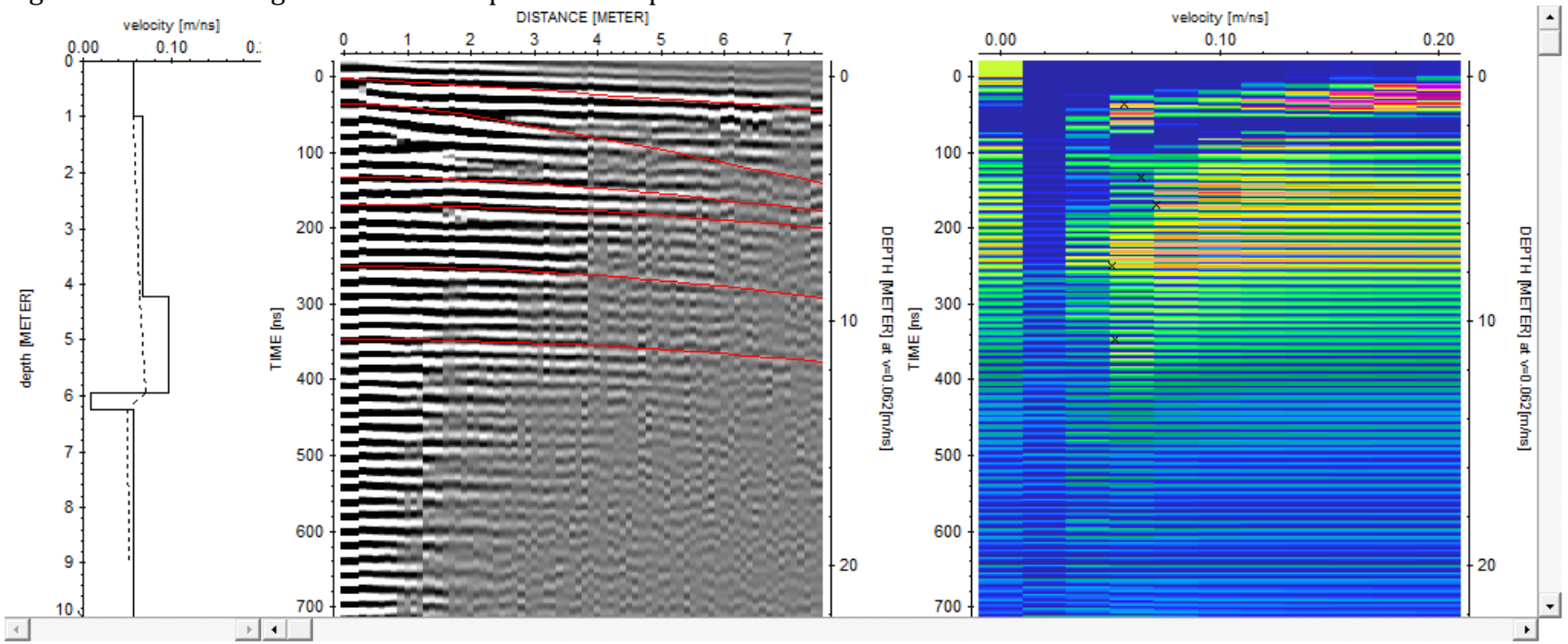

Figure 15. Same as Figure 1 but for oil plantation 3 plot 4.

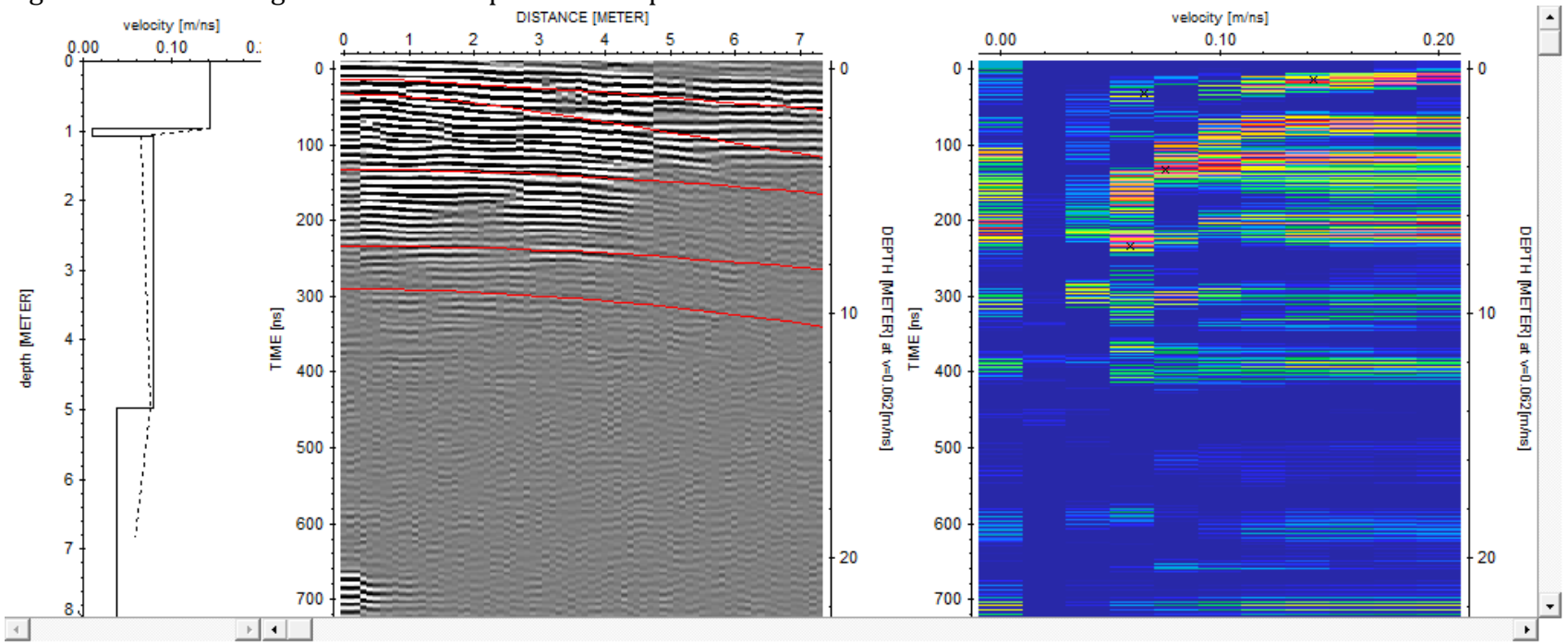

Figure 16. Same as Figure 1 but for oil plantation 3 plot 5.

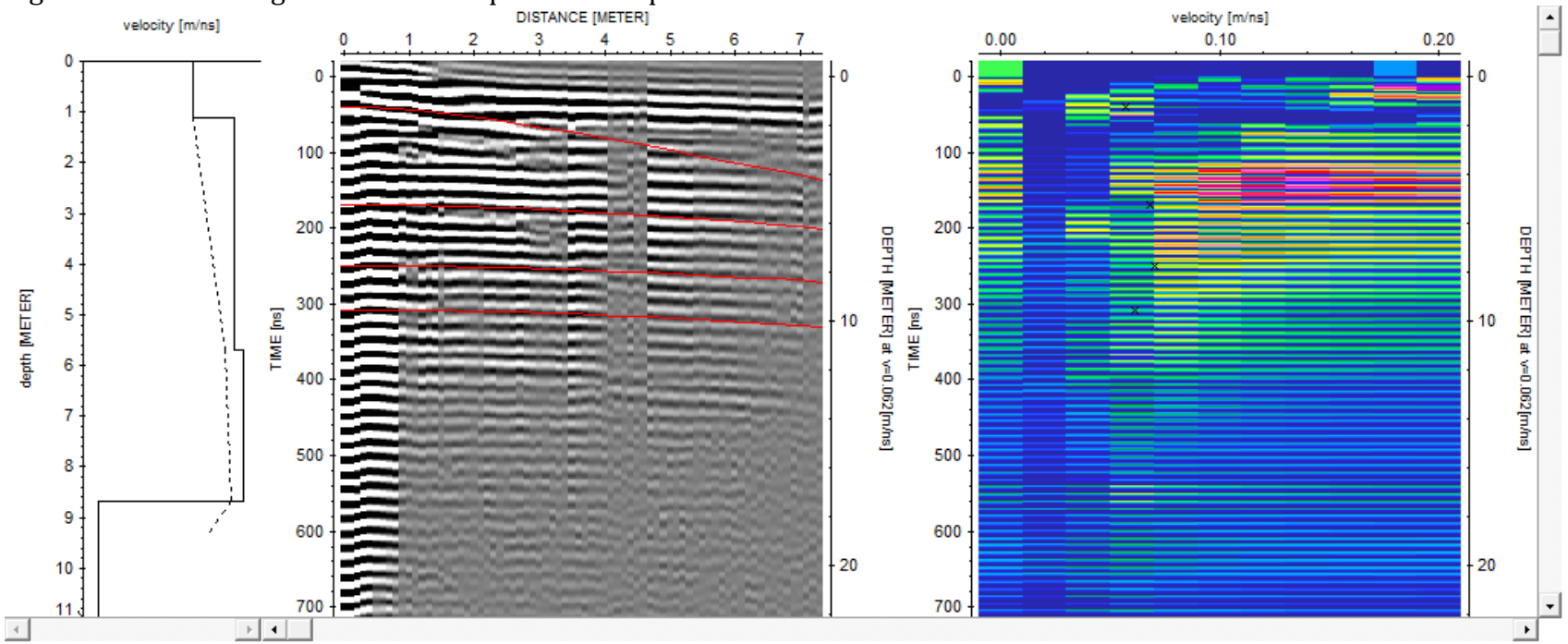

Figure 17. Same as Figure 1 but for oil plantation 3 plot 6.

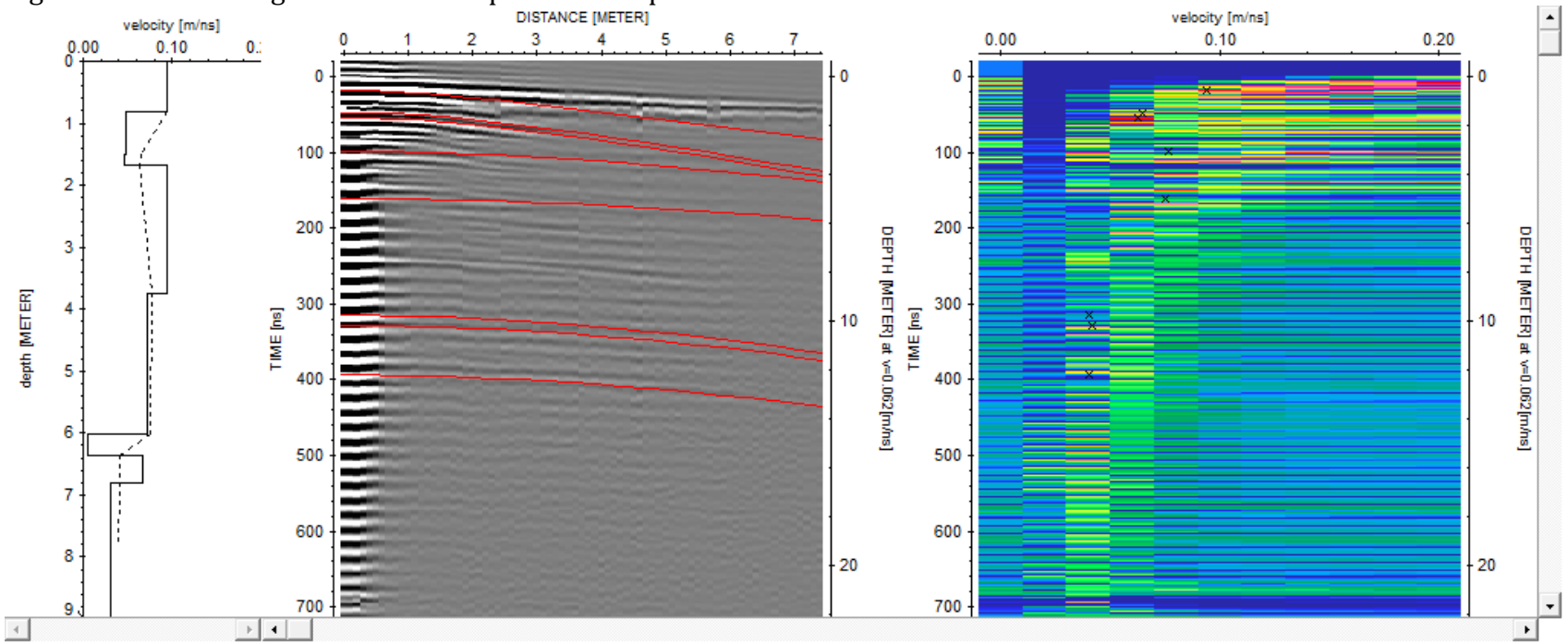

Figure 18. Same as Figure 1 but for Seral 1 plot 1.

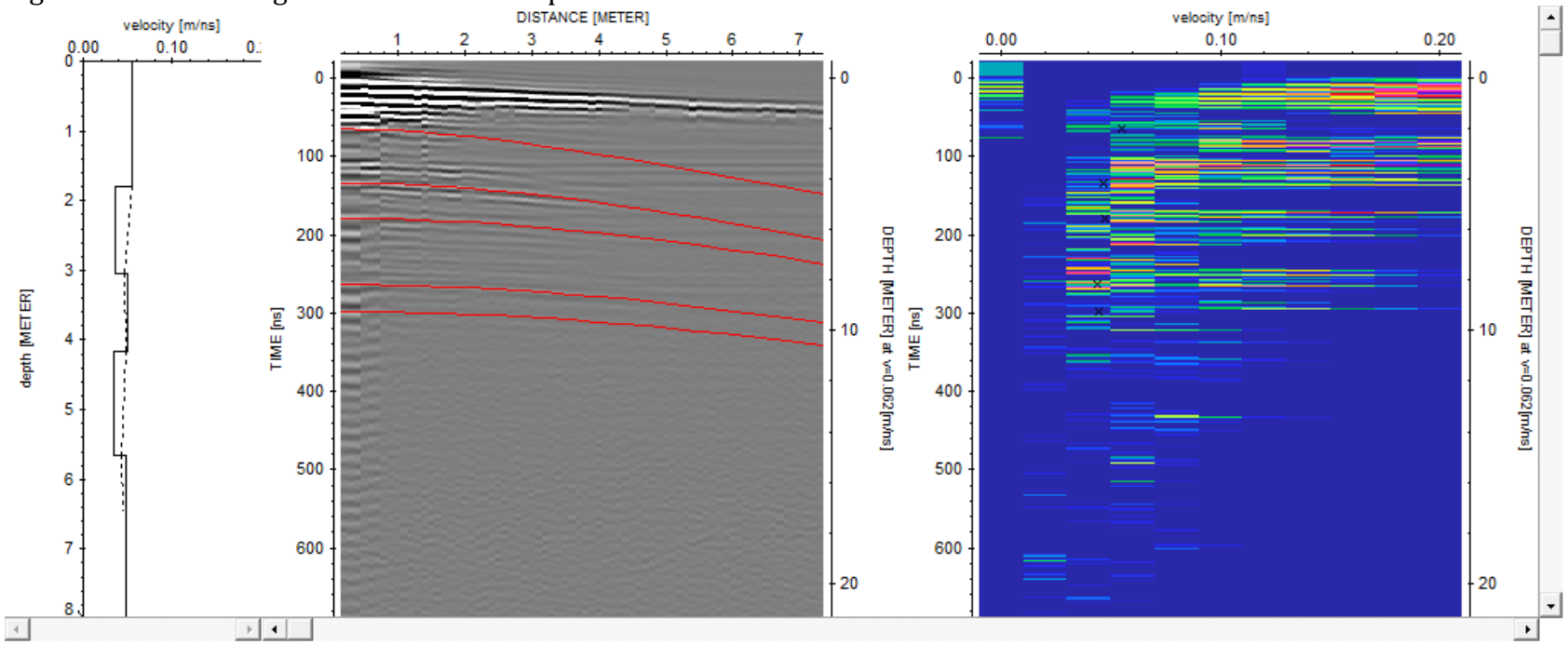

Figure 19. Same as Figure 1 but for Seral 1 plot 2.

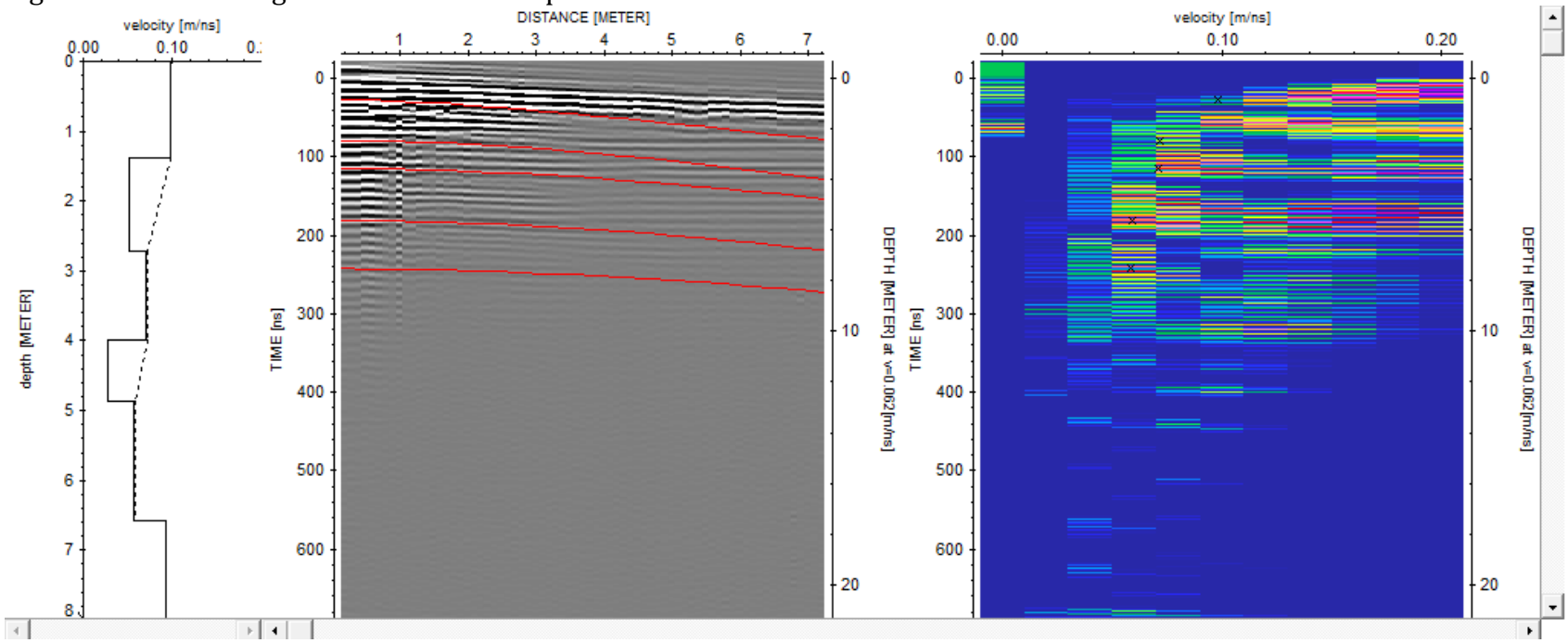

Figure 20. Same as Figure 1 but for Seral 1 plot 3.

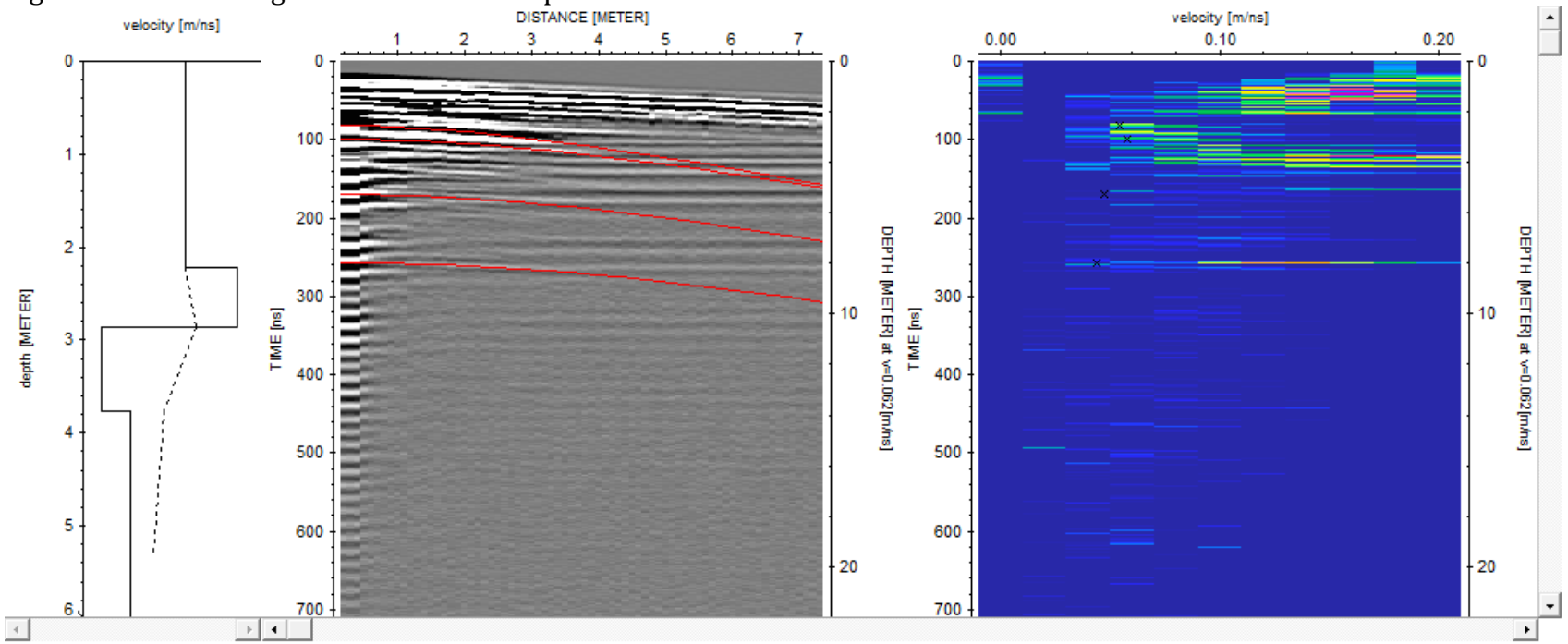

Figure 21. Same as Figure 1 but for Seral 1 plot 4.

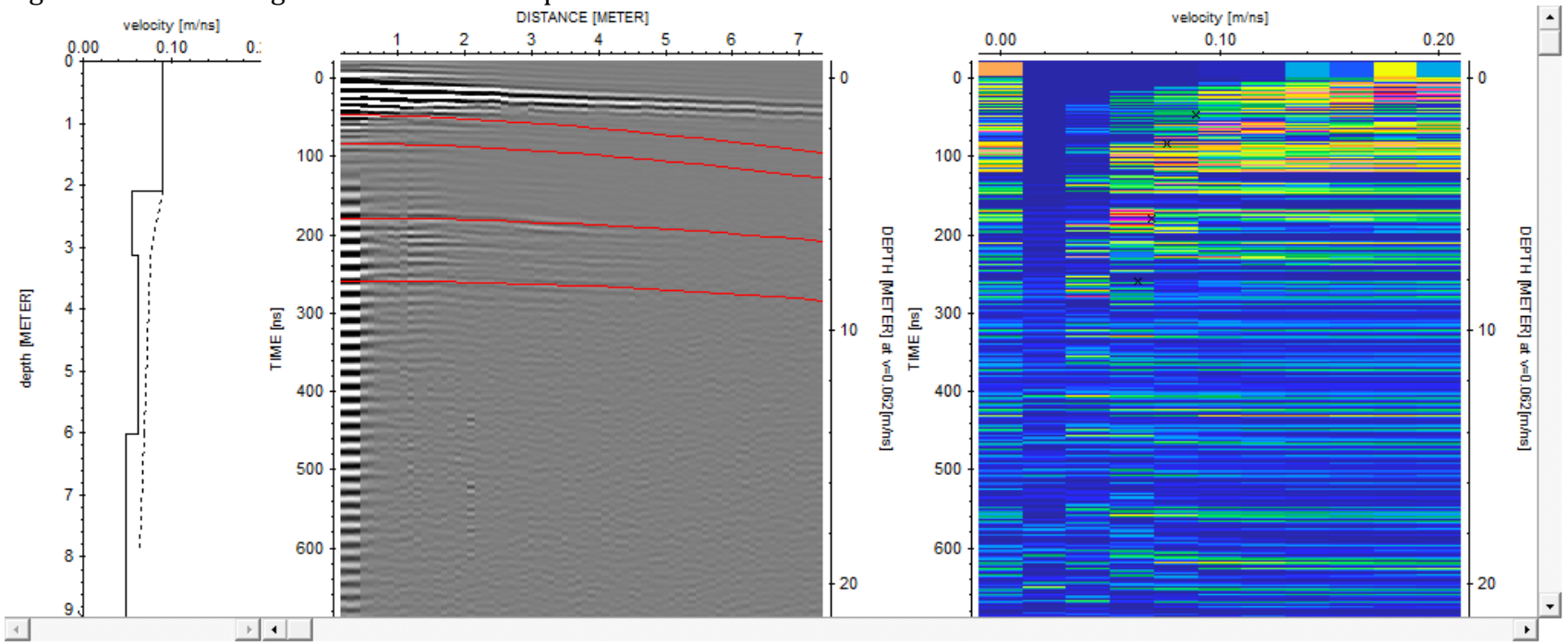

Figure 22. Same as Figure 1 but for Seral 1 plot 5.

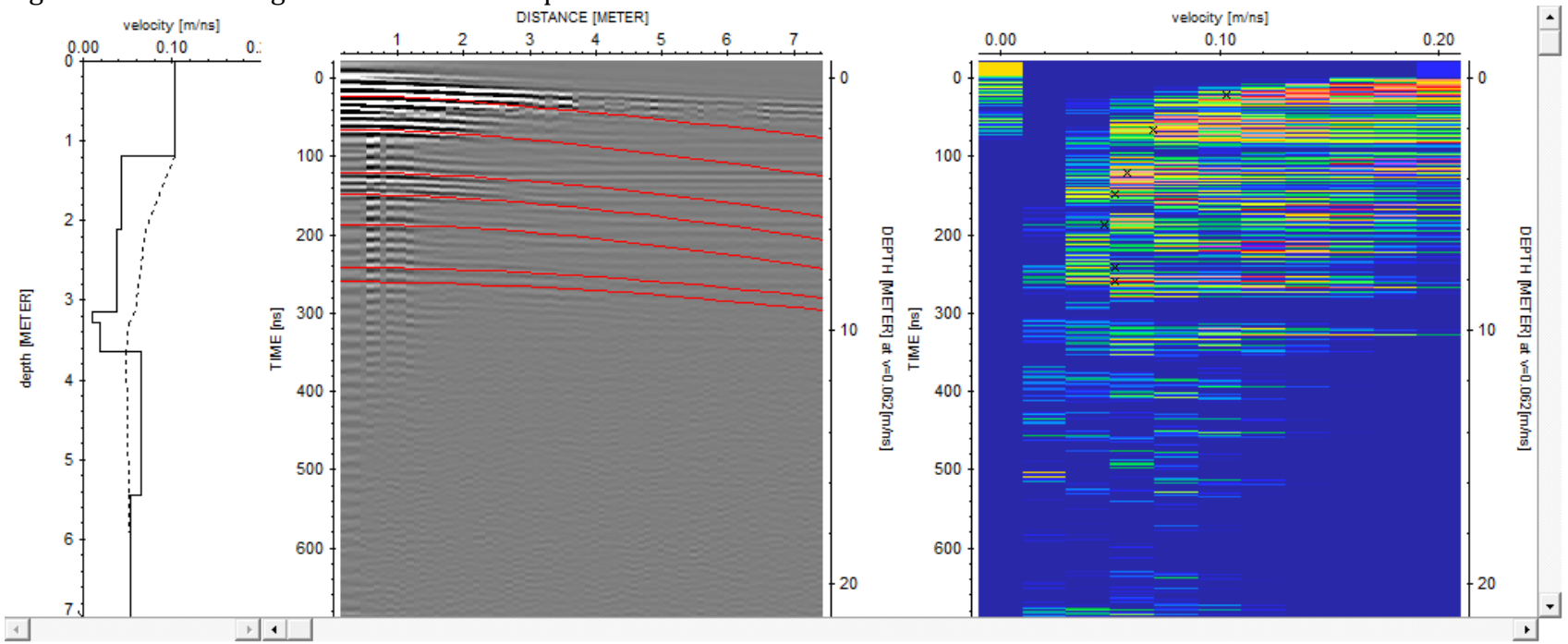

Figure 23. Same as Figure 1 but for Seral 1 plot 6.

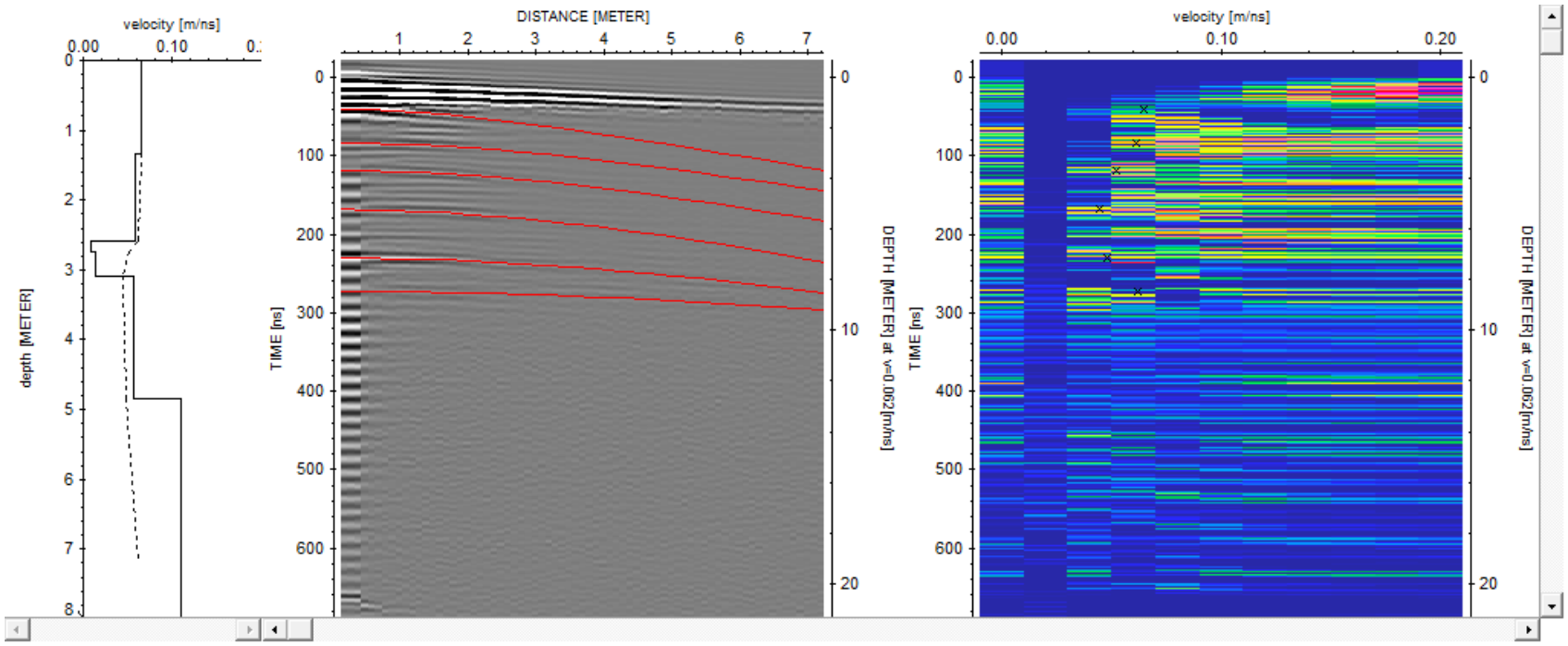

Figure 24. Same as Figure 1 but for Seral 2 plot 1.

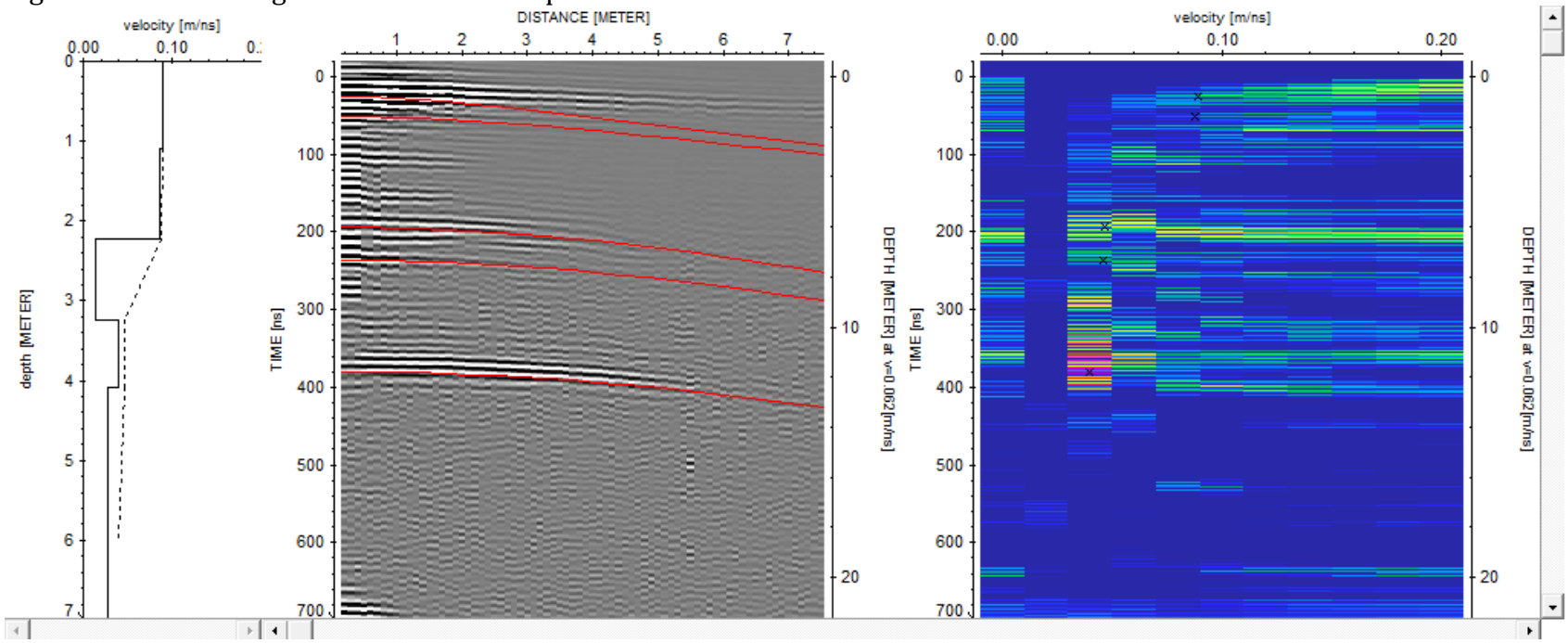

Figure 25. Same as Figure 1 but for Seral 2 plot 2.

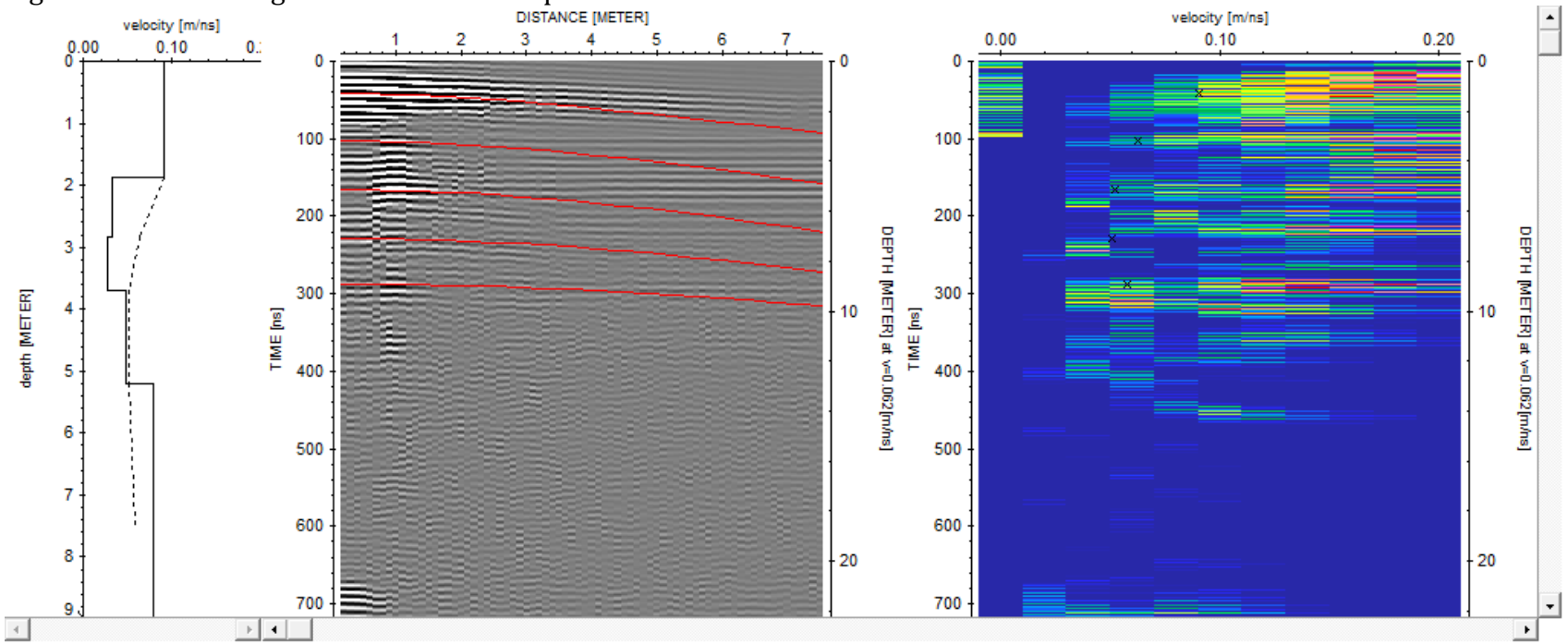

Figure 25. Same as Figure 1 but for Seral 2 plot 3.

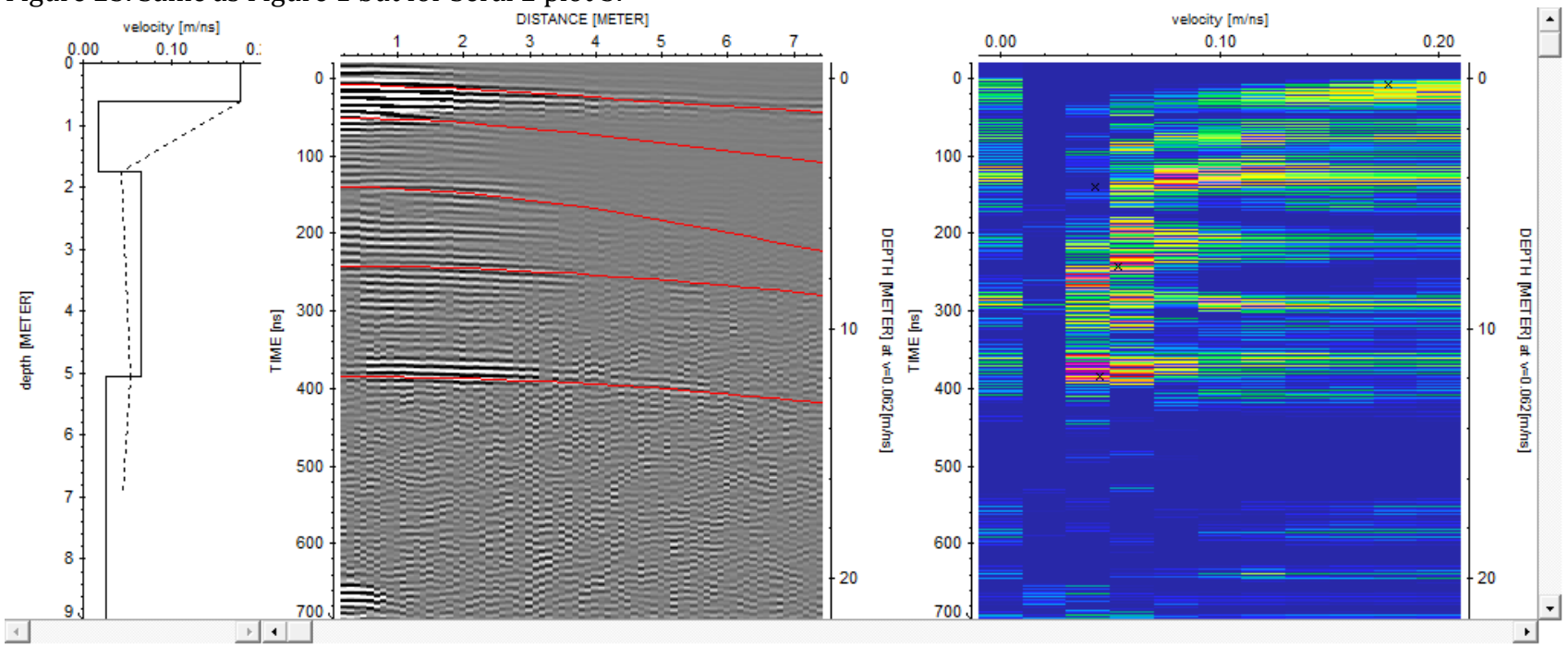

Figure 26. Same as Figure 1 but for Seral 2 plot 4.

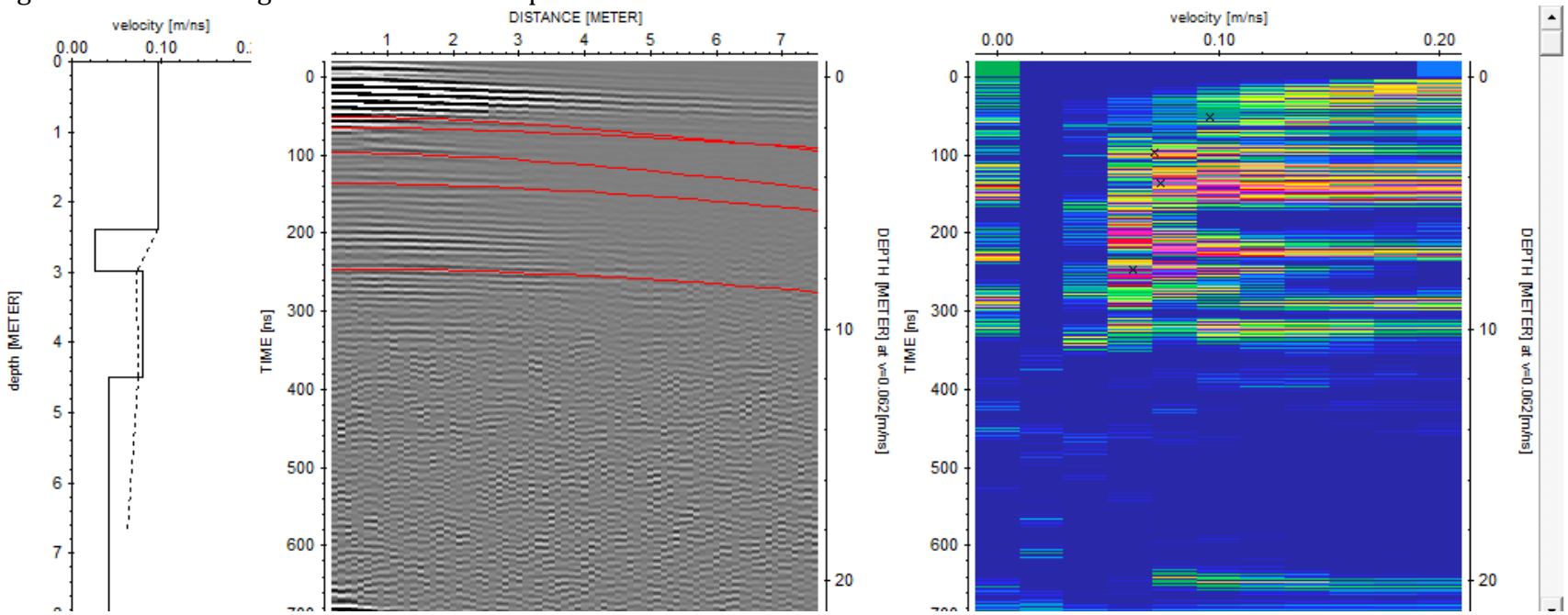

Figure 27. Same as Figure 1 but for Seral 2 plot 5.

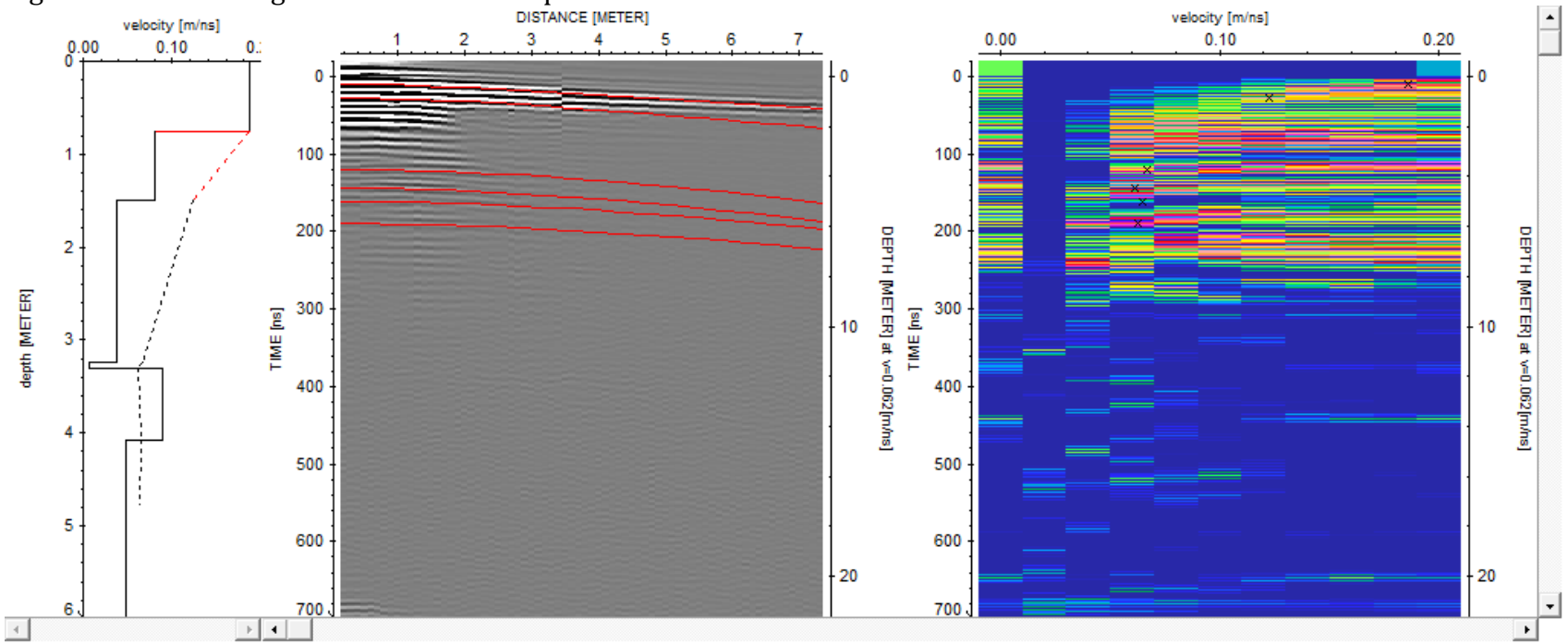

Figure 28. Same as Figure 1 but for Seral 2 plot 6.

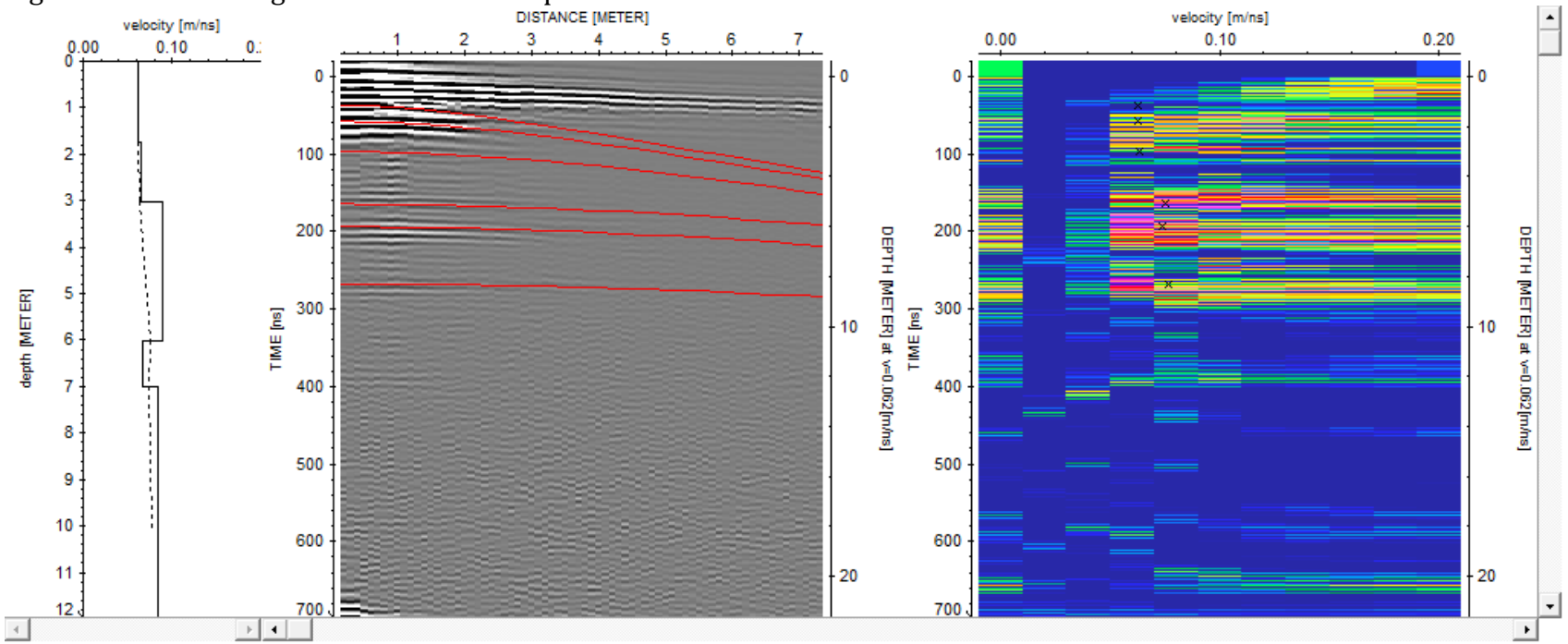

Figure 29. Same as Figure 1 but for Seral 3 plot 1.

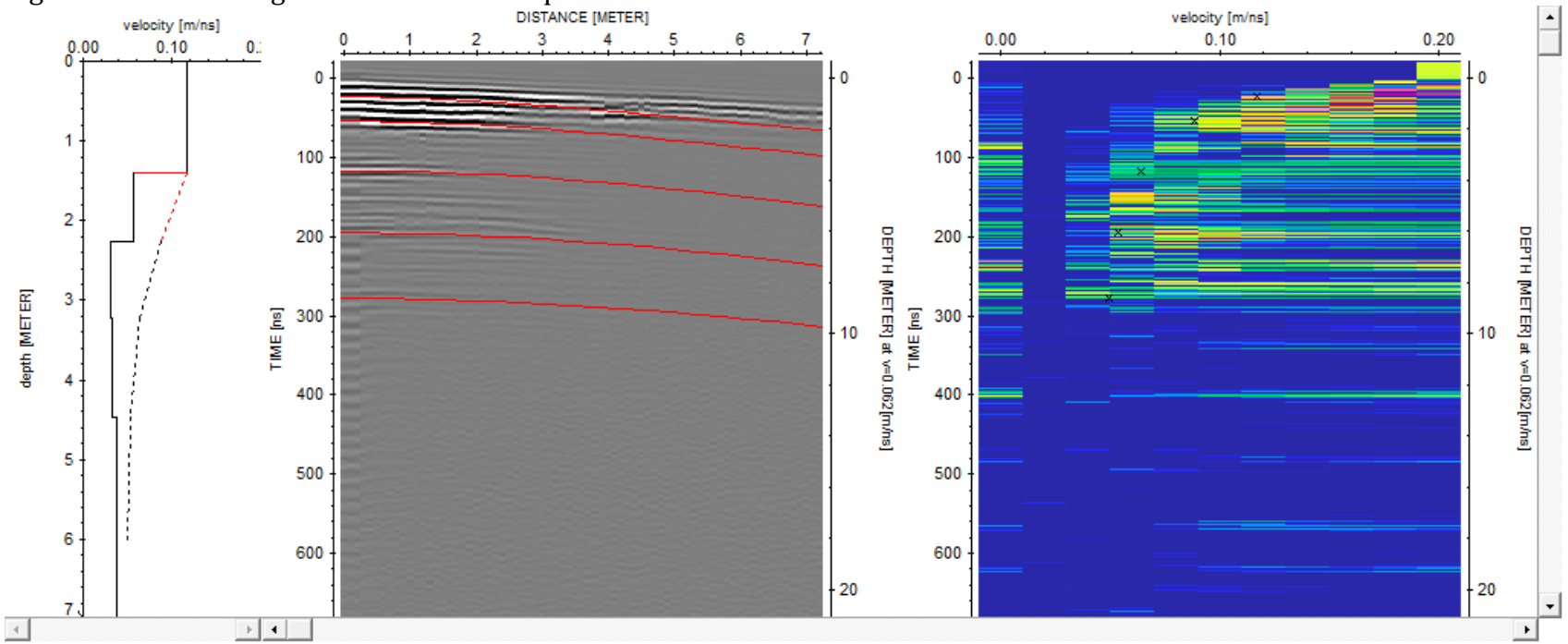

Figure 30. Same as Figure 1 but for Seral 3 plot 2.

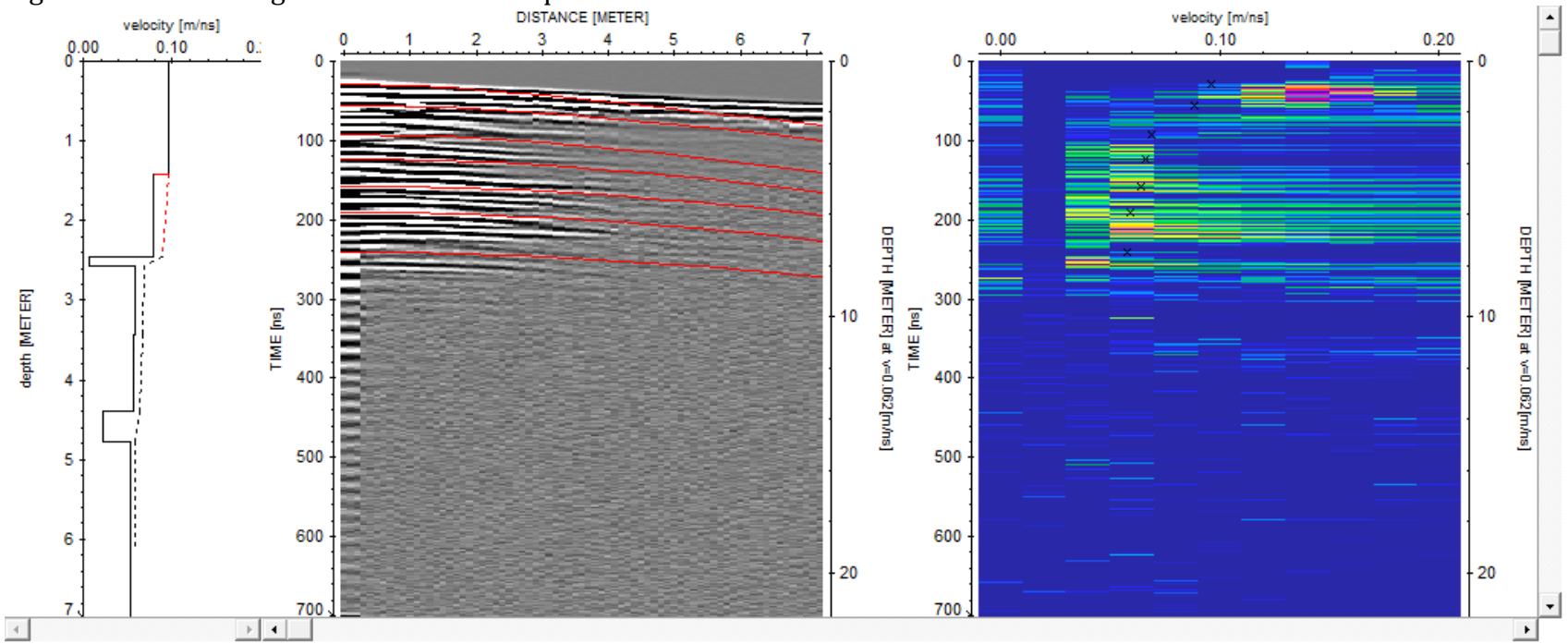

Figure 31. Same as Figure 1 but for Seral 3 plot 3.

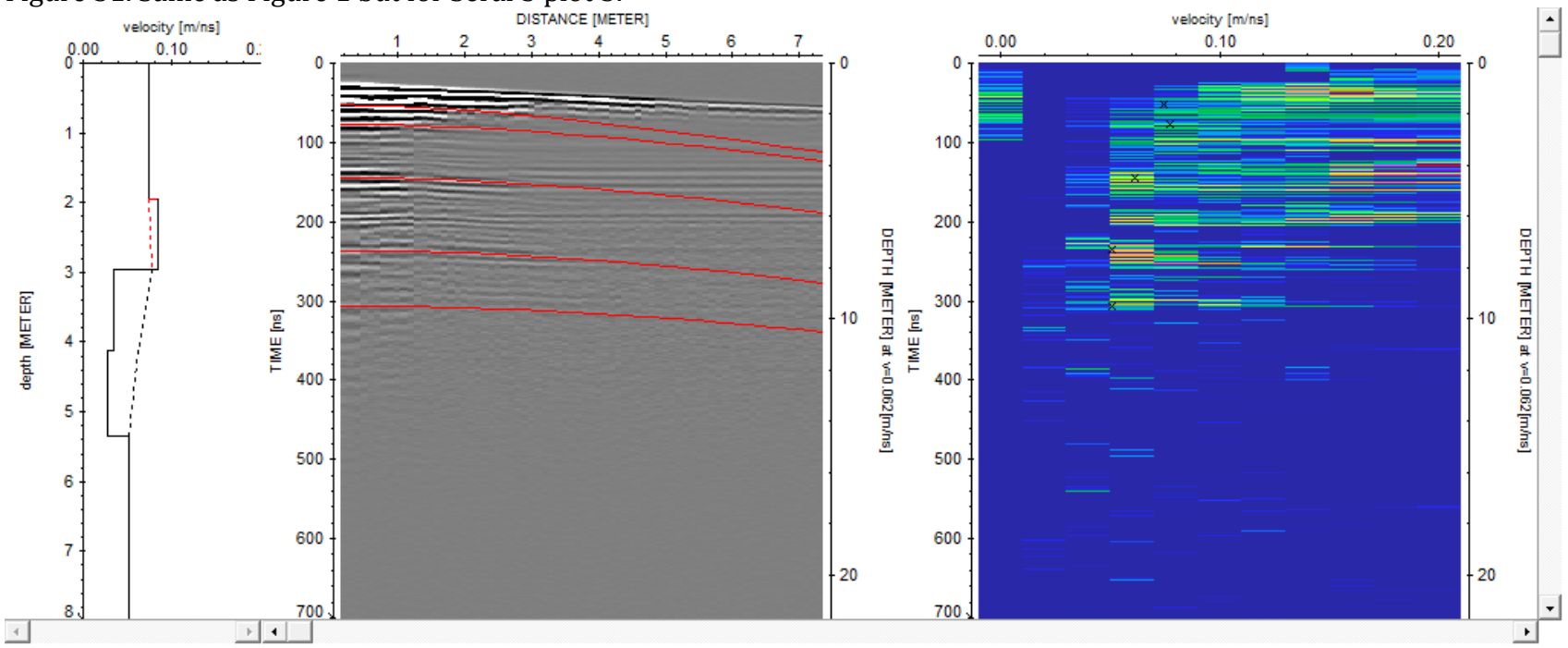

Figure 32. Same as Figure 1 but for Seral 3 plot 4.

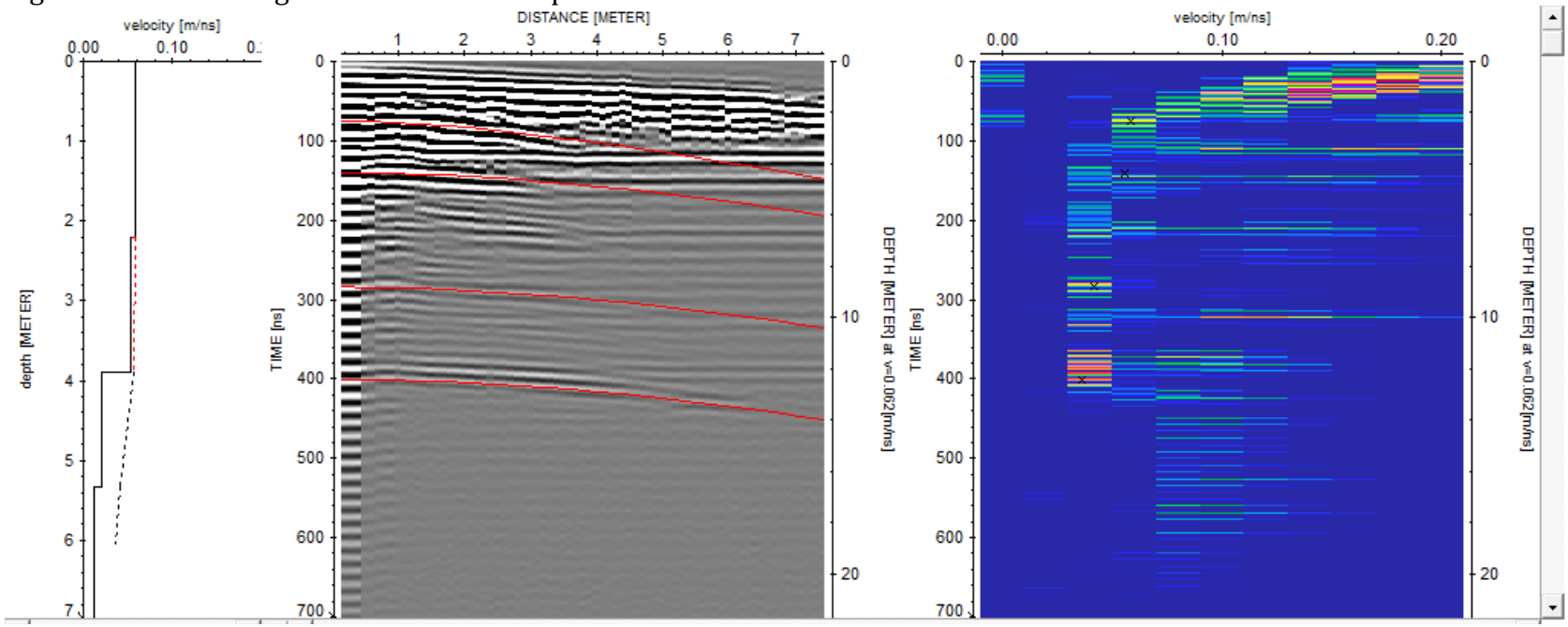

Figure 33. Same as Figure 1 but for Seral 3 plot 5.

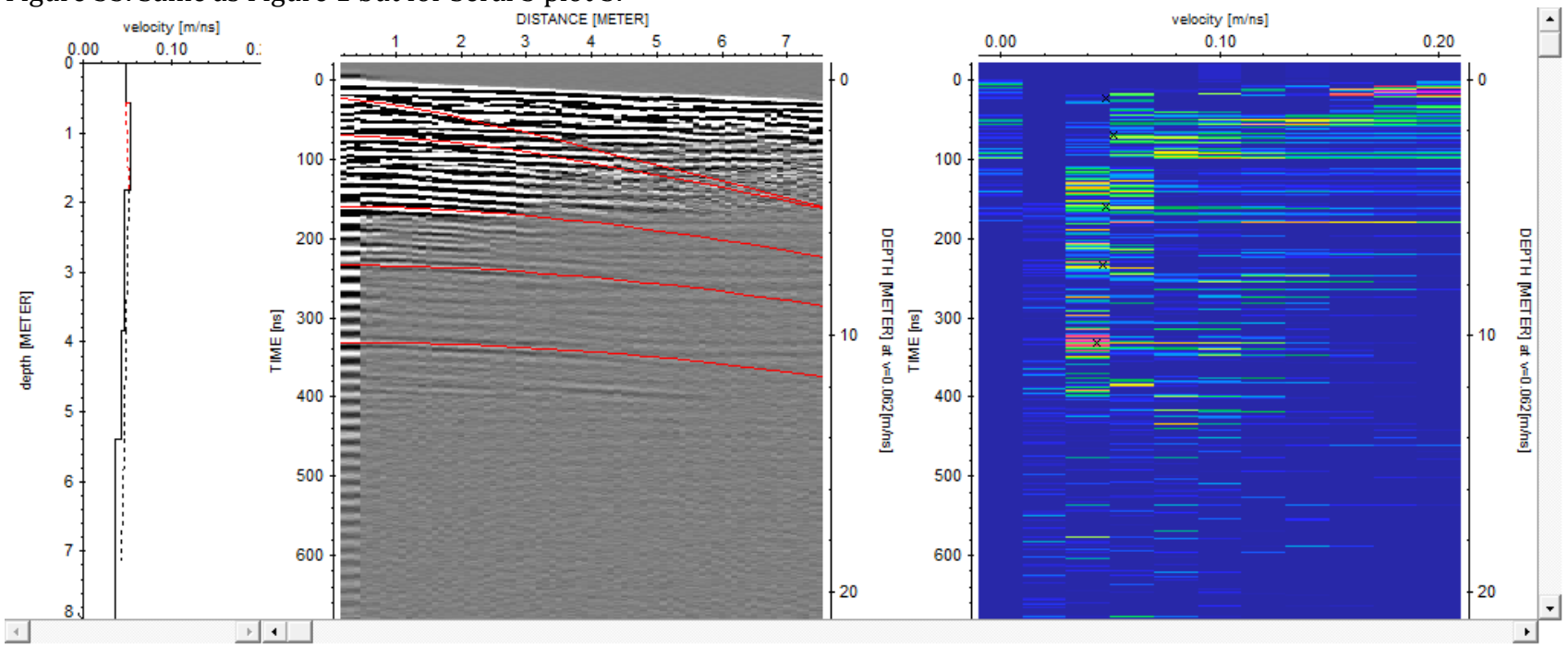

Figure 34. Same as Figure 1 but for Seral 3 plot 6.

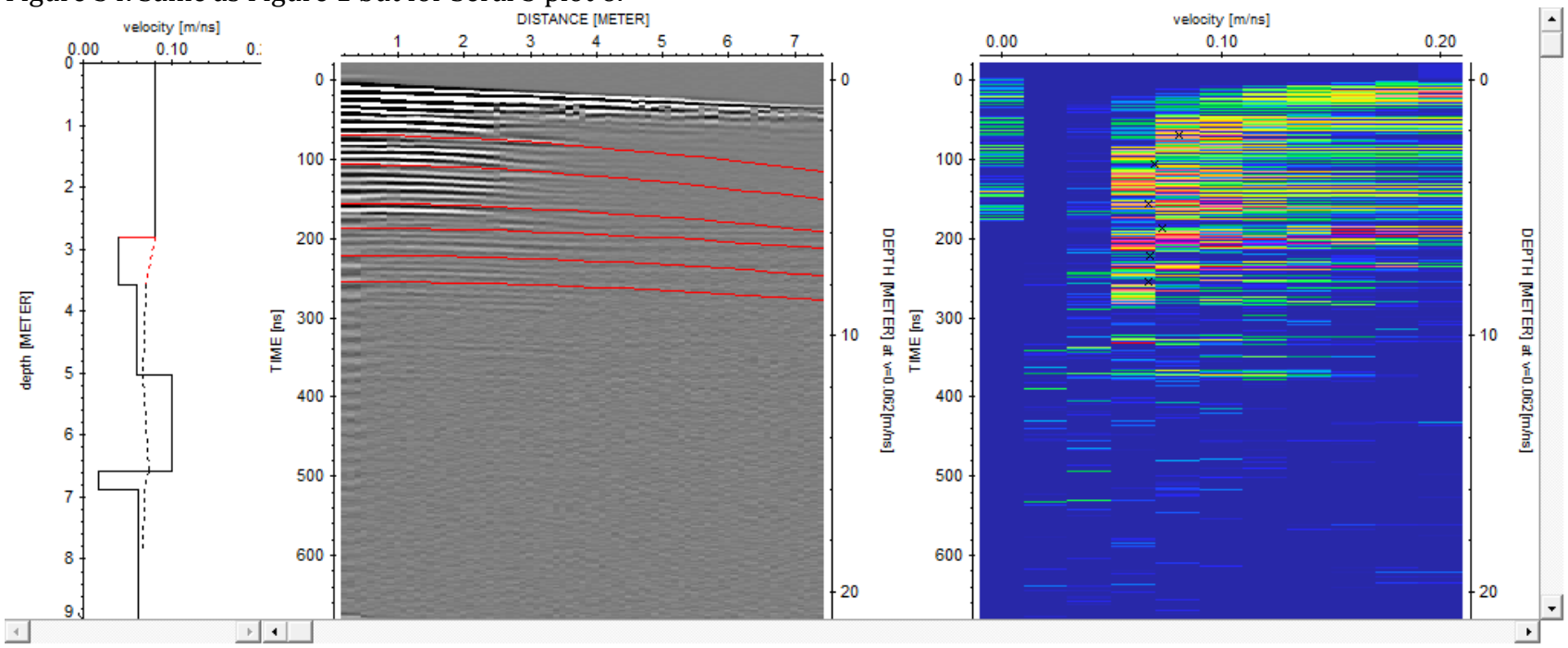

Table 1. Saturated hydraulic conductivity (K_s), carbon (C), nitrogen (N), carbon to nitrogen ratio (C/N), bulk density (BD), ash content, von Post degree of decomposition, and depth of measurement used for chapter 2.

Land cover	Site	Plot	Ks (m day^{-1})	C (%)	N (%)	C/N	BD (g cm^{-3})	Ash (%)	von Post	Depth (cm)
Forests	F1	2	0.035	59.2	0.9	65.8	0.063	51.8	5	350
Forests	F1	2	0.012	31.2	0.4	78.0	0.137	1.8	7	550
Forests	F1	3	0.046	53.3	1.5	35.5	0.091	10.6	7	75
Forests	F1	3	0.036	57.3	0.6	95.5	0.051	56.5	5	350
Forests	F1	4	0.074	54.4	1.6	34.0	0.115	1.1	8	75
Forests	F1	4	0.054	60.5	1.0	60.5	0.054	0.7	5	550
Forests	F1	5	0.174	53.7	1.6	33.6	0.093	2.2	8	75
Forests	F1	5	0.013	58.9	0.9	65.4	0.071	2.5	8	350
Forests	F1	5	1.105	34.3	0.4	85.8	0.153	1.5	6	550
Forests	F1	6	0.208	57.4	1.3	44.2	0.106	2.3	7	75
Forests	F1	6	0.029	58.5	1.0	58.5	0.067	1.5	7	350
Forests	F1	6	0.025	37.7	0.4	94.3	0.157	11.3	4	550
Forests	F2	1	1.927	50.9	1.1	46.3	0.093	1.3	8	75
Forests	F2	1	0.026	54.8	0.8	68.5	0.122	1.4	9	350
Forests	F2	1	0.018	50.1	0.8	62.6	0.106	5.9	5	550
Forests	F2	2	0.103	50.8	0.8	63.5	0.092	5.5	9	350
Forests	F2	2	0.021	22.3	0.3	74.3	0.22	52.3	7	550
Forests	F2	3	1.303	49.4	1.3	38.0	0.085	1.3	5	75
Forests	F2	3	0.045	53.7	0.9	59.7	0.087	1.7	5	350
Forests	F2	3	0.048	24.9	0.3	83.0	0.231	35.1	4	550
Forests	F2	4	2.943	49.1	1.4	35.1	0.095	2.9	5	75
Forests	F2	4	0.044	53.5	1.0	53.5	0.094	1.4	5	350

Forests	F2	4	0.038	19.5	0.3	65.0	0.301	56.6	8	550
Forests	F2	5	0.227	50.7	1.4	36.2	0.114	2.3	6	75
Forests	F2	5	0.053	53.7	0.9	59.7	0.093	2.0	8	350
Forests	F2	5	0.030	25.6	0.3	85.3	0.302	43.8	3	550
Forests	F2	6	0.131	51.3	1.4	36.6	0.088	2.6	6	75
Forests	F2	6	0.077	54.4	0.9	60.4	0.093	2.8	7	350
Forests	F2	6	0.012	19.8	0.2	99.0	0.252	54.7	5	550
Forests	F3	1	1.284	51.9	1.2	43.3	0.113	1.9	5	75
Forests	F3	1	0.024	52.7	1.0	52.7	0.091	1.2	5	350
Forests	F3	1	0.026	30.5	0.3	101.7	0.199	31.4	3	550
Forests	F3	2	0.314	52.4	1.3	40.3	0.097	11.3	9	75
Forests	F3	2	0.030	52.9	0.8	66.1	0.103	2.7	6	350
Forests	F3	2	0.059	31.9	0.3	106.3	0.181	33.1	5	550
Forests	F3	3	4.211	52.4	1.1	47.6	0.081	3.5	9	75
Forests	F3	3	0.021	53.1	0.9	59.0	0.08	2.9	7	350
Forests	F3	3	0.018	30.1	0.9	33.4	0.16	1.7	3	550
Forests	F3	4	13.871	52.0	1.1	47.3	0.101	2.1	4	75
Forests	F3	4	0.025	53.5	1.0	53.5	0.082	2.5	5	350
Forests	F3	4	0.020	34.6	0.4	86.5	0.068	30.7	3	550
Forests	F3	5	2.462	53.1	1.0	53.1	0.076	2.4	8	75
Forests	F3	5	0.014	52.0	1.0	52.0	0.069	2.7	4	350
Forests	F3	5	0.010	38.8	0.4	97.0	0.14	19.9	3	550
Forests	F3	6	1.617	50.5	1.3	38.8	0.117	1.6	8	75
Forests	F3	6	0.011	54.2	0.9	60.2	0.09	1.6	4	350
Forests	F3	6	0.011	32.8	0.4	82.0	0.125	32.8	3	550
Forests	F4	1	0.036	54.6	0.7	78.0	0.106	1.0	5	75
Forests	F4	1	0.088	54.0	0.9	60.0	0.095	1.2	5	350

Forests	F4	1	0.036	54.2	0.8	67.8	0.127	19.6	4	550
Forests	F4	2	0.038	53.5	1.0	53.5	0.129	2.1	7	75
Forests	F4	2	0.018	54.3	0.9	60.3	0.115	31.5	6	350
Forests	F4	2	0.030	54.1	0.7	77.3	0.109	1.4	5	550
Forests	F4	3	0.076	54.8	0.7	78.3	0.141	3.5	7	75
Forests	F4	3	0.055	54.2	2.8	19.4	0.113	1.2	4	350
Forests	F4	3	0.034	52.9	0.9	58.8	0.114	6.8	4	550
Forests	F4	4	0.012	53.6	0.8	67.0	0.137	1.5	8	75
Forests	F4	4	0.240	55.0	0.9	61.1	0.109	1.1	4	350
Forests	F4	4	0.045	54.2	0.8	67.8	0.126	2.3	9	550
Forests	F4	5	0.030	54.7	0.9	60.8	0.119	1.3	7	350
Forests	F4	5	0.019	54.7	0.7	78.1	0.148	1.7	5	550
Forests	F4	6	0.027	44.1	0.7	63.0	0.084	1.6	8	75
Forests	F4	6	0.018	46.4	0.7	66.3	0.16	1.5	5	350
Forests	F5	1	0.018	54.2	0.8	67.8	0.113	1.3	6	75
Forests	F5	1	0.049	55.2	0.8	69.0	0.126	1.3	5	350
Forests	F5	1	0.063	53.9	0.8	67.4	0.115	2.6	4	550
Forests	F5	2	0.061	54.2	1.2	45.2	0.153	21.7	6	75
Forests	F5	2	0.085	53.2	0.8	66.5	0.092	2.4	5	350
Forests	F5	2	0.038	54.1	0.8	67.6	0.118	3.8	5	550
Forests	F5	3	0.031	54.7	0.7	78.1	0.121	1.4	7	75
Forests	F5	3	0.142	54.4	0.7	77.7	0.101	2.0	6	350
Forests	F5	3	0.023	54.1	1.4	38.6	0.128	4.7	5	550
Forests	F5	4	0.028	54.8	0.9	60.9	0.162	1.9	5	75
Forests	F5	4	0.021	54.9	0.7	78.4	0.114	2.0	5	350
Forests	F5	4	0.028	54.7	0.7	78.1	0.108	2.4	5	550
Forests	F5	5	0.031	53.2	0.9	59.1	0.135	2.0	4	75

Forests	F5	5	0.041	54.6	0.8	68.3	0.106	2.8	5	350
Forests	F5	5	0.020	53.9	0.7	77.0	0.119	2.2	6	550
Forests	F5	6	0.025	54.2	0.7	77.4	0.137	2.7	8	75
Forests	F5	6	0.127	54.2	0.8	67.8	0.116	3.0	5	350
Forests	F5	6	0.026	53.7	0.9	59.7	0.12	1.2	5	550
Forests	F6	1	0.132	51.5	0.8	64.4	0.103	2.0	5	75
Forests	F6	1	0.022	51.0	1.2	42.5	0.117	4.8	6	350
Forests	F6	1	0.081	27.1	0.3	96.2	0.318	46.2	3	550
Forests	F6	2	0.186	49.8	1.3	39.2	0.119	2.5	6	75
Forests	F6	2	0.133	55.0	0.9	58.2	0.099	10.1	6	350
Forests	F6	2	0.096	46.4	0.9	52.3	0.107	12.6	5	550
Forests	F6	3	0.232	44.7	1.2	36.9	0.112	4.8	6	75
Forests	F6	3	0.046	53.5	1.0	51.8	0.117	2.5	6	350
Forests	F6	3	0.065	42.7	0.8	54.0	0.114	17.1	5	550
Forests	F6	4	2.138	48.7	1.2	39.4	0.106	4.8	6	75
Forests	F6	4	0.082	53.9	1.0	54.7	0.088	3.0	7	350
Forests	F6	4	0.076	52.7	1.0	54.4	0.103	4.4	5	550
Forests	F6	5	0.056	53.6	0.8	70.4	0.132	1.2	5	350
Forests	F6	5	0.123	41.8	0.6	72.9	0.11	22.4	6	550
Forests	F6	6	0.664	49.1	1.5	33.8	0.13	16.0	5	75
Forests	F6	6	0.026	58.9	0.7	85.5	0.112	3.7	5	350
Forests	F6	6	0.131	51.8	0.8	65.6	0.124	1.8	5	550
Forests	F7	1	0.387	53.5	1.0	55.8	0.092	3.1	7	75
Forests	F7	1	0.101	49.6	1.4	35.5	0.105	4.7	5	350
Forests	F7	1	0.244	51.9	1.1	46.1	0.087	2.8	4	550
Forests	F7	2	0.635	51.3	1.3	39.6	0.09	2.5	5	75
Forests	F7	2	0.086	31.4	0.3	93.4	0.12	33.7	7	350

Forests	F7	2	0.095	37.8	0.5	83.7	0.182	22.3	4	550
Forests	F7	3	0.738	50.7	0.9	58.6	0.077	4.4	5	75
Forests	F7	3	0.046	53.0	0.8	62.5	0.09	3.0	7	350
Forests	F7	3	0.107	31.4	0.4	78.6	0.148	33.6	5	550
Forests	F7	4	2.191	52.9	0.9	56.9	0.09	4.5	5	75
Forests	F7	4	0.087	45.9	1.4	32.2	0.136	2.6	5	350
Forests	F7	4	0.153	30.1	0.3	92.8	0.151	35.4	4	550
Forests	F7	5	1.173	47.9	1.1	41.8	0.108	5.4	7	75
Forests	F7	5	0.060	29.2	0.3	105.9	0.137	3.9	5	350
Forests	F7	5	0.141	29.2	0.3	107.2	0.159	36.7	4	550
Forests	F7	6	0.188	51.5	1.4	37.5	0.104	2.9	5	75
Forests	F7	6	0.038	50.8	1.0	50.5	0.073	6.6	9	350
Forests	F7	6	0.082	29.4	0.3	88.1	0.178	37.0	4	550
Burnt Forests	BF1	1	0.070	57.7	1.0	57.7	0.089	23.5	6	75
Burnt Forests	BF1	1	0.087	59.2	0.8	74.0	0.075	1.3	8	350
Burnt Forests	BF1	1	0.047	19.9	0.1	199.0	0.254	14.8	5	550
Burnt Forests	BF1	2	0.501	55.9	1.6	34.9	0.075	32.6	8	75
Burnt Forests	BF1	2	0.019	47.7	0.7	68.1	0.092	2.7	8	350
Burnt Forests	BF1	2	0.605	23.0	0.2	115.0	0.26	10.0	4	550
Burnt Forests	BF1	3	0.193	59.6	1.4	42.6	0.068	25.0	9	75
Burnt	BF1	3	0.033	52.5	0.7	75.0	0.096	1.9	8	350

Forests										
Burnt Forests	BF1	4	0.291	57.9	1.0	57.9	0.054	13.9	9	75
Burnt Forests	BF1	4	0.055	58.7	0.5	117.4	0.111	2.1	6	350
Burnt Forests	BF1	4	0.231	59.8	1.2	49.8	0.083	5.6	4	550
Burnt Forests	BF1	5	0.114	56.9	1.4	40.6	0.076	1.0	7	75
Burnt Forests	BF1	5	0.061	57.8	1.0	57.8	0.065	1.3	5	350
Burnt Forests	BF1	5	0.024	55.9	0.5	111.8	0.099	33.0	8	550
Burnt Forests	BF2	1	0.078	52.6	1.3	40.5	0.1	2.6	9	75
Burnt Forests	BF2	1	0.143	55.0	0.9	61.1	0.107	3.6	5	350
Burnt Forests	BF2	2	0.351	51.4	1.2	42.8	0.095	2.2	6	75
Burnt Forests	BF2	2	0.042	53.2	0.9	59.1	0.109	9.1	5	350
Burnt Forests	BF2	2	0.042	51.7	0.7	73.9	0.106	4.0	5	550
Burnt Forests	BF2	3	0.287	52.8	1.3	40.6	0.094	1.8	4	75
Burnt Forests	BF2	3	0.096	54.5	0.9	60.6	0.11	1.9	7	350
Burnt	BF2	4	0.251	49.3	1.6	30.8	0.116	4.4	6	75

Forests										
Burnt Forests	BF2	5	1.567	52.0	1.3	40.0	0.088	2.3	6	75
Burnt Forests	BF2	5	0.041	53.2	0.9	59.1	0.116	6.6	8	350
Burnt Forests	BF2	6	0.463	52.8	1.2	44.0	0.1	2.5	5	75
Burnt Forests	BF2	6	0.061	44.6	0.7	63.7	0.143	14.4	8	350
Burnt Forests	BF3	2	0.066	50.3	1.5	33.5	0.137	1.6	7	75
Burnt Forests	BF3	2	0.015	53.0	0.8	66.3	0.126	4.1	6	350
Burnt Forests	BF3	2	0.017	53.9	0.7	77.0	0.111	6.7	7	550
Burnt Forests	BF3	3	0.026	51.6	1.2	43.0	0.144	9.3	9	75
Burnt Forests	BF3	3	0.030	51.5	1.1	46.8	0.121	1.2	7	350
Burnt Forests	BF3	3	0.031	53.3	0.7	76.1	0.128	1.7	4	550
Burnt Forests	BF3	4	0.013	49.1	0.9	54.6	0.132	4.5	8	75
Burnt Forests	BF3	4	0.032	55.1	0.7	78.7	0.119	1.2	8	350
Burnt Forests	BF3	4	0.020	53.9	0.7	77.0	0.129	1.0	9	550
Burnt	BF3	5	0.051	50.5	1.5	33.7	0.131	15.3	9	75

Forests										
Burnt Forests	BF3	5	0.017	54.2	0.9	60.2	0.09	10.5	8	350
Burnt Forests	BF3	5	0.027	53.1	0.8	66.4	0.115	7.7	9	550
Burnt Forests	BF3	6	0.038	50.3	1.6	31.4	0.113	2.4	9	75
Burnt Forests	BF3	6	0.051	54.3	0.7	77.6	0.113	1.5	9	350
Burnt Forests	BF3	6	0.385	53.3	0.9	59.2	0.114	1.5	5	550
Shrubs	S1	1	0.080	45.4	0.5	84.0	0.082	11.2	8	75
Shrubs	S1	1	0.040	36.3	0.4	101.1	0.141	26.3	4	350
Shrubs	S1	1	0.023	46.1	0.6	76.1	0.141	10.0	7	550
Shrubs	S1	2	0.088	55.5	0.9	64.6	0.087	0.5	4	75
Shrubs	S1	2	0.012	41.8	0.4	94.5	0.16	16.8	4	350
Shrubs	S1	2	0.017	48.5	0.6	75.7	0.108	7.6	5	550
Shrubs	S1	3	0.010	54.8	0.9	60.8	0.083	0.8	5	75
Shrubs	S1	3	0.063	43.4	0.5	89.7	0.175	7.9	4	350
Shrubs	S1	3	0.036	41.5	0.6	71.6	0.33	8.2	5	550
Shrubs	S1	4	0.012	51.5	0.9	59.8	0.114	5.7	8	75
Shrubs	S1	4	0.063	44.0	0.5	97.8	0.185	5.8	4	350
Shrubs	S1	4	0.105	57.4	0.9	65.1	0.091	1.9	4	550
Shrubs	S1	5	0.046	57.9	1.0	57.9	0.065	1.0	5	75
Shrubs	S1	5	0.112	55.9	0.6	95.8	0.128	3.0	5	350
Shrubs	S1	5	0.115	55.2	0.7	75.9	0.091	6.6	4	550
Shrubs	S1	6	0.092	58.9	0.9	65.6	0.092	0.8	9	75

Shrubs	S1	6	0.074	57.6	0.9	62.3	0.084	0.9	4	350
Shrubs	S1	6	0.128	58.5	0.8	75.8	0.068	1.8	8	550
Shrubs	S2	1	1.739	53.2	1.2	43.6	0.091	1.8	9	75
Shrubs	S2	1	0.004	43.1	0.5	80.7	0.18	22.3	4	350
Shrubs	S2	1	0.022	25.3	0.3	88.2	0.197	48.6	9	550
Shrubs	S2	2	0.231	53.5	1.3	41.7	0.089	9.3	6	75
Shrubs	S2	2	0.013	47.3	0.7	64.9	0.126	16.7	5	350
Shrubs	S2	2	0.021	29.8	0.4	78.8	0.197	38.7	4	550
Shrubs	S2	3	0.083	52.7	1.2	43.1	0.104	2.7	9	75
Shrubs	S2	3	0.015	47.2	0.8	59.2	0.136	15.9	9	350
Shrubs	S2	3	0.042	28.9	0.5	63.6	0.229	40.1	5	550
Shrubs	S2	4	0.065	52.3	1.4	37.4	0.084	2.1	8	75
Shrubs	S2	4	0.022	35.7	0.6	56.6	0.176	5.3	8	350
Shrubs	S2	4	0.004	20.1	0.3	59.0	0.286	54.7	9	550
Shrubs	S2	5	0.142	52.8	1.6	33.2	0.122	2.7	9	75
Shrubs	S2	5	0.036	55.2	1.0	56.4	0.109	1.7	9	350
Shrubs	S2	5	0.051	53.4	0.9	56.9	0.098	3.8	7	550
Shrubs	S2	6	0.003	52.6	1.0	55.1	0.094	9.3	9	350
Shrubs	S2	6	0.026	42.1	0.4	118.9	0.168	16.6	7	550
Shrubs	S3	1	0.019	53.7	0.9	57.4	0.096	1.4	8	350
Shrubs	S3	1	0.044	53.8	0.9	58.5	0.113	1.8	9	550
Shrubs	S3	2	0.029	54.5	0.8	72.3	0.08	1.1	5	550
Shrubs	S3	3	0.132	54.0	0.9	63.3	0.102	1.1	8	350
Shrubs	S3	3	0.072	54.8	0.9	61.7	0.086	1.7	8	550
Shrubs	S3	4	0.010	54.2	0.7	76.3	0.15	12.2	8	75
Shrubs	S3	4	0.083	53.9	1.1	50.6	0.084	1.2	8	350
Shrubs	S3	4	0.027	54.2	0.8	67.2	0.101	1.7	9	550

Shrubs	S3	5	0.015	54.1	0.9	61.5	0.126	1.8	7	75
Shrubs	S3	5	0.015	54.1	0.9	59.0	0.108	2.6	9	350
Shrubs	S3	5	0.120	54.8	0.9	63.7	0.112	2.0	7	550
Shrubs	S3	6	0.014	52.8	0.6	87.9	0.127	1.5	7	75
Shrubs	S3	6	0.377	53.9	0.8	66.7	0.111	1.5	8	350
Shrubs	S3	6	0.037	54.7	0.8	70.3	0.122	1.6	9	550
Shrubs	S4	1	0.946	39.3	0.5	78.5	0.099	15.5	4	350
Shrubs	S4	1	0.139	29.1	0.3	106.6	0.155	40.4	4	550
Shrubs	S4	2	0.020	54.8	0.6	91.3	0.117	2.7	5	75
Shrubs	S4	2	0.051	35.2	0.5	76.2	0.102	26.2	4	350
Shrubs	S4	3	0.076	55.1	0.9	63.3	0.148	2.7	6	75
Shrubs	S4	3	0.051	36.1	0.4	83.0	0.065	19.7	4	350
Shrubs	S4	3	0.148	31.2	0.2	141.6	0.184	29.6	4	550
Shrubs	S4	4	1.424	55.8	0.9	63.7	0.146	4.4	5	75
Shrubs	S4	4	0.058	35.2	0.4	90.9	0.085	26.2	3	350
Shrubs	S4	4	0.354	31.2	0.3	107.1	0.116	35.9	3	550
Shrubs	S4	5	1.929	55.3	0.9	60.3	0.078	1.7	4	350
Shrubs	S4	5	0.243	32.9	0.2	133.6	0.158	28.3	4	550
Shrubs	S5	1	0.038	54.9	0.9	58.1	0.088	2.1	8	75
Shrubs	S5	1	0.027	54.5	0.9	59.0	0.052	1.8	5	350
Shrubs	S5	1	0.019	51.5	0.7	74.3	0.09	3.3	6	550
Shrubs	S5	2	0.029	54.3	1.0	56.8	0.07	8.3	8	75
Shrubs	S5	2	0.020	50.7	0.7	67.7	0.089	5.7	5	350
Shrubs	S5	2	0.173	15.0	0.1	153.3	0.355	16.4	4	550
Shrubs	S5	3	0.014	55.0	0.9	60.9	0.068	3.2	8	75
Shrubs	S5	3	0.165	44.8	0.5	88.2	0.174	9.4	3	350
Shrubs	S5	3	0.033	25.9	0.3	93.6	0.154	8.8	4	550

Shrubs	S5	4	0.037	26.6	0.2	106.9	0.078	6.0	8	75
Shrubs	S5	4	0.018	51.7	0.9	59.9	0.062	10.5	8	350
Shrubs	S5	4	0.027	33.1	0.5	72.9	0.119	31.2	5	550
Shrubs	S5	5	0.087	54.1	1.0	56.4	0.058	2.6	8	75
Shrubs	S5	5	0.053	28.6	0.2	120.3	0.164	2.2	5	350
Shrubs	S5	5	0.001	35.7	0.4	86.2	0.148	3.6	4	550
Shrubs	S5	6	0.095	53.3	1.1	50.5	0.061	3.7	8	75
Shrubs	S5	6	0.083	52.0	0.8	64.7	0.047	16.2	8	350
Shrubs	S5	6	0.018	25.7	0.2	145.4	0.064	49.6	4	550
OP	OP1	1	0.020	55.6	0.9	61.8	0.092	0.8	7	75
OP	OP1	1	0.064	40.0	0.4	100.0	0.106	20.4	3	350
OP	OP1	1	0.205	49.8	0.6	83.0	0.11	4.5	6	550
OP	OP1	2	0.050	55.7	0.9	61.9	0.102	1.9	8	75
OP	OP1	2	0.066	42.5	0.5	85.0	0.121	15.3	4	350
OP	OP1	2	0.085	30.0	0.4	75.0	0.105	30.1	5	550
OP	OP1	3	0.018	46.1	0.7	65.9	0.106	7.1	5	75
OP	OP1	3	0.146	44.6	0.5	89.2	0.147	9.4	3	350
OP	OP1	3	1.427	50.6	0.6	84.3	0.088	7.3	8	550
OP	OP1	4	0.039	57.3	0.8	71.6	0.12	1.1	8	75
OP	OP1	4	0.062	55.1	0.9	61.2	0.117	3.2	4	350
OP	OP1	4	0.028	54.4	0.8	68.0	0.092	3.5	7	550
OP	OP1	5	0.146	55.0	0.8	68.8	0.115	1.1	9	75
OP	OP1	5	0.378	54.7	0.8	68.4	0.13	0.6	4	350
OP	OP1	5	0.146	54.0	0.7	77.1	0.073	5.2	7	550
OP	OP1	6	0.084	56.5	0.8	70.6	0.106	1.0	8	75
OP	OP1	6	0.054	54.6	0.6	91.0	0.072	1.9	5	350
OP	OP1	6	0.153	55.1	0.8	68.9	0.065	2.8	7	550

OP	OP2	1	0.108	52.2	0.8	65.3	0.101	4.2	4	75
OP	OP2	1	2.845	33.2	0.3	110.7	0.154	32.4	4	350
OP	OP2	1	0.113	34.3	0.6	57.2	0.152	26.9	5	550
OP	OP2	2	4.334	53.8	0.9	59.8	0.089	3.8	5	75
OP	OP2	2	0.089	29.9	0.4	74.8	0.118	35.8	4	350
OP	OP2	2	0.040	45.0	0.7	64.3	0.181	11.5	4	550
OP	OP2	3	0.062	51.6	0.9	57.3	0.119	3.7	9	75
OP	OP2	3	0.070	33.1	0.3	110.3	0.174	28.2	4	350
OP	OP2	3	0.031	45.8	0.6	76.3	0.126	10.7	5	550
OP	OP2	4	0.050	53.0	0.9	58.9	0.093	3.1	7	75
OP	OP2	4	0.820	34.8	0.4	87.0	0.12	26.7	4	350
OP	OP2	4	0.378	48.3	0.7	69.0	0.104	7.3	4	550
OP	OP2	5	0.071	51.3	0.9	57.0	0.095	4.5	9	75
OP	OP2	5	0.172	42.6	0.5	85.2	0.14	14.6	4	350
OP	OP2	5	0.069	50.1	0.8	62.6	0.111	6.2	8	550
OP	OP2	6	4.211	53.6	0.8	67.0	0.087	3.5	5	75
OP	OP2	6	0.057	36.1	0.4	90.3	0.164	25.5	4	350
OP	OP2	6	0.032	37.6	0.5	75.2	0.15	27.8	5	550
OP	OP3	1	0.141	38.3	0.4	95.8	0.151	24.8	4	350
OP	OP3	1	0.016	42.0	0.5	84.0	0.132	19.1	5	550
OP	OP3	2	0.305	41.4	0.5	82.8	0.146	16.3	4	350
OP	OP3	2	0.017	39.6	0.7	56.6	0.19	17.1	4	550
OP	OP3	3	0.161	40.0	0.4	100.0	0.153	19.4	4	350
OP	OP3	3	0.010	30.3	0.3	101.0	0.194	38.1	8	550
OP	OP3	4	0.229	51.0	0.9	56.7	0.141	2.5	6	75
OP	OP3	4	0.150	42.8	0.4	107.0	0.157	10.8	5	350
OP	OP3	4	0.019	28.9	0.5	57.8	0.229	40.1	9	550

OP	OP3	5	0.048	51.6	0.8	64.5	0.136	4.1	5	75
OP	OP3	5	0.123	30.5	0.4	76.3	0.246	6.9	4	350
OP	OP3	5	0.011	16.9	0.2	84.5	0.345	57.2	7	550
OP	OP3	6	0.047	54.2	0.9	60.2	0.095	2.6	5	75
OP	OP3	6	0.044	48.3	0.6	80.5	0.138	5.0	4	350
OP	OP3	6	0.001	14.7	0.1	147.0	0.341	64.6	7	550
OP	OP4	1	0.095	53.8	0.9	59.8	0.072	1.5	5	75
OP	OP4	1	2.725	41.6	0.5	83.2	0.164	12.8	4	350
OP	OP4	1	0.094	30.9	0.4	77.3	0.169	39.1	5	550
OP	OP4	2	3.525	48.5	0.7	69.3	0.122	5.7	4	350
OP	OP4	2	0.015	38.6	0.4	96.5	0.151	25.0	4	550
OP	OP4	3	0.021	51.7	0.8	64.6	0.118	1.4	4	75
OP	OP4	3	0.025	45.5	0.6	75.8	0.125	8.5	4	350
OP	OP4	3	0.129	29.4	0.4	73.5	0.172	44.1	5	550
OP	OP4	4	0.014	54.1	0.9	60.1	0.104	2.3	7	75
OP	OP4	4	0.160	44.4	0.6	74.0	0.136	13.5	4	350
OP	OP4	4	0.111	37.6	0.4	94.0	0.144	25.8	4	550
OP	OP4	5	0.101	55.7	0.8	69.6	0.063	2.6	4	75
OP	OP4	5	0.210	42.8	0.6	71.3	0.13	3.5	4	350
OP	OP4	5	0.050	33.5	0.3	111.7	0.169	46.1	7	550
OP	OP4	6	0.019	54.4	0.8	68.0	0.085	2.5	4	75
OP	OP4	6	0.020	48.0	0.5	96.0	0.133	13.1	4	350
OP	OP4	6	0.329	32.6	0.4	81.5	0.172	33.4	4	550

Table 2. Bulk density (BD) and peat water content for several pressure (pF) as the raw data for chapter 3

Site	Distance to canal	BD (g cm^{-3})	pF0	pF1	pF1.5	pF2	pF2.5	pF3	pF4.2
drained1	1	0.093	0.940	0.657	0.643	0.643		0.286	0.114
drained1	10	0.078	0.950	0.672	0.668	0.564	0.610	0.316	0.115
drained1	50	0.084	0.946	0.630	0.509	0.455	0.421	0.243	0.086
drained1	100	0.118	0.924	0.837	0.812	0.627	0.540	0.352	0.136
drained1	200	0.076	0.951	0.653	0.539	0.520	0.402	0.270	0.093
drained2	1	0.108	0.930	0.877	0.706	0.696	0.540	0.349	0.110
drained2	10	0.117	0.925	0.933	0.774	0.720	0.722	0.411	0.140
drained2	50	0.078	0.950	0.519	0.509	0.423	0.360	0.247	0.083
drained2	100	0.091	0.942	0.719	0.661	0.502	0.391	0.252	0.193
drained2	200	0.111	0.928	0.716	0.673	0.521	0.406	0.257	0.112
Drained3	1	0.105	0.933	1.081	0.890	0.748	0.608	0.410	0.128
Drained3	10	0.121	0.923	1.178	1.025	0.872	0.649	0.407	0.139
Drained3	50	0.082	0.947	0.636	0.554	0.547	0.370	0.244	0.090
Drained3	100	0.068	0.956	0.556	0.497	0.386	0.356	0.217	0.080
Drained3	200	0.08	0.948	0.671	0.531	0.518	0.405	0.240	0.092
Forest ARTU		0.08	0.949	0.636	0.536	0.456	0.329	0.234	0.109
Forest ARTU		0.11	0.930	0.792	0.729	0.730	0.650	0.350	0.152
Forest ARTU		0.064	0.959	0.477	0.425	0.379	0.409	0.231	0.058
Forest ARTU		0.073	0.953	0.511	0.490	0.483	0.373	0.258	0.101

Forest ARTU		0.077	0.950	0.577	0.497	0.450	0.316	0.083	0.116
Forest ARTU		0.082	0.948	0.605	0.559	0.508	0.494	0.257	0.126
ForestLog		0.104	0.933	0.705	0.621	0.431	0.257	0.318	0.135
ForestLog		0.094	0.940	0.700	0.587	0.525	0.443	0.254	0.116
ForestLog		0.062	0.960	0.338	0.370	0.269	0.334	0.200	0.093
ForestLog		0.095	0.939	0.740	0.540	0.491	0.426	0.265	0.132
ForestLog		0.086	0.944	0.663	0.600	0.534	0.441	0.266	0.128
ForestLog		0.106	0.932	0.802	0.648	0.622	0.430	0.309	0.161
ForestOU		0.09	0.942	0.536	0.571	0.467	0.384	0.212	0.107
ForestOU		0.081	0.948	0.548	0.470	0.427	0.372	0.239	0.119
ForestOU		0.091	0.941	0.451	0.389	0.492	0.280	0.205	0.104
ForestOU		0.082	0.947	0.589	0.507	0.493	0.354	0.272	0.118
ForestOU		0.077	0.951	0.611	0.522	0.506	0.376	0.256	0.108
ForestOU		0.083	0.947	0.604	0.549	0.560	0.430	0.267	0.117